Title
The mechanisms underlying exacerbated autistic behavior induced by the circadian-disrupting environment of nightly illumination.

Author
Wang, Huei-Bin

Publication Date
2022

Peer reviewed|Thesis/dissertation

UNIVERSITY OF CALIFORNIA

Los Angeles

The mechanisms underlying exacerbated autistic behavior induced by the circadian-disrupting environment of nightly illumination.

A dissertation submitted in partial satisfaction of the requirements

for the degree Doctor of Philosophy

in Molecular, Cellular, and Integrative Physiology

by

Huei-Bin Wang

2022

ABSTRACT OF THE DISSERTATION

The mechanisms underlying exacerbated autistic behavior induced by the circadian-disrupting environment of nightly illumination.

by

Huei-Bin Wang

Doctor of Philosophy in Molecular, Cellular, and Integrative Physiology

University of California, Los Angeles, 2022

Professor Christopher S. Colwell, Chair

Autism spectrum disorders (ASD) are a set challenging neurodevelopmental disorders with extremely high prevalence and expensive social cost. There is a good evidence for a genetic contribution to ASD but environment factors also play a role and interact with the genetic loads as a “second-hit” that further exacerbated the syndrome. The later raise the possibility that dysfunctional circadian rhythms may contribute to the disease improving these rhythms may offer a mechanism to help with the management of ASD symptoms. Robust circadian rhythms and good quality of sleep are restorative and critical for many of the same behaviors that are compromised in ASD. However, the possibility that circadian disruption is one of the environmental factors that contribute to the disease has not been well studied. Using the contactin associated protein-like 2 knock out (*Cntnap2* KO) mouse model of ASD, this dissertation research addressed this issue by determine whether a mild circadian disruption caused by dim light at night (DLaN) impacts wild type (WT) and *Cntnap2* KO mice. In the first

study, I demonstrated that the *Cntnap2* mutants are vulnerable to DLaN exposure by showing light-evoked disruptions in sleep/wake cycles, the social impairments, and repetitive grooming behavior. Nightly treatment with melatonin was effective in counteracting the negative effects of DLaN. Next, I examined the pathways by which DLaN was detected and specifically explored the role of the photopigment melanopsin in mediating DLaN consequences. The effects of DLaN on circadian behavior, social behavior, and repetitive behavior were prevented in a line of mice in which the cells expressing melanopsin are genetically ablated. In addition, knowing the melanopsin is largely sensitive to light in the blue/green wavelengths, a specialized LED-system was used that minimized the melanopsin activation while still providing illumination for vision. The illumination produced by this lighting system prevented the negative impacts of DLaN. In the third study, I aimed to evaluate the role of inflammation in mediating the effects of DLaN. The *Cntnap2* mutation itself was found to alter the immune profiles in the plasma and the prefrontal cortex, and made the mutants even more vulnerable to the DLaN perturbation compared to the WT controls. Moreover, an inhibitor targeting COX-2 signaling effectively blocked DLaN-evoked inflammation as well as the behavioral changes caused by this environmental second hit. Together, this dissertation work supports a model in which DLaN activates inflammatory pathway. Increase in these inflammatory molecules drives behavioral changes. Widely used, inexpensive pharmacological treatments were found to prevent these adverse behavioral changes. Finally, in the last study, a second mouse model of ASD - the fragile X mental retardation 1 (Fmr1) KO mice, was used to test the principle hypothesis that circadian interventions can be beneficial to ASD.

The dissertation of Huei-Bin Wang is approved.

Gene D. Block

Cristina A. Ghiani

Weizhe Hong

Stephanie Correa Van Veen

Christopher S. Colwell, Committee Chair

University of California, Los Angeles

2022

Dedication

I would like to thank my family for their love and constant support, especially my mom who independently raised me and my two younger brothers. I was never the smartest in a group, but my mom always encouraged me and never lost faith in me. And even though I could tell that she would love me to be around, she remained supportive when I showed my interest in studying abroad at UCLA, where is thousands of miles away from home. This doctoral degree is not just an academic accomplishment of myself, but also a fruit of a motherhood and her love.

A big thank you to Dr. Christopher Colwell and Dr. Cristina Ghiani, who always patiently guide me and help me to become better. They are supportive with my learning in the lab, and never stopped showing me the big world and letting me have so many opportunities to learn and explore growing up. I am particularly grateful that they financially support me to attend academic symposiums including the Society for Research on Biological Rhythms and Society for Neuroscience. The experience of interacting with inspiring scientists and talented grad student peers were great inspirations to my scientific learning. I fall short of words to express my gratitude towards them.

I appreciate invaluable inputs from my committee members Drs. Gene Block, Stephanie Correa Van Veen, and Weizhe Hong. Especially their expertise in experimental designs. And they have been positive and supportive in all our committee meetings.

I would like to thank all the past and present lab members of the Colwell Lab and Ghiani Lab for all their help and friendship. Dawn, Chris L, Saemi, Olivia, Yu, Kathy, Sarah, Hye-In, and Daniel are the best colleagues and friends. I cherish all the wonderful time that we have together. I also want to thank my friends from MCIP cohort 2017: Abigail Aleman, Rozeta Avetisyan, Chieh Chen, Rockelle Guthrie, Jessica Nevarez-Mejia, and Jessica Yano. You guys are just amazing!

There are many Taiwanese friends along the way. Jerry, Derek, Yen-Wei, Yi-Wei, Cathy, Howard, Ting-Yuhan, Wie-chia, Te-Yuan, Yu-Tao, Yen-Ru, Yi-Chung, Hao-Yu, Ivy, Kimi, Ted, Yueh Jia, and Kido are particularly special to me. I am grateful to my girlfriend Raven Wang for her love and encouragement. She has been always there beside me for better or worse. I cannot thank enough Raven for her constant support.

Table of Contents

List of Figures

Melatonin treatment of repetitive behavioral deficits in the Cntnap2 mouse model of autism spectrum disorder

Long wavelength light reduces the negative consequences of dim light at night in the CNTNAP2 mouse model of autism.

Scheduled feeding improves behavioral outcomes and reduces inflammation in a mouse model of Fragile X syndrome.

Conclusion

List of Tables

Melatonin treatment of repetitive behavioral deficits in the Cntnap2 mouse model of autism spectrum disorder

Long wavelength light reduces the negative consequences of dim light at night in the CNTNAP2 mouse model of autism.

Role of inflammation in mediating the effects of dim light at night in the Cntnap2 KO mouse model of autism.

Scheduled feeding improves behavioral outcomes and reduces inflammation in a mouse model of Fragile X syndrome.

Acknowledgments

The UCLA Molecular, Cellular, and Integrative Physiology (MCIP) Graduate Program provided financial as well as academic support. And all chapters of this dissertation represent the collaborative efforts of multiple individuals as directed by PI Christopher S. Colwell and PI Cristina A. Ghiani. The chapter 2, chapter 3, chapter 4, and chapter 5 include materials from manuscripts that have been published, are currently in-press, or are currently in preparation. Chapter 2 is a version of “Wang, H.B., Tahara, Y., Luk, S.H.C., Kim, Y.S., Hitchcock, O.N., Kaswan, Z.A.M., Kim, Y.I., Block, G.D., Ghiani, C.A., Loh, D.H. and Colwell, C.S., 2020. Melatonin treatment of repetitive behavioral deficits in the Cntnap2 mouse model of autism spectrum disorder. Neurobiology of disease, 145, p.105064”. This work was supported by Takeda Pharmaceuticals. Chapter 3 is a version of “Wang, H.B., Zhou, D., Luk S.H., Cha, H.I., Mac, A., Chae, R., Matynia A., Harrison, B., Afsharim S., Block, G., Ghiani, C.A., Colwell, C.S. Long wavelength light reduces the negative consequences of dim light at night in the CNTNAP2 mouse model of autism”. This work was supported by Korrus Inc and the scholarship for study abroad provided by the Taiwan Ministry of Education (#1100090595).

Biographical Sketch

EDUCATION

University of California, Los Angeles (UCLA) — **Los Angeles, CA**

- PhD candidate, Molecular, Cellular, and Integrative Physiology (MCIP) — **Sep 2017 - Current**
- Thesis Title: The mechanisms underlying exacerbated autistic behavior induced by the circadian-disrupting environment of nightly illumination.

University of California, Los Angeles (UCLA) — **Los Angeles, CA**

- MS, Physiological Science — **Sep 2013 - Oct 2015**
- Thesis Title: Photo-Environment Affects Disease Progression in Bacterial Artificial Chromosome (BAC) Huntington s Disease Mouse Model

National Taiwan University (NTU) — **Taipei, Taiwan**

- BS, Animal Science — **Sep 2008 - Jun 2012**
- Undergraduate Research: Acute and Chronic Effects of Kisspeptin on Serum Level of Gonadotropin in Caprine

RESEARCH EXPERIENCE

PhD Student Researcher, Laboratory of Circadian and Sleep Medicine — **Los Angeles, CA**

- Applied circadian-based interventions (agonist of melatonin receptor, melanopsin-minimized photic stimuli, scheduled-feeding paradigm) and improved the circadian and sleep phenotypes as well as the autistic behavior in mouse models of autism spectrum disorder (ASD). Our work suggested improvements of 20-40% in measured outputs compared to the control groups[1-3]. — **Sep 2017 - Current**

Research Assistant, Semel Institute for Neuroscience and Human Behavior — **Los Angeles, CA**

- Rescued the motor symptoms and the circadian disturbances by leveraging the antagonist of Histamine-3 receptor, the blue light therapy, or the scheduled feeding in mouse models of Huntington's disease (HD), a desperate neurodegenerative disease[5-8]. — **Dec 2015 - Aug 2017**

Master Student Researcher, Laboratory of Circadian and Sleep Medicine — **Los Angeles, CA**

- Applied microarray analysis to discover biological pathways underlying the disease progression of cardiovascular abnormality in a mouse model of HD. — **Sep 2013 - Oct 2015**
- Conducted behavioral assays (e.g. learning and memory, aggression, depression) in mouse models to assess disease progressions.

Undergraduate Student Researcher, NTU — **Taipei, Taiwan**

- Measure the level of serum reproductive hormones (e.g. estrogen, progesterone) using ELISA assays. — **Jul 2009 - Jun 2012**
- Cell culture with immortalized cell lines to test biological pathways

AWARDS

Government scholarships for study abroad, Taiwan Ministry of Education	**2021**
BRI/Semel Institute Graduate Travel Award, UCLA	**2019**
Excellence Award, Society of Research in Biological Rhythm	**2018**
University Fellowship, UCLA	**2017**
Academic Fellowship, UCLA	**2014**
Research Scholarship, Taiwan National Science Council	**2011**

SELECTED RESEARCH PUBLICATIONS

1. **Wang HB**, Tahara Y, Luk SHC, Kim YS, Hitchcock ON, MacDowell Kaswan ZA, In Kim Y, Block GD, Ghiani CA, Loh DH, Colwell CS. Melatonin treatment of repetitive behavioral deficits in the Cntnap2 mouse model of autism spectrum disorder. Neurobiol Dis. 2020 145:105064. doi: 10.1016/j.nbd.2020.105064.
2. **Wang HB**, Zhou D, Cha HI, Ghiani CA, Colwell CS. Reducing the melanopic intensity of dim light at night is an effective countermeasure for behavioural deficits in the Cntnap2 mouse model of autism spectrum disorder. MS prep
3. **Wang HB**, Brown S, Smale N, Ghiani CA, Colwell CS. Timed-restricted feeding ameliorates reduced social discrimination, repetitive behavior, and sleep/wake cycles in the male Fmr1 KO mice. MS prep
4. **Wang HB**, Zhou D, Ghiani CA, Colwell CS. Non-steroid anti-inflammatory treatment (carprofen) counteracts the negative impacts of nightly-illumination circadian disruption on social behavior and repetitive grooming behavior in the Cntnap2 KO mice. MS prep
5. Whittaker DS, **Wang HB**, Loh DH, Cachope R, Colwell CS. Possible use of a H3R antagonist for the management of nonmotor symptoms in the Q175 mouse model of Huntington's disease. Pharmacol Res Perspect. 2017 Oct;5(5):e00344. doi: 10.1002/prp2.344.
6. **Wang HB**, Loh DH, Whittaker DS, Cutler T, Howland D, Colwell CS. Time-Restricted Feeding Improves Circadian Dysfunction as well as Motor Symptoms in the Q175 Mouse Model of Huntington's Disease. eNeuro. 2018 5(1):ENEURO.0431-17.2017. doi: 10.1523/ENEURO.0431-17.2017.
7. Whittaker DS, Loh DH, **Wang HB**, Tahara Y, Kuljis D, Cutler T, Ghiani CA, Shibata S, Block GD, Colwell CS. Circadian-based treatment strategy effective in the BACHD mouse model of Huntington's disease. Journal of biological rhythms. 2018 Oct;33(5):535-54.
8. **Wang HB,** Whittaker DS, Truong D, Mulji AK, Ghiani CA, Loh DH, Colwell CS. Blue light therapy improves circadian dysfunction as well as motor symptoms in two mouse models of Huntington's disease. Neurobiol Sleep Circadian Rhythms. 2017 2:39-52. doi: 10.1016/j.nbscr.2016.12.002.
9. Loh DH, Kuljis DA, Azuma L, Wu Y, Truong D, **Wang HB**, Colwell CS. Disrupted reproduction, estrous cycle, and circadian rhythms in female mice deficient in vasoactive intestinal peptide. Journal of biological rhythms. 2014 Oct;29(5):355-69.
10. Schroeder AM, **Wang HB**, Park S, Jordan MC, Gao F, Coppola G, Fishbein MC, Roos KP, Ghiani CA, Colwell CS. Cardiac Dysfunction in the BACHD Mouse Model of Huntington's Disease. PLoS One. 2016 11(1):e0147269. doi: 10.1371/journal.pone.0147269

Chapter 1

Chapter 1

The term “Autism” comes from Greek roots (from the Greek autos, meaning “self”) which highlights the isolation of patients from their surroundings. Generally the diagnosis umbrella known as “autism spectrum disorder (ASD) is used in recognition of the diversity of symptoms in these neurodevelopmental disorders. The ASD field needs more integrative research from diverse fields to elucidate the causes and develop treatments.

One area with emerging ties to autism is the field of circadian rhythms. The circadian system mediates a broad range of physiology including brain development, cognitive function, sleep gating and consolidation, and immune balance. A number of underlying genetic connections between circadian rhythms and ASD have been reported. More boardly, sleep and circadian disturbances are commonly observed in ASD patients. It is my hope that a better understanding of the role of circadian rhythms in ASD may bring new insights to disease mechanisms and assist in the development of novel treatments. For example, I believe it is likely that treating the sleep/wake disturbances can actually improve the ASD symptoms and provide a new therapeutic avenue.

Circadian Rhythms

Let time tell the clock story

Circadian rhythms are a biological timing system with a period of close to 24 hours. This timing system is endogenous and temperature compensated (Ruby et al., 1999; Reyes et al., 2008). It generates the daily rhythms of sleep/wake cycles, body temperature, and hormonal secretion (Reddy et al., 2018). In order to function adaptively, this timing system must be synchronized to the local environment (e.g. light/dark changes), which leads to the appropriate phasing of circadian outputs (e.g. sleep/wake cycles). The discovery of circadian rhythms and the understanding that these rhythms are critical for our health are still new concepts in the biomedical field.

The very first discovery of circadian rhythms was much earlier than the coined circadian term. It was made in 1729 by French astronomer Jean Jacques d'Ortous de Mairan. He observed that leaf movements of the Mimosa plant moved up and down with a daily cycle, and this daily cycle persisted even when the plants were placed in constant darkness. His observation led to the conclusion that the daily rhythms were intrinsically controlled rather than simply a response to the photic cycle of the Earth (de Mairan 1729). However, this insightful observation did not receive attention from many academics, and the field had no significant breakthrough until the early 1900s (almost 2 centuries later!). With the growing appreciation of Mendelian genetics, Dr. Erwin Bunning conducted genetic experiments by crossing bean plants with various circadian period lengths and demonstrated that the offspring period was an intermediate of the previous generation, suggesting that there was a genetic component in circadian rhythms (Bunning 1969). Later, observations of daily rhythms in physiological outputs under constant environmental conditions were reported in animal kingdom such as in rodents (Richter 1922), birds (Kramer 1952), and humans (Aschoff and Wever 1962). Then, two giants in the field, Dr. Colin Pittendrigh and Dr. Jurgen Aschoff, established a series of quantitative protocols and paved the foundation of the field in the 1960s. Moreover, Dr. Pittendrigh developed a non-parametric model describing how circadian rhythms can be reset or disrupted by a single pulse of light (Pittendrigh and Minis 1964), and Dr. Aschoff coined the term "Zeitgeber" (German: time-giver) to describe the environmental stimuli that can synchronize the intrinsically generated circadian rhythms (Aschoff 1955; Aschoff et al., 1975).

Even with the clear demonstration of the endogenous nature of circadian rhythmicity, the questions of, how and where the rhythms were generated remained elusive. In 1971, the field started gaining an understanding in the genetic basis of circadian clocks. The elucidation a circadian clock mechanism was initiated by Dr. Ronald Konopka and Dr. Seymour Benzer using a mutant screen in *Drosophila melanogaster* identified a critical circadian timing gene – *Period* (Konopka and Benzer 1971). Later, Dr. Jeffery Hall and Dr. Michael Rosbash

proposed a transcriptional translational feedback loop (TTFL) model with *Period* as the positive arm of TTFL, and the later discovery of the second clock gene *timeless* (tim) by Dr. Michael Young (Harms et al., 2003) served as the negative arm of TTFL. Together, their landmark studies identified essential components of the TTFL, leading to our first real insight into the molecular clock mechanism in living organisms. Their achievements were recognized by the 2017 Nobel Prize in Physiology or Medicine, honoring their pioneer work in establishing the molecular basis of circadian rhythm.

The historic progress in understanding the molecular basis of circadian rhythm generation in *Drosophila* facilitated circadian research into the molecular basis of mammalian circadian timing. The successful experience with Drosophila mutant screens paved the way for a large-scale mutant screen in mice. This definitive project supervised by Dr. Joseph Takahashi lead to the discovery and cloning of the first mammalian circadian gene, Clock (Circadian Locomotor Output Cycles Kaput; Vitaterna et al., 1994, King et al., 1997), followed by the discovery of its heterodimeric partner – BMAL1 in 1998 (Gekakis et al., 1998). By 2001, the Takashi team had mapped out the positive arms and the negative arms of the mammalian TTFL, dramatically broadening the circadian research in mammalian physiology. Research into the circadian field then grew steadily, with more circadian genes added to TTFLs and better understanding of the core circuitry. Moreover, along with the new understanding of the mechanisms underlying biological timing there was a steady growth of interest into understanding how circadian rhythms impact human health and disease states.

In the following sections, I will focus on the mammalian clocks and briefly introduce the molecular clock (TTFLs), the master circadian pacemaker, entertainment and the downstream peripheral clocks, and its relationship to psychiatric and developmental disorders.

The molecular TTFL driving mammalian circadian rhythms

As mentioned above, there are sophisticated genetic processes underlying the mammalian circadian clock. Our current understanding is that there are at least three core TTFLs underlying the circadian timing in mammals. The daily up-and-down rhythms result from the temporal interactions of a positive arm (promotes transcriptional activity) and a negative arm (inhibits transcriptional activity) of the TTFLs. Take the central TTFL for an example, the CLOCK and BMAL-1 (brain and muscle ARNT-like-1) form its positive arm, and PERIOD (PER) and CRYPTOCHROME (CRY) form its negative arm (Robinson et al., 2014). The circadian cycle starts when the heterodimer of CLOCK and BMAL1 promotes the mRNA expression of *Per* and *Cry* by the interaction with the E-box promoter of the two genes. Translation and post-translational phosphorylation increase their stability and the two proteins start accumulating in the cytoplasm. This cytoplasmic accumulation significantly increases the probability of PER and CRY to be dimerized and translocated back to the nucleus (Kondratov et al., 2003). However, the nucleic heterodimer PER/CRY interrupts the transcriptional activity of the heterodimer CLOCK /BMAL1; in other words, PER/CRY heterodimer inhibits the positive arm of the TTFLs and exerts negative feedback regulation on their own mRNA production (Van Der Horst et al., 1999). Therefore, with the increasing levels of PERs and CRYs over time, the positive arm of the central TTFL is gradually repressed. This repression of the positive arm consequently leads to less and less *Per* and *Cry* mRNA made, which in turn, weakens the negative arm of the central TTFL. The new cycle starts when the negative arm gets too weak and requires more time for the accumulation of PER and CRY.

The secondary and third TTFLs are looped with the central TTFL through the key clock proteins. The BMAL1 in the central loop is further regulated by retinoic acid-related orphan receptors (ROR, the positive arm) and REV-ERBα (the negative arm) in the second TTFL. The third TTFL involves the D-box binding protein (DBP) and the nuclear factor interleukin-3-regulated protein (NFIL3). DBP and NFIL3 are dimerized in the cytoplasm and

bind to the D-box element of many clock genes (e.g. PER and REV-ERB), adding additional regulatory layers on the molecular clock machinery.

The environmental zeitgebers align the circadian clocks to the environmental period by altering the level of clock genes, protein stability, and protein translocation to speed up or slow down the TTFLs (Mendoza-Viveros et al., 2017). This complex TTFL network driving circadian rhythms is resident in almost all cells. Recent studies suggest that more than half of protein-coding genes are rhythmic and under the regulations of circadian timing system (Zhang et al., 2014), making the circadian timing system a large regulatory network in physiology. Almost all diseases (e.g. cancers, metabolic disorders, brain diseases) are associated with disrupted profiles of clock genes, and disruptions of the circadian rhythms (e.g. shift work, light pollution, or nighttime snack) are commonly associated with increased risks of diseases (Rijo-Ferreira et al., 2019).

The suprachiasmatic nucleus: the master clock synchronizing physiological rhythms

The discovery of the suprachiasmatic nucleus (SCN) was a remarkable finding because it revealed, for the first time, a neural basis of circadian rhythms in mammals. The SCN was identified in 1972 (Moore & Eichler, 1972) and has proven to be the master pacemaker in the mammalian circadian system through experiments involving lesions, cell culture, and transplantation. The SCN exhibits self-sustained oscillations at tissue or individual neuron levels in in cell and tissue culture (Welsh, Logothetis, Meister & Reppert, 1995; Yamazaki et al., 2000). Moreover, SCN lesions abolished circadian rhythms at tissue and whole-animal levels, and the rhythmicity could be restored by the SCN transplantation with the circadian period of the donor rather than the recipient (Lehman, Silver, Gladstone, Kahn, Gibson & Bittman, 1987; Ralph, Foster, Davis & Menaker, 1990; Sujino et al., 2003). Together, these studies conclusively demonstrate that SCN is a self-sustained master clock driving mammalian circadian rhythms.

Anatomical studies reveal that the SCN is a bilaterally paired nucleus located just lateral to the third ventricle above the optic chiasm. It can be broadly divided into the ventral "core" region (vSCN) and the dorsal "shell" region (dSCN). The vSCN is thought to be an integrator of external inputs, and there are three afferent projections to vSCN: the retinohypothalamic tract (RHT), the geniculohypothalamic tract (GHT), and projections from the raphe nuclei. The RHT is the major pathway relaying the environmental photic signals from the intrinsically photosensitive retinal ganglion cells (ipRGCs, will be further introduced later) directly to the vSCN, as well as other brain areas (Chen et al., 2011; Fernandez et al., 2018). The GHT is thought to indirectly modulate SCN activity with gamma-aminobutyric acid (GABA) and neuropeptide Y (NPY) (Hanna et al., 2017). The projections from the raphe nuclei are another indirect pathway that sends serotonergic inputs to mediate SCN activity (Pontes et al., 2010). As the major information recipient part of the SCN, the vSCN neurons fire with low-amplitudes so that it can be easily reset by environmental stimuli, and integrate the inputs to the dSCN with neuropeptides such as vasoactive intestinal peptide (VIP) and gastrin-releasing peptide (GRP), as well as the neurotransmitter GABA. The dSCN is thought to be the output part of the SCN, and exhibit high-amplitude firing rhythms. The dSCN neurons primarily express the neuropeptide arginine vasopressin (AVP).

The SCN has a major responsibility in synchronizing the downstream peripheral clocks and adjusting them accordingly to the environmental light cycle. Without proper SCN coupling, the peripheral circadian rhythms would quickly be dampened and diminished due to the desynchronization among individual cells (Nagoshi et al., 2004). To synchronize the downstream peripheral clocks, the dSCN sends neural and endocrine signaling to critical regulatory hubs in other parts of the nervous system (Astiz et al., 2019; Welsh et al., 2010), such as the subparaventricular region and the paraventricular nuclei of the hypothalamus (PVH). For example, the hypothalamic-pituitary-adrenal (HPA) axis is under control of SCN rhythms through the regulation of corticotropin-releasing hormone (CRH) and vasopressin in the PVH (Jones et al., 2021).

Entrainment: timing the central and peripheral clocks

The synchronization of circadian clocks to the environmental light cycle with a predictiable phase relationship established between the circadian rhythm and the light cycle is referred to as stable “entrainment”. Clearly, being able to adapt and anticipate natural periodic changes, such as cycles of the light/dark transition, food availability, temperature, and social contacts, can significantly increase the survival rate in a periodically changing world. Among the temporal cues, light is the most dominant signaling in most circumstances.

The mammalian eye is a unique complex organ equipped with an image forming system where rods and cones dominate. The third photoreceptor - melanopsin (encoded by *OPN4*) has been discovered and characterized (Provencio et al., 1998), and is the major contributor in the non-image forming function of the retina such as circadian photoentrainment, negative masking, and pupillary light reflex. It is a vitamin A-based opsin photopigment and is most sensitive to the lighting wavelength at 480 nm (Fu et al., 2005). The classical visual receptors (rods and cones) also contribute photic information to the circadian system (Østergaard et al., 2007); however, they are not required for circadian regulation.

Recent studies have suggested that the ipRGCs are not a uniform population of cells; instead, there are at least 6 subtypes (M1-M6) that are anatomically, genetically, and functionally distinct (Quattrochi et al., 2019). Briefly, the M1-ipRGCs were the first to be discovered and express the highest levels of melanopsin compared with other subtypes. The Hattar group took the lead and further divided the M1-ipRGCs into two distinguishable populations based on their differential expression of the transcription factor *Brn3b* (Badea et al., 2009; Chen et al., 2011; Fernandez et al., 2018). The subpopulation of *Brn3b* positive-M1-ipRGC projects to limbic areas of the brain involved in mood regulation, such as the medial amygdala and the lateral habenula. However, *Brn3b* positive-M1-ipRGC do not project to the SCN. In contrast, the subpopulation of *Brn3b* negative-M1-ipRGC largely projects to the

SCN and drives photoentrainment of circadian rhythms. Because of the projections to the SCN and its role in circadian entrainment, it is the *Brn3b* negative-M1-ipRGCs that are particularly important for the research described in this dissertation.

The discovery and characterization of the Brn3b negative-M1-ipRGCs completed the mechanistic picture describing how light entrains circadian rhythms. The photic signals are captured by the melanopsin and then passed to the vSCN via the monosynaptic projections of the Brn3b negative-M1-ipRGCs. When the Brn3b negative-M1-ipRGCs are excited by the light stimulation, they release neurotransmitters such as glutamate (Glu) and Pituitary Adenylate Cyclase-Activating Polypeptide (PACAP) at their synaptic terminals (Moldavan et al., 2018). The neurotransmitter receptors including AMPA, NMDA, and PACAP are abundantly expressed in neurons in the vSCN (Prosser et al., 2001; Michel et al., 2006), and respond to this excitatory event by increasing the levels of intracellular Ca2+ in the vSCN. The downstream pathways mediated by the CaM kinase, cGMP/PKG, and MAPK increase the level of phosphorylated CREB (p-CREB), which alters the transcriptional level of the clock genes (e.g. *Period 1* and *Period 2*) of the TTFL network in the vSCN (Golombek et al., 2000). The activated signals are then transmitted from the vSCN to the dSCN through voltage-sensitive currents and GABA-mediated synaptic transmission (McNeill et al., 2018). Finally, the dSCN sends the output signals to the downstream peripheral clocks via the neuroendocrine system or the autonomic system of the hypothalamus (e.g. PVH, melatonin, and HPA-axis) (Patton et al., 2014).

The cells of the immune system are an example of a downstream peripheral clock. The TTFL molecular clock is present in all types of immune cells (Labrecque et al., 2015), and circadian rhythms are demonstrated on immune cell trafficking, inflammatory processes, responses to infection, expression of cytokines, chemokines and recognition receptors (Scheiermann et al., 2013; Man et al., 2016), suggesting that both innate and adaptive immunity are under circadian regulation. To entrain and coordinate the circadian rhythms, one way that the SCN communicates to the primary and secondary lymphoid

organs (i.e. thymus, spleen and lymph nodes) is through the PVH and HPA-axis to release norepinephrine, adrenaline, and glucocorticoids (Kalsbeek et al., 2012). In addition, light stimiulation of the SCN-melatonin pathway is another signal that can shift the clock genes in the immune system regulating diurnal rhythms of leukocyte proliferation, cytokine production, and NK cell activity in the bone marrow (Cardinali et al., 1999; Vishwas et al., 2013).

Perturbations from diseases, genetic risk factors, or the environment are commonly found to cause changes in the phase of the TTFLs in a tissue-specific manner (Golombek et al., 2013). The evoked misalignments are thought to create a condition of “internal jetlag” which negatively influences physiological well-being. In contrast to the detrimental impact of circadian misalignments, strengthening the entraining signals leading to more robust synchronization of circadian rhythms would be expected to help general health, increase disease resilience, improve symptoms, and improve wellness (Schroeder and Colwell 2013). In other words, paying attention to circadian hygiene should be a considered strategy for disease prevention, management, and treatment.

Circadian dysfunctions in psychiatric and developmental disorders

Circadian disturbances have been observed at behavioral and molecular clock levels in patients with psychiatric and developmental disorders (Valdez et al., 2012). It has been noted that fragmented and highly variable sleep/wake cycles are commonly reported with these disorders (Luik et al., 2013). Moreover, altered expression levels in members of the core TTFL (e.g *Per*, *Clock, BMLAL1, and Cry*) have been identified in a variety of psychiatric and developmental disorders. For example, patients with bipolar disorder (BD) show circadian and sleep disturbances in both mood episodes (Robillard et al., 2013; Takaesu et al., 2018): patients show increased insomnia (or hypersomnia) and extended sleep onset latency during the depressive episode, and reduced sleep needs as well as shorter circadian period during the manic episode. Altered circadian clock genes are found in BD patients

(Shi et al., 2008, Kripke et al., 2009, Nievergelt et al., 2006), and there are phase differences in clock gene profiles in the same individual between mood episodes (Nováková et al., 2015). Similarly, 25%-50% of patients with attention-deficit/hyperactivity disorder (ADHD) are observed with sleep fragmentation, delayed sleep phase syndrome, and excessive daytime fatigue/sleepiness (Gau et al., 2007). Changes in expression levels (Baird et al., 2011) as well as polymorphisms (Carpena et al., 2019) in circadian clock genes provide genetic links associating circadian rhythms and ADHD at molecular, endocrine, and behavioral levels. Finally, schizophrenia (SZ) patients show changes in their temporal pattern of sleep/wake cycle and melatonin profiles (Rao et al., 1994). In addition, the loss of rhythmic expression of CRY1 and PER2 is found in cultured fibroblasts from patient skin samples (Johansson et al., 2016). The animal model such as the “blind- drunk” (Bdr) mouse, which carries a mutation in the gene encoding synaptosomal- associated protein (Snap)-25, has phase-advanced locomotor activity rhythms with increased and fragmented activity bouts (Oliver et al., 2012). Together, a wealth of studies points to the fact that the circadian timing system is disturbed from levels of molecular clock gears to behavioral outputs in psychiatric and developmental disorders.

Disturbances in circadian rhythms may not simply be inconsequential correlates of disorders; instead, the underlying circadian misalignments may actively contribute to the development and mediate the severity of syndromes. This hypothesis is supported by at least two lines of work: first, genomic variability of circadian clock genes has been associated with many psychiatric and developmental disorders including BD (Shi et al., 2008), ADHD (Kissling et al., 2008; Jeong et al., 2014), major depressive disorder (Jiang et al., 2013), and SZ (Vacic et al., 2011). In addition, interventions aiming to realign the circadian rhythms are beneficial in helping alleviate symptoms (Penders et al., 2016; Wang et al., 2017; Fargason et al., 2017; Whittaker et al., 2018). Together, an increasing number of studies suggest that circadian disruptions, either caused by genetic mutations or the environmental perturbations, may actively interact with the disorders by making individuals

more susceptible to the development of psychiatric and developmental disorders, accelerating disease progression, or exacerbating symptoms after disease onset (Karatsoreos and McEwen, 2011, 2013).

Autism Spectrum Disorders (ASD)

A long way to conceptualize the puzzle

ASD is a group of neurodevelopmental disorders with increasing prevalence that occurs in all racial, ethnic, and socioeconomic groups (Maenner et al., 2021). In the United States, the estimated prevalence grew from one in 152 in 2002 (Centers for Disease Control and Prevention, 2007) to one in 54 in 2016 (Maenner et al., 2020), and the most recent survey suggested one in 44 (Maenner et al., 2021). The lifespan cost of supporting an ASD individual without intellectual disability is estimated to be $1.4 million and even higher in ASD patients with an intellectual disability (Ariane et al., 2014). The challenging behavior of ASD patients can be extremely stressful to their caregivers, and many families are devastated due to the unfortunate fact that there are not yet any effective treatments. Although the path has been demanding, there has been progress in understanding the disorder.

The term autism comes from the Greek word, “autós” meaning “self”. The term “autism” is thought to have originated from the Swiss psychiatrist Eugen Bleuler who describing some of the schizophrenic patients under his care. These “schizophrenic autism” patients were described as severely withdrawn into their own world (Bleuler et al., 1912). Another pioneer was American child psychiatrist Leo Kanner who studied a group of children who showed social impairments and repetition of vocalization. In addition, the patients showed difficulty in adapting to changes in routines, sensitivity to stimuli (especially sound), as well as resistance to certain food (Kanner, 1943). About 1 year later, Dr. Hans Asperger diagnosed his patients who display similar but not exactly, the same behavioral domains as what Kanner noted. Of note, his patients’ language development was not severely impaired

(Asperger et al., 1944). His description of the higher-functioning form of autism was later referred to as Asperger's syndrome. The autistic-like symptoms are also found in other forms of developmental disorders and can be confused with mental retardation and psychosis. In fact, "The Diagnostic and Statistical Manual of Mental Disorders, first edition (DSM-1)" published in 1952 did not have a category for autism. The word autism appeared only once, and it was under the category of schizophrenia (Sasson et al., 2011).

A decade later, investigators initiated studies in the neurological factors associated with autism (Rimland et al., 1964). However, the second edition of the DSM, DSM-II, still deemed autism a form of childhood schizophrenia when it was published in 1968. It was not until another decade before historic achievements were made. The concept of triad of impairment was introduced to the field by Dr. Lorna Wing. She proposed that autism patients show impairments in three big behavioral domains: social interaction, social communication and social imagination (Gillberg et al., 2015). This triad theory, although different from current diagnosis criteria, was foundational for the field by providing a framework to help interpret highly variable clinical observations. Another landmark achievement in the field was contributed by the psychologist Ivar Lovaas at UCLA who published a series of work showing that intensive behavior therapy could help children with autism (Smith et al., 2011). His contribution gave hope to autistic families. In 1988, the DSM-3 officially included diagnosis criteria for autism for the first time (Volkmar et al., 1988). Unfortunately, the development of the field and the public understanding of autism were detoured by a misleading hypothesis that the measles-mumps-rubella (MMR) vaccine triggers autism published by Dr. Andrew Wakefield in 1998. This work was eventually retracted and disproven. Still, it took a long time for the field to correct the public thinking about autism (DeStefano et al., 2019) and the idea that vaccines trigger ASD remains potent today.

Not until relatively recently did the field reach consensus that autism is not a single entity but a wide spectrum of symptoms. In 2013, the DSM-5 officially reflected this agreement and 4 subtypes of autism, including autistic disorder, Asperger syndrome,

childhood disintegrative disorder, and pervasive developmental disorder not otherwise specified, that were separate categories in DSM-4 have now been consolidated into one diagnosis umbrella by using the term “autism spectrum disorder”.

A closer look at a different brain

According to DSM-5, ASD patients are now diagnosed by 2 major behavioral domains that can be varied in degrees of severity: (1) Deficits in social communication/interaction and (2) Repetitive behavior and restricted interests. Impaired behavior in the first social-communicational domain includes problems in initiating or maintaining reciprocal social interaction (e.g. back-and-forth conversation, and reduced sharing of interests and emotions), adjusting to different social expectations, and using or understanding the nonverbal communication (e.g. eye contact, facial expressions, tone of voice, and gestures). The repetitive behavior includes stereotypic speech, motor movements, or use of objects. The restricted interest indicates observations that patients commonly show excessive adherence to routines, ritualized patterns of verbal or nonverbal behavior, and resistance to change with abnormally strong intensity. The unusual reactivity to sensory inputs (e.g. indifference to pain, and excessive response to sounds or textures) is also categorized under the second challenging behavior domain. All these behavioral syndromes are complex, and more than one brain region is involved. The prefrontal cortex, amygdala, hippocampus, striatum, and cerebellum are notably different in ASD patients (Wegiel et al., 2014). Next, I will consider the anatomical substraits with particular focus on the role of the prefrontal cortex, amygdala, and hippocampus to the social impairments and repetitive behavior in ASD.

Prefrontal Cortex

The prefrontal cortex (PFC) is connected with the hub regions of the “social brain” such as the nucleus accumbens and amygdala, and it is essential for social cognition including social adjustment (Karafin et al., 2004), social recognition (Amodio and Frith,

2006), and social motivation (Kas et al., 2014). Impairments in PFC lead to social isolation and apathy (Barrash et al., 2000). Abnormalities in PFC are consistent findings in ASD. Studies in postmortem PFC suggest altered neurogenesis and gliogenesis (Falcone et al., 2021; Zhang et al., 2020; Fiddes et al., 2018; Suzuki et al., 2018; Voineagu et al., 2011; Courchesne et al., 2011). For example, Falcone and the colleagues reported an increased number of neurons and reduced number of astrocytes in specific layers of the PFC (Falcone et al., 2021), suggesting altered cortical circuit patterning and function in ASD patients. In addition, imaging studies point atypical functional connections between the PFC and other brain areas in ASD patients (Zikopoulos et al., 2013; Cheng et al., 2015).

Better detailed neural mechanisms are suggested in preclinical models, and the role of PFC underlying social function have been widely demonstrated in rodents (Pellis et al., 2006; Rudebeck et al., 2007). The application of cutting-edge techniques such as the optogenetic manipulations in medial PFC (mPFC) convincingly demonstrate the role of mPFC abnormal activity in the development of autistic behavior, and the correction may be beneficial. For example, by using the engineered bistable step-function opsin, Yizhar et al., reported that region-specifically enhanced excitability in the mPFC induced social dysfunction (Yizhar et al., 2011). In line with this study, optogenetically exciting the parvalbumin neurons (inhibitory) or suppressing the pyramidal neurons (excitatory) in mPFC successfully increased social interactions in a mouse model of ASD even at adult age (Selimbeyoglu et al., 2017). The aberrant PFC-striatum circuits are also implicated in inducing stereotypic behavior (Mallet et al., 2002; Van den Heuvel et al., 2005). When being optogenetically excited, the repetitive behavior was evoked (Ahmari et al., 2013; Kim et al., 2015). The dopaminergic signaling is thought to be the underlying mediator. Overexcited PFC-dopamine release in the striatum was shown to result in repetitive behavior (Morency et al., 1985; Aliane et al., 2009; Kim et al., 2015).

Amygdala

The amygdala is well known for the association with environmental threats; however, its role has been extended into part of the "social brain" network that constitutes the neural basis of social cognition (Brothers et al., 1990; Kling and Brothers, 1992; Dunbar et al., 2009). Recent studies have even suggested that the amygdala is one of the most notable candidates underlying social impairments and repetitive behaviors in ASD.

First, people with damaged amygdala show autistic-like social impairments, such as avoiding eye contact and having difficulty judging facial expressions (Adolphs et al., 1999; Adolphs, Baron-Cohen, & Tranel, 2002; Heberlein & Adolphs 2004 ;Vuilleumier et al., 2005). In addition, postmortem and imaging studies show that the autistic amygdala exhibits altered volume and number of neurons, suggesting unusually structured amygdala in ASD patients (Abell et al., 1999; Rojas et al., 2004; Schumann et al., 2006). Besides the structural changes, functional connections between the amygdala and the PFC also appear to be reduced in ASD patients (Swartz et al., 2013; van dem Hagen et al., 2013; Pitskel et al., 2014), and the weaker connections are associated with greater social deficits (Shen et al., 2022).

Compared to the amount of studies investigating social impairments, the clinical studies examining the association between the restrictive and repetitive behaviors and the amygdala abnormalities are much fewer. Nevertheless, there are at least two studies reporting that the altered volume of amygdala was associated with increased repetitive behavior (Dziobek et al., 2006; Breece et al., 2013). The preclinical studies provide a more detailed neural mechanism on how amygdala regulates social impairments and repetitive behavior. Dr. Hong and his team at UCLA showed that, even in mice without carrying any mutations of the ASD risk gene, optogenetic activation of glutamatergic neurons in the medial amygdala (MeA) evoked self-grooming while suppressing social behavior. On the other hand, the activation of GABAergic neurons in the MeA triggered social interaction while

suppressing self-grooming (Hong et al., 2014). At least two regions are implicated as downstream effectors of the amygdala pathway. First, two independent research teams demonstrated that the microcircuit of the basolateral amygdala (BLA)-mPF mediated the ASD-like behavior. Felix-Ortiz and colleagues used the optogenetic approaches to either activate or inhibit BLA inputs to the mPFC during behavioral assays, and showed that the excited BLA-mPFC microcircuit reduced social interaction while the suppression initiated the social behavior (Felix-Ortiz et al., 2016). The other group, Sun and colleagues, further demonstrated that the glutamatergic neurons from the BLA preferentially projected to GABAergic neurons in the mPFC. Both their optogenetic and chemogenetic stimulations of this pathway resulted in reduced mPFC activity and stereotypic checking behavior (Sun et al., 2019). The second downstream effector of BLA pathway is the ventral hippocampus (vHp). When the glutamatergic projection of BLA-vHp was optogenetically activated, the social behavior was reduced while the self-grooming was increased. This finding was further confirmed by showing that treatment of glutamate receptor antagonists led to attenuated optogenetic-evoked changes (Felix-Ortiz et al., 2014).

Hippocampus

Evidence from the neuropathological and imaging studies (Raymond et al., 1989; Lawrence; Bauman et al., 2005) indicated altered hippocampal structure and functional connections to other brain regions in patients, suggesting that this key limbic structure is impacted in ASD. Nevertheless, only a few studies directly investigated the relationships between the hippocampus and social impairments and repetitive behavior, and the mechanistic picture of the hippocampal contributions still seems far from reach.

One possible explanation for the underlying social impairments are deficits in social memory (Tzakis et al., 2019). This speculation arises from reports showing impaired facial memory in ASD patients (Klin et al., 1999; McPartland & Panagiotides, 2001; Blair et al., 2002; William et al., 2005). Animal studies suggest that the dorsal CA2 and ventral CA1

hippocampal subregions (Hitti et al., 2014; Bertoni et al., 2021; Paterno et al., 2021) are involved in impairments in social memory. In addition, a chemogenetic study further demonstrated that the microcircuit of vHp projections to mPFC was necessary for recalling social memories (Phillips et al., 2019). Whether or not ASD patients have altered dorsal CA2 and ventral CA1 hippocampal subregions and if they are responsible for their impaired facial memory require further study.

A second possibility of how an altered hippocampus may contribute to social deficits is the ability to map social distance. Being able to maintain an appropriate physical distance from others is a critical aspect of social function in real-life; however, ASD patients were found to have atypical social distancing behavior (Kennedy et al., 2014). This hypothesis still needs to be tested and the neural mechanism remains elusive. However, the recent discovery of hippocampal “social place-cells” in an animal study (Omer et al., 2018) may provide a neural basis for how disrupted hippocampal function would “mis-map” the interpersonal space between a patient's location and the others in a social environment.

The links between the hippocampus and stereotypic behavior has not yet been established in clinical studies. However, there are suggestions about this linkage from research studies. Bilateral chemical lesions of the hippocampus in the juvenile rhesus monkeys resulted in stereotypic head-twist behavior (Bauman et al., 2008). Rats that received an excitotoxic lesion of the vHp region showed increased stereotypy (Lipska and Weinberger, 1993; Wood et al., 1997). Finally, hippocampal disruption by genetic manipulation evoked repetitive grooming behavior in mice (Cai et al., 2018).

Collectively, numerous studies support the essential role of the PFC- amygdala-hippocampus network in performance of normal behavior. Stressor to the microcircuits among them, either by genetic alterations or environmental disruptions, are likely to increase the risk of the development of social impairments and repetitive behavior.

Testing core ASD behavior in mouse models

Preclinical models generate great value in studying disease mechanisms, the interactions between risk genes and the environment, as well as the search for effective treatments. Non-human primates (Zhao et al., 2018), mice (Bey et al., 2014), rats (Gilby et al., 2008), guinea pigs (Grandgeorge et al., 2019), voles (Horie et al., 2019), zebrafish (Liu et al., 2019), and *Drosophila* (Ueoka et al., 2019) have all been used to study the ASD mechanisms at multiple levels including genetics, epigenetics, molecules, cells, synapses and behaviors. Mouse models of ASD are preferable for many reasons. Although models of non-human primates are more similar to human physiology, they are difficult to keep and to conduct manipulations at the neurounal circuit and synaptic level of analysis. In this regard, mouse models show advantages including genetic and neuronal manipulations (e.g. optogenetic/chemogenetic tools), smaller laboratory space requirements and infrastructur, and faster generation time with large litters.

Social impairments

Many mouse behavioral tests have been developed to measure and report the deficits in the two behavioral domains defined by DSM-5. Mice are a social species and known to have internal drive for engaging social exploration or social play (Crawley, 2007; Silverman et al., 2010). The reciprocal social interaction test and the three-chamber test are mostly commonly used. In the reciprocal social interaction test, a novel and never-met stranger mouse that matches sex, age and genotype is introduced to the testing mouse, and the time that the testing mouse actively spends on physical contact, crawling over and under each other, chasing, mounting, wrestling, nose-to-nose sniffing and nose-to-anogenital sniffing to the conspecific is measured (Bolivar et al., 2007).

The three-chamber test consists of two stages: the first stage assesses the social preference toward the stranger mouse, and the second stage assesses the ability of social recognition of the testing mouse. During the first testing stage, the testing mouse can freely

move and choose to spend time in a chamber with a non-social object or a chamber with a social conspecific. The stranger conspecific is confined within a wired cup so that aggressive behavior between 2 males can be prevented. In the second stage (social recognition), the first stranger mouse remained the same while a second never-met stranger conspecific was introduced. Thus, the recognition between the socially familiar chamber and the socially novel chamber is tested in this second testing stage.

Another way to test social recognition is the 5-trial social test (Hitti et al., 2014). The testing mouse is first habituated to a never-met conspecific for 4 trials. Then, a second stranger conspecific is introduced to the testing mouse during the 5th trial. Between trials, there are resting intervals. If the testing mouse can memorize the conspecific that it interacted with before, the time spent on social exploration would reduce gradually in later trials (e.g. Trial 3 & 4), and be boosted again when it meets the second novel mouse in the 5th trial.

Communication deficits

Communicational deficits can be tested in mouse models by evaluating the olfactory or auditory cues emitted by mice as well as how they respond to receiving such cues. This is mainly because, unlike human or non-human primates who communicate primarily through speech with assistance of non-verbal expressions, mice primarily communicate through olfactory pheromones and ultrasonic vocalizations (Shekel et al., 2021). The test of urinary pheromones counts sniffing bout and the duration in proximity to olfactory cues to evaluate their communication behavior. Mouse pups use ultrasonic vocalization to communicate to their mothers, and this type of communication is commonly evaluated in newborn or juvenile ASD mice (Wöhr et al., 2011).

Stereotypy

Among the assessments of repetitive behavior and restricted interests, stereotypic self-grooming is perhaps the most consistent phenotype compared to other repetitive

behaviors (e.g. circling, backflips, jumping) in ASD mouse models. In the grooming test, the testing mouse can freely move in the testing arena, and camcorders are used to record and score the grooming behavior. The digging behavior is also frequently reported in studies. The marble bury test is mostly used to assess the repetitive digging behavior (Hoffman et al., 2016). In this test, the marbles are laid out on thick sawdust to trigger the digging behavior. Camcorders are used to record and score the digging behavior, and the number of marbles that are at least two-thirds buried are counted at the end of the test. The "insistence on sameness" is commonly tested by the T-maze in mouse models of ASD. Instead of having roughly the same frequency in visiting both arms, they show inflexibility and spend more time in one arm of the maze (Guariglia et al., 2013).

The combination of behavioral tests modeling the ASD-like behavior and circuit-manipulating tools in mouse models has assisted the field in constructing a mechanistic picture of ASD, especially the output part of the disorder. However, the etiology of ASD still remains relatively elusive compared to many other brain diseases. The barrier is likely due to the fact that more than one risk genes are contributing to ASD plus the involvement of environmental factors.

The genetic and non-genetic mediators

Genetic mediators

The rapidly increasing studies of the whole-exome and whole-genome sequencing (WES and WGS, respectively) of families with at least one child with ASD, and the identification of genetic variants [include but not limited to: copy number variants (Sebat et al., 2007), de novo single nucleotide variants (Iossifov et al., 2014; Nealeet al., 2012; Sanders et al., 2012), common genetic variants (Gaugler et al., 2014), mosaicism (Lim et al., 2017), non-coding and regulatory pathogenic variations (Turner et al., 2016), and inherited recessive variants (Morrow et al., 2008)] provide foundations for the genetic risk to the development of ASD. Moreover, the strong trait of heritability is commonly observed in

ASD families. For example, the proportion of ASD-related challenging behavior is higher in the first-degree relatives than the general population (Lyall et al., 2014; Virkud et al., 2009).

The field has established that ASD is not a monogenic disorder, but rather associated with a group of risk genes. Since 2013, Abrahams and the collaborators have established the SFARI database (https://gene.sfari.org/) where comprehensive and up-to-date information of identified ASD-risk genes can be found (Abrahams et al., 2013). The risk genes are classed into 1 (High Confidence), 2 (Strong Candidate) or 3 (Suggestive Evidence) based on the current studies supporting the function of a certain risk gene in ASD development. These identified genes are primarily important for brain development and function (Sztainberg et al., 2016; Tian et al., 2017; Yuen et al., 2016), such as synaptogenesis and synaptic plasticity (e.g. CNTNAP2, FMRP), cytoskeleton dynamics (e,g, SHANK3), protein synthesis and degradation (e.g. mTOR and UBE3A), and chromatin remodeling (e.g. MECP2).

To further understand how these identified genes alter the brain circuits and the output behaviors, genetic mouse models of ASD have been made and widely used for the discovery of detailed mechanisms as well as the search of the treatments. In this dissertation research, the *Cntnap2* knockout (KO) mouse model is primarily used as the testing model. CNTNAP2, which locates on 7q35-q36.1, is a transmembrane scaffolding protein (Dean and Dresbach, 2006) and highly expressed throughout the brain (Kang et al., 2011). It is expressed in dendritic spines, axons, and soma (Varesa et al., 2015), and it plays an essential role in mediating cell-cell interactions in the nervous system. In fact, it is one of widely replicated ASD-predisposition genes (Alarcon et al., 2008; Arking et al., 2008; Bakkaloglu et al., 2008; Li et al., 2010), and convincingly considered as one of the high-risk genes for ASD. At least one study reported that the homozygous mutations can lead to as high as 67% of ASD diagnoses. Even the heterozygous mutations are reported to have impacts on brain structure and functional connectivity (Scott-Van Zeeland AA, et al., 2010; Dennis et al., 2011; Whalley et al., 2011).

The *Cntnap2* KO mouse model replicates ASD syndrome at many levels. At neuron/synapse level, different research groups have found deficits such as dysregulated excitatory/inhibitory balance in brain regions including the PFC (Selimbeyoglu et al., 2017; Lazaro; Park et al., 2022) and hippocampus (Jurgensen and Pablo 2015; Park et al., 2022), altered axonal myelination (Gordon et al., 2014), reduced number of GABAergic interneurons (Penagarikano et al., 2011), and impaired neuronal migration (Penagarikano et al., 2011). At the behavioral level, the mutants show deficits in social preference (Penagarikano et al., 2011; Park et al., 2022) and communication (Penagarikano et al., 2011), as well as strong repetitive grooming behavior (Penagarikano et al., 2011; Xing et al., 2019). They also have impaired response to olfactory sensory stimuli and lack preference for novel odors (Gordon et al., 2016), replicating the sensory abnormalities in ASD patients (Behrmann et al., 2015). In addition, the *Cntnap2* KO mice have been demonstrated as a validated model for ASD-relevant drug discovery. For example, rescuing effects of risperidone (Penagarikano et al., 2011), oxytocin (Peñagarikano et al., 2015), and rapamycin (Xing et al., 2019) have been successfully demonstrated in the mutants.

Even though the field has significantly advanced the understanding of how ASD risk genes have impacts on brain development and the downstream behavior, there are still more than 70% of ASD cases that are idiopathic (Abrahams and Geschwind, 2008). This discrepancy suggests that non-genetic factors must play a role in the trajectory of ASD.

Non-genetic mediators

The key study challenging the long-time mainstream hypothesis that genetic factors play the dominant role in ASD is the work by Hallmayer and colleagues published in 2011. Their work was one of the largest twin-pair studies (192 twin-pair studies) and their analysis concluded that the shared environment (58%) had a greater impact on ASD development than genetic similarity among monozygotic twins (Hallmayer et al., 2011). This report was then supported by other groups (Sandin et al., 2014) and further indicated that the non-

genetic factors determined up to 40 – 50% of variance in ASD liability (Deng et al., 2015; Gaugler et al., 2014).

A large proportion of studies have investigated possible environmental contributions to ASD at early- life stages, especially the prenatal period. Factors such as the mother's condition, and advanced maternal age (Shelton et al., 2010), maternal obesity (Krakowiak et al., 2012), later birth order (Turner et al., 2011) and shorter pregnancy spacing interval (Cheslack-Postava et al., 2011) have all been reported to contributing to risk of ASD. The maternal exposure to environmental toxicity such as air pollution (Kalkbrenner et al., 2010) and pesticides (Roberts et al., 2007) have also been associated with increased ASD risks. The paternal contribution is less studied but evidence for involvement is emerging. The paternal age is suggested to be important (Yoshizaki et al., 2016), and speculated to account for as many as 20-30% of ASD cases (Callaway et al., 2012).

In practice it is extremely difficult to distinguish the interactions between genetics and the environment. In fact, variations in the interplay between different environmental influences and inherited genetic susceptibility most likely account for the observed heterogeneity in ASD. However, in the laboratory, the assessments of the environment component can be achieved by exposing wild-type (WT) mice (i.e. without carrying any known ASD risk mutations) to a specific environmental risk. The most studied non-genetic risk is the prenatal exposure to valproic acid (VPA). VPA was first used for treating epilepsy, bipolar disorder, and migraines (Cipriani et al., 2013; Rahman et al., 2021); however, it was later consistently reported to be particularly neurotoxic to embryonic development (Taleb et al., 2021). Specifically, its adverse effects are most prominent during the window of the closure of the neural tube, and thus perturbing neurogenesis, migration, and synapse formation of the fetus brain (Finnell et al., 2021). Studies consistently report that if the WT pregnant mothers are exposed to VPA, their offspring are more likely to show significant immunological, neurodevelopmental, and behavioral changes that resemble ASD-like phenotypes (Yang et al., 2016; Mahmood et al., 2018; Wang et al., 2018).

Role of circadian disruption in ASD

Recent studies estimate that 50%-80% patients experience at least some sleep disturbances (Leader et al., 2021). The commonly reported complaints include difficulty falling asleep, reduced sleep duration, frequent nighttime awakening, and nightmares. In addition, the sleep architecture is also altered. For example, reduced rapid-eye- movement (REM) sleep and slow-wave sleep (Gagnon et al., 2021). Sleep behavior is regulated by both the homeostasis regulations and circadian rhythms, and there is evidence suggesting that both systems are affected in ASD.

Reduced REM sleep (Miano et al., 2007), higher rate of REM sleep disorders (Thirumalai et al., 2002), decreased density of spindle activity and slow-wave sleep (Rochette et al., 2018; Lehoux et al., 2019) taken together suggest sleep problems may be common among ASD patients. Alongside the dysfunctional sleep homeostasis, evidence of disrupted circadian timing in ASD patients can be found at many levels. At the genetic level, the clock genes that compose the core TTFLs of circadian rhythms (such as PER1, PER2, CLOCK) are highly polymorphic in ASD and associated with ASD risks (Yang et al., 2016). At the endocrine level, growing studies indicate disrupted circadian rhythms in levels of melatonin (Yenen et al., 2020), serotonin (Yuwiler et al., 1971; Badcock et al., 1987), and cortisol (Tordjman et al., 2014). Melatonin, for example, is a multifunctional hormone that not only signals the brain of the timing of nights but also mediates inflammatory events and oxidative stress (Galano et al., 2018; Hardeland et al., 2018). Mis-timed melatonin rhythms are likely to evoke desynchronization among peripheral circadian clocks, which may further induce high levels of inflammation and oxidative stress (Faraut et al., 2013; Wright et al., 2015; Espino et al., 2019; Inokawa et al., 2020), and ultimately exacerbate the challenging behavior in ASD patients. In line with this speculation, supplements of melatonin ameliorates sleep/wake cycles and alleviates behavior in ASD patients (Malow et al., 2012). At behavioral level, ASD patients show unstable sleep/wake temporal patterns, with imprecise onsets and frequent nighttime awakening commonly reported. In addition, compared to

control subjects, a higher proportion of ASD patients meet the criteria for circadian rhythm sleep-wake disorders (Baker et al., 2017).

The possible role of disrupted circadian clocks in ASD has not received much attention to date. The consequences of circadian disturbances are not just limited to patients because the sleep problems likely generate secondary effects on the sleep quality of their caregivers (e.g. parents). This will ultimately increase stress and frustrations, both psychologically and socially, among family members (Wiggs et al., 2001), adding challenges to taking care of ASD patients.

Although it is not yet determined if mutations in clock genes are risk factors contributing to ASD or if the disrupted circadian rhythms is an outcome of other ASD-driven pathology, the association is likely to be bidirectional. In other words, disrupted profiles of circadian rhythms are likely to exacerbate ASD symptoms, and correcting their circadian rhythms of ASD patients could be an effective treatment.

Conclusion and research aim

In summary, the field of circadian rhythms has evolved dramatically in the past two decades, and now chronobiologists are better equipped with the tools and knowledge to study the underlying mechanisms by which circadian timing impacts diseases development and treatments. Even in complex brain disorders such as ASD, there is evidence that consideration of circadian rhythms may contribute to the understanding and treatment of ASD, not simply by improving the sleep problems in patients but also by actively unraveling the interactions between them. This work raises our awareness of the possible costs of environmental perturbations that disturb the circadian system.

Robust circadian rhythms and good quality of sleep are restorative and critical for cognitive function and mental health. However, it should be noted that multiple lines of evidence suggest that ASD patients have compromised circadian clocks, and yet, unlike exposures to toxicants, the impacts and the underpinning mechanisms of environmental

circadian disruptions to ASD are not well studied. This is a concern because the intrinsic sleep problems in ASD patients likely hinder them from adapting their behavior to the social environment.

One commonly overlooked environmental disruption surrounding us is light at night. Unlike natural light-dark cycles with robust daytime lights and clean nighttime darkness, lights at night (LaN) are biologically inappropriate and dramatically diminishes the clear day to night transitions that synchronize our circadian timing system. Studies have shown that LaN significantly dampens the circadian rhythms in the SCN (Ikeno et al., 2016). In addition, chronic exposures to LaN not only suppress melatonin secretion (Touitou et al., 2017) but also leads to adverse effects on sleep quality (Jniene et al., 2019), reduced cognitive function (Taufique et al., 2019), increased cardiometabolic risks (Nagai et al., 2019), and abnormal immune responses (Okuliarova et al., 2020). This is a concern that needs to be addressed because ASD patients are reported to be high screen users (Montes et al., 2014), and such excessive screen time is associated with the severity of ASD symptoms i.e. the longer the screen time, the more severe the ASD symptoms (Wu et al., 2017; Dong et al., 2021). One possible explanation of the observed association between screen time and ASD severity is that enhanced screen time leads to circadian disruption. It is likely that the excessive use of screens leads to reduced sunlight in the day due to spending additional time indoors and then too much artificial lights from electrical screens at night. Together, the ASD patients maybe predisposed to sleep disruptions by their genetic background, and the circadian-disrupting LaN is likely to further worsen their symptom outputs.

I feel that this is an urgent issue that should be studied and resolved. If LaN is indeed detrimental to the ASD symptoms, then constructing a clean photic environment should be seriously considered as part of the disease management. Moreover, studying the role of environmental factors and its interaction with ASD risk genes can potentially inform both primary prevention and evidence-based interventions. Therefore, my dissertation research is devoted to studying this urgent issue and filling the gap in the field. Using the *Cntnap2*

KO mouse model of ASD, my primary aim is to test the 2-hit hypothesis that the ASD risk genes (the first hit) predispose the mutants, and the environmental disruption (i.e. dim LaN or DLaN) is the second hit leading to exaggerated ASD symptoms.

My first study aims to determine if the *Cntnap2* KO mice are selectively vulnerable to the exposure of DLaN. To achieve this goal, circadian analysis at both TTFL and behavior levels, as well as the assessments of social impairments and repetitive behavior, were conducted. In the same study, we also tested if restoring circadian rhythms by giving a supplement of melatonin is effective in counteracting DLaN. Next, I started to map out the pathway underlying DLaN impacts in the *Cntnap2* KO model. First, I investigated the role of melanopsin in mediating DLaN consequences. To achieve this goal, the circadian behavior and social behavior was compared between the WT controls and the *Opn4*^{aDTA} mutants. Furthermore, a specialized LED-system that emits lights designed to minimize the melanopsin excitement was used. Sleep/wake cycles as well as the ASD behavior were tested to determine if shifting the spectrum of lights to reduce melanotic illuminations can also reduce the negative impact of DLaN. The third study aimed to explore the downstream pathway connecting circadian disruption and affected ASD behavior. Imbalanced immune activities are frequently evoked by circadian disruptions and commonly observed in ASD patients. To pursue this line of study, the immune profile at both peripheral level and central nervous system was assessed to determine this seemingly convergent mechanism. An inhibitor targeting the dysregulated immune network was used to test the role of immune abnormalities underlying DLaN mechanism. Finally, a second mouse model of ASD - the *Fmr1* KO mice, was used to highlight the principal hypothesis that circadian interventions are beneficial to ASD population.

References

Abell, Frances, et al., "The neuroanatomy of autism: a voxel-based whole brain analysis of structural scans." Neuroreport 10.8 (1999): 1647-1651.

Aliane V, Pérez S, Nieoullon A, Deniau JM, Kemel ML. Cocaine-induced stereotypy is linked to an imbalance between the medial prefrontal and sensorimotor circuits of the basal ganglia. Eur J Neurosci. 2009;30(7):1269–79.

doi:10.1111/j.1460-9568.2009.06907.x.

ASCHOFF J. Zeitgeber der 24-Stunden-Periodik [Time signal transmitter for twenty-four hour period]. Acta Med Scand Suppl. 1955;307:50-2. German. PMID: 13301414.

Aschoff J, Hoffmann K, Pohl H, Wever R. Re-entrainment of circadian rhythms after phase-shifts of the Zeitgeber. Chronobiologia. 1975 Jan-Mar;2(1):23-78. PMID: 1192905.

Asperger, H. (1944). Die autistisehen Psychopathen im Kindesalter. Archiv für Psychiatrie und Nervenkrankheit, 117, 76–136.

Badcock, N. R., J. G. Spence, and L. M. Stern. "Blood serotonin levels in adults, autistic and non-autistic children—with a comparison of different methodologies." Annals of clinical biochemistry 24.6 (1987): 625-634.

Badea TC, Cahill H, Ecker J, Hattar S, Nathans J. Distinct roles of transcription factors brn3a and brn3b in controlling the development, morphology, and function of retinal ganglion cells. Neuron. 2009 Mar 26;61(6):852-64. doi: 10.1016/j.neuron.2009.01.020. PMID: 19323995; PMCID: PMC2679215.

Bauman, Margaret L., and Thomas L. Kemper. "Neuroanatomic observations of the brain in autism: a review and future directions." International journal of developmental neuroscience 23.2-3 (2005): 183-187.

Bauman, M. D.; Toscano, J. E.; Babineau, B. A.; Mason, W. A.; Amaral, D. G. (2008). Emergence of stereotypies in juvenile monkeys (Macaca mulatta) with neonatal amygdala or hippocampus lesions.. Behavioral Neuroscience, 122(5), 1005–1015. doi:10.1037/a0012600

Bertoni, Alessandra, et al., "Oxytocin administration in neonates shapes hippocampal circuitry and restores social behavior in a mouse model of autism." Molecular Psychiatry (2021): 1-14.

Behrmann, Marlene, and Nancy J. Minshew. "Sensory processing in autism." Autism spectrum disorders. Vol. 180. Karger Publishers, 2015. 54-67.

Bey AL, Jiang YH. Overview of mouse models of autism spectrum disorders. Curr Protoc Pharmacol. 2014 Sep 2;66:5.66.1-26. doi: 10.1002/0471141755.ph0566s66. PMID: 25181011; PMCID: PMC4186887.

Bleuler E. Freud, Psychoanalytic Remarks on an Autobiographically Described Case of Paranoia (Dementia paranoides). Central Journal for Psychoanalysis. 1912; 2 343-348

Bozek K, Relo´gio A, Kielbasa SM, et al., (2009). Regulation of clock-controlled genes in mammals. PLoS ONE, 4, e4882.

Breece, E., Paciotti, B., Nordahl, C. W., Ozonoff, S., Van de Water, J. A., Rogers, S. J., Amaral, D., & Ashwood, P. (2013). Myeloid dendritic cells frequencies are increased in children with autism spectrum disorder and associated with amygdala volume and repetitive behaviors. Brain, Behavior, and Immunity, 31, 69–75

Brumback, Audrey C., et al., "Identifying specific prefrontal neurons that contribute to autism-associated abnormalities in physiology and social behavior." Molecular psychiatry 23.10 (2018): 2078-2089.

BÜNNING, E. R. W. I. N. "Common features of photoperiodism in plants and animals." Photochemistry and Photobiology 9.3 (1969): 219-228.

Callaway, Ewen. "Fathers bequeath more mutations as they age." Nature 488.7412 (2012): 439.

Cai, Yulong, et al., "Liver X receptor β regulates the development of the dentate gyrus and autistic-like behavior in the mouse." Proceedings of the National Academy of Sciences 115.12 (2018): E2725-E2733.

Cardinali DP, Brusco LI, Cutrera RA, Castrillón P, Esquifino AI. Melatonin as a time-meaningful signal in circadian organization of immune response. Biol Signals Recept. 1999 Jan-Apr;8(1-2):41-8. doi: 10.1159/000014567. PMID: 10085461.

Centers for Disease Control and Prevention. "Prevalence of autism spectrum disorders--autism and developmental disabilities monitoring network, 14 sites, United States, 2002." Morbidity and mortality weekly report. Surveillance summaries (Washington, DC: 2002) 56.1 (2007): 12-28.

Chen SK, Badea TC, Hattar S. Photoentrainment and pupillary light reflex are mediated by distinct populations of ipRGCs. Nature. 2011 Jul 17;476(7358):92-5. doi: 10.1038/nature10206. PMID: 21765429; PMCID: PMC3150726.

Cho Y, Ryu SH, Lee BR, Kim KH, Lee E, Choi J. Effects of artificial light at night on human health: A literature review of observational and experimental studies applied to exposure assessment. Chronobiol Int. 2015;32(9):1294-310. doi: 10.3109/07420528.2015.1073158. Epub 2015 Sep 16. PMID: 26375320.

Cipriani A, Reid K, Young AH, Macritchie K, Geddes J. Valproic acid, valproate and divalproex in the maintenance treatment of bipolar disorder. Cochrane Database Syst Rev. 2013 Oct 17;2013(10):CD003196. doi: 10.1002/14651858.CD003196.pub2. PMID: 24132760; PMCID: PMC6599863.

Crespi B., Badcock C. Psychosis and autism as diametrical disorders of the social brain. Behav. Brain Sci.

de Mairan, J. Observation botanique (Histoire de l'Academie des Sciences, Paris, 1729)

DeStefano F, Shimabukuro TT. The MMR Vaccine and Autism. Annu Rev Virol. 2019 Sep 29;6(1):585-600. doi: 10.1146/annurev-virology-092818-015515. Epub 2019 Apr 15. PMID: 30986133; PMCID: PMC6768751.

Dunbar, Robin IM. "The social brain hypothesis and its implications for social evolution." Annals of human biology 36.5 (2009): 562-572.

Dziobek, Isabel, et al., "The ‘amygdala theory of autism’revisited: linking structure to behavior." Neuropsychologia 44.10 (2006): 1891-1899.

Do MTH. Melanopsin and the Intrinsically Photosensitive Retinal Ganglion Cells: Biophysics to Behavior. Neuron. 2019 Oct 23;104(2):205-226. doi: 10.1016/j.neuron.2019.07.016. PMID: 31647894; PMCID: PMC6944442.

Ebisawa, Takashi. "Circadian rhythms in the CNS and peripheral clock disorders: human sleep disorders and clock genes." Journal of pharmacological sciences 103.2 (2007): 150-154.

Espino J, Rodríguez AB, Pariente JA. Melatonin and Oxidative Stress in the Diabetic State: Clinical Implications and Potential Therapeutic Applications. Curr Med Chem. 2019;26(22):4178-4190. doi: 10.2174/0929867325666180410094149. PMID: 29637854.

Faraut B, Bayon V, Léger D. Neuroendocrine, immune and oxidative stress in shift workers. Sleep Med Rev. 2013 Dec;17(6):433-44. doi: 10.1016/j.smrv.2012.12.006. Epub 2013 Apr 22. PMID: 23618533.

Felix-Ortiz, Ada C., and Kay M. Tye. "Amygdala inputs to the ventral hippocampus bidirectionally modulate social behavior." Journal of Neuroscience 34.2 (2014): 586-595.

Felix-Ortiz, Ada C., et al., "Bidirectional modulation of anxiety-related and social behaviors by amygdala projections to the medial prefrontal cortex." Neuroscience 321 (2016): 197-209.

Fernandez DC, Fogerson PM, Lazzerini Ospri L, Thomsen MB, Layne RM, Severin D, Zhan J, Singer JH, Kirkwood A, Zhao H, Berson DM, Hattar S. Light Affects Mood and Learning through Distinct Retina-Brain Pathways. Cell. 2018 Sep 20;175(1):71-84.e18. doi: 10.1016/j.cell.2018.08.004. Epub 2018 Aug 30. PMID: 30173913; PMCID: PMC6190605.

Finnell RH, Caiaffa CD, Kim SE, Lei Y, Steele J, Cao X, Tukeman G, Lin YL, Cabrera RM, Wlodarczyk BJ. Gene Environment Interactions in the Etiology of Neural Tube Defects. Front Genet. 2021 May 10;12:659612. doi: 10.3389/fgene.2021.659612. PMID: 34040637; PMCID: PMC8143787.

Fu, Yingbin, et al., "Intrinsically photosensitive retinal ganglion cells detect light with a vitamin A-based photopigment, melanopsin." Proceedings of the National Academy of Sciences 102.29 (2005): 10339-10344.

Hoffman AE, Zheng T, Stevens RG, et al., (2009). Clock-cancer connection in non-Hodgkin's lymphoma: a genetic association study and pathway analysis of the circadian gene cryptochrome 2. Cancer Res, 69, 3605–13.

Horie K, Inoue K, Suzuki S, Adachi S, Yada S, Hirayama T, Hidema S, Young LJ, Nishimori K. Oxytocin receptor knockout prairie voles generated by CRISPR/Cas9 editing show reduced preference for social novelty and exaggerated repetitive behaviors. Horm Behav. 2019 May;111:60-69. doi: 10.1016/j.yhbeh.2018.10.011. Epub 2018 Nov 8. PMID: 30713102; PMCID: PMC6506400.

Gagnon K, Bolduc C, Bastien L, Godbout R. REM Sleep EEG Activity and Clinical Correlates in Adults With Autism. Front Psychiatry. 2021 Jun 8;12:659006. doi: 10.3389/fpsyt.2021.659006. PMID: 34168578; PMCID: PMC8217632.

Galano A, Reiter RJ. Melatonin and its metabolites vs oxidative stress: From individual actions to collective protection. J Pineal Res. 2018 Aug;65(1):e12514. doi: 10.1111/jpi.12514. PMID: 29888508.

Gery, Sigal, and H. Philip Koeffler. "Circadian rhythms and cancer." Cell cycle 9.6 (2010): 1097-1103.

Gilby KL. A new rat model for vulnerability to epilepsy and autism spectrum disorders. Epilepsia. 2008 Nov;49 Suppl 8:108-10. doi: 10.1111/j.1528-1167.2008.01851.x. PMID: 19049604.

Gillberg, Christopher. "Lorna Wing OBE, MD, FRCPsych: Formerly psychiatrist and physician, Social Psychiatry Unit, Institute of Psychiatry, King's College London, co-founder of the UK National Autistic Society." BJPsych Bulletin 39.1 (2015): 52-53.

Golombek, Diego A., et al., "Neurochemistry of mammalian entrainment: Signal transduction pathways in the suprachiasmatic nuclei." Biological Rhythm Research 31.1 (2000): 56-70.

Gordon, Aaron, et al., "Caspr and caspr2 are required for both radial and longitudinal organization of myelinated axons." Journal of Neuroscience 34.45 (2014): 14820-14826.

Gordon, Aaron, et al., "Expression of Cntnap2 (Caspr2) in multiple levels of sensory systems." Molecular and Cellular Neuroscience 70 (2016): 42-53.

Grandgeorge M, Dubois E, Alavi Z, Bourreau Y, Hausberger M. Do Animals Perceive Human Developmental Disabilities? Guinea Pigs' Behaviour with Children with Autism Spectrum Disorders and Children with Typical Development. A Pilot Study. Animals (Basel). 2019 Aug 2;9(8):522. doi: 10.3390/ani9080522. PMID: 31382429; PMCID: PMC6719160.

Guariglia, Sara Rose, and Kathryn K. Chadman. "Water T-maze: a useful assay for determination of repetitive behaviors in mice." Journal of neuroscience methods 220.1 (2013): 24-29.

Golombek, Diego A., et al., "Neurochemistry of mammalian entrainment: Signal transduction pathways in the suprachiasmatic nuclei." Biological Rhythm Research 31.1

(2000): 56-70.

Golombek, Diego A., et al., "The times they're a-changing: effects of circadian desynchronization on physiology and disease." Journal of Physiology-Paris 107.4 (2013): 310-322.

Hardeland R. Melatonin and inflammation-Story of a double-edged blade. J Pineal Res. 2018 Nov;65(4):e12525. doi: 10.1111/jpi.12525. Epub 2018 Oct 12. PMID: 30242884.

Harms E, Young MW, Saez L. CK1 and GSK3 in the Drosophila and mammalian circadian clock. Novartis Found Symp. 2003;253:267-77; discussion 102-9, 277-84.

PMID: 14712927.

Hitti, Frederick L., and Steven A. Siegelbaum. "The hippocampal CA2 region is essential for social memory." Nature 508.7494 (2014): 88-92.

Hoffman, K. "Animal models for studying obsessive-compulsive and related disorders." Modeling Neuropsychiatric Disorders in Laboratory Animals (2016): 161-241.

Hong, Weizhe, Dong-Wook Kim, and David J. Anderson. "Antagonistic control of social versus repetitive self-grooming behaviors by separable amygdala neuronal subsets." Cell 158.6 (2014): 1348-1361.

Ikeno T, Yan L. Chronic Light Exposure in the Middle of the Night Disturbs the Circadian System and Emotional Regulation. J Biol Rhythms. 2016 Aug;31(4):352-64. doi: 10.1177/0748730416642065. Epub 2016 Apr 13. PMID: 27075857.

Inokawa H, Umemura Y, Shimba A, Kawakami E, Koike N, Tsuchiya Y, Ohashi M, Minami Y, Cui G, Asahi T, Ono R, Sasawaki Y, Konishi E, Yoo SH, Chen Z, Teramukai S, Ikuta K, Yagita K. Chronic circadian misalignment accelerates immune senescence and abbreviates lifespan in mice. Sci Rep. 2020 Feb 13;10(1):2569. doi: 10.1038/s41598-020-59541-y. PMID: 32054990; PMCID: PMC7018741.

Jniene A, Errguig L, El Hangouche AJ, Rkain H, Aboudrar S, El Ftouh M, Dakka T. Perception of Sleep Disturbances due to Bedtime Use of Blue Light-Emitting Devices and Its Impact on Habits and Sleep Quality among Young Medical Students. Biomed Res Int. 2019 Dec 24;2019:7012350. doi: 10.1155/2019/7012350. PMID: 31950050; PMCID: PMC6944959.

Jones, Jeff R., et al., "Circadian neurons in the paraventricular nucleus entrain and sustain daily rhythms in glucocorticoids." Nature communications 12.1 (2021): 1-15.

Jones, Stephanie G., and Ruth M. Benca. "Circadian disruption in psychiatric disorders." Sleep medicine clinics 10.4 (2015): 481-493.

Jurgensen, Sofia, and Pablo E. Castillo. "Selective dysregulation of hippocampal inhibition in the mouse lacking autism candidate gene CNTNAP2." Journal of Neuroscience 35.43 (2015): 14681-14687.

Kalsbeek A, van der Spek R, Lei J, Endert E, Buijs RM, Fliers E. Circadian rhythms in the hypothalamo-pituitary-adrenal (HPA) axis. Mol Cell Endocrinol. 2012 Feb 5;349(1):20-9. doi: 10.1016/j.mce.2011.06.042. Epub 2011 Jul 18. PMID: 21782883.

Kanner, Leo. "Autistic disturbances of affective contact." Nervous child 2.3 (1943): 217-250.

Kennedy, D.P. and Adolphs, R. (2014) Violations of personal space by individuals with autism spectrum disorder. PLoS One 9, e103369

Kim, Il Hwan, et al., "Spine pruning drives antipsychotic-sensitive locomotion via circuit control of striatal dopamine." Nature neuroscience 18.6 (2015): 883-891.

Kondratov, Roman V., et al., "BMAL1-dependent circadian oscillation of nuclear CLOCK: posttranslational events induced by dimerization of transcriptional activators of the mammalian clock system." Genes & development 17.15 (2003): 1921-1932.

Labrecque N, Cermakian N. Circadian Clocks in the Immune System. J Biol Rhythms.

2015 Aug;30(4):277-90. doi: 10.1177/0748730415577723. Epub 2015 Apr 20. PMID: 25900041.

Lawrence, Y. A., et al., "Parvalbumin-, calbindin-, and calretinin-immunoreactive hippocampal interneuron density in autism." Acta Neurologica Scandinavica 121.2 (2010): 99-108.

Lazaro, Maria T., et al., "Reduced prefrontal synaptic connectivity and disturbed oscillatory population dynamics in the CNTNAP2 model of autism." Cell reports 27.9 (2019): 2567-2578.

Leader G, Barrett A, Ferrari C, Casburn M, Maher L, Naughton K, Arndt S, Mannion A. Quality of life, gastrointestinal symptoms, sleep problems, social support, and social functioning in adults with autism spectrum disorder. Res Dev Disabil. 2021 May;112:103915. doi: 10.1016/j.ridd.2021.103915. Epub 2021 Mar 4. PMID: 33676088.

Lehoux T, Carrier J, Godbout R. NREM sleep EEG slow waves in autistic and typically developing children: Morphological characteristics and scalp distribution. J Sleep Res. 2019 Aug;28(4):e12775. doi: 10.1111/jsr.12775. Epub 2018 Oct 12. PMID: 30311707.

Liu CX, Li CY, Hu CC, Wang Y, Lin J, Jiang YH, Li Q, Xu X. CRISPR/Cas9-induced shank3b mutant zebrafish display autism-like behaviors. Mol Autism. 2018 Apr 2;9:23. doi: 10.1186/s13229-018-0204-x. PMID: 29619162; PMCID: PMC5879542.

Luik, Annemarie I., et al., "Stability and fragmentation of the activity rhythm across the sleep-wake cycle: the importance of age, lifestyle, and mental health." Chronobiology international 30.10 (2013): 1223-1230.

Mahmood, Usman, et al., "Dendritic spine anomalies and PTEN alterations in a mouse model of VPA-induced autism spectrum disorder." Pharmacological research 128 (2018): 110-121.

Maenner, Matthew J., Kelly A. Shaw, and Jon Baio. "Prevalence of autism spectrum

disorder among children aged 8 years—autism and developmental disabilities monitoring network, 11 sites, United States, 2016." MMWR Surveillance Summaries 69.4 (2020): 1.

Maenner, Matthew J., et al., "Prevalence and characteristics of autism spectrum disorder among children aged 8 years—autism and developmental disabilities monitoring network, 11 sites, United States, 2018." MMWR Surveillance Summaries 70.11 (2021):1.

Mendoza-Viveros, Lucia, et al., "Molecular modulators of the circadian clock: lessons from flies and mice." Cellular and Molecular Life Sciences 74.6 (2017): 1035-1059.

McDonald AJ, Mascagni F, Guo L (1996): Projections of the medial and lateral prefrontal cortices to the amygdala: A Phaseolus vulgaris leucoagglutinin study in the rat.

Neuroscience 71:55–75.

McNeill IV, John K., James C. Walton, and H. Elliott Albers. "Functional significance of the excitatory effects of GABA in the suprachiasmatic nucleus." Journal of biological rhythms 33.4 (2018): 376-387.

Miano S, Bruni O, Elia M, Trovato A, Smerieri A, Verrillo E, Roccella M, Terzano MG, Ferri R. Sleep in children with autistic spectrum disorder: a questionnaire and polysomnographic study. Sleep Med. 2007 Dec;9(1):64-70. doi: 10.1016/j.sleep.2007.01.014. Epub 2007 Aug 28. PMID: 17728182.

Michel, Stephan, et al., "Regulation of glutamatergic signalling by PACAP in the mammalian suprachiasmatic nucleus." BMC neuroscience 7.1 (2006): 1-11.

Moldavan MG, Sollars PJ, Lasarev MR, Allen CN, Pickard GE. Circadian Behavioral Responses to Light and Optic Chiasm-Evoked Glutamatergic EPSCs in the Suprachiasmatic Nucleus of ipRGC Conditional vGlut2 Knock-Out Mice. eNeuro. 2018 May 10;5(3):ENEURO.0411-17.2018. doi: 10.1523/ENEURO.0411-17.2018. PMID: 29756029; PMCID: PMC5944003.

Morency MA, Stewart RJ, Beninger RJ. Effects of unilateral microinjections of sulpiride into the medial prefrontal cortex on circling behavior of rats. Prog Neuropsychopharmacol Biol Psychiatry. 1985;9(5–6):735–8. doi:10.1016/0278-5846(85)90051-X.

Murugan, Malavika, et al., "Combined social and spatial coding in a descending projection from the prefrontal cortex." *Cell* 171.7 (2017): 1663-1677.

Nagai N, Ayaki M, Yanagawa T, Hattori A, Negishi K, Mori T, Nakamura TJ, Tsubota K. Suppression of Blue Light at Night Ameliorates Metabolic Abnormalities by Controlling Circadian Rhythms. Invest Ophthalmol Vis Sci. 2019 Sep 3;60(12):3786-3793. doi: 10.1167/iovs.19-27195. PMID: 31504080.

Nakamura, Takahiro J., et al., "Age-related decline in circadian output." Journal of Neuroscience 31.28 (2011): 10201-10205.

Okuliarova M, Mazgutova N, Majzunova M, Rumanova VS, Zeman M. Dim Light at Night Impairs Daily Variation of Circulating Immune Cells and Renal Immune Homeostasis. Front Immunol. 2021 Jan 22;11:614960. doi: 10.3389/fimmu.2020.614960. PMID: 33552079; PMCID: PMC7862740.

Omer, D.B. et al., (2018) Social place-cells in the bat hippocampus. Science 359, 218 – 224

Østergaard J, Hannibal J, Fahrenkrug J. Synaptic contact between melanopsin-containing retinal ganglion cells and rod bipolar cells. Invest Ophthalmol Vis Sci. 2007 Aug;48(8):3812-20. doi: 10.1167/iovs.06-1322. PMID: 17652756.

Patton AP, Hastings MH. The suprachiasmatic nucleus. Curr Biol. 2018 Aug 6;28(15):R816- R822. doi: 10.1016/j.cub.2018.06.052. PMID: 30086310.

Park, Gaeun, et al., "Decreased in vivo glutamate/GABA ratio correlates with the social behavior deficit in a mouse model of autism spectrum disorder." Molecular brain 15.1 (2022): 1-12.

Paterno, Rosalia, et al., "Hippocampal gamma and sharp-wave ripple oscillations are altered in a Cntnap2 mouse model of autism spectrum disorder." Cell reports 37.6 (2021): 109970.

Patton AP, Hastings MH. The suprachiasmatic nucleus. Curr Biol. 2018 Aug 6;28(15):R816- R822. doi: 10.1016/j.cub.2018.06.052. PMID: 30086310.

Pitskel, N. B., et al., "Neural systems for cognitive reappraisal in children and adolescents with autism spectrum disorder. Dev. Cogn. Neurosci. 10, 117–128." (2014).

Peñagarikano, Olga, et al., "Exogenous and evoked oxytocin restores social behavior in the Cntnap2 mouse model of autism." Science translational medicine 7.271 (2015): 271ra8-271ra8.

Pittendrigh, CS, Minis, DH (1964) The entrainment of circadian oscillations by light and their role as photoperiodic clocks. Am Nat 98(902):261-294

Phillips, Mary L., Holly Anne Robinson, and Lucas Pozzo-Miller. "Ventral hippocampal projections to the medial prefrontal cortex regulate social memory." Elife 8 (2019): e44182.

Prosser, Rebecca A. "Glutamate blocks serotonergic phase advances of the mammalian circadian pacemaker through AMPA and NMDA receptors." Journal of Neuroscience 21.19 (2001): 7815-7822.

Provencio, Ignacio, et al., "Melanopsin: An opsin in melanophores, brain, and eye." Proceedings of the National Academy of Sciences 95.1 (1998): 340-345.

Quattrochi, Lauren E., et al., "The M6 cell: A small-field bistratified photosensitive retinal ganglion cell." Journal of Comparative Neurology 527.1 (2019): 297-311.

Rahman M, Nguyen H. Valproic Acid. 2021 Oct 11. In: StatPearls [Internet]. Treasure Island (FL): StatPearls Publishing; 2022 Jan–. PMID: 32644538.

Raymond, G. "The hippocampus in autism: Golgi analysis." Ann. Neurol. 26 (1989): 483-484.

Rao, Maria Luise, et al., "Circadian rhythm of tryptophan, serotonin, melatonin, and pituitary hormones in schizophrenia." Biological Psychiatry 35.3 (1994): 151-163.

Reddy, Sujana, Vamsi Reddy, and Sandeep Sharma. "Physiology, circadian rhythm." (2018).

Reyes, Bryan A., Julie S. Pendergast, and Shin Yamazaki. "Mammalian peripheral circadian oscillators are temperature compensated." Journal of biological rhythms 23.1 (2008): 95-98.

Rijo-Ferreira, Filipa, and Joseph S. Takahashi. "Genomics of circadian rhythms in health and disease." Genome medicine 11.1 (2019): 1-16.

Robinson, I., and A. B. Reddy. "Molecular mechanisms of the circadian clockwork in mammals." FEBS letters 588.15 (2014): 2477-2483.

Rochette AC, Soulières I, Berthiaume C, Godbout R. NREM sleep EEG activity and procedural memory: A comparison between young neurotypical and autistic adults without sleep complaints. Autism Res. 2018 Apr;11(4):613-623. doi: 10.1002/aur.1933. Epub 2018 Jan 30. PMID: 29381247.

Rojas, Donald C., et al., "Hippocampus and amygdala volumes in parents of children with autistic disorder." American Journal of Psychiatry 161.11 (2004): 2038-2044.

Ruby, Norman F., D. Erik Burns, and H. Craig Heller. "Circadian rhythms in the suprachiasmatic nucleus are temperature-compensated and phase-shifted by heat pulses in vitro." Journal of Neuroscience 19.19 (1999): 8630-8636.

Russart KLG, Nelson RJ. Light at night as an environmental endocrine disruptor. Physiol Behav. 2018 Jun 1;190:82-89. doi: 10.1016/j.physbeh.2017.08.029. Epub 2017 Sep 7. PMID: 28870443; PMCID: PMC5839924.

Selimbeyoglu, Aslihan, et al., "Modulation of prefrontal cortex excitation/inhibition balance rescues social behavior in CNTNAP2-deficient mice." Science translational medicine 9.401 (2017): eaah6733.

Schumann, Cynthia Mills, and David G. Amaral. "Stereological analysis of amygdala neuron number in autism." Journal of Neuroscience 26.29 (2006): 7674-7679.

Schroeder AM, Colwell CS. How to fix a broken clock. Trends Pharmacol Sci. 2013 Nov;34(11):605-19. doi: 10.1016/j.tips.2013.09.002. Epub 2013 Oct 10. PMID: 24120229; PMCID: PMC3856231.

Selimbeyoglu, Aslihan, et al., "Modulation of prefrontal cortex excitation/inhibition balance rescues social behavior in CNTNAP2-deficient mice." Science translational medicine 9.401 (2017): eaah6733.

Shen, Mark D., et al., "Subcortical Brain Development in Autism and Fragile X Syndrome: Evidence for Dynamic, Age-and Disorder-Specific Trajectories in Infancy." American Journal of Psychiatry (2022): appi-ajp.

Shekel, Itay, et al., "Isolation-Induced Ultrasonic Vocalization in Environmental and Genetic Mice Models of Autism." Frontiers in Neuroscience 15 (2021).

Smith, Tristram, and Svein Eikeseth. "O. Ivar Lovaas: Pioneer of applied behavior analysis and intervention for children with autism." Journal of autism and developmental disorders 41.3 (2011): 375-378.

Swartz, Johnna R., et al., "Amygdala habituation and prefrontal functional connectivity in youth with autism spectrum disorders." Journal of the American Academy of Child & Adolescent Psychiatry 52.1 (2013): 84-93.

Sun, Tingting, et al., "Basolateral amygdala input to the medial prefrontal cortex controls obsessive-compulsive disorder-like checking behavior." Proceedings of the National Academy of Sciences 116.9 (2019): 3799-3804.

Stefanacci L, Amaral DG (2002): Some observations on cortical inputs to the macaque monkey amygdala: an anterograde tracing study. J Comp Neurol 451:301–323

Touitou Y, Reinberg A, Touitou D. Association between light at night, melatonin secretion,

sleep deprivation, and the internal clock: Health impacts and mechanisms of circadian disruption. Life Sci. 2017 Mar 15;173:94-106. doi: 10.1016/j.lfs.2017.02.008. Epub 2017 Feb 16. PMID: 28214594.

Taufique ST, Prabhat A, Kumar V. Light at night affects hippocampal and nidopallial cytoarchitecture: Implication for impairment of brain function in diurnal corvids. J Exp Zool A Ecol Integr Physiol. 2019 Feb;331(2):149-156. doi: 10.1002/jez.2238. Epub 2018 Oct 4. PMID: 30288960.

Taleb A, Lin W, Xu X, Zhang G, Zhou QG, Naveed M, Meng F, Fukunaga K, Han F. Emerging mechanisms of valproic acid-induced neurotoxic events in autism and its implications for pharmacological treatment. Biomed Pharmacother. 2021 May;137:111322. doi: 10.1016/j.biopha.2021.111322. Epub 2021 Feb 16. PMID: 33761592.

Tordjman S, Anderson GM, Kermarrec S, Bonnot O, Geoffray MM, Brailly-Tabard S, Chaouch A, Colliot I, Trabado S, Bronsard G, Coulon N, Botbol M, Charbuy H, Camus F, Touitou Y. Altered circadian patterns of salivary cortisol in low-functioning children and adolescents with autism. Psychoneuroendocrinology. 2014 Dec;50:227-45. doi: 10.1016/j.psyneuen.2014.08.010. Epub 2014 Aug 27. PMID: 25244637.

Trinkler, I. et al., (2009) Neural bases of autobiographical support for episodic recollection of faces. Hippocampus 19, 718 – 730

Tzakis, N. and Holahan, M.R. (2019) Social memory and the role of the hippocampal CA2 region. Front. Behav. Neurosci. 13, 233

Ueoka I, Pham HTN, Matsumoto K, Yamaguchi M. Autism Spectrum Disorder-Related Syndromes: Modeling with Drosophila and Rodents. Int J Mol Sci. 2019 Aug 21;20(17):4071. doi: 10.3390/ijms20174071. Erratum in: Int J Mol Sci. 2020 Oct 30;21(21): PMID: 31438473; PMCID: PMC6747505.

Valdez, Pablo, Candelaria Ramírez, and Aída García. "Circadian rhythms in cognitive performance: implications for neuropsychological assessment." Chronophysiology and therapy 2.81 (2012): 12.

Van Der Horst, Gijsbertus TJ, et al., "Mammalian Cry1 and Cry2 are essential for maintenance of circadian rhythms." Nature 398.6728 (1999): 627-630.

Varea, Olga, et al., "Synaptic abnormalities and cytoplasmic glutamate receptor aggregates in contactin associated protein-like 2/Caspr2 knockout neurons." Proceedings of the National Academy of Sciences 112.19 (2015): 6176-6181.

Vishwas DK, Haldar C. Photoperiodic induced melatonin regulates immunity and expression pattern of melatonin receptor MT1 in spleen and bone marrow mononuclear cells of male golden hamster. J Photochem Photobiol B. 2013 Nov 5;128:107-14. doi: 10.1016/j.jphotobiol.2013.08.018. Epub 2013 Sep 11. PMID: 24090924.

von dem Hagen, Elisabeth AH, et al., "Reduced functional connectivity within and between 'social'resting state networks in autism spectrum conditions." Social cognitive and affective neuroscience 8.6 (2013): 694-701.

Vuilleumier, Patrik. "How brains beware: neural mechanisms of emotional attention." Trends in cognitive sciences 9.12 (2005): 585-594.

Wang, Ruanna, et al., "Aberrant development and synaptic transmission of cerebellar cortex in a VPA induced mouse autism model." Frontiers in cellular neuroscience (2018): 500.

Williams, Diane L., Gerald Goldstein, and Nancy J. Minshew. "Impaired memory for faces and social scenes in autism: Clinical implications of memory dysfunction." Archives of clinical neuropsychology 20.1 (2005): 1-15.

Wöhr, Markus, et al., "Communication impairments in mice lacking Shank1: reduced levels of ultrasonic vocalizations and scent marking behavior." PloS one 6.6 (2011): e20631.

Yang, Eun-Jeong, et al., "Early behavioral abnormalities and perinatal alterations of PTEN/AKT pathway in valproic acid autism model mice." PloS one 11.4 (2016): e0153298.

Yoshizaki, Kaichi, et al., "Paternal aging affects behavior in Pax6 mutant mice: a gene/environment interaction in understanding neurodevelopmental disorders." PloS one 11.11 (2016): e0166665.

Wright KP Jr, Drake AL, Frey DJ, Fleshner M, Desouza CA, Gronfier C, Czeisler CA. Influence of sleep deprivation and circadian misalignment on cortisol, inflammatory markers, and cytokine balance. Brain Behav Immun. 2015 Jul;47:24-34. doi: 10.1016/j.bbi.2015.01.004. Epub 2015 Jan 29. PMID: 25640603; PMCID: PMC5401766.

Wulff, Katharina, et al., "Sleep and circadian rhythm disruption in psychiatric and neurodegenerative disease." Nature Reviews Neuroscience 11.8 (2010): 589-599.

Xing, Xiaoliang, et al., "Suppression of Akt-mTOR pathway rescued the social behavior in Cntnap2-deficient mice." Scientific reports 9.1 (2019): 1-9.

Yenen AS, Çak HT. Melatonin and Circadian Rhythm in Autism Spectrum Disorders. Turk Psikiyatri Derg. 2020 Fall;31(3):201-211. English, Turkish. doi: 10.5080/u25160. PMID: 32978956.

Yizhar, Ofer. "Optogenetic insights into social behavior function." Biological psychiatry 71.12 (2012): 1075-1080.

Yuwiler, Arthur, et al., "Examination of circadian rhythmicity of blood serotonin and platelets in autistic and non-autistic children." Journal of autism and childhood schizophrenia 1.4 (1971): 421-435.

Zhao H, Jiang YH, Zhang YQ. Modeling autism in non-human primates: Opportunities and challenges. Autism Res. 2018 May;11(5):686-694. doi: 10.1002/aur.1945. Epub 2018 Mar 23. PMID: 29573234; PMCID: PMC6188783.

Zhang, Ray, et al., "A circadian gene expression atlas in mammals: implications for biology and medicine." Proceedings of the National Academy of Sciences 111.45 (2014): 16219-16224.

Zink CF, Stein JL, Kempf L, Hakimi S, Meyer-Lindenberg A (2010): Vasopressin modulates medial prefrontal cortex-amygdala circuitry during emotion processing in humans. J Neurosci 30:7017–7022.

Chapter 2

Chapter 2

Melatonin treatment of repetitive behavioral deficits in the *Cntnap2* mouse model of autism spectrum disorder.

Abstract

Nighttime light pollution is linked to metabolic and cognitive dysfunction. Many patients with autism spectrum disorders (ASD) show disturbances in their sleep/wake cycle, and may be particularly vulnerable to the impact of circadian disruptors. In this study, we examined the impact of exposure to dim light at night (DLaN, 5 lux) in a model of ASD: the contactin associated protein-like 2 knock out (*Cntnap2* KO) mice. DLaN was sufficient to disrupt locomotor activity rhythms, exacerbate the excessive grooming and diminish the social preference in *Cntnap2* mutant mice. On a molecular level, DLaN altered the phase and amplitude of PER2::LUC rhythms in a tissue-specific manner *in vitro.* Daily treatment with melatonin reduced the excessive grooming of the mutant mice to wild-type levels and improved activity rhythms. Our findings suggest that common circadian disruptors such as light at night should be considered in the management of ASD.

Introduction

There is a growing concern that nighttime light pollution may be negatively impacting human health, as much of the world's urban populations do not experience true night due to the widespread use of artificial lighting (Falchi et al., 2016). Previous studies have shown that night time light exposure leads to cognitive, skeletal motor, and metabolic dysfunction in laboratory animals (Bedrosian et al., 2016; Bedrosian et al., 2011; Borniger et al., 2014; Fonken et al., 2013a; Fonken et al., 2012; Fonken & Nelson, 2011; Lucassen et al., 2016; Walker et al., 2019). The deleterious effects of night time light pollution also affect animals in the wild (Dominoni et al., 2013; Raap et al., 2015; Stevenson et al., 2015). Despite all of the social and economic benefits of artificial lighting, we may be paying a price for inappropriate light exposure (Czeisler, 2013; Roenneberg & Merrow, 2016; Rybnikova et al., 2016). One of the major factors leading to disrupted sleep is an inappropriate photic environment caused by nighttime exposure to electric lights and light-emitting devices as well as diminished exposure to daylight while indoors.

A significant proportion of individuals with neurodevelopmental disorders such as autism spectrum disorders (ASD) experience disruptions to their daily sleep/wake cycles. Among the most common complaints is delayed bedtime with frequent nocturnal awakenings (Devnani & Hegde, 2015; Elrod & Hood, 2015; Mazurek & Sohl, 2016; Robinson-Shelton & Malow, 2016; Veatch et al., 2015). Perhaps because of this disrupted temporal pattern of sleep, these patients are exposed to more light via electronic screens during the night (Engelhardt et al., 2013; Mazurek et al., 2016). This nocturnal light exposure by itself has been shown to delay sleep in healthy young people (Chang et al., 2015; Gronli et al., 2016; Wood et al., 2013). Melatonin as well as conventional sleeping aids are commonly used as counter-measures to help sleep onset in patients with neurodevelopmental disorders (Goldman et al., 2014; Kawabe et al., 2014; Malow et al., 2012; Rossignol & Frye, 2014; Schwichtenberg & Malow, 2015). Animal models are helpful to better understand the mechanisms underlying

circadian and sleep disorders as well as in developing strategies for disease management focused on restoring the sleep/wake cycle.

In this study, we set out to test the possibility that mice with a genetic risk factor associated with ASD are more vulnerable to the detrimental effects of nighttime light exposure. Rare and common variants of the contactin associated protein-like 2 *(Cntnap2)* gene are associated with ASD, intellectual disabilities, and seizures in patients (Arking et al., 2008; Bakkaloglu et al., 2008; Nord et al., 2011; O'Roak et al., 2011; Strauss et al., 2006) as well as in mouse models (Penagarikano et al., 2011; Poliak et al., 1999). We examined the impact of nighttime light exposure by housing the mutant animals and their wild-type (WT) controls under conditions that mimic experiencing very dim LED-generated light in the bedroom at night. We describe the deleterious effect of dim light at night (DLaN) on daily rhythms of activity, sleep, and on the molecular circadian clock as measured by PERIOD2-driven bioluminescence. In addition, we examined the impact of DLaN on repetitive behavior and sociability in *Cntnap2* mutant mice and examined the persistence of the effects of DLaN after returning the mice to a normal lighting cycle. Finally, we tested the ability of melatonin to counteract the effects of DLaN on repetitive behavior and circadian disruption.

Materials and Methods

Animals

All animal procedures were performed in accordance with the UCLA animal care committee's regulations. *Cntnap2*^{tm2Pele} mutant mice backcrossed to the C57BL/6J background strain were acquired (B6.129(Cg)-*Cntnap2*^{tm2Pele}/J, https://www.jax.org/strain/017482 , (Poliak et al, 1999). *Cntnap2* null mutant (KO) and wild-type (WT) mice were obtained from heterozygous breeding pairs. Weaned mice were genotyped (TransnetYX, Cordova, TN) and group-housed prior to experimentation. We limited our studies to mice between the ages of 2 and 4 months as the circadian system is mature at this age and it is prior to the development of epilepsy in the mutant mice (Penagarikano et al, 2011). Only male animals were used in this study as it has previously been determined that the C57BL/6J strain of mice exhibit subtle sex differences in circadian rhythms of locomotor activity (Kuljis et al, 2013).

Home cage lighting manipulations

Mice were housed in light-tight ventilated cabinets in temperature- and humidity-controlled conditions, with free access to food and water. Young adult (2–3 mo old) *Cntnap2* KO and age-matched WT littermate controls were first entrained to a normal lighting cycle: 12 hr light : 12 hr dark (LD). Light intensity during the day was 300 lux as measured at the base of the cage, and 0 lux during the night. Following entrainment to normal LD, mice were singly housed under 1 of 2 lighting conditions for 2 weeks: LD, or dim light at night (DLaN, nighttime dim light 5 lux). The spectral properties of the DLaN are shown in **S. Fig. 1.1**. The melanoptic light intensity in the cage was 2.8 lux. The body weights of the mice are shown in **S. Fig. 1.3**.

Cage activity

Home cage activity (Loh et al., 2013; Wang et al., 2017) was monitored using a top-mounted passive infra-red (PIR) motion detector reporting to a VitalView data recording system (Mini Mitter, Bend, OR). Detected movements were recorded in 3 min bins, and 10 days of data were averaged for analysis using the El Temps chronobiology program (A. Diez-Noguera, Barcelona, Spain; http://www.el-temps.com/principal.html). Cage activity was determined by averaging 10 days of PIR-detected motion (movements/hr), and the relative distribution of activity during the day versus the night was determined (day activity, %). The strength of the rhythm was determined from the amplitude of the $\chi 2$ periodogram at 24 hr, to produce the rhythm power (%V) normalized to the number of data points examined. The periodogram analysis uses a $\chi 2$ test with a threshold of 0.001 significance, from which the amplitude of the periodicities is determined at the circadian harmonic to obtain the rhythm power. Precision was determined using the Clocklab program (Actimetrics, Wilmette, IL; http://actimetrics.com/products/clocklab/) by first determining the daily onset of activity over 10 days, and then determining the deviation from the best-fit line drawn through the 10 onset times. To produce the representative waveforms, hourly running averages of the same series of activity data was plotted against time of day (Zeitgeber Time, ZT, where ZT 0 indicates the time of lights-on).

Monitoring of immobility-defined sleep behavior

Immobility-defined sleep was determined as described previously (Whittaker et al., 2018). Singly housed *Cntnap2* KO and WT littermate controls (2–3 mo old) were first entrained to a normal lighting cycle (LD 12:12, 7 days). Mice were then kept in the LD or exposed to DLaN for 2 weeks prior to 2 days of measurement of sleep behavior. Mice were housed in see-through plastic cages containing bedding (without the addition of nesting material). A side-on view of each cage was obtained, with minimal occlusion by the food bin or water bottle,

both of which were top-mounted. Cages were top-lit using IR-LED lights. Video capture was accomplished using surveillance cameras with visible light filters (Gadspot Inc., City of Industry, CA) connected to a video-capture card (Adlink Technology Inc., Irvine, CA) on a Dell Optiplex computer system. ANY-maze software (Stoelting Co., Wood Dale, IL) was used for automated tracking of mouse immobility.

Immobility was registered when 95% of the area of the animal stayed immobile for more than 40 sec, as was previously determined to have 99% correlation with simultaneous EEG/EMG defined sleep (Fisher et al., 2012). Continuous tracking of the mice was performed for a minimum of 5 sleep-wake cycles, with randomized visits (1-2 times/day) by the experimenter to confirm mouse health and video recording. The 3rd and 4th sleep-wake cycles were averaged for further analysis. Immobility-defined sleep data were exported in 1 min bins, and total sleep time was determined by summing the immobility durations in the rest phase (ZT 0-12) or active phase (ZT 12-24). An average waveform of hourly immobile-sleep over the two sleep-wake cycles was produced. Variability of sleep onset and awake time was determined using Clocklab to draw the best-fit line over the sleep cycles, and the differences between sleep offset and best-fit regression of each sleep cycle were averaged.

Recordings of neurons in suprachiasmatic nucleus (SCN)

Male *Cntnap2* mutant mice and WT littermates (3-4 mo old) entrained on a 12:12 LD or DL cycle were anesthetized in an isoflurane chamber at ZT 4.5 and ZT 16.5 for ZT 6-8 and ZT 18-20 recordings respectively. Anesthetized mice were decapitated, brains extracted, and brains incubated in ice-cold slice solution for 5 minutes. Coronal slices (300μm) of mid-SCN were collected in slice solution (in mM: 26 $NaHCO_3$, 1.25 NaH_2PO_4, 10 glucose, 125 NaCl, 3 KCl, 5 $MgCl_2$, 1 $CaCl_2$) using a vibratome, and then incubated for 1hr at 34°C in artificial cerebrospinal fluid (ACSF, in mM; 26 $NaHCO_3$, 1.25 NaH_2PO4, 10 glucose, 125 NaCl, 3 KCl, 2 $MgCl_2$, 2 $CaCl_2$) while continually being aerated with 95% O2/5% CO2. Slices were placed

in a recording chamber (PH-1, Warner Instruments, Hamden, CT) attached to the stage of a fixed stage upright DIC microscope (OLYMPUS, Tokyo, Japan), and superfused continuously (2 ml/min) with ACSF aerated with 95% O_2/5% CO_2 at 34°C. Two sets of experiments were carried out to measure spontaneous firing rate (SFR) from SCN neurons. First, extracellular single-unit recordings from the SCN were taken with recording electrodes. These micropipettes (4–7 MΩ) were pulled from borosilicate tubing (Sutter Instrument) and filled with 3 M NaCl, pH 7.4. Second, cell-attached SCN recordings were made using electrode micropipettes (3-7MΩ) pulled from glass capillaries and recording electrodes were filled with ACSF. Recordings were obtained with the AXOPATCH 200B amplifier (Molecular Devices, Sunnyvale, CA) and monitored on-line with pCLAMP (Ver 10, Molecular Devices). The daytime SFR measured from WT mice was virtually identical between these two techniques (3.0 ± 0.2 Hz extracellular vs 3.0 ± 0.4 Hz cell-attached).

***In vitro* bioluminescence**

In vitro measurements of bioluminescence were performed as previously described (Whittaker et al., 2018). *Cntnap2* KO and WT PER2::LUC male mice were subjected to control LD or DLaN for 2 weeks prior to sampling. Mice were sacrificed after anesthesia (isoflurane) between ZT 10 and 11, and 1-2 mm^3 explants were immediately dissected in ice-cold Hanks' balanced salt solution (HBSS; Sigma) supplemented with 4.5 mM $NaHC0_3$, 10 mM HEPES and 100 U/ml penicillin-streptomycin. Brains were incubated in ice-cold slice solution (in mM: 26 $NaHCO_3$, 1.25 NaH_2PO_4, 10 glucose, 125 NaCl, 3 KCl, 5 MgCl2, 1 $CaCl_2$) aerated with 95% O_2 / 5% CO_2 for 5 min, and 300 µm coronal sections were collected using a vibratome and further microdissected in HBSS under a 10X dissecting microscope. The SCN was cut away from the rest of the section using two cuts with a surgical scalpel (No. 21 blade, Fisher Sci.). All explants were individually transferred to Millicell membranes (0.4 µm, PICMORG50, Millipore, Bedford, MA) resting on 1.2 ml of recording media: (1X DMEM (Sigma), 1X B27 supplement (Gibco), 4.5 mM $NaHCO_3$, 10 mM HEPES, 40 mM Glutamax (Gibco), 4.5 mg/ml

D-glucose, 25 U/ml penicillin, 25 U/ml streptomycin, 0.1 mM sodium salt monohydrate luciferin (Biosynth, Staad, Switzerland)) in a 35 mm dish sealed with autoclaved vacuum grease (Dow Corning, Midland, MI). SCN, hippocampus, and liver explants were inserted into the Lumicycle photometer (Actimetrics, Wilmette, IL), incubated at 37 ºC, and bioluminescence was continuously monitored for 7 consecutive days. Raw bioluminescence values were normalized by baseline subtraction (24 hr running average) and smoothed with 2 hr windows to prepare the representative bioluminescence traces. The phase and amplitude of each explant were determined as previously described (Whitaker et al., 2018). Period was determined using the sine-wave fit function in Lumicycle Analysis (Actimetrics).

Behavioral tests

During the 14th day of LD or DLaN treatment, mice were placed in a novel arena for 10 min, and their grooming and exploration behavior was recorded. Following habituation to the arena, mice were tested using the three chamber sociability protocol (Yang et al, 2011). In this test, mice are freely mobile in an arena with three chambers where the central chamber remains empty. In each of the flanking chambers, an up-turned metal-grid pencil cup is placed: one remains empty as the novel object (O), and an age- and sex-matched WT stranger mouse (S1) is placed in the second up-turned cup. The stranger mice were previously habituated to the cups for 3 x 15 min sessions. To test for social preference, the mice were presented with the choice of the object (O) or the stranger mouse (S1). Social preference was determined by comparing the dwell time of the tested mouse in the two chambers, and a social preference index was calculated using the following: $(S1 - O)/(S1 + O)$, where a higher value indicates greater social preference. The time that the tested mouse spent investigating the object and the stranger mouse was also determined.

Grooming and investigating behaviors were manually scored and averaged post-hoc by two independent observers who were blind to the treatment and genotype conditions.

All three chamber tests were performed under dim red light (<2 lux at arena level) during the animals' night between 2 to 4 hrs after lights-off (ZT 14-16). Video recordings of each arena were captured using surveillance cameras, supplemented with infra-red lighting, connected to a video-capture card (Adlink Technology Inc., Irvine, CA) on a Dell Optiplex computer system. Automated tracking of the mice was achieved using ANY-maze software (Stoelting, Wood Dale, IL), which allowed us to determine distance travelled and chamber dwell time.

Drug treatments

WT and *Cntnap2* KO mice were randomly distributed into one of two groups and housed under DLaN conditions. One group of mice was treated daily with melatonin (3.0 mg/kg) suspended in a small amount of condensed milk (10 mg condensed milk/g body weight). The second group of mice was treated daily with the suspension vehicle (10 mg condensed milk/g body weight). Both groups were first habituated to the ceramic food bowls containing condensed milk for 3 days prior to the start of the light and drug treatment. All mice in the study learnt to find and consume the condensed milk within the food bowls within 15 min of presentation. All food bowls were weighed at 15 min post-presentation to confirm that the treatment was fully consumed throughout the duration of the drug treatment. Mice in both groups were given free access to the treatments at ZT 11.5 (30 min prior to lights off) daily from the first day of the DLaN treatment. The total treatment duration was 2 weeks to match the duration of DLaN.

Morphometrical and histoanatomical analyses of the SCN

Structural analysis of the SCN was performed as previously described (Lee et al., 2018). WT and *Cntnap2* KO mice (males, 3-4 mo) were anesthetized with isoflurane at a specific time during the night (ZT 14) and transcardially perfused with phosphate buffered saline (PBS, 0.1 M, pH 7.4) containing 4% (w/v) paraformaldehyde (PFA, Electron Microscopy Sciences, Hatfield, PA). The brains were rapidly dissected out, post-fixed overnight in 4% PFA

at 4°C, and cryoprotected in 15% sucrose. Coronal sections were obtained using a cryostat (Leica, Buffalo Grove, IL), collected sequentially and then processed for Nissl staining using cresyl violet (Sigma) or immunofluorescence. The histomorphological and stereological assessments were performed by two independent observers “masked” to the treatment and genotype.

Nissl Staining

Coronal brain sections (20-30 µm) containing the entire left and right SCN were stained with 1% cresyl violet solution (Sigma). Photographs were acquired on a Zeiss Axioskop equipped with a Zeiss colour Axiocam using a 10x objective, to include both left and right SCN, and the AxioVision software (Zeiss, Pleasanton, CA) and then, used to estimate the area, height and width of the SCN. Measurements (in µm) were obtained using the AxioVision. For each animal, the three measurements were performed in consecutive slices of the SCN. Those from the 2 most central sections (largest area), the 2 sections anterior and 3 posterior to these were summed (a total of 7 consecutive sections). No significant differences between the measurements in the left or right SCN were found so the results were averaged.

Immunofluorescence

Free-floating coronal sections (30 µm) containing the entire SCN were blocked for 1 hr at RT in carrier solution (1% BSA, 0.3% Triton X-100, PBS) containing 10% normal donkey serum and then incubated with gentle shacking for 2h at 37°C with the primary antibodies against arginine vasopressin (AVP; 1:500, guinea pig polyclonal, Peninsula Lab, San Carlos, CA) and vasoactive intestinal peptide (VIP; 1:1000, rabbit polyclonal, ImmunoStar, Hudson, WI) diluted in the carrier solution containing 5% normal donkey serum, followed by incubation in the appropriate secondary antibody conjugated to Cy3 or AlexaFluor 488 (Jackson ImmunoResearch Laboratories, Bar Harbor, ME). Sections were mounted and coverslips applied onto a drop of Vectashield mounting medium containing DAPI (4’-6-diamidino-2-

phenylinodole; Vector Laboratories, Burlingame, CA). Stereological analysis was performed using a Zeiss AxioImager M2 microscope (Zeiss, Pleasanton, CA) equipped with a motorized stage controlled by the StereoInvestigator software (MicroBrightField Biosciences, Williston, VT). Due to the SCN's small area and the low number of VIP+ and AVP+ neurons in the SCN, stereological parameters were designed to cover the entire area of interest. All immunopositive cell bodies were counted directly using a 40x objective. Images were acquired on a Zeiss AxioImager M2 microscope equipped with an AxioCam MRm and the ApoTome imaging system, using a 10x objective and the Zeiss Zen digital imaging software.

Statistics

To determine the impact of DLaN on waveform, we used a repeated measures two-way analysis of variance (ANOVA) with time and treatment as factors. To determine the impact of DLaN on other behavioral measures, we used a two-way ANOVA with genotype and treatment as factors. *Post hoc* Holm-Sidak pairwise comparisons were applied after the ANOVA. A *t*-test was used to compare Nissl measurements and cell counts in WT and *Cntnap2* KO mice. Values were reported as the mean ± standard error of the mean (SEM). Differences were deemed significant if $P < 0.05$.

Results

Nighttime light exposure alters daily rhythms of cage activity in WT and Cntnap2 KO mice.

To determine whether DLaN altered the daily rhythms in locomotor activity, separate cohorts of KO and WT mice were housed under either control conditions (LD) or DLaN for 2 weeks. We first examined the impact of DLaN on the average waveform (1 hr bins) of each genotype using a 2-way ANOVA for repeated measures (**Fig. 1.1A, B**). Both *Cntnap2* KO (*n*=10) and WT controls (*n*=10) exhibited clear rhythms in activity under both lighting conditions. The *Cntnap2* KO activity levels significantly varied with time but not treatment; while in WT mice, there were significant effects of both time and treatment. Post-hoc analysis by Multiple Comparison Procedures (Holm-Sidak method) indicated significant reductions in activity caused by DLaN exposure at a number of phases during the night in both genotypes (**Fig. 1.1A, B**). To provide another measure, DLaN equally reduced the peak/trough amplitude of the WT (63.9 ± 4.0 to 9.2 ± 1.0) and *Cntnap2 KO* (61.8 ± 7.5 to 12.0 ± 2.9). Quantitative analysis of all the activity rhythms (2-way ANOVA; **Table 1.1**) found that, under normal lighting conditions, *Cntnap2* KO mice exhibited reduced rhythm strength (**Fig. 1.1D**), increased daytime activity (**Fig. 1.1E**) and decreased precision in the daily onset of activity (**Fig. 1.1F**) compared to WT controls. DLaN significantly reduced cage activity (**Fig. 1.1C**) and rhythm power (**Fig. 1.1D**), while increasing the amount of activity during the day (**Fig. 1.1E**) and the cycle-to-cycle variation (**Fig. 1.1F**) in both genotypes. After return to the original LD cycle, both genotypes of mice exhibited partial recovery of their activity rhythms (**S. Fig. 1.4**). These results indicate that the *Cntnap2* KO mice exhibit some deficits in the generation of diurnal rhythms in cage activity and that DLaN negatively affected most of the locomotor activity parameters in both genotypes.

Nighttime light exposure alters the temporal pattern of sleep in Cntnap2 KO mice.

We sought to determine whether loss of *Cntnap2* had an impact on the amount or temporal pattern of sleep behavior measured with video recording in combination with an automated mouse tracking analysis software system (Wang et al., 2017; 2018). Both *Cntnap2* KO (*n*=10) and WT controls (*n*=10) exhibited clear rhythms in sleep under both lighting conditions (**Fig. 1.2A, B; Table 1.1**). Further analysis showed significant effects of time and treatment in the mutants while, in the WT mice, there were significant effects of time but not treatment. Post-hoc analysis by Multiple Comparison Procedures (Holm-Sidak method) revealed significant changes in sleep caused by DLaN exposure at a number of phases during the night in both genotypes (**Fig. 1.2 A, B**). Quantitative analysis of all the sleep rhythms (2-way ANOVA; **Table 1.1**) found that the total amount of sleep (per 24 hr-day; **Fig. 1.2C**) was not affected by genotype but did increase with treatment. Analysis of the same animals before and after the exposure confirmed that DLaN significantly increased the total amount of sleep in the mutant and mice. Significant day/night differences in the amount of sleep behavior (**Fig. 1.2D**) were seen in *Cntnap2* KO and WT with higher amounts of sleep during the day. In contrast, the treated groups lost the day/night difference. Sleep fragmentation as measured by the total number of sleep bouts (**Fig. 1.2E; Table 1.1**) was not affect by genotype or treatment. However, the maximum sleep bout length (**Fig. 1.2F**) was increased by treatment but not genotype. Post-hoc analysis indicated that DLaN increased the duration of sleep in individual bouts in the *Cntnap2* KO and WT mice. Finally, sleep onset **(Fig. 1.2 G, H**) was altered by both genotype and treatment (**Table 1.1**). Thus, the *Cntnap2* KO mice exhibited a disruption in sleep onset, but other parameters were no different from WT mice. Both genotypes exhibited disrupted temporal patterns in sleep behavior driven by the DLaN treatment.

***Daytime neural activity in the central clock is compromised in the Cntnap2 KO mice*.**

A characteristic property of SCN neurons is that these cells generate a circadian rhythm of neural activity with higher spontaneous activity during the day and low activity during

the night. This neural activity is critical for the synchrony of cells within the SCN circuit as well as the ability of this nucleus to drive outputs throughout the body. Thus, we measured the SFR of the dorsal SCN neurons in *Cntnap2* KO and WT. Each of these cells was determined to be within the dorsal region of the SCN by directly visualizing the location of the cell with infrared DIC video microscopy. First, we found that the *Cntnap2* mutants exhibited a reduced daytime firing rate compared to WT controls (**Fig. 1.3A**) which was accompanied by a shift in the distribution of SFR with the mutants exhibiting more cells firing below 2 Hz (**Fig. 1.3B**). In a second set of experiments, we measured the SFR from *Cntnap2 KO* and WT mice held under a normal LD or DLaN for 2 weeks prior to the preparation of the brain slice. With this data set, we observed that the *Cntnap2* KO mice exhibited a reduced SFR and the DLaN treatment did not have any obvious impact of the daytime or nighttime firing rate (**Fig. 1.3C**). In WT mice, the normal day/night rhythm as lost when the mice were held under DLaN (**Fig. 1.3C**). The SFR is a direct measure of the output of the SCN and our data indicate that the *Cntnap2 KO* mice exhibit a modestly reduced spontaneous neural activity.

DLaN shifted the phase and amplitude of the PER2::LUC rhythms in the Cntnap2 KO mice.

Next, we used *in vitro* imaging of tissue from *Cntnap2* KO and WT PER2::LUC mice to examine the impact of DLaN on bioluminescence rhythms. For both genotypes, we observed robust daily rhythms from the SCN, the hippocampus and liver under control conditions (**Fig. 1.4, 1.5; Table 1.2; S. Fig. 1.5**). The SCN was clearly impacted by the DLaN treatment (**Fig. 1.4**). In the central clock, the amplitude was reduced by treatment, but there were no differences between the genotypes. The peak phase varied with both treatment and genotype (**Table 1.2**). The *Cntnap2* KO exhibited a significant phase advance, while the phase of the WT SCN was unaltered (**Fig. 1.4 E, F**). In the hippocampus (**Fig. 1.5**), the KO mice exhibited a strong reduction in amplitude that was not seen in the WT (**Fig. 1.5C, Table 1.2**). The peak phase varied with treatment but not genotype (**Table 1.2**). The phase advances (4-6 hrs) were

of larger magnitude than what we observed in the SCN. In the liver (**Table 1.2, S. Fig. 1.5**), the amplitude was not altered by treatment or genotype. The DLaN treatment also advanced the phase of the liver rhythms. There was no significant effect of genotype or treatment on the endogenous tau (free-running period) measured from any of the three tissues (**Table 1.2**). Overall, our data indicated that the *Cntnap2* KO still presents robust PER2:LUC rhythms, but DLaN altered the amplitude and phase of these rhythms in a tissue- specific manner. The KO exhibited more sensitivity to the impact of treatment on phase in the SCN.

Nighttime light exposure alters social behavior in Cntnap2 KO mice

A key symptom in ASD is difficulty with social interactions, which has been demonstrated in both juvenile (Penagarikano et al, 2011) and adult (Thomas et al., 2017) *Cntnap2* KO mice. When the three-chamber social approach test was administered to adult mice during the night (ZT 14-16), Cntnap2 KO mice under LD conditions did not exhibit a preference for the stranger chamber, whilst under DLaN, they actually preferred the object (**Fig. 1.6A**). WT typically spent more time in the chamber with a stranger mouse than in the one containing the object (**Fig. 1.6B, Table 1.3**). This social preference was eliminated by DLaN (**Fig. 1.6B**). The chamber dwell times were converted to a social preference index by normalizing the chamber preference to the total time spent in the two chambers of interest (**Fig. 1.6C**). The two-way ANOVA indicated that there were significant effects of both genotype and treatment. Post hoc analysis indicated that DLaN decreased preference for the stranger mouse in both WT and *Cntnap2* KO, but the negative social effects of the exposure were stronger in the *Cntnap2* KO mice. There were no genotypic or treatment differences in the time spent in the center chamber (**Table 1.3**). These findings indicate that exposure to DLaN disrupted social behavior in both genotypes, with the mutants being more susceptible.

Nighttime light exposure aggravates repetitive behavior in Cntnap2 KO mice

A hallmark of ASD in humans is repetitive behavior, which is recapitulated in the *Cntnap2* mutants in the form of increased grooming behavior during the day (Penagarikano et al, 2011; Thomas et al., 2017). We examined grooming behavior in the night (ZT 14-16) for each of the four groups and observed that the amount of grooming was significantly impacted by both genotype and treatment (**Fig. 1.7A, Table 1.3**). Post hoc analysis indicated that the mutants exhibited more grooming behavior than WT mice and that this aberrant grooming behavior was exacerbated by DLaN treatment. WT mice housed under DLaN did not display increased grooming compared to WT mice in LD housing. The DLaN exposure decreased exploratory behavior as measured by distance traveled during the test (**Fig. 1.7B**, **Table 1.3**). There were no genotypic or treatment differences in the time spent in the center chamber (**Fig. 1.7C**). In the absence of DLaN, the *Cntnap2* KO exhibited high levels of spontaneous grooming during the day but not in the night (**S. Fig. 1.6**). Therefore, the DLaN exposure drove a large increase in repetitive behavior in the *Cntnap2* KO but not in WT mice.

Treatment with melatonin ameliorates the effects of nighttime light exposure on activity rhythms and repetitive behavior

Melatonin has been proposed as a safe and effective treatment to help with the sleep/wake disruptions common in neurodevelopmental disabilities (Goldman et al, 2014; Kawabe et al, 2014; Schwichtenberg & Malow, 2015). Levels of melatonin are normally high during the night and low during the day. Therefore, we sought to determine whether nightly treatment with melatonin (3 mg/kg) would improve the excessive grooming behavior seen in the *Cntnap2* mutant exposed to DLaN. WT and KO mice housed under DLaN conditions were treated daily (ZT 11.5) with melatonin or vehicle for 2 weeks (**Fig. 1.8A, Table 1.4**). Significant effects were seen for both genotype and treatment as well as their interaction. Post hoc analysis revealed that melatonin treatment in the night significantly reduced grooming behavior in the mutant mice. As a control for the time of administration, another group of KO mice was treated with melatonin in the day (ZT 23.5). No amelioration in excessive grooming

behavior was observed (**Fig. 1.8A**).

Finally, we determined the effects of the same nightly melatonin treatment on activity rhythms in the *Cntnap2* KO exposed to DLaN. Cohorts of mutant mice were held under DLAN and treated with either melatonin (3 mg/kg) or vehicle (**Fig. 1.8B, Table 1.4**). Melatonin significantly improved the power of the daily rhythms by decreasing inappropriate activity during the day as well as reducing the cycle-to-cycle variation in activity onset. Therefore, melatonin successfully rescued the excessive grooming and disrupted activity rhythms seen in the *Cntnap2* KO under DLaN.

Discussion

Cntnap2 homozygous null (*Cntnap2* KO) mice were chosen because of their strong construct validity and the human genetic evidence that implicate this gene in autism. Recessive loss-of-function mutations in *Cntnap2* cause Pitt-Hopkins-like syndrome (Peippo & Ignatius, 2012; Zweier et al., 2009), symptoms of which include severe intellectual disability, lack of speech, and seizures. In addition, a homozygous single base pair deletion, resulting in a truncated protein, causes Recessive Symptomatic Focal Epilepsy, which presents with autistic symptoms as well as cortical dysplasia and epilepsy (Strauss et al., 2006). The *Cntnap2* KO mice have the first exon of *Cntnap2* gene replaced by a *neo* gene that results in the absence of the Cntnap2 protein in the brains in homozygous mice (Poliak et al., 1999).

One of the key assessments in this study was the evaluation of the mutant mice compared to WT controls. We found that *Cntnap2* KO mice have weaker daily cage activity rhythms, are more day-active and have less precision in activity onset than WT mice (**Fig. 1.1; Table 1.1**). Previous work with this model reported acute hyperactivity when the mice were placed in a testing field in the light phase of the LD cycle (Penagarikano et al., 2011; Brunner et al., 2015; Thomas et al., 2017). We also observed some evidence for acute hyperactivity in the mutants when the mice were placed in an open arena (**Fig. 1.7**) as has also been seen with home cage activity (Angelakos et al., 2019). However, when the activity rhythms are measured over a 24-hr cycle, the *Cntnap2* KO mice show reduced locomotor activity, especially during the night. (**Fig. 1.1**; Thomas et al., 2017; Angelakos et al., 2019). We found that sleep behavior was relatively unaffected in the *Cntnap2* KO (**Fig. 1.2; Table 1.1**) with overall sleep duration or fragmentation unaltered. Previous analysis on electroencephalogram (EEG)-defined sleep in the *Cntnap2* KO mice enabled the authors to parse vigilance states into wake, rapid eye movement (REM) and non-REM sleep. They were able to demonstrate blunted rhythms in each of the states along with fragmented bouts of wakefulness (Thomas et al., 2017). The authors found a reduced spectral power of the EEG in the alpha (9-12 Hz)

range (Thomas et al., 2017), suggesting a disruption in the coherence in the electrical activity of thalamic pacemaker cells that are thought to be responsible for the alpha waves.

The alterations in the amplitude of the diurnal rhythms in activity, sleep (NREM, REM) and core body temperature could be most simply explained if the *Cntnap2* mutation caused disruption in the circadian timing system. The *Cntnap2* transcript is highly expressed in the SCN as well as the paraventricular nucleus in the adult mouse (Lein et al. 2007). However, behaviorally, there does not appear to be an alteration in free-running circadian period (Tau) when activity is measured in constant darkness (Angelakos et al., 2019). Similarly, we did not see a difference in Tau between the WT (23.67 ± 0.07, n=14) and mutant (23.53 ± 0.17, n=8) mice when housed in constant darkness (DD). The free-running period, as measured by locomotor behavior in DD, is an extremely sensitive marker of output of the core molecular clock that drives circadian oscillations (Takahashi et al., 2008). Thus, the behavioral data do not suggest a disruption in the core clock in the *Cntnap2* KO mice. In addition, we did not observe anomalies in the morphology of the SCN or in the number of cells expressing the peptides VIP and AVP (**S. Fig. 1.7**). We went on to measure PER2-driven bioluminescence from the SCN. Using this direct read out of the molecular clock (Yoo et al., 2004), we found that the key circadian parameters of amplitude, phase and free-running period did not vary between the genotypes (**Fig. 1.4, 1.5; Table 1.3**). We did see a reduction in daytime SFR measured from the mutant SCN (**Fig. 1.3**) so there may be some circadian disruption that could explain the deficits in the diurnal rhythms. Collectively, this work indicates that the *Cntnap2* KO mice exhibit disruptions in the temporal patterning of activity and sleep which fits with a general pattern of deficits seen in mouse models of monogenic neurological disorders (Angelakos et al., 2019; Brown et al., 2019; Shi and Johnson, 2019; Takumi et al., 2019).

Social deficits were observed in the *Cntnap2* KO as measured by the 3-chamber test (**Fig. 1.6; Table 1.3**), where they had decreased preference for spending time in close vicinity to a stranger mouse compared to WT. However, the time that the mutant mice spent

investigating the stranger mouse was not different from the controls. Prior work with this model found robust social deficits in juvenile *Cntnap2* mutants (Penagarikano et al., 2011) that responded positively to treatment with oxytocin (Penagarikano et al, 2015). Working with slightly older mice, another group observed social deficits in one test (urine-open field) but not in the 3-chamber or reciprocal social interaction test (Brunner et al., 2015). Another study using adult mutants found reduced social interactions when the KO mice were allowed to interact in a cage (Thomas et al., 2017). The reasons for these differences among the different laboratories' measurements of social behavior are not clear. The strongest phenotype that we observed with the *Cntnap2* KO model was increased repetitive behavior. The mutant mice spent more time grooming (**Fig. 1.7; Table 1.3**) than WT controls. This repetitive behavior has been shown in prior work in the *Cntnap2* model (Penagarikano et al., 2011; Thomas et al., 2017) and can be normalized by treatment with Risperidone (Penagarikano et al., 2011), demonstrating the predictive validity of the model.

Genetic studies have revealed heterogeneity in ASD, predicting hundreds of rare genetic associations (Iossifov et al., 2012; O'Roak et al., 2012; Sanders et al., 2012). Despite evidence of genetic risk factors, environmental risk factors are very likely to be playing an important role in the symptoms and serving as a "second hit". Nightly light exposure is a common environmental perturbation and has been shown to cause a number of ill effects (Bedrosian et al., 2016; Bedrosian et al., 2011; Borniger et al., 2014; Fonken et al., 2013a; Fonken et al., 2012; Fonken & Nelson, 2011; Lucassen et al., 2016). Therefore, we investigated the impact of dim light at night on locomotor activity, sleep, PER2::LUC bioluminescence rhythms, social and grooming behavior in both WT and mutant mice. The DLaN treatment had a dramatic effect on measures of locomotor activity rhythms (**Fig. 1.1; S. Fig. 1.2**) and the temporal pattern of sleep (**Fig. 1.2**). For example, the normal day/night rhythms in the amount of sleep is lost under DLaN treatment, and the amount of time sleeping in the day and night were not significantly different in either genotype. The DLaN treatment did not altered SFR (**Fig. 1.3C**)

although the day/night rhythm in SFR was lost under DLaN exposure. DLaN also dramatically reduced the amplitude of the PER2:LUC rhythm measured at the level of the SCN (**Fig. 1.4**). Since we do not have single cell resolution for the bioluminescence, we cannot resolve whether the reduction in amplitude is driven by a loss of synchrony in the cell population or damping of the single cell oscillation. Based on prior work examining the impact of constant light on SCN neurons (Ohta et al., 2005), we would expect that DLaN desynchronizes clock neurons but does not compromise their ability to generate circadian rhythms. Finally, DLaN reduced social behavior in both genotypes (**Fig. 1.6**) and increased grooming in the mutants (**Fig. 1.7**).

We expected that the mutants may be more sensitive to the effects of circadian disruption and found some evidence for selective vulnerability in the *Cntnap2* model i.e. DLaN produced significantly worse effects in the KO compared to WT controls. This selective vulnerability was seen with changes in the amplitude and phase of the PER2 rhythms measured in the hippocampus, reduced social index, and increase time spent grooming. In our hands, the impact on activity onset and grooming were particularly robust. In the present study, using a shorter circadian disruption of 2 weeks, the negative impact of the light at night proved to be reversible when conditions of true darkness were restored (**S. Fig. 1.4**). It remains to be determined if longer durations under DLaN lead to permanent deficits. Circadian disruptions have been observed in a number of neurodevelopmental disorders (Angelakos et al., 2019; Brown et al., 2019; Shi and Johnson, 2019; Takumi et al., 2019), and it will be important to explore whether there is a selectively vulnerable developmental period for long-term effects of DLaN on behavior (e.g. Borniger et al., 2014; Logan & McClung, 2019).

The mechanisms underlying the negative impact of DLaN are not known and could be mediated by multiple factors. Based on recent work, our assumption is that the effects of DLaN are mediated by intrinsically photosensitive retinal ganglion cells (ipRGCs) (Lazzerini et al., 2017). For example, work from the Hattar laboratory indicates that ipRGCs that project to

the SCN mediate the effects of light on learning (Fernandez et al., 2018). Mood regulation by light, on the other hand, requires an SCN-independent pathway linking ipRGCs to the perihabenular nucleus (PHb). The PHb is anatomically integrated in a distinct circuit with the limbic system and appears to be both necessary and sufficient for driving the effects of light on affective behavior. An important area for future work will be to determine which of these ipRGC pathways underlie the impact of DLaN observed in the present study. Notably, recent work on the mouse forebrain has found evidence that a variety of the genes coding for transcripts linked to synaptic transmission are regulated by the circadian timing system, while the proteome is more highly influenced by the sleep/wake cycle (Noya et al., 2019). Many of these same synaptic transcripts have been shown to be down-regulated in cortical regions of patients with neurodevelopmental disorders (Gandal et al., 2018). Therefore, by altering both the circadian clock and sleep behavior, DLaN would be expected to have a major impact on synaptic transmission throughout the forebrain.

In this study, we show that treatment with melatonin improves some of the symptoms seen in the *Cntnap2* model, with striking improvements in repetitive behaviors i.e. excessive grooming (**Fig. 1.8A; Table 1.4**). In addition, nightly melatonin improved the power and precision of cage activity rhythms (**Fig. 1.8B**). Thus, two key parameters in which the *Cntnap2* mutants show selective vulnerability to DLaN are both improved and, in the case of grooming behavior, returned to WT levels. Exogenous melatonin treatment has also been proposed as a treatment for circadian rhythm disorders (e.g. Burke et al, 2013; Riemersma-van der Lek et al, 2008; Schroeder & Colwell, 2013) and is particularly appealing for use in young and adolescent patients (Eckerberg et al, 2012), as most indications are that it is well-tolerated. Perhaps for this reason, melatonin is one of the most commonly used medications for sleep disturbances in children and adolescents with developmental disabilities (Rossignol & Frye, 2014; Schwichtenberg & Malow, 2015). For example, a survey of ASD patients found that medications for sleep were prescribed in 46% of 4- to 10-year-olds given a sleep diagnosis,

with melatonin being the most commonly used medication (Malow et al, 2016). Mostly relying on self-reports by patients and family members, the studies to date have found consistent evidence that sleep latency is improved in many of the patients taking melatonin (Andersen et al, 2008; Garstang & Wallis, 2006; Giannotti et al, 2006; Malow et al, 2012; Wirojanan et al, 2009; Wright et al, 2011). There has been at least one study which found that treatment with the melatonin receptor agonist Ramelteon improved insomnia and behavioral symptoms in a small number of ASD patients (Kawabe et al, 2014). Recent work examined the association between repetitive behaviors and sleep problems in children with ASD. Patients with repetitive behaviors, but not restrictive behaviors like the insistence on routine, experienced significant reported sleep problems even after controlling for anxiety (Hundley et al, 2016). This suggests that melatonin may be better suited as an intervention for the subset of ASD patients with repetitive behaviors and sleep problems (Schroder et al., 2019). Understandably, the work in patients is focused on treating the symptoms rather than understanding the underlying biology. With animal models, it is possible to explore the underlying mechanisms and develop improved therapeutics with caveats. For example, in the context of the present work, it is worth noting that many commonly used mouse strains like the C57 line do not produce melatonin (Ebihara et al., 1986).

The *Cntnap2* model has strong construct validity, as mutations in this gene are found in humans with autism. Nevertheless, not all mouse models can recapitulate all of the autism domain deficits due to the broad spectrum of causes and symptoms in ASD. In our hands, the locomotor and repetitive behavior phenotypes were most robust in the adult mouse and were the focus of our study. Dim light at night is a mild environmental disruptor of circadian rhythms and one that may be commonly experienced by patients with ASD. At least two studies have shown that these young patients are more exposed to light at night via electronic screens than age-matched controls (Engelhardt et al., 2013; Mazurek et al., 2016). This light exposure by itself has been shown to delay sleep in healthy young people (Chang et al., 2015;

Gronli et al,, 2016; Wood et al., 2013). Our work raises the possibility that sleep and circadian disruption may be an environmental factor that makes at least some of the core symptoms of developmental disabilities worse. While this remains to be rigorously tested, the data suggests that patients and caregivers may benefit from living in a temporally structured environment with particular attention paid to lighting conditions. While melatonin levels would be suppressed by light exposure during the night, melatonin supplements or melatonin receptor agonists may prove to be an appropriate countermeasure.

Figures

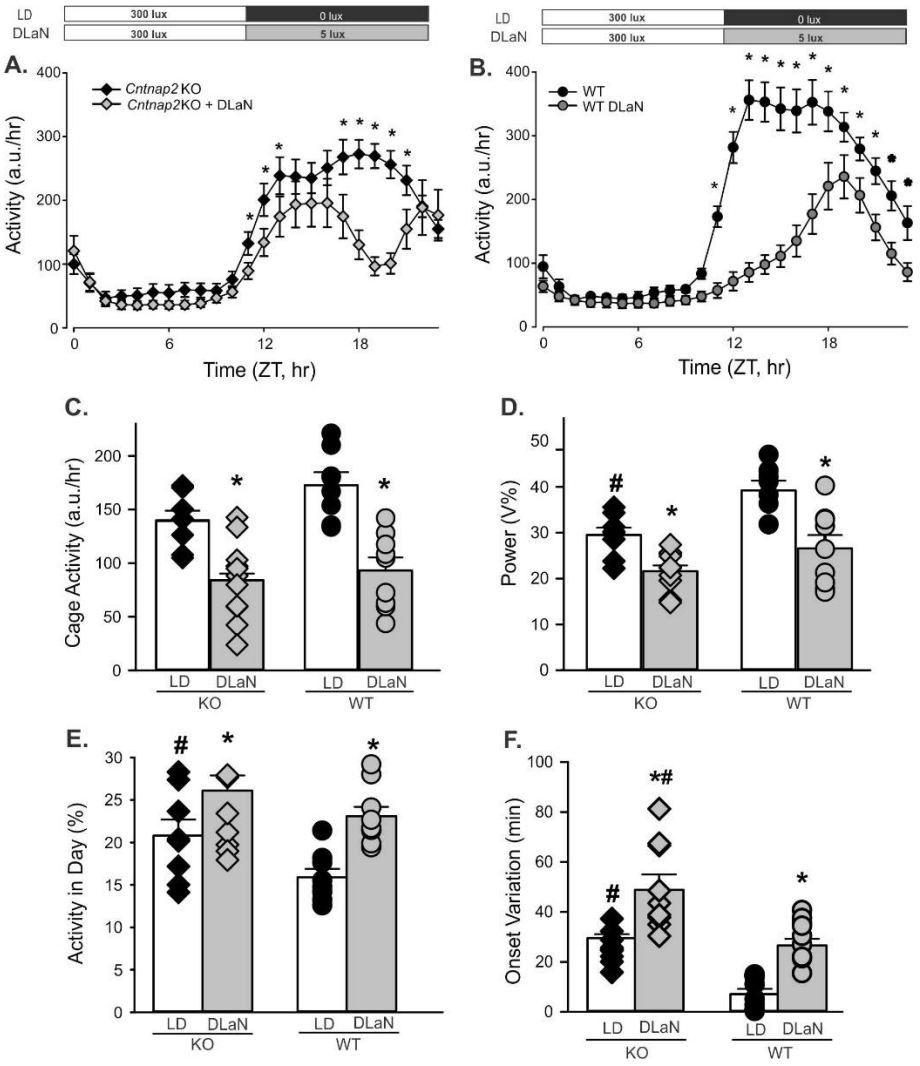

Fig. 1.1: Rhythms in cage activity are altered by dim light at night (DLaN). Waveforms of daily rhythms in cage activity under LD and DLaN show the activity-depressing effect of DLaN (5 lux) in both *Cntnap2* KO (**A**) and WT (**B**) mice. The mean ± SEM is shown at each time point. For this and all other figures, the mutants are shown as diamonds while the WT values are shown as circles. For this and all other figures, black symbols are from mice in normal LD while grey symbols are from mice in DLaN. The activity waveform (1 hr bins) of each genotype was analyzed using a 2-way ANOVA for repeated measures with genotype and time as factors. Both *Cntnap2* KO (n=10) and WT controls (n=10) exhibited clear rhythms in activity under both lighting conditions. Overall, the *Cntnap2* KO exhibited significant effects of time ($F_{(23, 383)}$ = 23.491, P < 0.001) but not treatment ($F_{(1, 383)}$ = 3.353, P = 0.089). The WT mice exhibited significant effects of both time ($F_{(23, 383)}$ = 79.375, P = 0.001) and treatment ($F_{(1, 383)}$ = 25.744, P < 0.001). Post-hoc analysis by Multiple Comparison Procedures (Holm-Sidak method) indicated significant reductions in activity caused by DLaN exposure at a number of phases during the night in both genotypes. Significant (P < 0.05) differences between the genotypes are indicated with an asterisk over the untreated values. Histograms (**C—F**) show means ± SEM with the values from individual animals overlaid. The locomotor activity parameters were analyzed using a 2-way ANOVA with genotype and

treatment as factors. Significant ($P < 0.05$) differences as a result of treatment are indicated with an asterisk (*) over the treated values while the number sign (#) indicates a genotypic difference. (**C**) Cage activity was reduced by treatment ($F_{(1, 35)} = 37.428$, $P < 0.001$) but there were no effects of genotype ($F_{(1,35)} = 3.716$, $P = 0.063$). (**D**) The power of the rhythms (% variation) was reduced by treatment ($F_{(1, 35)} = 26.780$, $P < 0.001$) as well as genotype ($F_{(1,35)} = 13.789$, $P < 0.001$). (**E**) The amount of activity during the day (%) was increased by the treatment ($F_{(1, 35)} = 15.346$, $P < 0.001$) as well as genotype ($F_{(1,35)} = 6.097$, $P = 0.019$). (**F**) The precision of the activity onset (cycle-to-cycle variation) was reduced by the treatment ($F_{(1, 35)} = 41.644$, $P < 0.001$) and genotype ($F_{(1,35)} = 29.686$, $P < 0.001$). Overall, DLaN negatively impacted most measures of activity rhythms and the mutant mice exhibited more activity in the day and increased variability of activity onset which resulted in an overall reduction in the strength of the daily rhythm.

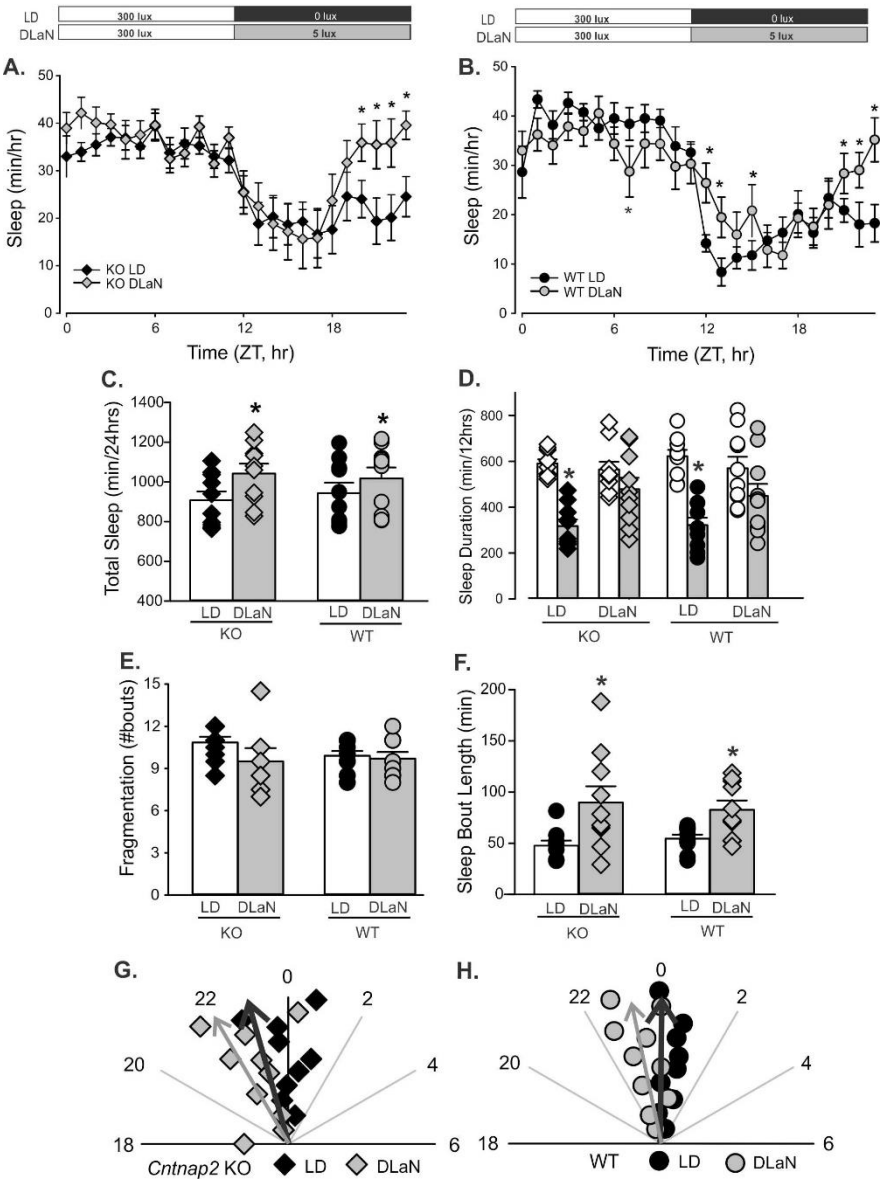

Fig. 1.2: Rhythms in sleep behavior are altered by DLaN. Waveforms of daily rhythms in sleep behavior under LD and DLaN in both *Cntnap2* KO (**A**) and WT (**B**) mice. The sleep waveform (1 hr bins) of each genotype using a 2-way ANOVA for repeated measures with genotype and time as factors. All *Cntnap2* KO (n=10) and WT controls (n=10) exhibited clear rhythms in sleep under both lighting conditions. The *Cntnap2* KO exhibited significant effects of time ($F_{(23, 479)} = 8.426$, $P < 0.001$) and treatment ($F_{(1, 479)} = 7.279$, $P = 0.024$). The WT mice exhibited significant effects of both time ($F_{(23, 432)} = 16.133$, $P < 0.001$) but not treatment ($F_{(1, 432)} = 0.838$, $P = 0.360$). There were significant interactions between treatment and time ($F_{(23, 479)} = 2.812$, $P < 0.001$). Post-hoc analysis by Multiple Comparison Procedures (Holm-Sidak method) indicated significant reductions in activity caused by DLaN exposure at a number of phases during the night in both genotypes. Significant ($P < 0.05$) differences between the genotypes are indicated with an asterisk over the treated values. Several aspects of sleep behavior were measured from each genotype (*Cntnap2* KO, WT) under each lighting condition (LD, DLaN) and the resulting data analyzed with 2-way ANOVA. Histograms

show means ± SEM with the values from individual animals overlaid. Significant ($P < 0.05$) differences because of treatment are indicated with an asterisk (*) over the treated values while the number sign (#) indicates a genotypic difference. (**C**) Total sleep was increased by treatment ($F_{(1, 39)} = 4.762$, $P = 0.036$) but there were no effects of genotype ($F_{(1,39)} = 0.011$, $P = 0.914$). (**D**) Day/night differences in the amount of sleep were disrupted by treatment. Both WT ($t_{(9)} = 8.960$, $P < 0.001$) and *Cntnap2* KO ($Z_{(9)} = 2.805$, $P = 0.002$) exhibited increased sleep in the day than in the night. These differences were lost in both WT ($t_{(9)} = 1.347$, $P = 0.211$) and KO ($t_{(9)} = 1.228$, $P = 0.251$) mice under DLaN. (**E**) The number of sleep bouts was unaltered by treatment ($F_{(1, 39)} = 1.880$, $P = 0.179$) or genotype ($F_{(1,39)} = 0.440$, $P = 0.511$). (**F**) The sleep bout length was increased by treatment ($F_{(1, 39)} = 14.676$, $P < 0.001$) but not genotype ($F_{(1,39)} = 0.001$, $P = 0.979$). (**G, H)** Polar plots show the time of sleep onset for the mice measured under each condition. The numbers show the phases (ZT) with ZT 0 showing the time of light-onset. The onset of sleep was altered by both treatment ($F_{(1, 39)} = 20.617$, $P < 0.001$) and genotype ($F_{(1,39)} = 5.6$, $P = 0.023$). The vector indicates the peak phase and the amplitude relative to WT controls. Overall, DLaN increased sleep behavior by shifting the onset of sleep to an earlier phase. This change had the effect of eliminating the normal day/night difference in sleep duration.

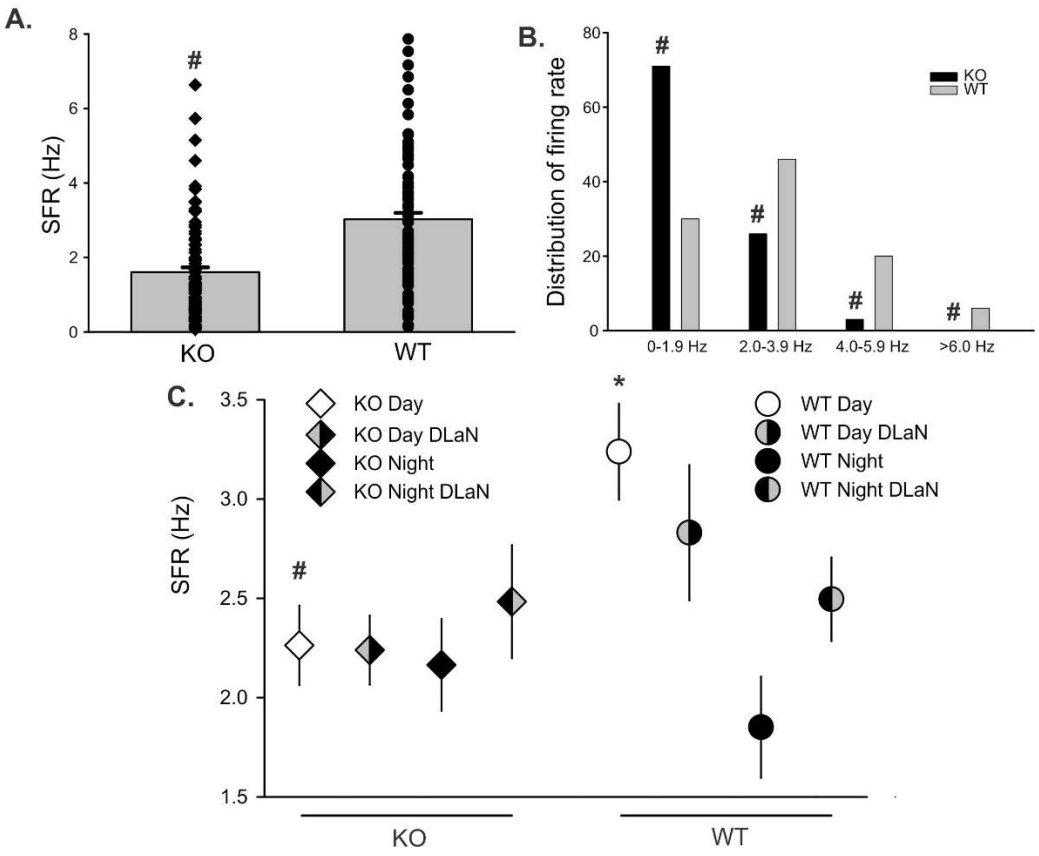

Fig. 1.3: DLaN did not alter the daytime spontaneous frequency rate (SFR) of SCN neurons measured in a brain slice preparation. (**A**) Extracellular recording techniques indicated that SCN neurons from the *Cntnap2* KO (n = 101) exhibited a modestly reduced daytime (ZT 5-7) firing rate compared to WT (n = 102) controls (Mann-Whitney Rank Sum test with $U = 2499$, $P < 0.001$). (**B**) The distribution of SFR was shifted lower in the mutants with highly significant changes in the number of neurons firing at the 0-2 Hz rate (Z score = -6.050, $P = 0.001$). In a separate experiment (**C**), cell-attached recording techniques were used to measure the SFR of *Cntnap2* KO and WT mice in brain slices prepared from mice held in normal LD and under DLaN. In WT mice (one-way ANOVA), there were significant differences ($H = 19.744$, $P < 0.001$) driven by a day/night difference in firing rate ($Q = 4.418$; $P < 0.001$). In *Cntnap2* KO, the day/night difference was lost ($H = 0.338$; $P < 0.953$). If we consider only day-time firing rate, the WT exhibits significantly higher SFR ($H = 11.722$; $P = 0.029$) than the KO. There was no significant day/night difference in SFR under DLaN. In short, DLaN did not produce changes in SCN firing rate that we could measure in the slice preparation, but the *Cntnap2* KO did show a reduced SCN output.

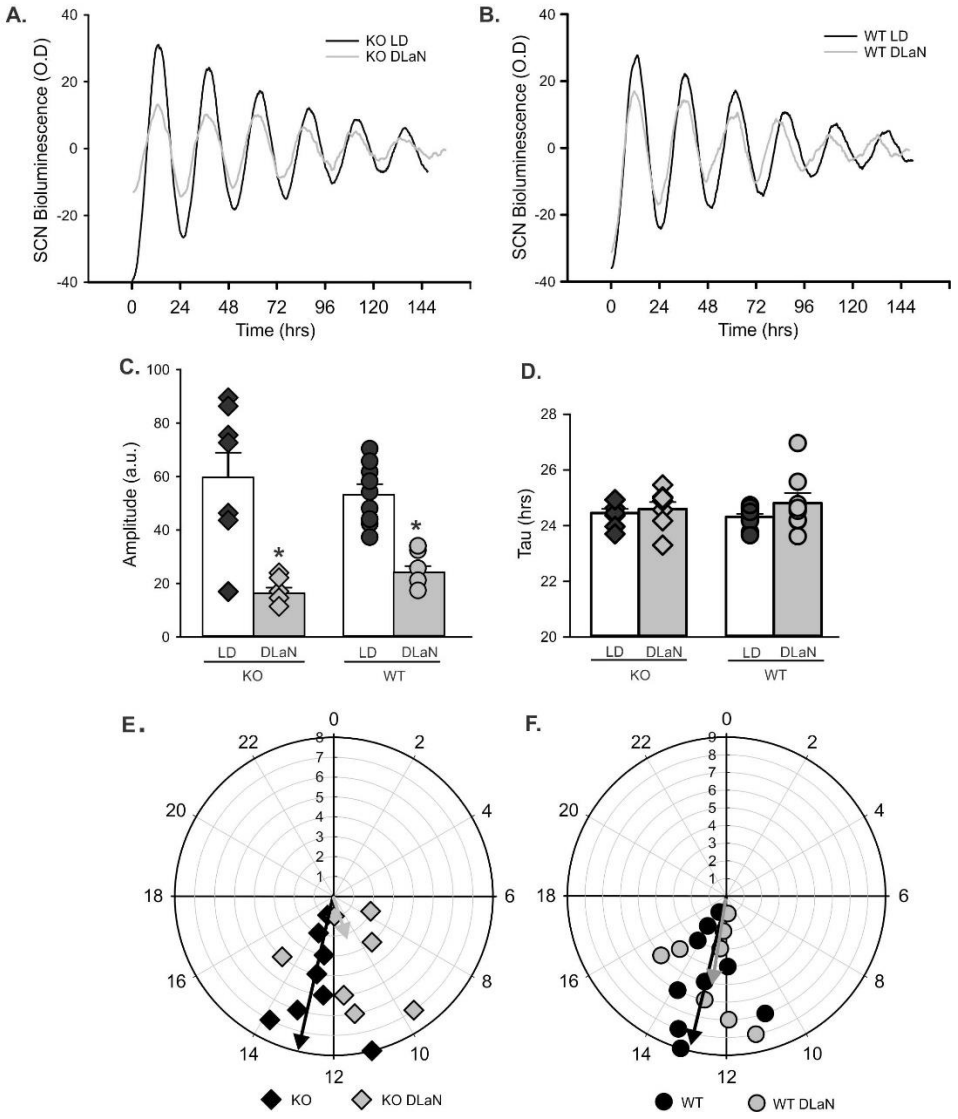

Fig. 1.4: **DLaN alters the PER2::LUC bioluminescence rhythms measured in the SCN.** Representative examples of bioluminescence rhythms measured from the *Cntnap2* KO (**A**) and WT (**B**) SCN under LD and DLaN conditions. Several parameters were measured from the bioluminescence rhythms and analyzed with 2-way ANOVA. Histograms show means ± SEM with the values from individual animals overlaid. Significant ($P < 0.05$) differences because of treatment are indicated with an asterisk (*) over the treated values while the number sign (#) indicates a genotypic difference. (**C**) The amplitude was reduced by treatment ($F_{(1,31)} = 47.458$, $P < 0.001$) but there was no differences between the genotypes ($F_{(1,31)} = 0.014$, $P = 0.907$). (**D**) There was no difference in the tau (free-running period) measured by treatment ($F_{(1,31)} = 1.838$, $P = 0.186$) or genotype ($F_{(1,31)} = 0.024$, $P = 0.879$). (**E, F**) Polar plots show the peak phase of the rhythms measured under each condition. The numbers show the phases (ZT) with ZT 0 showing the time of light-onset. The peak phase varied with both treatment ($F_{(1,31)} = 4.726$, $P = 0.038$) and genotype ($F_{(1,31)} = 4.424$, $P = 0.045$). The vector indicates the peak phase and the amplitude relative to WT controls. Overall, DLaN decreased the amplitude of rhythms in both genotypes and caused a phase advance in the mutants only.

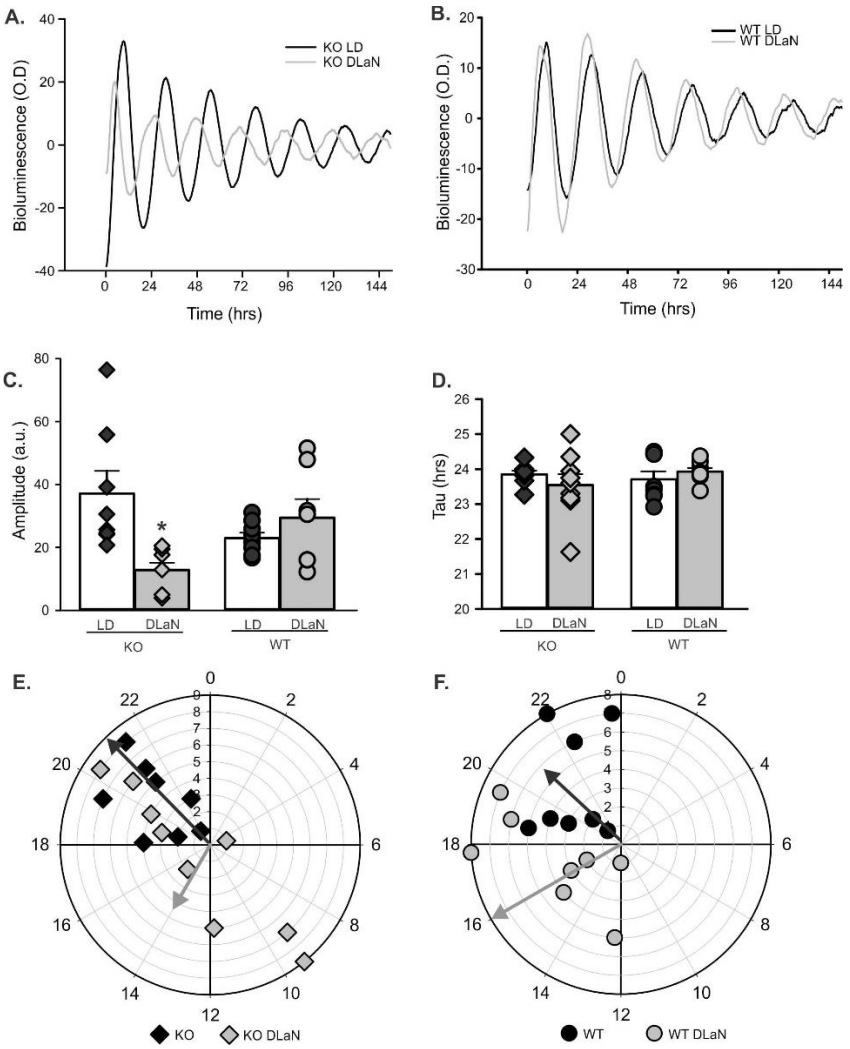

Fig. 1.5: **DLaN alters the PER2::LUC bioluminescence rhythms measured in the hippocampus.** Representative examples of bioluminescence rhythms measured from the *Cntnap2* KO (**A**) and WT (**B**) hippocampus under LD and DLaN conditions. Several parameters were measured from the bioluminescence rhythms and analyzed with 2-way ANOVA. Histograms show means ± SEM with the values from individual animals overlaid. Significant ($P < 0.05$) differences because of treatment are indicated with an asterisk (*) over the treated values while the number sign (#) indicates a genotypic difference. (**C**) Overall, the amplitude of the rhythms was not altered by treatment ($F_{(1,32)} = 3.566$, P = 0.069) or genotype ($F_{(1,32)} = 0.065$, P = 0.800). However, the treatment did dramatically reduce the amplitude of the KO rhythms, an effect that was significant in post-hoc tests. (**D**) There was no difference in the tau (free-running period) measured by treatment ($F_{(1,32)} = 0.205$, $P = 0.654$) or genotype ($F_{(1,32)} = 0.629$, $P = 0.450$). (**E, F**) Polar plots show the peak phase of the rhythms measured under each condition. The numbers show the phases (ZT) with ZT 0 showing the time of light-onset. The peak phase varied with treatment ($F_{(1,32)} = 20.108$, P < 0.001) but not genotype ($F_{(1,32)} = 0.602$, P = 0.444). The vector indicates the peak phase and the amplitude relative to WT controls. Overall, DLaN caused a phase advance in both genotypes and decreased the amplitude in the mutants only.

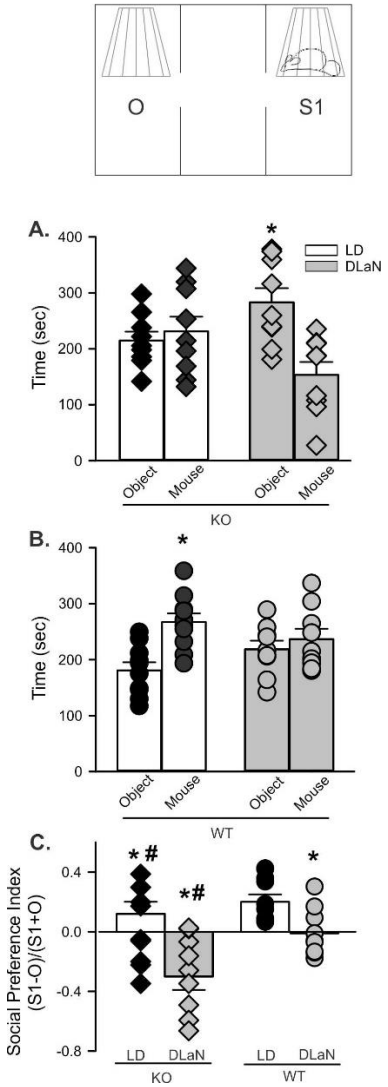

Fig. 1.6: Social preference is reduced by DLaN. Performance on the 3-chamber social test was assessed in mice of each genotype (*Cntnap2* KO, WT) under each lighting condition (LD, DLaN) and the resulting data analyzed with 2-way ANOVA. During the social preference stage of the three chamber test, mice freely explored the arena with a novel object (O) in one chamber, and an age- and sex-matched WT stranger mouse (S1) in the other chamber while dwell time is measured. (**A**) *Cntnap2 KO* mice do not show a preference for the mouse over an object ($t_{(8)}$ = 0.533, P = 0.601). Under DLaN, the mutants actually prefer the object and avoid the mouse ($t_{(8)}$ = 3.791, P = 0.002). (**B**) WT mice prefer to spend time with the stranger mouse over the object ($t_{(9)}$ = 4.391, P < 0.001). This preference is lost under DLaN conditions ($t_{(8)}$ = 0.751, P = 0.464). (**C**) Normalizing the difference between chamber dwell times by time spent in both chambers produced the social preference index. This index shows significant effects of genotype ($F_{(1,36)}$ = 11.757, P = 0.002) and treatment ($F_{(1, 36)}$ = 13.892, P < 0.001). Significant (P < 0.05) differences because of treatment are indicated with an asterisk (*) over the treated values while the number sign (#) indicates a genotypic difference. DLaN reduced social performance in both genotypes with the mutant mice appearing to avoid the test mouse.

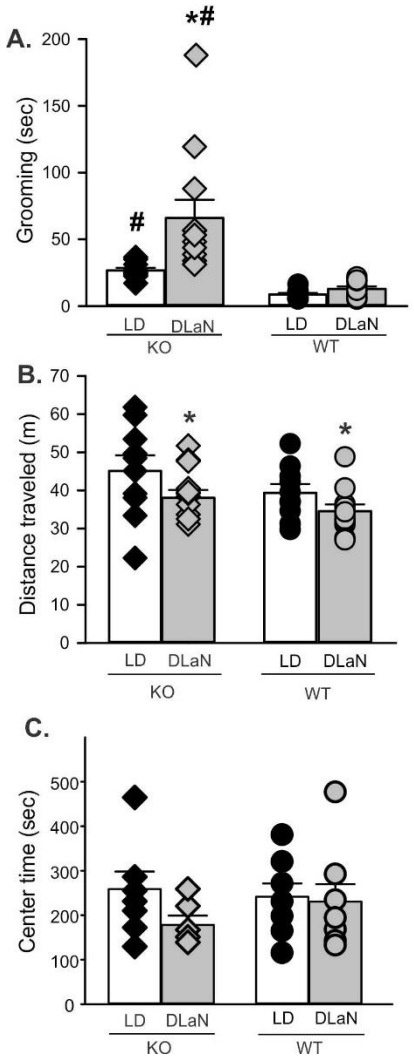

Fig. 1.7: Repetitive and exploratory behavior are altered by DLaN. Grooming and movement was assessed in a novel arena from mice of each genotype (*Cntnap2* KO, WT) under each lighting condition (LD, DLaN) and the resulting data analyzed with 2-way ANOVA. Histograms show means ± SEM with the values from individual animals overlaid. Significant ($P < 0.05$) differences because of treatment are indicated with an asterisk (*) over the treated values while the number sign (#) indicates a genotypic difference. (**A**) Grooming behavior was significantly increased by genotype ($F_{(1,43)} = 21.986$, $P < 0.001$) and treatment ($F_{(1, 43)} = 8.231$, $P = 0.007$). There was a significant interaction between the two factors ($F_{(1, 43)} = 5.296$, $P = 0.027$). (**B**) Novel arena exploration was decreased by the treatment ($F_{(1, 43)} = 5.846$, $P = 0.020$) but not genotype ($F_{(1,43)} = 3.603$, $P = 0.065$). **(C)** The time spent in the center of the open field did not vary with genotype ($F_{(1, 29)} = 0.254$, $P = 0.619$ or treatment ($F_{(1,29)} = 1.688$, $P = 0.205$). There was no significant interaction between the two factors ($F_{(1, 29)} = 0.981$, $P = 0.331$).

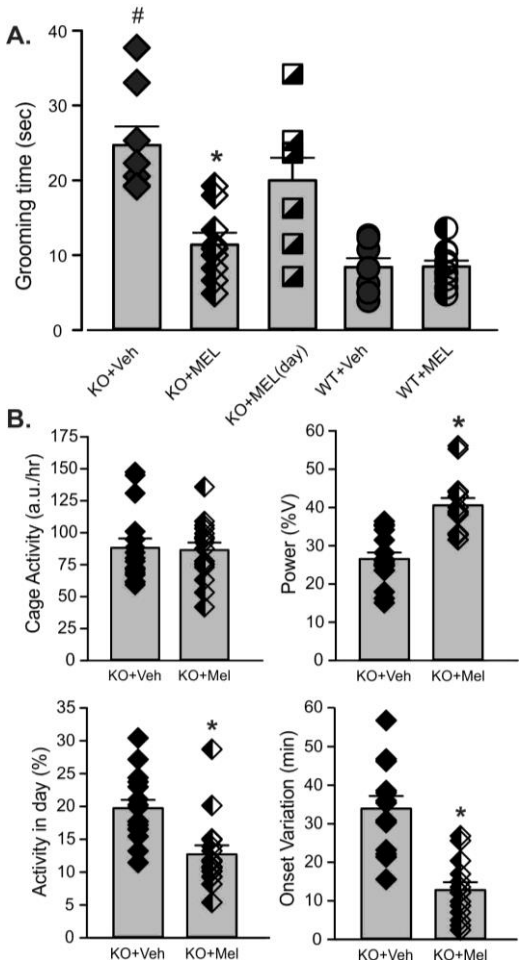

Fig. 1.8: Treating mice with melatonin counteracts the effects of DLaN on repetitive behavior. Both WT and *Cntnap2* KO mice were housed under DLaN for 2 weeks. During the same 2 weeks, mice were treated with either vehicle or a melatonin (3.0 mg/kg), given daily at ZT 11.5 (30 min before the night phase). (**A**) Grooming was assessed in a novel arena and the resulting data analyzed with 2-way ANOVA. Histograms show means ± SEM with the values from individual animals overlaid. A separate group of *Cntnap2* KO mice treated with melatonin at ZT 23.5 are shown as squares. Half-tone symbols indicate mice that were treated with melatonin. Significant ($P < 0.05$) differences because of treatment are indicated with an asterisk (*) over the treated values while the number sign (#) indicates a genotypic difference. Grooming behavior was significantly increased by genotype ($F_{(1,34)} = 25.338$, $P < 0.001$) and reduced by the melatonin treatment ($F_{(1, 34)} = 7.074$, $P = 0.012$). There was a significant interaction between the two factors ($F_{(1, 34)} = 11.615$, $P = 0.002$). The mutant mice treated with melatonin at dawn were not different from vehicle controls ($t_{(13)} = 1.070$, $P = 0.304$). (**B**) The impact of melatonin treatment on cage activity of a separate group of *Cntnap2* KO mice under DLaN was assessed. Compared to vehicle controls, melatonin did not alter activity levels ($t_{(30)} = 0.181$, $P = 0.857$). Melatonin treatment did improve the power ($t_{(30)} = 3.605$, $P = 0.001$) and precision ($U_{(30)} = 25$, $P = 0.001$) of the activity rhythm. Treatment with melatonin effectively reduced the repetitive behavior and improved the activity rhythms of the *Cntnap2* KO mice under DLaN.

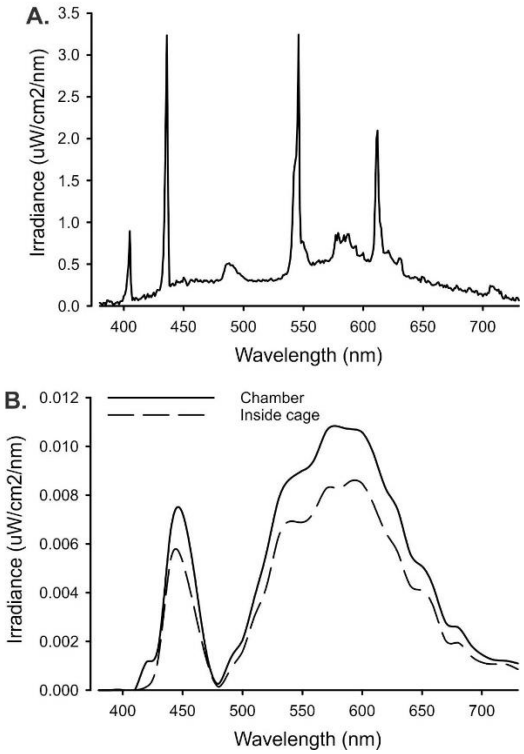

S. Fig. 1.1: **A**) The irradiance of the DLaN illumination was measured inside the animal holding chamber as well as inside the mouse cage. The overall light intensity was measured at 5.2 lux while the melanoptic light intensity inside the mouse cage was calculated to be 2.8 lux. **B**) For comparison, the irradiance of the fluorescent light generated a light intensity of 300 lux for the normal LD cycle.

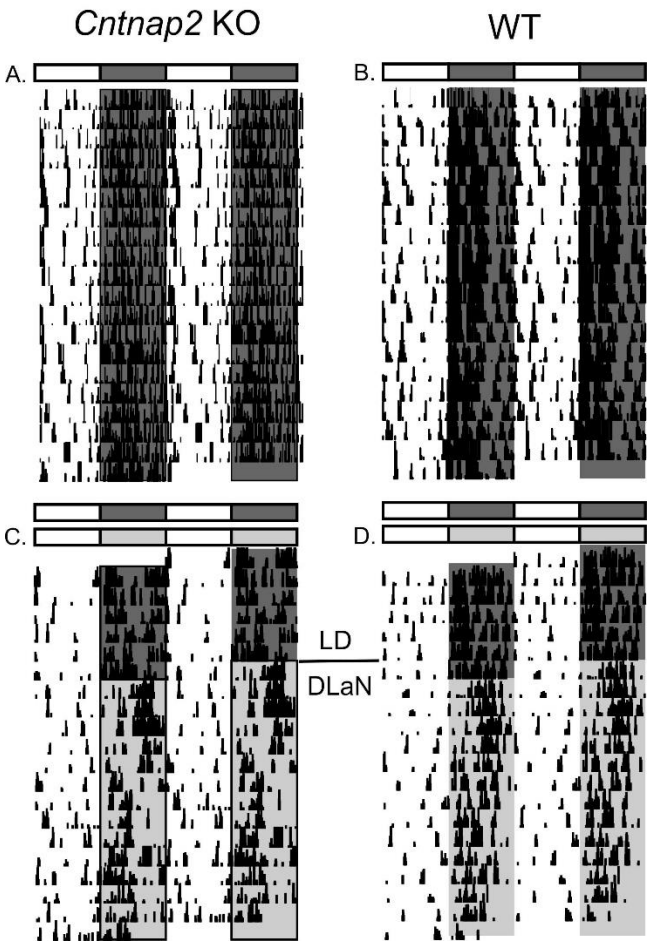

S. Fig. 1.2: Rhythms in cage activity are altered by dim light at night (DLaN). Example actograms of daily rhythms in cage activity under LD (**A, B**) and DLaN (**C, D**) show the activity-depressing effect of DLaN (5 lux) in both *Cntnap2* KO (**C**) and WT (**D**) mice.

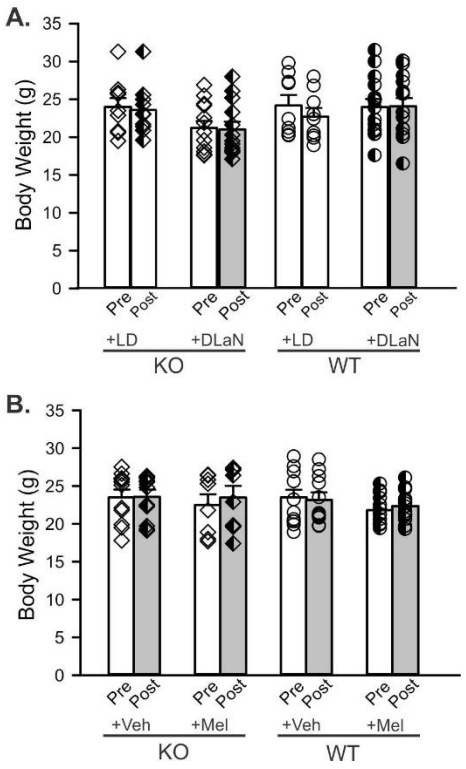

S. Fig. 1.3: Body weights were not altered by DLaN. There is ample evidence that disruption of the circadian system causes metabolic disruption. Therefore, we measured the body weight of each genotype before and after treatment with DLaN (**A**) or DLaN plus melatonin (**B**). Histograms show means ± SEM with the values from individual animals overlaid. Half-tone symbols indicate mice that were exposed to DLaN. Data from the mutants are shown as diamonds while the WT values are shown as circles. The body weight of each group before and after treatment were evaluated using a paired *t*-test. None of the groups exhibited significant differences ($P > 0.05$).

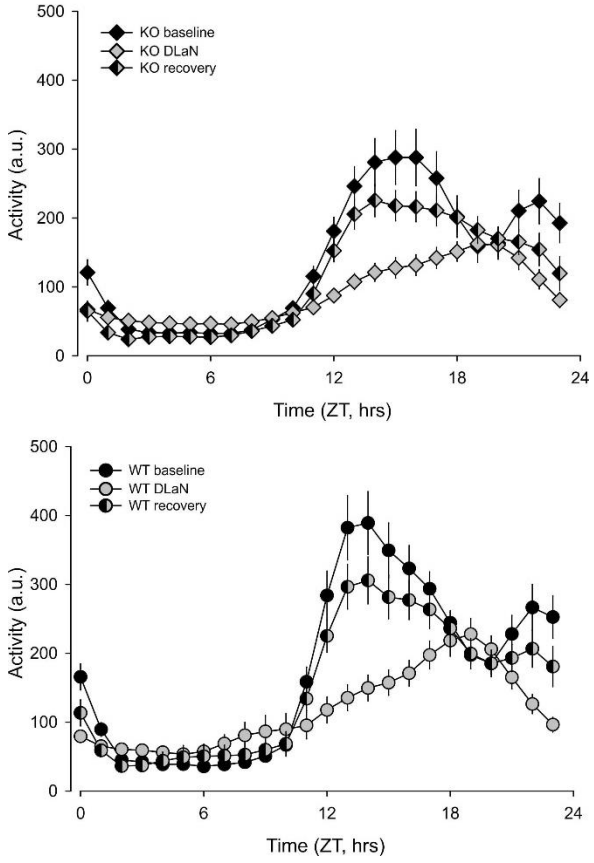

S. Fig. 1.4: The *Cntnap2* KO and WT mice recovered from the DLaN treatment. Cage activity of mutant and WT mice was measured before, during and 2 weeks after treatment with DLaN in new cohort of mice. Both *Cntnap2* KO (**A**) and WT (**B**) mice showed the expected suppression in the amplitude of the activity rhythm as shown with the earlier mice. The mutants were also obviously hypoactive compared to controls. Activity levels were largely recovered to baseline after 2 weeks in the normal LD cycle.

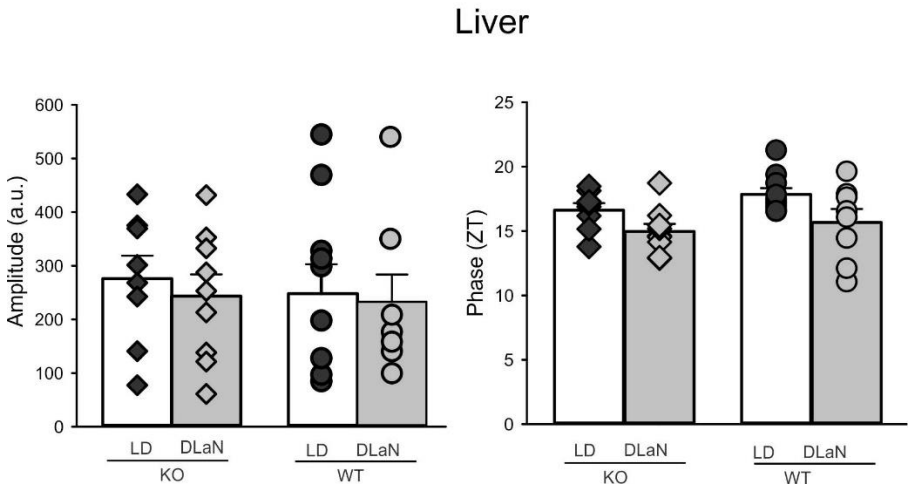

S. Fig. 1.5: DLaN did not alter the PER2::LUC bioluminescence rhythms measured in the liver. Bioluminescence rhythms measured from the *Cntnap2* KO and WT liver under LD and DLaN conditions. Several parameters were measured from the bioluminescence rhythms and analyzed with 2-way ANOVA. Amplitude and phase did not appear to be altered by the treatment ($P > 0.05$). Histograms show means ± SEM with the values from individual animals overlaid.

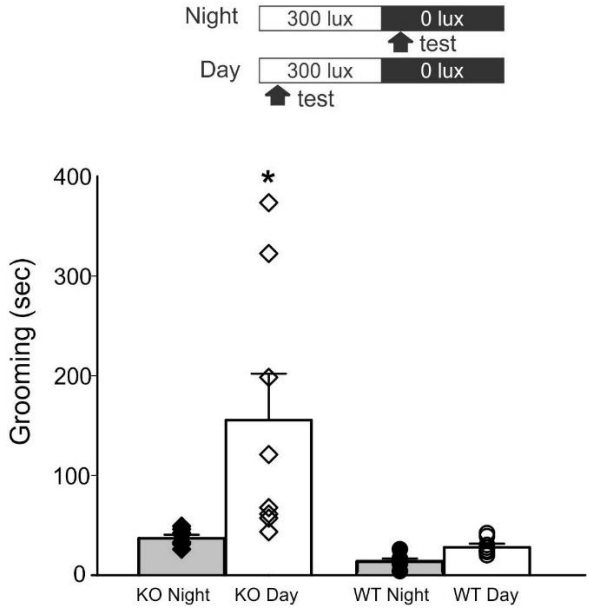

S. Fig. 1.6: Repetitive behavior was highest in the day in *Cntnap2* mutants. Grooming was assessed in a novel arena from mice of each genotype (*Cntnap2* KO, WT; *n*=8 per group) in the light and dark portion of the LD cycle. In the day, the grooming behavior was higher in the *Cntnap2* KO compared to WT. Grooming behavior was significantly increased by genotype ($F_{(1,31)}$ = 11.053, P = 0.002) and time ($F_{(1, 31)}$ = 8.643, P = 0.007). There was a significant interaction between the two factors ($F_{(1, 31)}$ = 4.760, P = 0.038). Post-hoc comparison found that the mutants showed increased grooming compared to WT in the day (t = 3.894, P <0.001) but not in the night (t = 0.808, P = 0.426). Histograms show means ± SEM with the values from individual animals overlaid.

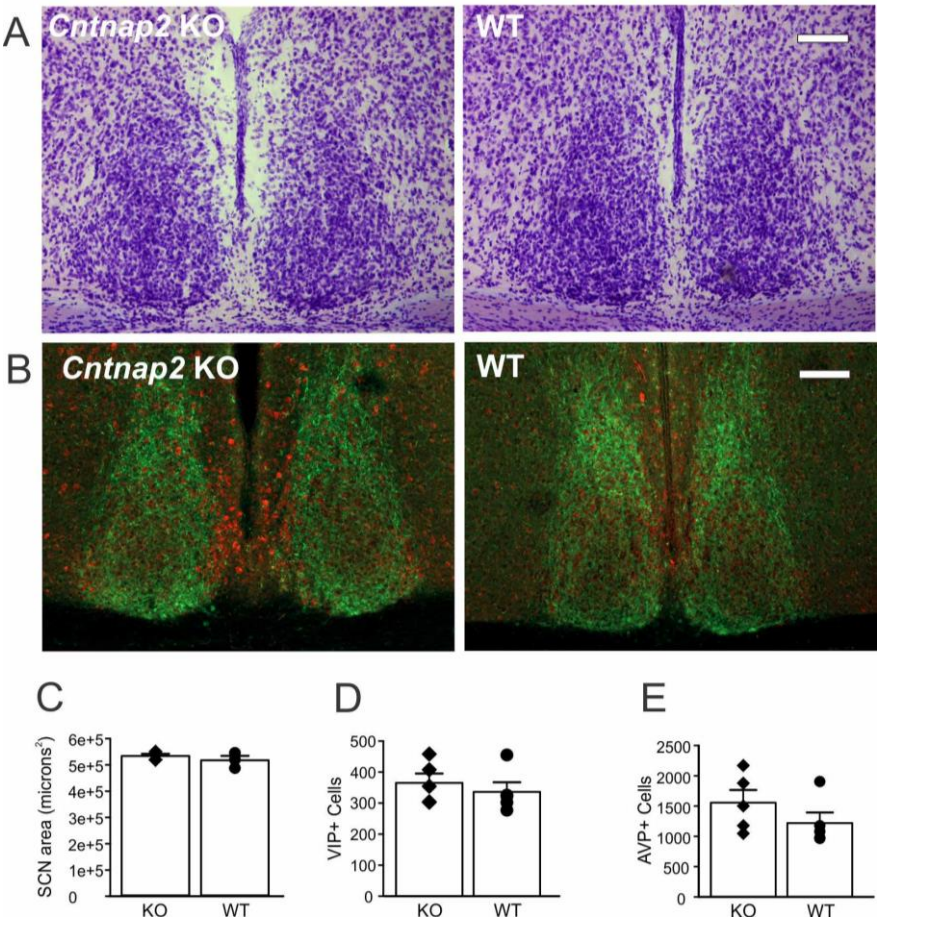

S. Fig. 1.7: No changes in SCN morphology or peptide expression in *Cntnap2* KO mice. Animals were perfused during the night (ZT 14), and serial coronal slices containing the whole SCN were stained with cresyl violet (Nissl staining) (**A**) or with antibodies against the neuropeptides VIP (green) & AVP (red) (**B**). Gross morphometric measurements of the Nissl-defined SCN revealed no differences in the area of the SCN of *Cntnap2* KO mice compared to WT mice (**C**). Individual data points represent the average ± SEM of the left and right SCN values measured in 7 consecutive slices/animal (n=4 animals/genotype). No genotypic differences were found in the number of VIP (**D**) and AVP (**E**) positive neurons. Individual data points represent the number of positive cell counted per animal for each group (n=5 animals/genotype). Columns represent the mean ± SEM. Scale bar=100µm

Tables

Table 1.1. Rhythms in locomotor activity and sleep behavior in Cntnap2 KO mice were disrupted by dim light at night (DLaN). Comparisons of age-matched WT and Cntnap2 KO mice under LD or DLaN regimen (n = 8/group). Values are shown as averages ± SEM. Data were analyzed with a two-way ANOVA using genotype and treatment as factors. The Holm-Sidak test for multiple comparisons was used when appropriate. * indicates significant differences between LD controls and those exposed to DLaN. P values < 0.05 were considered significant and are shown in bold.

Locomotor Activity rhythms

	Cntnap2 KO	*Cntnap2* KO + DLaN	WT	WT + DLaN	Genotype	Treatment
Power (% variance)	29.5 ± 2.1	21.6 ± 1.8*	39.2 ± 2.1	26.6 ± 1.9*	**F=13.789; P<0.001**	**F=26.780; P<0.001**
Cage Activity (a.u./hr)	139.2 ± 11.6	84.1 ± 9.9*	172.6 ± 11.6	93.1 ± 10.9*	F=3.716; P=0.063	**F=37.428; P<0.001**
Activity in day (%)	20.8 ± 1.9	26.1 ± 1.8*	15.9 ± 1.0	23.1 ± 1.1*	**F=6.097; P=0.019**	**F=15.346; P<0.001**
Onset Variability (min)	25.7 ± 2.1	48.8 ± 6.2*	7.1 ± 2.1	29.4 ± 6.5*	**F=29.686; P<0.001**	**F=41.644; P<0.001**
Fragmentation	9.8 ± 0.9	11.6 ± 0.9	9.0 ± 0.9	11.3 ± 0.9	F=1.173; P=0.287	F=2.888; P=0.089

Sleep Behavior rhythms

	Cntnap2 KO	*Cntnap2* KO + DLaN	WT	WT + DLaN	Genotype	Treatment
Daily sleep (min)	908.6 ± 43.8	1042.6 ± 49.4*	943.5 ± 52.8	1018.0 ± 54.7*	F=0.011; P=0.914	**F=4.762; P=0.036**
Sleep in day (min)	590.9 ± 17.6	564.6 ± 33.1	622.0 ± 27.8	569.4 ± 50.3	F=0.274; P=0.604	F=1.318; P=0.258
Sleep in night (min)	317.7 ± 28.2	478.0 ± 49.8*	321.5 ± 32.3	448.6 ± 53.2*	F=0.091; P=0.764	**F=11.533; P=0.002**
Bouts in day (#)	3.7 ± 0.5	3.9 ± 0.2	4.3 ± 0.2	3.3 ± 0.5	F=1.118; p=0.299	**F=14.492; p<0.001**
Bouts in night (#)	6.3 ± 0.4	5.7 ± 0.4	5.8 ± 0.6	6.1 ± 0.5	F=0.067; p=0.797	F=1.966; p=0.172
Bout duration day	177.4 ± 26.7	207.5 ± 33.0	229.0 ± 54.7	161.2 ± 27.1	F=1.581; P=0.217	F=1.329; P=0.257
Bout duration night	47.7 ± 4.8	89.8 ± 15.8*	54.4 ± 3.9	82.7 ± 9.2*	F=0.007; P=0.979	**F=14.676; P<0.001**
Sleep onset (ZT)	21.2 ± 2.4	22.2 ± 0.6*	24.4 ± 0.2	23.2 ± 0.2*	**F=5.639; P=0.023**	**F=20.617; P<0.001**

Table 1.2. DLaN alters the peak phase and amplitude of the PER2::LUC rhythms measured in SCN, hippocampus, and liver. Comparisons of age-matched WT and Cntnap2 KO mice under standard LD or DLaN regimen (n=7-9/group). Data were analyzed with a two-way ANOVA using genotype and treatment as factors. The Holm-Sidak test for multiple comparisons was used when appropriate. * indicates significant differences between LD controls and those exposed to DLaN. P values < 0.05 were considered significant and are shown in bold.

	Cntnap2 KO	Cntnap2 KO + DLaN	WT	WT + DLaN	Genotype	Treatment
SCN						
Tau	24.4 ± 0.2	24.6 ± 0.2	24.3 ± 0.2	24.8 ± 0.2	F=0.024; P=0.879	F=1.838; P=0.186
Amplitude	59.8 ± 5.2	16.5 ± 5.6*	53.3 ± 4.9	24.3 ± 5.2*	F=0.014; P=0.907	**F=47.458; P<0.001**
Phase	12.8 ± 0.5	10.9 ± 0.6*	13.1 ± 0.5	12.8 ± 0.5	**F=4.424; P=0.045**	**F=4.726; P=0.038**
Damping rate	-0.33 ± 0.03	-0.29 ± 0.04	-0.30 ± 0.02	-0.36 ± 0.04	F=0.540;P=0.469	F=0.211; P=0.105
Hippocampus						
Tau	23.8 ± 0.2	23.5 ± 0.2	23.8 ± 0.2	23.9 ± 0.2	F=0.629; P=0.450	F=0.205 P=0.654
Amplitude	37.2 ± 4.7	12.9 ± 4.4*	22.9 ± 4.7	29.5 ± 5.0	F=0.065; P=0.800	F=3.566; P=0.069
Phase	20.6 ± 1.2	14.4 ± 1.2*	20.9 ± 1.2	16.0 ± 1.2*	F=0.602; P=0.444	**F=20.108; P<0.001**
Damping rate	-0.30 ± 0.02	-0.27 ± 0.06	-0.35 ± 0.04	-0.323 ± 0.06	F=1.355; P=0.254	F=0.344; P=0.562
Liver						
Tau	23.0 ± 0.2	22.9 ± 0.2	23.0 ± 0.2	23.4 ± 0.2	F=1.502; p=0.752	F=0.444; P=0.510
Amplitude	276.2 ± 50.6	243.7 ± 47.7	248.3 ± 45.2	232.9 ± 50.6	F=0.158; P=0.694	F=0.242; P<0.626
Phase	16.6 ± 0.7	15.0 ± 0.7	17.8 ± 0.6	15.72 ± 0.7*	F=2.002; P=0.167	**F=7.903; P=0.008**
Damping rate	-0.22 ± 0.07	-0.12 ± 0.05	-0.14 ± 0.04	-0.17 ± 0.05	F=0.116; P=0.736	F=0.518; P=0.477

Table 1.3. DLaN impacted social and grooming behavior. Two-way ANOVA followed by Holm-Sidak's multiple comparisons test was used to evaluate the effects of genotype and time, and their interaction. Degrees of freedom are reported in parentheses. Data are reported as the mean ± SEM. P values < 0.05 were considered significant and are shown in bold.

Three chambered social test

	Cntnap2 KO	*Cntnap2* KO + DLaN	WT	WT + DLaN	Genotype	Treatment
Center chamber (sec)	153.9 ± 19.1	163.6 ± 19.7	154.5 ± 15.4	144.8 ± 13.3	F=0.265; P=0.610	F=0.001; P=0.999
Social chamber (sec)	231.2 ± 26.3.6	164.4 ± 15.8*	271.3 ± 15.1	236.6 ± 16.8	**F=8.066 P=0.008**	**F=6.669; P=0.014**
Object chamber (sec	218.6 ± 13.8	283.0 ± 22.9*	166.8 ± 11.7	218.6 ± 13.8	**F=8.111; P=0.008**	**F=9.326; P=0.004**
Social Index	0.02 ± 0.09	-0.26 ± 0.07*	0.24 ± 0.5	0.04 ± 0.06*	**F=11.757; P=0.002**	**F=13.892; P<0.001**

Grooming

	Cntnap2 KO	*Cntnap2* KO + DLaN	WT	WT + DLaN	Genotype	Treatment
Grooming (sec)	26.7 ± 2.0	66.0 ± 14.2*	8.6 ± 1.7	13.7 ± 1.8	**F=21.986; P<0.001**	**F=8.231; P=0.007**
Distance (m)	47.1 ± 3.1	38.1 ± 2.0	39.4 ± 2.3	34.6 ± 1.8	F=3.603; P=0.065	**F=5.846; P=0.020**

Table 1.4. Melatonin effective counter-measure for DLaN-evoked grooming behavior. Two-way ANOVA followed by Holm-Sidak's multiple comparisons test was used to evaluate the effects of genotype and treatment. Data are reported as the mean ± SEM. P values < 0.05 were considered significant and are shown in bold.

Grooming

	Cntnap2 KO DLaN vehicle	*Cntnap2* KO DLaN melatonin	WT DLaN vehicle	WT DLaN melatonin	Genotype	Treatment
Grooming (sec)	27.7 ± 2.5	11.4 ± 1.6	8.4 ± 1.1	8.5 ± 1.1	**F = 25.338; P<0.001**	**F=7.074; P=0.012**

Activity rhythms

	Cntnap2 KO LD vehicle	*Cntnap2* KO DLaN melatonin	WT LD vehicle	WT DLaN melatonin	Genotype	Treatment
Power (% variance)	29.6 ± 2.3	40.6 ± 1.9	26.2 ± 2.1	33.7 ± 1.6	F=3.816; P<0.058	**F=12.350; P=0.001**
Activity (a.u./24 hr)	2116.1 ± 173.6	2075.8 ± 139.4	2864.4 ± 249.7	4200.4 ± 484.8	**F=37.432; P<0.001**	**F=7.614; P=0.009**
Daytime activity (%)	18.5 ± 1.3	12.7 ± 1.4	16.2 ± 1.6	11.7 ± 0.8	F = 0.939; P=0.338	**F = 9.649; P=0.003**
Onset Variability (min)	30.1 ± 3.9	12.8 ± 2.0	43.3 ± 1.8	36.7 ± 3.8	**F = 15.366; P<0.001**	**F = 9.099; P=0.005**
Fragmentation	11.8 ± 0.4	10.7 ± 0.5	8.6 ± 0.5	9.4 ± 0.6	**F=14.213; P<0.001**	F=0.089; P=0.763

References

Andersen IM, Kaczmarska J, McGrew SG, Malow BA (2008). Melatonin for insomnia in children with autism spectrum disorders. *J Child Neurol* 23(5), 482-485. doi:10.1177/0883073807309783

Angelakos CC, Tudor JC, Ferri SL, Jongens TA, Abel T (2019). Home-cage hypoactivity in mouse genetic models of autism spectrum disorder. *Neurobiol Learn Mem* 165, 107000. doi:10.1016/j.nlm.2019.02.010.

Arking DE, Cutler DJ, Brune CW, Teslovich TM, West K, Ikeda M, Rea A, Guy M, Lin S, Cook EH, Chakravarti A (2008). A common genetic variant in the neurexin superfamily member CNTNAP2 increases familial risk of autism. *Am J Hum Genet* 82(1), 160-164. doi:10.1016/j.ajhg.2007.09.015

Bakkaloglu B, O'Roak BJ, Louvi A, Gupta AR, Abelson JF, Morgan TM, Chawarska K, Klin A, Ercan-Sencicek AG, Stillman AA, Tanriover G, Abrahams BS, Duvall JA, Robbins EM, Geschwind DH, Biederer T, Gunel M, Lifton RP, State MW (2008). Molecular cytogenetic analysis and resequencing of contactin associated protein-like 2 in autism spectrum disorders. *Am J Hum Genet* 82(1), 165-173. doi:10.1016/j.ajhg.2007.09.017

Bedrosian TA, Fonken LK, Nelson RJ (2016). Endocrine Effects of Circadian Disruption. *Annu Rev Physiol* 78, 109-131. doi:10.1146/annurev-physiol-021115-105102

Bedrosian TA, Fonken LK, Walton JC, Haim A, Nelson RJ (2011). Dim light at night provokes depression-like behaviors and reduces CA1 dendritic spine density in female hamsters. *Psychoneuroendocrinology* 36(7), 1062-1069. doi:10.1016/j.psyneuen.2011.01.004

Borniger JC, McHenry ZD, Abi Salloum BA, Nelson RJ (2014). Exposure to dim light at night during early development increases adult anxiety-like responses. *Physiol Behav* 133, 99-106. doi:10.1016/j.physbeh.2014.05.012

Brown, L. A., Fisk, A. S., Pothecary, C. A., & Peirson, S. N. (2019). Telling the Time with a Broken Clock: Quantifying Circadian Disruption in Animal Models. *Biology (Basel)* 8(1), 18. doi:10.3390/biology8010018

Brunner D, Kabitzke P, He D, Cox K, Thiede L, Hanania T, Sabath E, Alexandrov V, Saxe M, Peles E, Mills A, Spooren W, Ghosh A, Feliciano P, Benedetti M, Luo Clayton A, Biemans B (2015). Comprehensive Analysis of the 16p11.2 Deletion and Null Cntnap2 Mouse Models of Autism Spectrum Disorder. *PLoS One* 10(8), e0134572. doi:10.1371/journal.pone.0134572

Burke TM, Markwald RR, Chinoy ED, Snider JA, Bessman SC, Jung CM, Wright KP, Jr. (2013). Combination of light and melatonin time cues for phase advancing the human circadian clock. *Sleep* 36(11), 1617-1624. doi:10.5665/sleep.3110

Chang AM, Aeschbach D, Duffy JF, Czeisler CA (2015). Evening use of light-emitting eReaders negatively affects sleep, circadian timing, and next-morning alertness. *Proc Natl Acad Sci USA* 112(4), 1232-1237. doi:10.1073/pnas.1418490112

Czeisler CA (2013). Perspective: casting light on sleep deficiency. *Nature* 497(7450), S13. doi:10.1038/497S13a

Devnani PA, Hegde AU (2015). Autism and sleep disorders. *J Pediatr Neurosci* 10(4), 304-307. doi:10.4103/1817-1745.174438

Dominoni D, Quetting M, Partecke J (2013). Artificial light at night advances avian reproductive physiology. *Proc Biol Sci* 280(1756), 20123017. doi:10.1098/rspb.2012.3017

Ebihara S, Marks T, Hudson DJ, Menaker M (1986). Genetic control of melatonin synthesis in the pineal gland of the mouse. *Science* 231(4737),491-493. doi:10.1126/science.3941912.

Eckerberg B, Lowden A, Nagai R, Akerstedt T (2012). Melatonin treatment effects on adolescent students' sleep timing and sleepiness in a placebo-controlled crossover study. *Chronobiol Int* 29(9), 1239-1248. doi:10.3109/07420528.2012.719962

Elrod MG, Hood BS (2015). Sleep differences among children with autism spectrum disorders and typically developing peers: a meta-analysis. *J Dev Behav Pediatr* 36(3), 166-177. doi:10.1097/DBP.0000000000000140

Engelhardt CR, Mazurek MO, Sohl K (2013). Media use and sleep among boys with autism spectrum disorder, ADHD, or typical development. *Pediatrics* 132(6), 1081-9. doi:10.1542/peds.2013-2066.

Falchi F, Cinzano P, Duriscoe D, Kyba CCM, Elvidge CD, Baugh K, Portnov BA, Rybnikova NA, Furgoni R (2016). The new world atlas of artificial night sky brightness. *Science Advances* 2(6), e1600377. doi:10.1126/sciadv.1600377.

Fernandez DC, Fogerson PM, Lazzerini Ospri L, Thomsen MB, Layne RM, Severin D, Zhan J, Singer JH, Kirkwood A, Zhao H, Berson DM, Hattar S. (2018). Light Affects Mood and Learning through Distinct Retina-Brain Pathways. *Cell* 175(1), 71-84.e18. doi:10.1016/j.cell.2018.08.004.

Fisher SP, Schwartz MD, Wurts-Black S, Thomas AM, Chen TM, Miller MA, Palmerston JB, Kilduff TS, Morairty SR (2016) Quantitative Electroencephalographic Analysis Provides an Early-Stage Indicator of Disease Onset and Progression in the zQ175 Knock-In Mouse Model of Huntington's Disease. Sleep. 39(2),379-91. doi:10.5665/sleep.5448.

Fonken LK, Aubrecht TG, Melendez-Fernandez OH, Weil ZM, Nelson RJ (2013). Dim light at night disrupts molecular circadian rhythms and increases body weight. *J Biol Rhythms* 28(4), 262-27. doi:10.1177/0748730413493862

Fonken LK, Kitsmiller E, Smale L, Nelson RJ (2012). Dim nighttime light impairs cognition and provokes depressive-like responses in a diurnal rodent. *J Biol Rhythms* 27(4), 319-327. doi:10.1177/0748730412448324

Fonken LK, Nelson RJ (2011). Illuminating the deleterious effects of light at night. *F1000 Med Rep* 3, 18. doi:10.3410/M3-18

Gandal MJ, Zhang P, Hadjimichael E, Walker RL, Chen C, Liu S, Won H, van Bakel H, Varghese M, Wang Y, Shieh AW, Haney J, Parhami S, Belmont J, Kim M, Moran Losada P, Khan Z, Mleczko J, Xia Y, Dai R, Wang D, Yang YT, Xu M, Fish K, Hof PR, Warrell J, Fitzgerald D, White K, Jaffe AE; PsychENCODE Consortium, Peters MA, Gerstein M, Liu C, Iakoucheva LM, Pinto D, Geschwind DH (2018). Transcriptome-wide isoform-level dysregulation in ASD, schizophrenia, and bipolar disorder. *Science* 362(6420). pii, eaat8127. doi:10.1126/science.aat8127

Garstang J, Wallis M (2006). Randomized controlled trial of melatonin for children with autistic spectrum disorders and sleep problems. *Child Care Health Dev* 32(5), 585-589. doi:10.1111/j.1365-2214.2006.00616.x

Giannotti F, Cortesi F, Cerquiglini A, Bernabei P (2006). An open-label study of controlled-release melatonin in treatment of sleep disorders in children with autism. *J Autism Dev Disord* 36(6), 741-752. doi:10.1007/s10803-006-0116-z

Goldman SE, Adkins KW, Calcutt MW, Carter MD, Goodpaster RL, Wang L, Shi Y, Burgess HJ, Hachey DL, Malow BA (2014). Melatonin in children with autism spectrum disorders: endogenous and pharmacokinetic profiles in relation to sleep. *J Autism Dev Disord* 44(10), 2525-2535. doi:10.1007/s10803-014-2123-9

Gronli J, Byrkjedal IK, Bjorvatn B, Nodtvedt O, Hamre B, Pallesen S (2016). Reading from an iPad or from a book in bed: the impact on human sleep. A randomized controlled crossover trial. *Sleep Med* 21, 86-92. doi:10.1016/j.sleep.2016.02.006

Hundley RJ, Shui A, Malow BA.(2016). Relationship Between Subtypes of Restricted and Repetitive Behaviors and Sleep Disturbance in Autism Spectrum Disorder. *J Autism Dev Disord* 46(11),3448-3457. doi: 10.1007/s10803-016-2884-4.

Iossifov I, Ronemus M, Levy D, Wang Z, Hakker I, Rosenbaum J, Yamrom B, Lee YH, Narzisi G, Leotta A, Kendall J, Grabowska E, Ma B, Marks S, Rodgers L, Stepansky A, Troge J, Andrews P, Bekritsky M, Pradhan K, Ghiban E, Kramer M, Parla J, Demeter R, Fulton LL, Fulton RS, Magrini VJ, Ye K, Darnell JC, Darnell RB, Mardis ER, Wilson RK, Schatz MC, McCombie WR, Wigler M (2012). De novo gene disruptions in children on the autistic spectrum. *Neuron* 74(2), 285-299. doi:10.1016/j.neuron.2012.04.009

Kawabe K, Horiuchi F, Oka Y, Ueno S (2014). The melatonin receptor agonist ramelteon effectively treats insomnia and behavioral symptoms in autistic disorder. *Case Rep Psychiatry* 2014, 561071. doi:10.1155/2014/561071

Kuljis DA, Loh DH, Truong D, Vosko AM, Ong ML, McClusky R, Arnold AP, Colwell CS (2013). Gonadal- and sex-chromosome-dependent sex differences in the circadian system. *Endocrinology* 154(4), 1501-12. doi:10.1210/en.2012-1921.

Lazzerini Ospri L, Prusky G, Hattar S (2017). Mood, the Circadian System, and Melanopsin Retinal Ganglion Cells. *Annu Rev Neurosci.* 40, 539-556. doi:10.1146/annurev-neuro-072116-031324.

Lee FY, Wang HB, Hitchcock ON, Loh DH, Whittaker DS, Kim YS, Aiken A, Kokikian C, Dell'Angelica EC, Colwell CS, Ghiani CA (2018). Sleep/Wake Disruption in a Mouse Model of BLOC-1 Deficiency. Front Neurosci. 12:759. doi: 10.3389/fnins.2018.00759.

Lein, E., Hawrylycz, M., Ao, N. et al (2007). Genome-wide atlas of gene expression in the adult mouse brain. *Nature* 445(7124), 168–176 doi:10.1038/nature05453

Logan RW, McClung CA (2019). Rhythms of life: circadian disruption and brain disorders across the lifespan. *Nat Rev Neurosci*. 20(1), 49-65. doi:10.1038/s41583-018-0088-y.

Loh DH, Kudo T, Truong D, Wu Y, Colwell CS. (2013) The Q175 mouse model of Huntington's disease shows gene dosage- and age-related decline in circadian rhythms of activity and sleep. *PLoS One*.8(7),e69993. doi:10.1371/journal.pone.0069993.

Lucassen EA, Coomans CP, van Putten M, de Kreij SR, van Genugten JH, Sutorius RP, de Rooij KE, van der Velde M, Verhoeve SL, Smit JW, Lowik CW, Smits HH, Guigas B, Aartsma-Rus AM, Meijer JH (2016). Environmental 24-hr Cycles Are Essential for Health. *Curr Biol* 26(14), 1843-1853. doi:10.1016/j.cub.2016.05.038

Malow B, Adkins KW, McGrew SG, Wang L, Goldman SE, Fawkes D, Burnette C (2012). Melatonin for sleep in children with autism: a controlled trial examining dose, tolerability, and outcomes. *J Autism Dev Disord* 42(8), 1729-1737; author reply 1738. doi:10.1007/s10803-011-1418-3

Malow BA, Katz T, Reynolds AM, Shui A, Carno M, Connolly HV, Coury D, Bennett AE (2016). Sleep Difficulties and Medications in Children With Autism Spectrum Disorders: A Registry Study. *Pediatrics* 137 Suppl 2, S98-S104 doi:10.1542/peds.2015-2851H

Mazurek MO, Engelhardt CR, Hilgard J, Sohl K (2016). Bedtime Electronic Media Use and Sleep in Children with Autism Spectrum Disorder. *J Dev Behav Pediatr* 37(7), 525–531. doi:10.1097/DBP.0000000000000314

Mazurek MO, Sohl K (2016). Sleep and Behavioral Problems in Children with Autism Spectrum Disorder. *J Autism Dev Disord* 46(6), 1906-1915. doi:10.1007/s10803-016-2723-7

Nord AS, Roeb W, Dickel DE, Walsh T, Kusenda M, O'Connor KL, Malhotra D, McCarthy SE, Stray SM, Taylor SM, Sebat J, Network SP, King B, King MC, McClellan JM (2011). Reduced transcript expression of genes affected by inherited and de novo CNVs in autism. *Eur J Hum Genet* 19(6), 727-731. doi:10.1038/ejhg.2011.24

Noya SB, Colameo D, Brüning F, Spinnler A, Mircsof D, Opitz L, Mann M, Tyagarajan SK, Robles MS, Brown SA (2019). The forebrain synaptic transcriptome is organized by clocks but its proteome is driven by sleep. *Science* 366(6462). pii, eaav2642. doi:10.1126/science.aav2642.

Ohta H, Yamazaki S, McMahon DG (2005). Constant light desynchronizes mammalian clock neurons. *Nat Neurosci.* 8(3), 267-269. doi:10.1038/nn1395.

O'Roak BJ, Deriziotis P, Lee C, Vives L, Schwartz JJ, Girirajan S, Karakoc E, Mackenzie AP, Ng SB, Baker C, Rieder MJ, Nickerson DA, Bernier R, Fisher SE, Shendure J, Eichler EE (2011). Exome sequencing in sporadic autism spectrum disorders identifies severe de novo mutations. *Nat Genet* 43(6), 585-589. doi:10.1038/ng.835

O'Roak BJ, Vives L, Girirajan S, Karakoc E, Krumm N, Coe BP, Levy R, Ko A, Lee C, Smith JD, Turner EH, Stanaway IB, Vernot B, Malig M, Baker C, Reilly B, Akey JM, Borenstein E, Rieder MJ, Nickerson DA, Bernier R, Shendure J, Eichler EE (2012). Sporadic autism exomes reveal a highly interconnected protein network of de novo mutations. *Nature* 485(7397), 246-250. doi:10.1038/nature10989

Peippo M, Ignatius J (2012). Pitt-Hopkins Syndrome. *Mol Syndromol* 2(3-5), 171-180. doi:10.1159/000335287

Peñagarikano O, Abrahams BS, Herman EI, Winden KD, Gdalyahu A, Dong H, Sonnenblick LI, Gruver R, Almajano J, Bragin A, Golshani P, Trachtenberg JT, Peles E, Geschwind DH

(2011). Absence of CNTNAP2 leads to epilepsy, neuronal migration abnormalities, and core autism-related deficits. *Cell* 147(1), 235-246. doi:10.1016/j.cell.2011.08.040

Peñagarikano O, Lázaro MT, Lu XH, Gordon A, Dong H, Lam HA, Peles E, Maidment NT, Murphy NP, Yang XW, Golshani P, Geschwind DH. (2015). Exogenous and evoked oxytocin restores social behavior in the Cntnap2 mouse model of autism. *Sci Transl Med.* 7(271), 271ra8. doi:10.1126/scitranslmed.3010257.

Poliak S, Gollan L, Martinez R, Custer A, Einheber S, Salzer JL, Trimmer JS, Shrager P, Peles E (1999). Caspr2, a new member of the neurexin superfamily, is localized at the juxtaparanodes of myelinated axons and associates with K+ channels. *Neuron* 24(4), 1037-1047. doi:10.1016/s0896-6273(00)81049-1

Raap T, Pinxten R, Eens M (2015). Light pollution disrupts sleep in free-living animals. *Sci Rep* 5, 13557. doi:10.1038/srep13557

Riemersma-van der Lek RF, Swaab DF, Twisk J, Hol EM, Hoogendijk WJ, Van Someren EJ (2008). Effect of bright light and melatonin on cognitive and noncognitive function in elderly residents of group care facilities: a randomized controlled trial. *JAMA* 299(22), 2642-2655. doi:10.1001/jama.299.22.2642

Robinson-Shelton A, Malow BA (2016). Sleep Disturbances in Neurodevelopmental Disorders. *Curr Psychiatry Rep* 18(1), 6. doi:10.1007/s11920-015-0638-1

Roenneberg T, Merrow M (2016). The Circadian Clock and Human Health. *Curr Biol* 26(10), R432-443. doi:10.1016/j.cub.2016.04.011

Rossignol DA, Frye RE (2014). Melatonin in autism spectrum disorders. *Curr Clin Pharmacol* 9(4), 326-334. doi:10.2174/15748847113086660072

Rybnikova NA, Haim A, Portnov BA (2016). Does artificial light-at-night exposure contribute to the worldwide obesity pandemic? *Int J Obes (Lond)* 40(5), 815-823. doi:10.1038/ijo.2015.255

Sanders SJ, Murtha MT, Gupta AR, Murdoch JD, Raubeson MJ, Willsey AJ, Ercan-Sencicek AG, DiLullo NM, Parikshak NN, Stein JL, Walker MF, Ober GT, Teran NA, Song Y, El-Fishawy P, Murtha RC, Choi M, Overton JD, Bjornson RD, Carriero NJ, Meyer KA, Bilguvar K, Mane SM, Sestan N, Lifton RP, Gunel M, Roeder K, Geschwind DH, Devlin B, State MW (2012). De novo mutations revealed by whole-exome sequencing are strongly associated with autism. *Nature* 485(7397), 237-241. doi:10.1038/nature10945

Schroder CM, Malow BA, Maras A, Melmed RD, Findling RL, Breddy J, Nir T, Shahmoon S, Zisapel N, Gringras P (2019). Pediatric Prolonged-Release Melatonin for Sleep in Children with Autism Spectrum Disorder: Impact on Child Behavior and Caregiver's Quality of Life. *J Autism Dev Disord*.49(8), 3218-3230. doi: 10.1007/s10803-019-04046-5.

Schroeder AM, Colwell CS (2013). How to fix a broken clock. *Trends Pharmacol Sci* 34(11), 605-619. doi:10.1016/j.tips.2013.09.002

Schwichtenberg AJ, Malow BA (2015). Melatonin Treatment in Children with Developmental Disabilities. *Sleep Med Clin* 10(2), 181-187. doi:10.1016/j.jsmc.2015.02.008

Shi SQ, Johnson CH (2019). Circadian biology and sleep in monogenic neurological disorders and its potential application in drug discovery. *Curr Opin Behav Sci* 25, 23-30. doi:10.1016/j.cobeha.2018.06.006.

Stevenson TJ, Visser ME, Arnold W, Barrett P, Biello S, Dawson A, Denlinger DL, Dominoni D, Ebling FJ, Elton S, Evans N, Ferguson HM, Foster RG, Hau M, Haydon DT, Hazlerigg DG, Heideman P, Hopcraft JG, Jonsson NN, Kronfeld-Schor N, Kumar V, Lincoln GA, MacLeod R, Martin SA, Martinez-Bakker M, Nelson RJ, Reed T, Robinson JE, Rock D,

Schwartz WJ, Steffan-Dewenter I, Tauber E, Thackeray SJ, Umstatter C, Yoshimura T, Helm B (2015). Disrupted seasonal biology impacts health, food security and ecosystems. *Proc Biol Sci* 282(1817), 20151453. doi:10.1098/rspb.2015.1453

Strauss KA, Puffenberger EG, Huentelman MJ, Gottlieb S, Dobrin SE, Parod JM, et al., (2006). Recessive symptomatic focal epilepsy and mutant contactin-associated protein-like 2. *N Engl J Med* 354(13), 1370-1377. doi:10.1056/NEJMoa052773

Takahashi JS, Shimomura K, Kumar V (2008). Searching for genes underlying behavior: lessons from circadian rhythms. *Science* 322(5903), 909-12. doi: 10.1126/science.1158822.

Takumi T, Tamada K, Hatanaka F, Nakai N, Bolton PF (2019). Behavioral neuroscience of autism. *Neurosci Biobehav Rev.* pii, S0149-7634(18)30372-5. doi:10.1016/j.neubiorev.2019.04.012.

Thomas AM, Schwartz MD, Saxe MD, Kilduff TS (2017). Cntnap2 Knockout Rats and Mice Exhibit Epileptiform Activity and Abnormal Sleep-Wake Physiology. *Sleep*. 40(1), 10.1093/sleep/zsw026. doi:10.1093/sleep/zsw026.

Veatch OJ, Maxwell-Horn AC, Malow BA (2015). Sleep in Autism Spectrum Disorders. *Curr Sleep Med Rep* 1(2), 131-140. doi:10.1007/s40675-015-0012-1

Walker WH 2nd, Borniger JC, Gaudier-Diaz MM, Hecmarie Meléndez-Fernández O, Pascoe JL, Courtney DeVries A, Nelson RJ (2019). Acute exposure to low-level light at night is sufficient to induce neurological changes and depressive-like behavior. *Mol Psychiatry* 25(5), 1080-1093. doi:10.1038/s41380-019-0430-4.

Wang H-B, Whittaker DS, Truong D, Mulji AK, Ghiani CA, Loh DH, Colwell CS (2017). Blue light therapy improves circadian dysfunction as well as motor symptoms in two mouse models of Huntington's disease. *Neurobiol Sleep Circadian Rhythms* 2, 39–52. doi:10.1016/j.nbscr.2016.12.002.

Wang HB, Loh DH, Whittaker DS, Cutler T, Howland D, Colwell CS (2018). Time-Restricted Feeding Improves Circadian Dysfunction as well as Motor Symptoms in the Q175 Mouse Model of Huntington's Disease. *eNeuro*. 5(1). pii, ENEURO.0431-17.2017. doi:10.1523/ENEURO.0431-17.2017

Whittaker DS, Loh DH, Wang HB, Tahara Y, Kuljis D, Cutler T, Ghiani CA, Shibata S, Block GD, Colwell CS (2018). Circadian-based Treatment Strategy Effective in the BACHD Mouse Model of Huntington's Disease. *J Biol Rhythms* 33(5), 535-554. doi:10.1177/0748730418790401.

Wirojanan J, Jacquemont S, Diaz R, Bacalman S, Anders TF, Hagerman RJ, et al., (2009). The efficacy of melatonin for sleep problems in children with autism, fragile X syndrome, or autism and fragile X syndrome. *J Clin Sleep Med* 5(2), 145-150

Wood B, Rea MS, Plitnick B, Figueiro MG (2013). Light level and duration of exposure determine the impact of self-luminous tablets on melatonin suppression. *Appl Ergon* 44(2), 237-240. doi:10.1016/j.apergo.2012.07.008

Wright B, Sims D, Smart S, Alwazeer A, Alderson-Day B, Allgar V, et al., (2011). Melatonin versus placebo in children with autism spectrum conditions and severe sleep problems not amenable to behaviour management strategies: a randomised controlled crossover trial. *J Autism Dev Disord* 41(2), 175-184. doi:10.1007/s10803-010-1036-5

Yang M, Silverman JL, Crawley JN (2011). Automated three-chambered social approach task for mice. *Curr Protoc Neurosci* Chapter 8, Unit-8.26. doi:10.1002/0471142301.ns0826s56

Yoo SH, Yamazaki S, Lowrey PL, Shimomura K, Ko CH, Buhr ED, Siepka SM, Hong HK, Oh WJ, Yoo OJ, Menaker M, Takahashi JS (2004). PERIOD2::LUCIFERASE real-time reporting

of circadian dynamics reveals persistent circadian oscillations in mouse peripheral tissues. *Proc Natl Acad Sci USA* 101(15), 5339-46. doi:10.1073/pnas.0308709101

Zweier C, de Jong EK, Zweier M, Orrico A, Ousager LB, Collins AL, et al., (2009). CNTNAP2 and NRXN1 are mutated in autosomal-recessive Pitt-Hopkins-like mental retardation and determine the level of a common synaptic protein in *Drosophila*. *Am J Hum Genet* 85(5), 655-666. doi:10.1016/j.ajhg.2009.10.004

Chapter 3

Chapter 3

Long wavelength light reduces the negative consequences of dim light at night in the CNTNAP2 mouse model of autism.

Abstract

Many patients with autism spectrum disorders (ASD) show disturbances in their sleep/wake cycles, and may be particularly vulnerable to the impact of circadian disruptors. We have previously shown that exposure to dim light at night (DLaN) in contactin associated protein-like 2 knock out (*Cntnap2* KO) mice disrupts diurnal rhythms, increases repetitive behaviors while reducing social interactions. These negative effects of DLaN may be mediated by intrinsically photosensitive retinal ganglion cells (ipRGCs) expressing the photopigment melanopsin, which is maximally sensitive to blue light (480nm). In this study, we used a light-emitting diod (LED) array that enabled us to shift the spectral properties of the DLaN stimulus while keeping the photic energy and intensity. First, using wild-type (WT) mice, we confirmed that the short wavelength enriched lighting produced strong acute suppression of locomotor activity (masking), robust light-induced phase shifts, and evoked robust c-Fos expression in the suprachiasmatic nucleus while the long wavelength enriched lighting evoked much weaker responses as measured by the same assays. Next, we found that exposure of WT mice to the short wavelength light at night reduced the amplitude of locomotor activity rhythms as well as impaired social interactions. Mice lacking the melanopsin expressing ipRGCs ($OPN4^{dta/dta}$ mice) were resistant to these negative effects of DLaN. Importantly, the shift of the DLaN stimulus to longer wavelengths also ameliorated the negative impact on activity rhythms and autistic behaviors (i.e. reciprocal social interactions, repetitive grooming) in the *Cntnap2* KO model. The short-, but not the long-wavelength enriched, DLaN drove c-Fos expression in the peri-habenula region as well as in the basolateral amygdala (BLA). We found that the DLaN driven cFos activation occurred in glutamatergic (vGlut2 expressing) neurons in the BLA

indicating that these cells may be particularly vulnerable to the effects of photic disruption. Broadly, our findings suggest that the spectral properties of light at night should be considered in the management of ASD and other neurodevelopmental disorders.

Introduction

Dim light at night (DLaN) is a common environmental perturbation of the circadian timing system and has been linked to a range of negative consequences (Stevenson et al., 2015; Lunn et al., 2017). Prior work in pre-clinical models has demonstrated that light at night negatively impacts the metabolism (Fonken et al., 2013a; Plano et al., 2017), immune function (Bedrosian et al., 2011; Fonken et al., 2013b; Lucassen et al., 2016), mood and cognition (Lazzerini Ospri et al., 2017; An et al., 2020; Walker et al., 2020). With people spending much of their time inside, the impact of DLaN needs to be considered in our hospitals, long-term care centers classrooms, and even our homes (Fournier and Wirz-Justice, 2010; Burgess and Molina, 2014; Osibona et al., 2021; Xiao et al., 2021). People diagnosed with autism spectrum disorders (ASD) commonly experience disturbances in their circadian rhythms (Cohen et al., 2014; Devnani and Hegde, 2015; Mazurek and Sohl, 2016; Baker and Richdale, 2017; Shelton and Malow, 2021), and they might be one of populations vulnerable to such environmental perturbation. For example, studies investigating the exposure time to the electronic screens pointed out a longer screen exposure among ASD patients compared with their age-matched controls (Engelhardt et al., 2013; Stiller et al., 2019; Healy et al., 2020; Dong et al., 2021). It has been speculated that this exposure to DLAN could be detrimental to ASD populations. In support of this speculation, we previously demonstrated that the animal model with a genetic risk factor associated with ASD (contactin associated protein-like 2, *Cntnap2*) showed reduced social preference and increased stereotypic grooming behavior after a 2-week exposure to DLaN (Wang et al., 2020).

The negative effects of nightly light exposure may be mediated by intrinsically photosensitive retinal ganglion cells (ipRGCs) expressing the photopigment melanopsin, which is maximally sensitive to blue light, with a peak response to 480nm light (Hattar et al., 2002; Panda et al., 2005). In addition, ipRGCs also receive input from rod and cone photoreceptors (Hattar et al., 2002; Lucas et al., 2012; Van Diepen et al., 2021) with rods driving the circadian response to sensitivity to low-intensity light (Altimus et al., 2010; Lall et

al 2010). These findings demonstrate that the circadian system is sensitive to blue light but other wavelengths as well (Foster et al., 2020) raise questions whether changes in the spectral properties of light can be effective to minimize the negative effects of light at night.

In our prior work (Wang et al., 2020), we used white light comprised of a mix of wavelengths to generate DLaN. In this present study, we used an array of light-emitting diodes (LEDs) to generate dim illumination (10 lx) with a spectral composition that was short wavelength enriched or diminished with the goal of evaluating the contribution of melanopsin photopigment to the effects of DLaN. First, using wild-type (WT) mice, we ascertained whether the long wavelength enhanced lighting effectively reduced negative masking behaviour, light-induced phase shifts of circadian behaviour as well as reduced light-evoked c-Fos response in the suprachiasmatic nucleus (SCN). A transgenic line of mice ($OPN4^{dta/dta}$) without melanopsin expression and with diminished ipRGCs due to the targeted expression of attenuated diphtheria toxin A in the Opn4 expressing cells (Güler et al., 2008) was further used to access the contribution of ipRGC in mediating the effects of DLaN. Next, we determined whether long wavelength enhanced DLaN reducing light-driven changes in daily patterns of activity in both WT and *Cntnap2* knock-out (KO) mice. We also tested whether long wavelength enhanced DLaN reduced the impacts of light on autistic behavior (grooming and sociability) in *Cntnap2* KO mice. Finally, we examined whether long wavelength enhanced DLaN altered light-evoked changes in the number of c-Fos+ cells in selected brain regions in both WT and *Cntnap2* KO mice.

Materials and Methods

Animals

All animal procedures were performed in accordance with the UCLA animal care committee's regulations. Both adult male and female mice (3-4 month of age) were used in this study. *Cntnap2*^{tm2Pele} mutant mice backcrossed to the C57BL/6J background strain were acquired (B6.129(Cg)-*Cntnap2*^{tm2Pele}/J, https://www.jax.org/strain/017482 as previously described (Wang et al., 2020). *Cntnap2* null mutant (KO) and WT mice were obtained from heterozygous breeding pairs. Weaned mice were genotyped (TransnetYX, Cordova, TN) and group-housed prior to experimentation. Mice lacking the melanopsin expressing cells (OPN4$^{dta/dta}$ mice, stock number 035927) and their littermate WT controls were kindly provided by Dr. Anna Mathynia (Jules Stein Eye Institute, UCLA). Male and female cohorts of mice were group housed before the study and tested at adult age. From JAX, we obtained vGlut2-ires-Cre knock-in mice that have Cre recombinase expression directed to excitatory glutamatergic neuron cell bodies (Strain #:028863), as well as Ai6 mice that express robust ZsGreen1 fluorescence following Cre-mediated recombination (Strain #:007906**)**. The Ai6 is a Cre reporter allele designed to have a loxP-flanked STOP cassette preventing transcription of a CAG promoter-driven enhanced green fluorescent protein variant (ZsGreen1) - all inserted into the Gt(ROSA)26Sor locus. We bred this floxed reporter gene into the Cntnap2 mutant to create *Cntnap2* KO mice that are either heterozygous for vGlut2 Cre-Ai6 (ZsGreen1).

Lighting manipulations

Mice were housed in light-tight ventilated cabinets in temperature- and humidity-controlled conditions, with free access to food and water. All experimental mice were first entrained to a normal lighting cycle: 12:12 hr light:dark (LD). Light intensity during the day was 300 lux as measured at the base of the cage, and 0 lux during the night. The time of lights-on defines Zeitgeber Time (ZT) 0 and the time of lights-off defines ZT 12. Following entrainment to normal LD, mice were singly housed under different lighting conditions for 2 weeks: nightly

light with the spectral composition aimed to minimize the stimulation of melanopsin (long wavelength enriched lights), or light with the spectral composition aimed to maximize the stimulation of melanopsin (short wavelength-enriched lights). The treated mice were exposed nightly to one of these lights from ZT 12 to 24. Control mice were held on the normal LD 12:12 schedule. The short- and long wavelength (10 lx intensity) were generated by the Korrus (Los Angeles, CA) LED lighting system (**Fig. 2.1A)**. Following recent recommendations (Lucas et al., 2014), the LED output was measured using UPRtek spectrophotometer (Model MK350S, Taiwan) at the level of the cage floor. Using the International Commission on Illumination (CIE) S 026 α-opic Toolbox (DOI: 10.25039/S026.2018), the melanopic α-opic irradiance of the long wavelength enhanced output was estimated at 0.001 W/m^2 while short wavelength enhanced output was estimated to be 0.020 W/m^2. The melanopic α-opic equivalent daylight (D65) illuminance of the long wavelength output was estimated at 1 melanopic lx while the short wavelength output was estimated at 15 melanopic lx.

Cage activity

Daily pattern of activity was monitored using a top-mounted passive infra-red (IR) motion detector reporting to a VitalView data recording system (Mini Mitter, Bend, OR) as previously described (Wang et al., 2017; 2018). Detected movements were recorded in 3 min bins, and 10 days of data were averaged for analysis using the El Temps chronobiology program (A. Diez-Noguera, Barcelona, Spain; http://www.el-temps.com/principal.html). The strength of the rhythm was determined from the amplitude of the χ2 periodogram at 24 hr, to produce the rhythm power (%V) normalized to the number of data points examined. The periodogram analysis uses a χ2 test with a threshold of 0.001 significance, from which the amplitude of the periodicities is determined at the circadian harmonic to obtain the rhythm power. The percentage of sleep-phase activity was determined by the relative distribution of activity during the day versus the night. Fragmentation and onset variability were determined using the Clocklab program (Actimetrics, Wilmette, IL; http://actimetrics.com/products/clocklab/). Fragmentation was determined by the number of

activity bouts. Each bout was counted when activity bouts were separated by a gap of 21 min. The onset variability was by first determining the daily onset of activity over 10 days, and then determining the deviation from the best-fit line drawn through the 10 onset times. To produce the representative waveforms, hourly running averages of the same series of activity data was plotted against time of day.

Photic suppression on nocturnal activity (negative light masking)

A separate cohort of WT mice (3-4 month of age) were housed under a 12:12 LD cycle to determine the effects of LED lights (Korrus, Los Angeles, CA) at night on masking of nocturnal activity. Animals were individually housed in cages with IR motion detector in light-tight chambers with the same housing conditions as described above. Their locomotor activity was recorded per 3-min interval, and monitored to ensure the entrainment to the housing LD cycles. The animals were subjected to one hour of light (enriched for long or short wavelengths) at ZT 14. The activity level during this light exposure was compared to the activity level during the equivalent hour (ZT 14 to 15) on the day before the treatment. The fold change (%) was reported.

Phase shift of wheel-running activity

After the habituation to the running-wheel cages, a different cohort of WT mice (3-4 mo) were released into constant darkness (DD) for 10 days. The circadian time (CT) of their free-running sleep/wake cycles were monitored with the VitalView. The time of activity onset under DD was defined as CT 12. On day 11, mice were exposed to long- or short-wavelength light (10 lx, 60 min) at CT 16. After the treatment, the mice stayed in DD for following 10 days. And best-fit lines of the activity onsets of sleep/wake cycles before and after the treatment were determined and compared. No other behavioral assays were performed on these animals.

Photic induction of c-Fos in the SCN

A different cohort of WT mice (3-4 month of age) were housed in DD conditions with access to a running wheel as described above. The animals were exposed to long- or short-wavelength light (10 lx, 15 min) at CT 16. Brains were fixed 45 mins after the end of the light exposure. The testing mice were anesthetized with isoflurane and transcardially perfused with phosphate buffered saline (PBS, 0.1 M, pH 7.4) containing 4% (w/v) paraformaldehyde (PFA, Sigma). The brains were rapidly dissected out, post-fixed overnight in 4% PFA at 4 °C, and cryoprotected in 15% sucrose in 1xPBS. Sequential coronal sections (40 μm) containing the middle SCN were collected using a cryostat (Leica, Buffalo Grove, IL) and then further processed for c-Fos immunostaining as reported below.

Behavioral tests

The reciprocal social interaction test was used to assess general sociability and interest in social novelty. On days of testing, the animals were taken out from the light-tight chambers, and habituated to the testing room for at least 30 mins. To avoid sleep disruptions, all behavioral tests were conducted in the middle of the dark phase (ZT 16-18). The social behavior was evaluated by familiarizing the testing mouse with the testing arena first (habituation for 30 mins), and then introducing a never-met stranger mouse into the same arena. The stranger mouse had the same age, sex, and genotype as the testing mouse. The two mice were allowed to interact for 10 mins, and the testing trials were recorded. Duration of sniffing (nose to nose sniff and nose to anogenital sniff), social grooming (the testing mouse grooms the novel stranger mouse on any part of the body) and touching was timed and reported for the time of social behavior.

The grooming test were performed to evaluate the level of their stereotypic behaviour (ZT 16-18). After the habituation to the testing room for at least 30 mins, the testing mice were introduced to the testing arena and their behavior was recorded by a camcorder for 30 mins. The duration of grooming behavior was scored as previously described (Wang et al., 2020).

c-Fos immunochemistry staining

The immunochemistry staining of c-Fos was performed as previously described (Lee et al., 2018). The free-floating coronal sections (50 µm) containing regions of interest were blocked for 1 hr at room temperature (1% BSA, 0.3% Triton X-100, 10% normal donkey serum in 1xPBS) and then incubated overnight at 4°C with the rabbit polyclonal antibody against c-Fos (1:1000, Cell Signaling) followed by a Cy3-conjugated donkey-anti-rabbit secondary antibody (Jackson ImmunoResearch Laboratories, Bar Harbor, ME). Sections were mounted on coverslips and applied with Vectashield mounting medium containing DAPI (4'-6-diamidino-2-phenylinodole; Vector Laboratories, Burlingame, CA). Images were acquired on a Zeiss AxioImager M2 microscope equipped with an AxioCam MRm and the ApoTome imaging system.

c-Fos positive cell counting

Images for counting were acquired using either a 20X or 40X objective and the Zeiss Zen digital imaging software. Both male and female mice, in equal number, were used for each assessment and two observers masked to genotype and experimental group performed the cell counting.

Photic induction of cFos in the SCN

Images of both the left and right middle SCN were acquired with a 20X objective using the tile tool of the Zen software. The SCN was then manually traced in each image using the NIH ImageJ software (https://imagej.net/software/fiji/), and the cells immunopositive for c-Fos were counted with the aid of the cell counter plugin of ImageJ in two consecutive sections at the level of the mid-SCN. Values from the left and right SCN in the two slices were averaged to obtain one value per animal and are presented as the mean ± SEM of 4 animals/experimental group.

Expression of c-Fos in other different brain regions of interest

Images of all the regions of interest (both right and left hemisphere) were acquired with a 20X objective using the tile tool of the Zen software. Each brain area was manually traced to define the regions of interest and all the c-Fos+ cells were counted with the aid of the cell counter plugin of ImageJ in two consecutive sections. Values from the left and right hemispheres in the two slices were averaged to obtain one value per animal and are presented as the mean ± SEM of 6 animals/genotype/experimental group.

Expression cFos in the basolateral amygdala of vGlut2-ZsGreen expressing mice

Seven to fifteen images from the left and right Basolateral Amygdala (BLA) were randomly acquired with a 40X objective from 6 consecutive slices/animal. Two investigators masked to genotype and treatment group performed the cell counting using the Zen software tools in 5-7 images/animal. The followings were determined in each image: (1) the total number of vGlut2-ZsGreen+ cells; (2) the number of vGlut2-ZsGreen+ cells immunopositive for c-Fos. The percentage of cFos positive cells/vGlut-ZsGreen cells per image was determined and then averaged to obtain a single value/animal. On average, each image contained about 30-45 vGlut2-ZsGreen+ cells. Data are shown as the mean ± SEM. N = 4 animals/genotype/experimental group, 2 males and 2 females were present in each group.

Statistics

To determine the impact of long or short wavelength enriched DLaN on three assays for the light input to the circadian system in WT mice, we used a one-way analysis of variance (ANOVA) (**Table 2.1**). Given the low sample size of the *OPN4*$^{DTA/DTA}$ mutants and littermate controls, we used student's *t*-tests or Mann Whitney rank-sum tests to determine whether DLaN altered activity parameters and their social behavior (**Table 2.2**). To analyse the activity waveforms, we used a two-way ANOVA with time and treatment as factors. The Holm-Sidak test for multiple comparisons was used when appropriate. To determine the consequent behavioral measures (**Table 2.3**) as well as the number of c-Fos+ cells across brain areas after the 2 weeks of treatment (**Table 2.4**), we used a two-way ANOVA with genotype and

treatment as factors. Again, the Holm-Sidak test for multiple comparisons was used when appropriate. Values were reported as the mean ± standard error of the mean (SEM). Differences were determined significant if $P < 0.05$.

Results

Long wavelength illumination reduces negative masking, light-induced phase shifts of the circadian activity rhythm, and induction of c-Fos in the SCN of WT mice.

In these first set of experiments, we compared the impact of long- and short-wavelength enhanced lighting (**Fig. 2.1 A**) on three classic tests of the ipRGC input to the circadian system. First, we examined the impact of the lighting on light-driven masking of activity as measured with a passive infra-red activity assay with WT mice. We confirmed a significant reduction in masking behaviour with the short wavelength-enriched lights (10 lx, 60 min, ZT 14) in WT mice (51 ± 5%). The long wavelength illumination produced a low level of masking (14 ± 7%) (**Fig. 2.1 B, Table 2.1).** Next, we measured the impact of the two lights on light-induced phase shifts of the circadian system using wheel-running activity (**Fig. 2.1 C**). The WT mice were exposed to one of two lights (10 lx, 15-min, CT 16) while activity was monitored in DD. The mice exposed to short-wavelength light exhibited significantly larger phase delay (-117 ± 6 min) compared to those mice exposed to the long-wavelength shifted light (-26 ± 4 min) (**Fig. 2.1 D, Table 2.1).** Finally, we examined the impact of the two lights (10 lx, 15 min, CT 16) on the number of c-Fos expressing cells in the SCN (**Fig. 2.1 E).** The SCN of the mice exposed to the shorter wavelengths light exhibited in robust induction of c-Fos+ cells (94 ± 6 cells per SCN section) while those exposed to the longer wavelength light exhibited significantly fewer cells (19 ± 2 per SCN section) (**Fig. 2.1 F, Table 2.1**). Taking together, shifting the wavelengths of illumination toward longer wavelengths significantly reduced the impact of light on negative masking, light-induced phase shifts and light-induction of c-Fos in the SCN.

Melanopsin (OPN4+) mediates the impacts of DLaN on both activity cycles and social behavior.

It is well-established that the melanopsin (OPN4+) expressing ipRGC mediate the effects of light on the circadian system and we sought to test their role in mediating the behavioural

impact of DLaN. For these experiments, we utilized a transgenic line of mice (*OPN4*$^{DTA/DTA}$) that lack melanopsin expression and with diminished ipRGCs due to the targeted expression of attenuated diphtheria toxin A in the Opn4 expressing cells (Güler et al., 2008). First, *OPN4*$^{DTA/DTA}$ mice and their WT littermates were held under either LD control environment on a short wavelength enriched DLaN for 2 weeks (n= 5/group). While the WT mice exhibited a clear reduction in the strength of the activity rhythm (activity levels, power, amplitude), the mutant mice did not show any clear changes to their activity rhythms (**Fig. 2.2 A & B, Table 2.2**)**.** Next, we examined negative masking as described above. Here again, the WT mice exhibited a robust suppression of activity (42 ± 7%) while the OPN4$^{DTA/DTA}$ did not exhibit a significant light-evoked suppression of activity (9 ± 9%; **Fig. 2.2 C, Table 2.2**). Finally, we had previously demonstrated that white DLaN reduces social behaviour in C57 mice (Wang et al., 2020), we examined the impact of the short wavelength illumination. In WT mice, the DLaN robustly reduced social interactions (71%) while the OPN4$^{DTA/DTA}$ mice were resistant to this negative effect of night-time illumination (18%, **Fig. 2.2 D, Table 2.2**). Together this data indicates that the ipRGCs are required for at least some of the negative effects of DLaN.

Reduced melanoptic illumination prevents disruption of daily rhythms in activity in WT and Cntnap2 KO mice from DLaN.

Next, we sought to use the LED array to determine whether long wavelength illumination would ameliorate DLaN disruption of locomotor activity rhythms. Cohorts of *Cntnap2* KO and WT mice were first housed under control conditions (LD 12:12) and then randomly treated under either long- or short wavelength enriched DLaN (10 lx) for 2 weeks (**Fig. 2.3 A)**. We examined the waveforms of each genotype and each lighting condition (**Fig. 2.3 B**). Under baseline conditions, both *Cntnap2* KO mice and WT controls exhibited robust rhythms in activity, although several parameters (total activity, power, amplitude) measured from the *Cntnap2* KO mice are consistent weaker rhythms as has been previously described (Thomas et al., 2017; Wang et al., 2020). When treated with short wavelength-enriched DLaN, the average waveform (1 hr bins) of both genotypes was significantly altered (**Fig. 2.3 B; Table**

2.3) The WT and the *Cntnap2* KO mice exhibited a significant reduction in a number of activity rhythm parameters (**Table 2.3**) while the long wavelength illumination did not produce significant changes compared to baseline. These differences in the effects of the short and long wavelength illumination are strikingly shown when we examine some of the key activity parameters before and after treatment (**Fig. 2.4**). These results indicate that the negative effects of DLaN are sensitive to the spectral properties of the light used for illumination in both WT and *Cntnap2* KO mice.

Reduced melanoptic illumination prevents worsened social deficits in WT and Cntnap2 KO mice from DLaN.

DLaN reduced social behaviour in both *Cntnap2* KO mutants as well as WT controls (Wang et al., 2020) and here we sought to determine the impact of the two illuminations. We measured the social behavior and demonstrated that the short wavelength-enriched DLaN treatment decreased social behaviour in both *Cntnap2* KO and WT mice while the long wavelength light was without effect (**Fig. 2.5, Table 2.3**). Looking at individual mice before and after DLaN, the short wavelength DLaN decreased social interactions (>10%) in 10 out of 12 KO mice evaluated while the long wavelength reduced social interactions in 5 out of 12 KO mice (**Fig. 2.5 B & C**). Our findings indicate that exposures to short wavelength-enriched DLaN disrupted social behavior in both genotypes, and the use of long wavelength illumination could effectively reduce the impact of DLaN on social behavior.

Reduced melanoptic illumination prevents evoked repetitive behaviour in Cntnap2 KO mice from DLaN.

We have previously shown that DLaN increases repetitive grooming behaviour in *Cntnap2* KO mutants but not WT controls (Wang et al., 2020) and here we sought to determine the impact of the two illuminations. We measured the grooming behavior in the middle of night (ZT 16-18) and demonstrated that the short wavelength-enriched DLaN treatment increased the time of grooming selectively in the *Cntnap2* KO mice (**Fig. 2.6, Table 2.3**). As we had previously observed, the *Cntnap2* KO exhibited higher levels of grooming than WT mice under baseline conditions (**Table 2.3**). Neither DLaN treatment altered the levels of grooming in WT mice. In contrast, the short wavelength selectively increased the time spent grooming in the *Cntnap2* KO mice. Looking at individual animals, the short wavelength DLaN increased grooming (>10%) in 16 out of 22 KO mice evaluated while the long wavelength increased grooming in only 4 out of 22 KO mice (**Fig. 2.6 B, C**). Our observations demonstrate that the impact of DLaN on repetitive grooming in the *Cntnap2* KO was dependent upon the wavelength of light used and that the mutants are selectively vulnerable to the effects of DLaN on repetitive behavior.

Reduced melanoptic illumination diminishes DLaN induction of c-Fos in the basolateral amygdala implicated in the control of repetitive behavior in WT and Cntnap2 KO mice.

Finally, to unravel possible mechanisms underlying the impacts of DLaN on autistic behavior, we examined the response of c-Fos levels across different brain regions. Prior work has shown that activation of ipRGC can drive c-Fos expression in several brain regions including those in the hypothalamus and limbic system (Milosavljevic et al., 2016; Fernandez et al., 2018). In this experiment, WT and *Cntnap2* KO mice to 2 weeks of short or long wavelength enriched DLaN (n=5/genotype/treatment). Compared to mice held on a standard LD cycle, we found that the short wavelength light inducted c-Fos immunoreactivity in the basolateral amygdala (BLA) and perihabenular nucleus (pHb), but not other brain regions of

interest including the paraventricular hypothalamus (PVH), and the lateral hypothalamus (LH) (**Fig. 2.7, Table 2.4**). In contrast, the long wavelength enriched DLaN did not induced c-Fos expression in any of these regions. Prior work suggested that the glutamatergic cell population in the BLA was a critical part of a circuit responsible for repetitive behavior (Felix-Ortiz et al., 2016). Therefore we crossed the *Cntnap2* KO line into mice that expressed both vGluT2-Cre (Vong et al., 2011) and a Cre-dependent reporter ZsGreen (Ai6) (Madisen et al., 2010), which provides strong cell body labelling. We generated WT and *Cntnap2* KO mice with these reporters and exposed them to short wavelength DLaN. We confirmed that cells within the BLA region robustly expressed the vGlut2 reporter. Importantly, the short wavelength DLaN drove a high degree of co-expression in the *Cntnap2* KO mice (55 ± 5%) compared to mutants under LD conditions (20 ± 5%). Both genotypes exhibited significantly higher co-labeling in the light treated group (**Table 2.5**). This data demonstrates that the glutamatergic cells within the BLA are activated by DLaN and raise the possibility that this cell population contributes to the impact of DLaN on repetitive behaviour.

Discussion

Nightly light exposure is a common environmental perturbation and has been shown to cause a number of ill effects (Lucassen et al., 2016; Bumgarner et al., 2021). Some populations may be more vulnerable to the negative effects of the exposure of light at night. For example, in the *Cntnap2* KO mouse model of ASD, we have found that DLaN selectively increases repetitive behaviour as measured by grooming while WT mice were not impacted (Wang et al., 2020). On the other hand, DLaN negatively impacted other behaviors including social interactions and daily activity rhythms in both the *Cntnap2* KO and WT mice. In the present study, we confirmed these negative impacts of nocturnal lighting on activity rhythms, social interactions, and repetitive behaviours (**Table 2.3**). Logically, the simplest approach to reducing these negative effects would simply be to decrease light intensity at night while ensuring a robust exposure to sunlight during the day. However, according to surveys, people spend a majority of time indoors (as high as 90%) and have need for illumination after the sun sets (e.g. Klepeis et al., 2001). Therefore an appealing alternative approach would be to adjust the spectral quality of lighting to minimize the negative effects. As a test case, in the present study, we used an array of light-emitting diodes (LEDs) to generate dim illumination (10 lx) to determine whether the spectral composition of nightly illumination would make a difference in the *Cntnap2* KO model of autism.

The retinal photoreceptor system has unique intensity and wavelength dependent characteristics (Lucas et al., 2014). We considered the possibility that the negative effects of nightly light exposure are likely to be mediated by ipRGCs expressing the photopigment melanopsin, which is maximally sensitive to blue light, with a peak response to 480nm light (Hattar et al., 2002; Panda et al., 2005). Indeed a number of studies have found evidence that short wavelength enriched lighting is more effective for circadian responses (for review see Brown, 2020). However, recent work emphasizes that ipRGCs also receive input from rod and cone photoreceptors (Hattar et al., 2003; Lucas et al., 2012; Van Diepen et al., 2021; Schoonderwoerd et al., 2022) with rods driving the circadian response to sensitivity to low-

intensity light (Altimus et al., 2010; Lall et al 2010) like the 10 lx used in the present study. Here we used an LED lighting system (Korrus Lighting) to tailor the spectral properties of the DLaN used to manipulate melanoptic stimulation. The output of the LEDs was measured as power (Watts) over a defined wavelength (380-780nm) using a spectrophotometer. This data was input into CIE toolkit which enables us to estimate that the short wavelength illumination was at 15 melanopic lx while the long wavelength illumination was 1 melanopic lx.

Using these two lighting conditions with predicted high and low melanopic stimulation, we measured the impact of the illumination on three classic tests of the ipRGC input to the circadian system (**Fig. 2.1**). We demonstrated that the low melanopic stimulation reduced the impact of light on negative masking, light-induced phase shifts and light-induction of c-Fos in the SCN. Next, we examined the impact of the high melanopic illumination on activity and social behaviour of WT and *OPN4*$^{DTA/DTA}$ in which the ipRGCs are lost due to targeted diphtheria toxin expression. We found that the high melanopic illumination showed greatly diminished ability to disrupt activity rhythms including negative masking as well as alter social behaviour in the mutant mice (**Fig. 2.2**). Together, this data indicates that ipRGCs are required for a majority of the negative effects of DLaN and that controlling melanopic stimulation altered activation of the ipRGC/SCN pathway.

With this validated lighting system in hand, we sought to use the LED array to determine whether long wavelength illumination would ameliorate DLaN disruption of behaviour in WT and *Cntnap2* KO mice. Both lines of mice exhibited a significant reduction in a number of activity rhythm parameters when exposed to the high melanopic illumination while the low melanoptic illumination did not produce significant changes compared to baseline (**Fig. 2.3 & 2.4**). Similarly, exposure to high melanopic illumination disrupted social behavior in both genotypes while the low melanopic DLaN had little impact on social interactions (**Fig. 2.5**). Finally, we found that exposure to high melanopic illumination increased repetitive grooming in the *Cntnap2* KO but not the low melanopic DLaN (**Fig. 2.6**).

Together, these data show that minimizing the melanopic activation of the light source was an effective strategy to minimize the negative effects of night-time light exposure.

There is a strong male bias in ASD prevalence with a common reported ratio of ~4:1 (Fombonne, 2009) and there has been evidence for significant interactions between sex and genotype for the *Cntnap2* gene in human populations (e.g. Hsu et al., 2019). Some of these sex differences may be driven in part by male/female differences in phenotypic presentation, including fewer repetitive behaviors in females (e.g. Werling and Geschwind, 2013). On the other hand, sleep disturbances appear to be more common in female with ASD (Elkhatib Smidt et al., 2021). Prior work with the *Cntnap2* KO mouse model found clear evidence for a sex difference with home cage activity with robust hypo-activity in the males but not the female mutants (Angelakos et al., 2019). In addition, the functional responses of cortical circuitry in male mice are more strongly affected by *Cntnap2* mutations than females (Townsend and Smith, 2017). Therefore, we powered the activity analysis to be able to examine possible sex differences in activity rhythms. We found clear sex differences in the activity rhythms in the WT mice that were lost in the *Cntnap2* KO line (**S. Fig. 2.1; S. Table 2.1**). We did see evidence that the excessive grooming that we take, as a measure of repetitive behavior was more pronounced in the males than the females although both sexes showed significantly higher grooming than WT controls. Finally, the social deficits were seen in both sexes. So, in our assays, both sexes of *Cntnap2* KO exhibited the phenotypes of disrupted activity rhythms, higher repetitive behavior and less social interactions compared to WT mice. Interestingly, prior work as found that LPS-induced maternal immune activation caused male-specific deficits in behavior and gene expression in the *Cntnap2* KO line (Schaafsma et al., 2017). Our data also allows us to determine if female mice are more resilience in the face of environmental perturbation. With our three assays (activity, grooming, and social interactions), we found that both sexes were negatively impacted by the DLaN (**S. Fig. 2.2; S. Table 2.2**). Therefore, with our assays, the female mutants were equally impacted and our data supports the use of both sexes in this mouse model of ASD.

Prior work has shown that activation of ipRGC can drive c-Fos expression in several brain regions including those in the hypothalamus and limbic system (Milosavljevic et al., 2016; Fernandez et al., 2018). We sought to determine whether the 2-weeks of DLaN would alter c-Fos expression in some of those brain regions (**Fig. 2.7**). In contrast to the effects of the light when the mice were held in DD (**Fig. 2.1**), we did not see any evidence that the chronic nightly high melanopic illumination increased c-Fos in the SCN. Similarly, we did not see increased c-Fos expression in the PVH and LH. Interestingly, the chemogenetic activation of ipRGCs, did induced c-Fos expression in these two regions (Milosavljevic et al., 2016). The difference may well be the relatively weak light stimulus used in the present study or the difference between acute chemogenetic activation vs. chronic stimulation with the DLaN. We did find that our high melanopic DLaN did increases c-Fos expression in the pHb and BLA region of the amygdala. Prior work has implicated the pHb as a region critically involved in the effects of light on mood (Fernandez et al., 2018). Specifically there is support for circuit by which the ipRGC regulation of the dorsal region of the pHb projects to the nucleus accumbens (NAc) to drive depressive-like behaviors (An et al., 2020). Thus we would expect to see DLaN driven alterations in depressive behaviors in our mouse models (Fonken et al., 2012; Bedrosian et al., 2013; Walker et al., 2020) and this will be an important area for future work. More critical for the present study, prior work suggests that the BLA may regulate repetitive behaviors (Felix-Ortiz and Tye, 2014; Sun et al., 2019). Using a reporter for a glutamate transporter (vGlut2), we were able to show that the c-Fos induction occurs robustly, although certainly not exclusively, in a glutamatergic cell population in the BLA (**Fig. 2.7**).

Prior work has suggested that the microcircuit of the basolateral amygdala (BLA) to mPFC contributes to ASD-like behaviour in mice. Felix-Ortiz and Tye (2014) used optogenetic approaches to either activate or inhibit BLA inputs to the mPFC during behavioral assays, and showed that the excited BLA/mPFC microcircuit reduced social interaction whereas suppression favoured social behavior. Sun and colleagues (2019) demonstrated that the glutamatergic neurons from the BLA preferentially projected to GABAergic neurons in the

mPFC. Both their optogenetic and chemogenetic stimulations of this pathway resulted in reduced mPFC activity and stereotypic behavior. The ventral hippocampus (vHp) is the second downstream target. When the glutamatergic projection from the BLA to the vHp mice was activated, social interaction was reduced while the self-grooming was increased. This glutamatergic BLA/vHp pathway was further confirmed by giving glutamate receptor antagonists to the vHPC 30 min before testing, and observed attenuated optogenetic-evoked changes (Felix-Ortiz and Tye, 2014). Therefore we speculate that the DLaN driven activation of the glutamatergic cell population in the BLA (**Table 2.5**) is what drives the grooming behaviour observed in the present study.

With rapidly growing studies reporting the effects of lights on not only circadian rhythms but also the brain health (Stevenson et al., 2015; Lunn et al., 2017; Bumgarner and Nelson, 2021), the consequences of worldwide prevalence of DLaN should be taken into concern of disease management seriously, especially to those patients with neurodevelopmental disorders and neurodegenerative diseases who are vulnerable to environmental perturbations. Nightly light pollution is a very common environmental disruption to our circadian rhythms all over the world, and this present study shows that the undesired outcomes of DLaN on sleep/wake cycles and autistic behavior can be ameliorated by tailoring the spectral content of light sources to minimize melanopic stimulation.

Figures

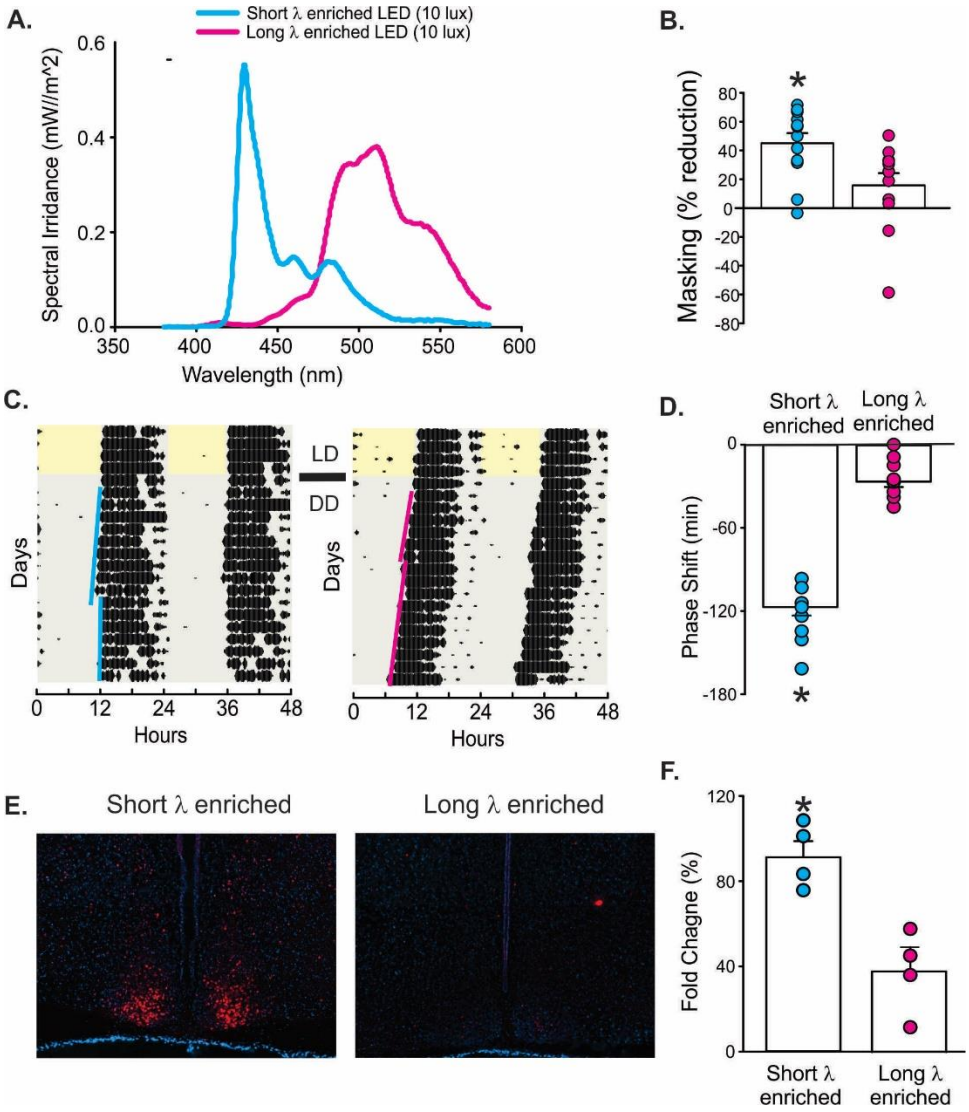

Fig. 2.1: Shift to longer wavelength (λ) illumination reduces negative masking, light-induced phase shifts of the circadian activity rhythm, and induction of c-Fos in the suprachiasmatic nucleus of WT mice. **(A)** Spectral irradiance of the light emitted by the LED array using two lighting paradigms: a short wavelength (λ) enriched (10 lx, peak at 478 nm) and a long λ enriched illumination (10 lx, peak at 608 nm). These two lighting conditions were compared throughout this study. **(B)** Light-induced masking of activity in mice exposed to either short λ or long λ enriched light for one hour at ZT 14. The activity level during this light exposure was compared to the activity level during the equivalent hour (ZT 14-15) on the day before the treatment (baseline activity). In this and other figures, the histogram shows the mean and standard error of the mean. The responses of the individual animals are shown by the symbols with teal representing the short λ enhanced lighting while the magenta representing the long λ enhanced lighting. **(C)** Examples of light-induced phase shifts of wheel-running activity onsets. After the entrainment to the standard light:dark (LD) cycle, the WT mice were placed into constant darkness (DD) for 10 days and then exposed to either short λ or long λ enriched illumination (10 lx, 15 min) at CT 16 (4 hours after activity onset). **(D)** The short λ enhanced illumination produced significant phase delays of the circadian system. **(E)** Examples of light-evoked c-Fos expression in the suprachiasmatic nucleus (SCN). Mice were exposed to either short λ - or long λ enriched illumination (10 lx, 15 min) at CT 16. **(F)** The short λ enhanced illumination produced significant c-Fos induction in the SCN. Data was analyzed using one way ANOVA (**Table 2.1**) with an asterisk (*) indicating significant difference ($P < 0.05$).

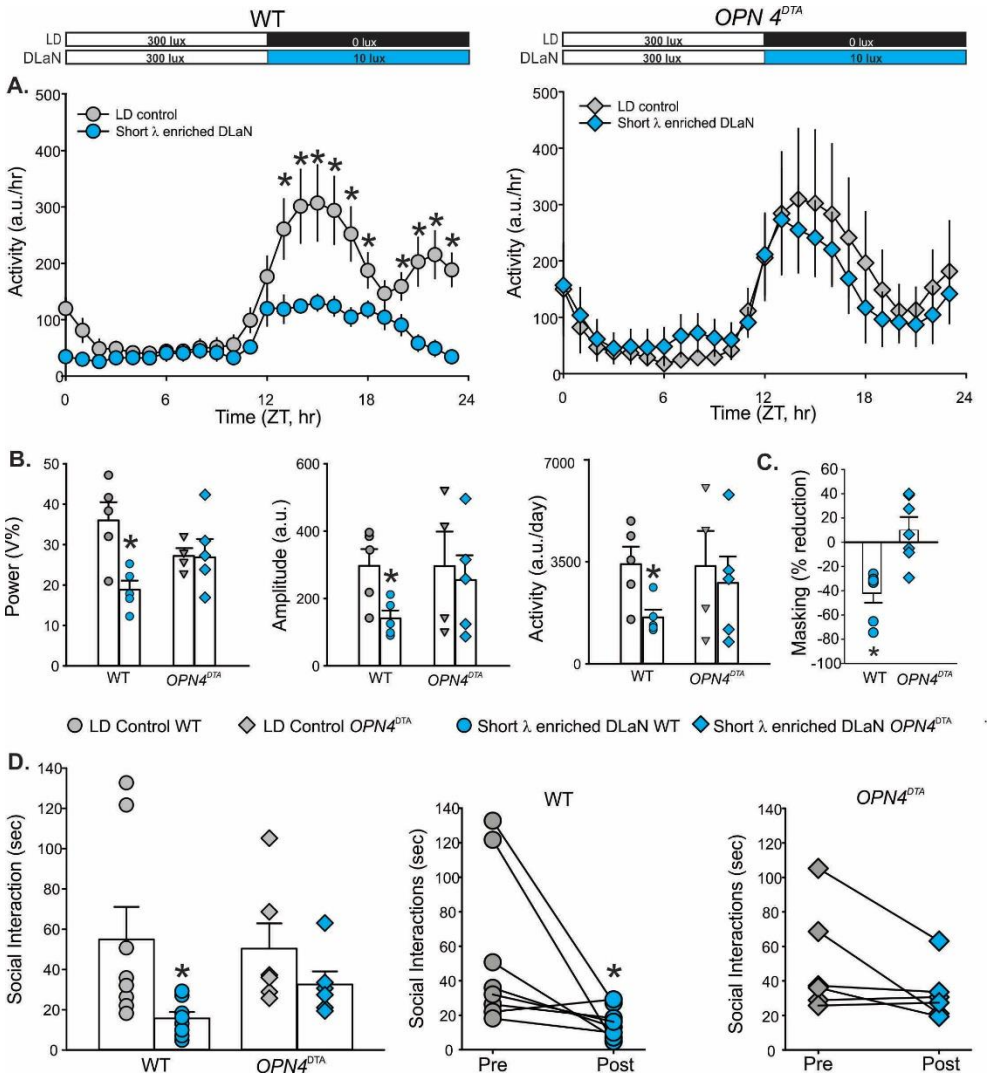

Fig. 2.2: Melanopsin (*OPN4*+) mediates the impacts of DLaN on activity rhythms and social behavior. (A) Waveforms of daily rhythms in cage activity under LD control conditions as well as short-enriched DLaN (10 lx) in WT (left) and *OPN4*$^{dta/dta}$ mice (right). The activity waveform (1 hr bins) of each treatment group was analyzed using a 2-way ANOVA for repeated measures with treatment and time as factors (n = 5 per group). The WT mice exhibited a significant effect of treatment ($F_{(1, 239)} = 95.39$; $P < 0.001$), time ($F_{(23, 239)} = 11.674$; $P < 0.001$) as well as a significant interaction between the two factors ($F_{(23, 239)} = 3.047$, $P < 0.001$). In contrast, the *OPN4*$^{dta/dta}$ mice exhibited a significant effect of time ($F_{(23,215)} = 4.73$; $P < 0.001$) but not treatment ($F_{(1, 215)} = 0.636$, $P = 0.426$). There was not any evidence for an interaction ($F_{(23,215)} = 0.611$; $P = 0.917$) *indicates significant ($P < 0.05$) differences between the 1 hr bins as measured by Holm-Sidak test for multiple comparisons. **(B)** The properties of the daily activity rhythms (10 day recordings) including power, amplitude, and overall activity levels were measured under LD and short λ wavelength enhanced DLaN (n=5 per group). Histograms show means ± SEM with the values from individual animals overlaid. (**C**) Light-evoked negative masking was measured by exposing the mice to one of light (10 lx) at ZT14 and comparing the prior day's activity. **(D)** The impact of DLaN on social interactions was measured by comparing social behavior under LD to mice illuminated with the short λ illumination. A paired *t*-test was used to analyze the changes before and after the treatment. The impact of DLaN in WT and OPN4$^{dta/dta}$ was evaluated using the student's *t*-tests (**Table 2.2**) with an asterisk indicating significant difference ($P < 0.05$).

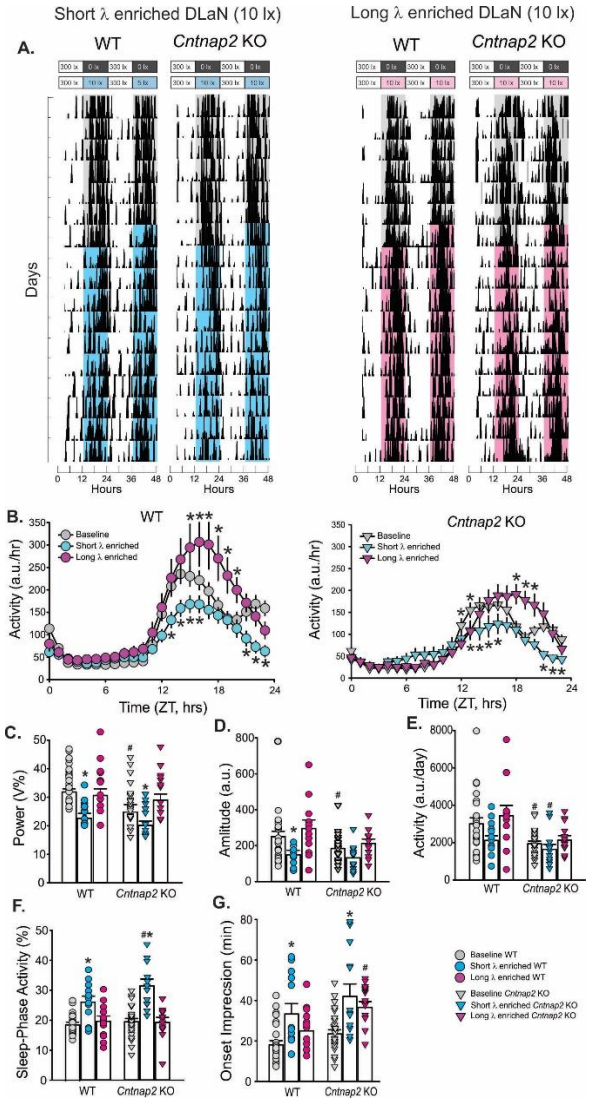

Fig. 2.3: Long λ illumination minimizes DLaN disruption of daily activity rhythms in WT and *Cntnap2* KO mice. (A) Examples of actograms of daily rhythms in cage activity under short λ (left) and long λ (right) enriched DLaN (10 lx) in both WT and *Cntnap2* KO mice. The activity levels in the actograms were normalized to the same scale (85% of the maximum of the most active individual. Each row represents two consecutive days, and the second day is repeated at the beginning of the next row. The bars on the top of actograms indicates the time and intensity when the nightly lights are given. The teal shading represents the short λ enhanced lighting while the magenta shading represents the long λ enhanced lighting. **(B)** Waveforms of daily rhythms in cage activity under short (teal) and long (magenta) λ enriched DLaN in WT (circles) and *Cntnap2* KO (triangles) mice. The baseline values from the mice under LD control conditions are shown for comparison (grey). The activity waveform (1 hr bins) of each treatment group was analyzed using a 2-way ANOVA for repeated measures with treatment and time as factors. Both groups exhibited significant effects of time (WT: $F_{(23,1151)} = 43.29$, $P < 0.001$; *Cntnap2* KO: $F_{(23,1151)} = 44.96$, $P < 0.001$) and treatment (WT: $F_{(2,1151)} = 42.66$, $P < 0.001$; *Cntnap2* KO: $F_{(2,1151)} = 15.16$, $P < 0.001$), and the interaction between the two factors is identified (WT: $F_{(46,1151)} = 2.57$, $P < 0.001$; *Cntnap2* KO: $F_{(46,1151)} = 3.8$, $P < 0.001$). Asterisk indicates significant ($P < 0.05$) differences between the 1 hr bins as measured by Holm-Sidak test for multiple comparisons. **(C-G)** The properties of the daily activity rhythms (10 day recordings) were measured under short or long λ enhanced DLaN (n = 12 per group) and compared to baseline LD. Histograms show means ± SEM with the values from individual animals overlaid. The properties of the daily activity rhythms measured and analyzed using a 2-way ANOVA with genotype and treatment as factors. Significant ($P < 0.05$) differences as a result of treatment are indicated with an * while the crosshatch sign (#) indicates a genotypic difference (see **Table 2.3**).

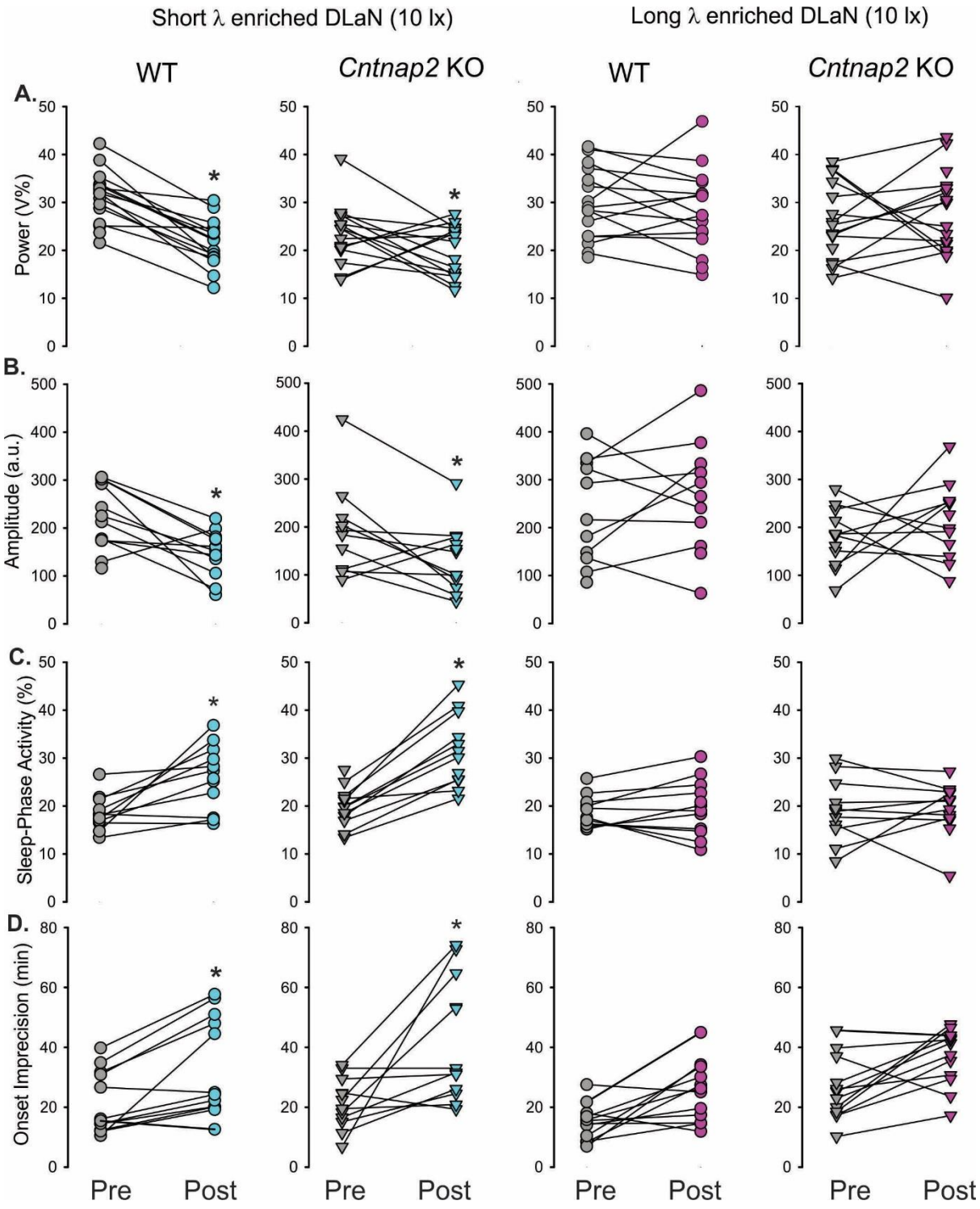

Fig. 2.4: Long λ illumination was less disruptive to activity rhythms in WT and *Cntnap2* KO mice. Key measures of the daily activity rhythms were measured before and after treatment. Values from individual animals under short λ (teal) and long λ enriched (magenta) enriched DLaN in WT (circles) and *Cntnap2* KO (triangles) mice are shown. Paired *t*-test was used to analyze the changes before and after the treatment, and an * over the treated values indicates significant difference ($P < 0.05$).

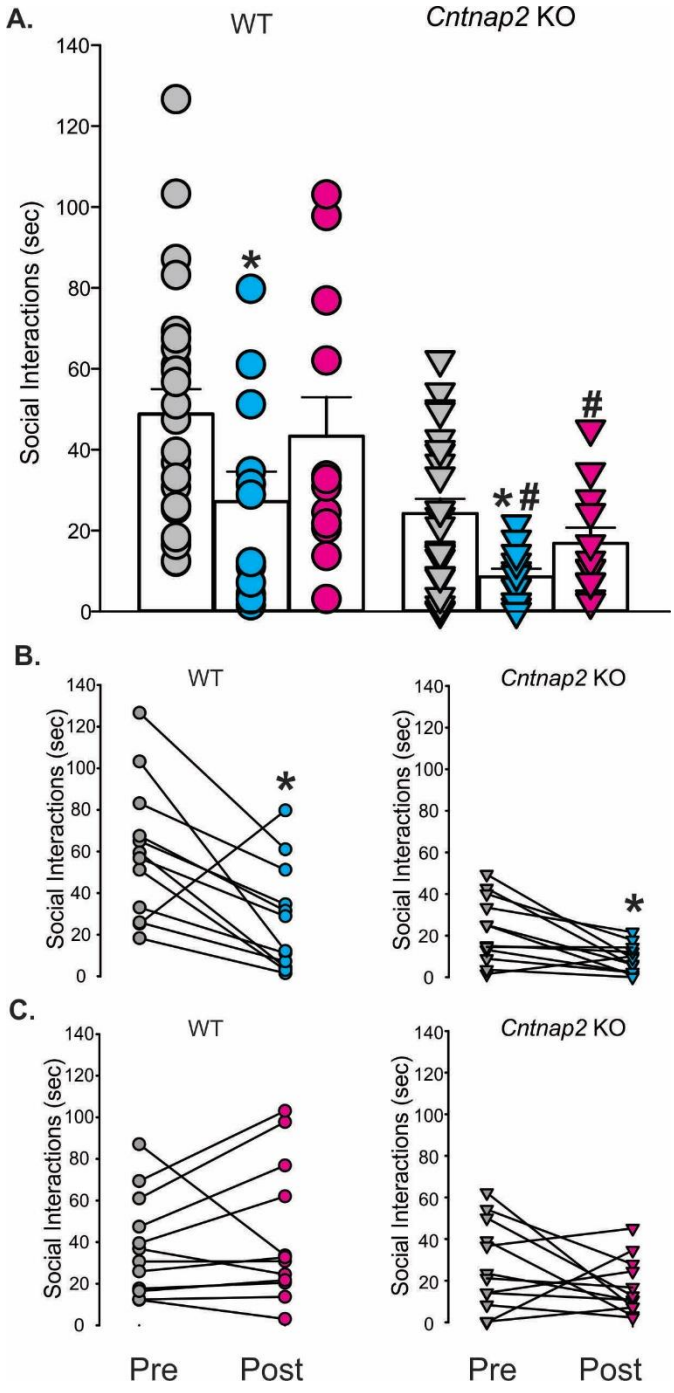

Fig. 2.5: Long λ illumination ameliorates DLaN evoked social deficits in WT and *Cntnap2* KO mice. The social behavior was evaluated by analyzing the time actively spent in social interactions by the testing mouse with the novel stranger mouse. The stranger and testing mice were matched for age, sex, and genotype. Experiments were conducted at ZT 18. **(A)** Time spent in social interaction. Values from individual animals under short λ (teal) and long λ enriched (magenta) enriched DLaN in WT (circles) and *Cntnap2* KO (triangles) mice are reported. Data were analyzed using a 2-way ANOVA with genotype and treatment. Significant ($P < 0.05$) treatment differences are indicated with an * while the # indicates a genotypic difference. **(B, C)** Values from individual animals under short λ (teal) and long λ (magenta) enriched DLaN in WT (circles) and *Cntnap2* KO (triangles) mice are shown. Paired *t*-test was used to analyze the changes before and after the treatment. An * over the treated values indicates significant difference ($P < 0.05$).

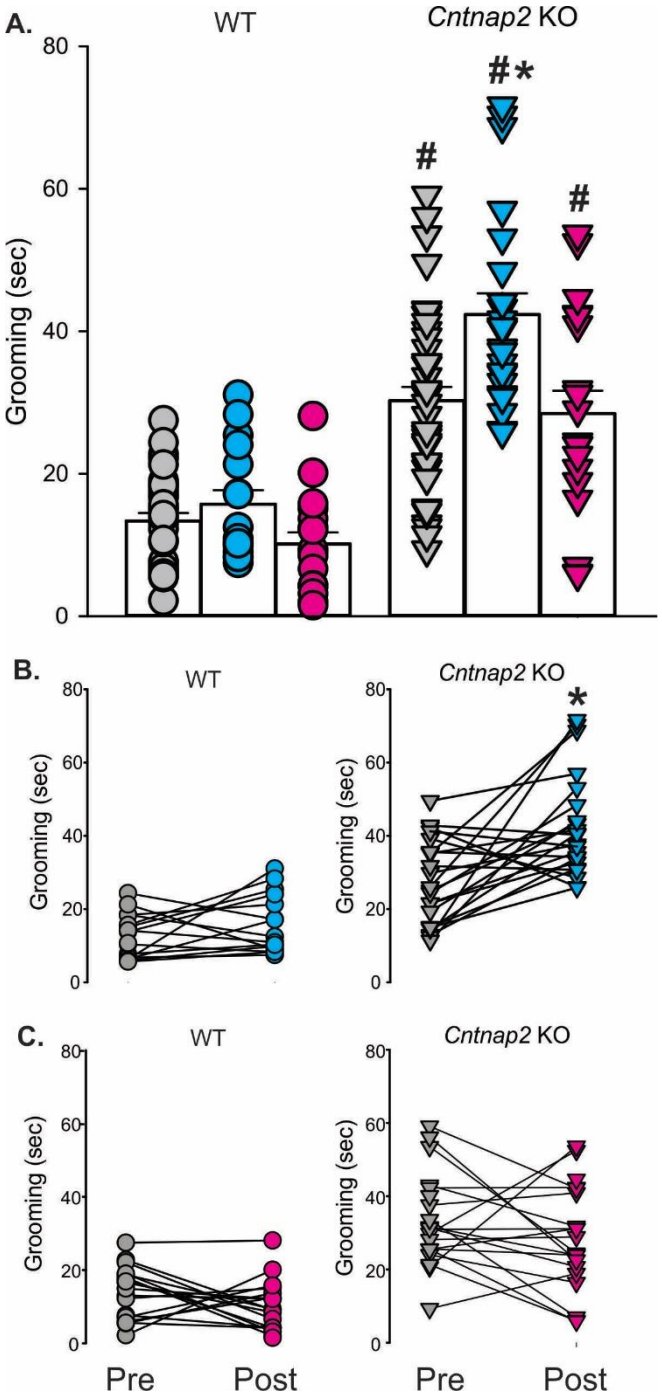

Fig. 2.6: Long λ illumination ameliorates DLaN evoked repetitive behavior in the *Cntnap2* KO mice. Grooming was assessed in a novel arena from mice of each genotype under each lighting condition (LD baseline, short λ enriched DLaN, long λ enriched DLaN. Measurements were conducted at ZT 18. **(A)** Time spent grooming under short λ (teal) and long λ enriched (magenta) enriched DLaN in WT (circles) and *Cntnap2* KO (triangles) mice are shown. Data were analyzed using a 2-way ANOVA with genotype and treatment as factors **(Table 2.3)**. Significant ($P < 0.05$) effects of treatment are indicated with an * while the # indicates a genotypic difference. **(B, C)** Values from individual animals under short - (teal) and long- (magenta) enriched DLaN in WT and *Cntnap2* KO mice. Paired *t*-test was used to analyze the changes before and after the treatment, and an * over the treated values indicates significant difference ($P < 0.05$).

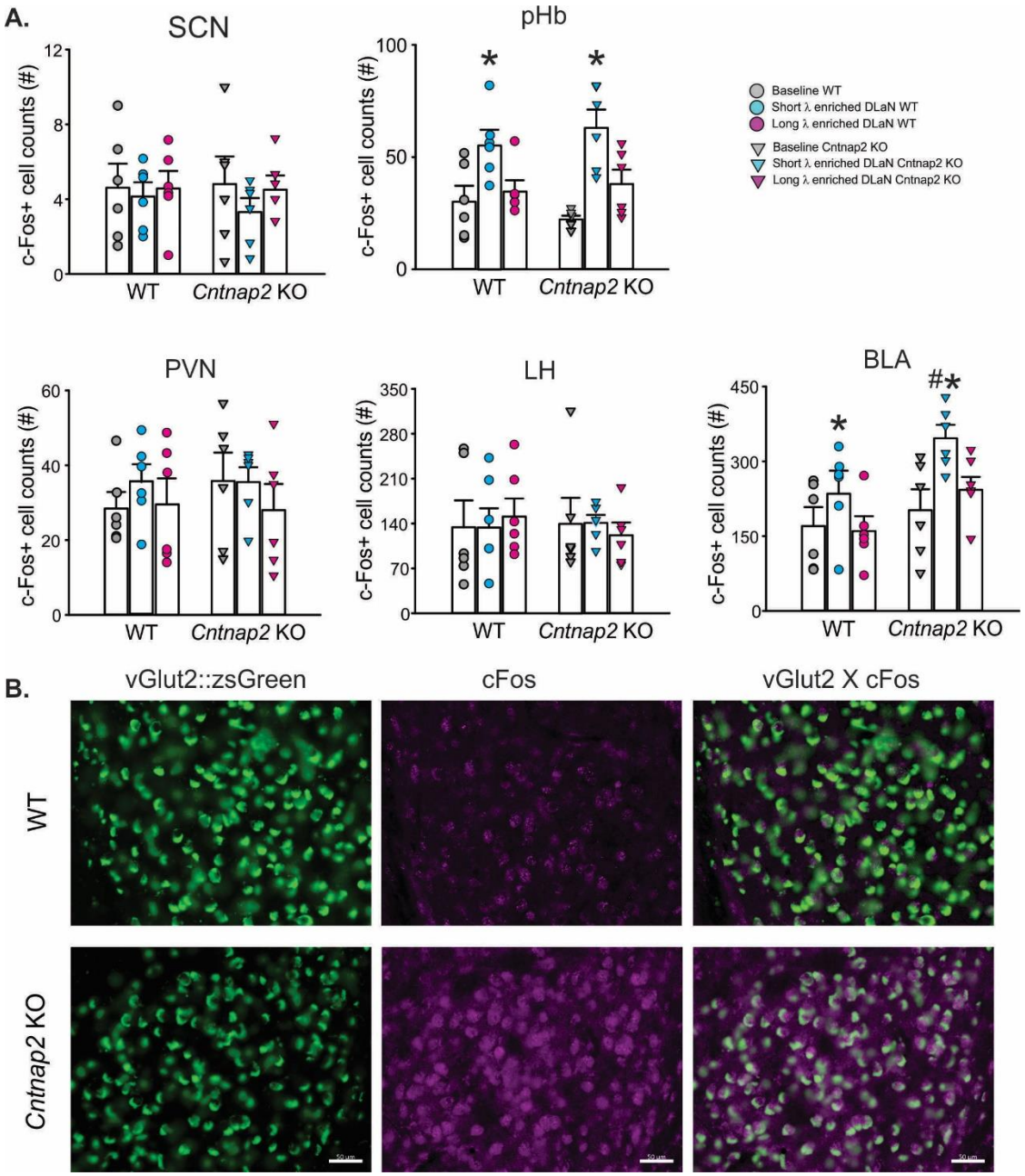

Fig. 2.7: Short, but not long, λ illumination evokes c-Fos in the basolateral amygdala region of in WT and *Cntnap2* KO mice. Tissue was collected from mice held under control LD as well as short λ (teal) or long λ (magenta) enriched DLaN (10 lux) in WT (circles) and *Cntnap2* KO (triangles) mice. The tissue was collected at ZT 18. (**A**) The number c-Fos positive cells were counted by two investigators masked to the experimental conditions in several brain regions including the SCN, peri-Hebenula (pHb), paraventricular nucleus (PVN), lateral hypothalamus (LH) and basolateral amygdala (BLA). The numbers obtained by the two investigators masked to the experimental condition were averaged and values per animal shown. Data were analyzed with a 2-way ANOVA with genotype and treatment as factors **(Table 2.4)**. Significant ($P < 0.05$) effects of treatment are indicated with an * while the # indicates a genotypic difference. (**B**) vGlut2+ neurons in the BLA are activated after DLaN exposure. WT and *Cntnap2* KO mice heterozygous for vGlut2 Cre and Rosa-LSL-ZsGreen (Ai6) were exposed to DLaN. Green, ZsGreen native fluorescence, Magenta, c-Fos immunostaining. Scale bars represent 50 µm. (**C**) Percentage of ZsGreen+ cells expressing c-fos. n = 4 animals for each condition. The DLaN treatment increased c-Fos in both WT and *Cntnap2* KO mice with the mutants showing greater c-Fos in the BLA as well as higher co-expression with vGlut2+ cells.

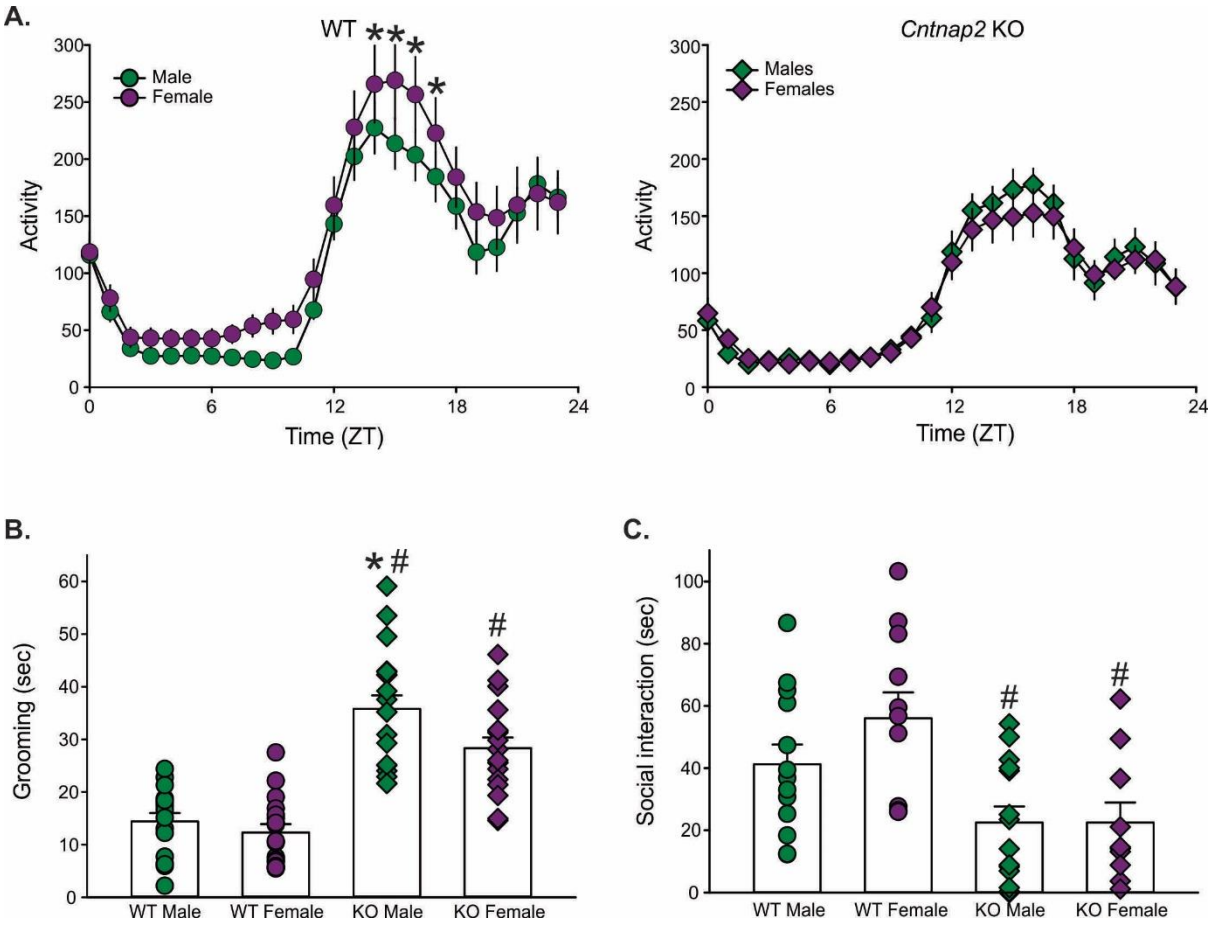

S. Fig. 2.1: Sex differences between the WT and *Cntnap2* KO mice under baseline conditions. (A) Waveforms of daily rhythms in cage activity in male (green) and female (purple) under baseline conditions in WT (circles) and *Cntnap2* KO (diamonds) mice. The activity waveform (1 hr bins) of each treatment group was analyzed using a 2-way ANOVA for repeated measures with time and sex as factors. The WT mice exhibited significant effects of time ($F_{(23,551)}$ = 31.64, P < 0.001) and sex ($F_{(1,551)}$ = 20.99, P < 0.001; but no interaction between the two factors was identified ($F_{(23,551)}$ = 0.55, P = 0.959). The *Cntnap2* KO exhibited significant effects of time ($F_{(23,575)}$ = 38.92, P < 0.001) but not sex ($F_{(1,575)}$ = 0.93, P = 0.336). There were no significant interaction between the time and sex ($F_{(23,575)}$ = 0.37, P = 0.997). Asterisk indicates significant (P = 0.959) differences between the 1 hr bins as measured by Holm-Sidak test for multiple comparisons. **(B)** Grooming was assessed in a novel arena from mice of each genotype under LD baseline conditions at ZT 18. Time spent grooming for male (green) and female (purple) in WT (circles) and *Cntnap2* KO (triangles) mice are shown. Data were analyzed using a 2-way ANOVA with genotype and sex as factors (**S. Table 2.1**). Significant (P < 0.05) effects of treatment are indicated with an * while the # indicates a genotypic difference. **(C)** Social interactions were assessed by measuring the time actively spent in social interactions with a novel stranger mouse under LD baseline conditions at ZT 18. Time spent grooming for male (green) and female (purple) in WT (circles) and *Cntnap2* KO (triangles) mice are shown. Data were analyzed using a 2-way ANOVA with genotype and sex as factors (**S. Table 2.1**). Significant (P < 0.05) effects of treatment are indicated with an * while the # indicates a genotypic difference.

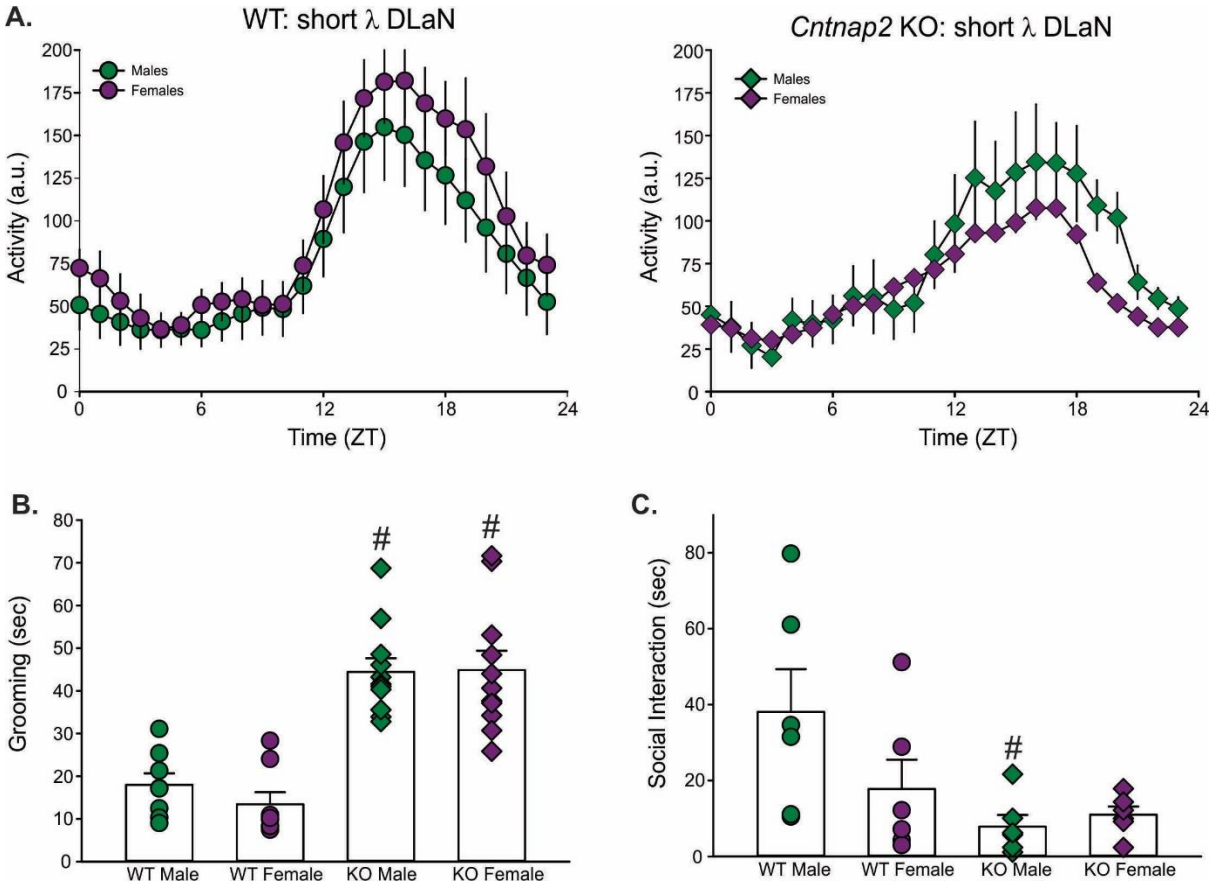

S. Fig. 2.2: Lack of sex differences between the WT and *Cntnap2* KO mice under DLaN conditions. (A) Waveforms of daily rhythms in cage activity in male (green) and female (purple) under short λ DLaN conditions in WT (circles) and *Cntnap2* KO (diamonds) mice. The activity waveform (1 hr bins) of each treatment group was analyzed using a 2-way ANOVA for repeated measures with sex and time as factors. The WT mice exhibited significant effects of time ($F_{(23,287)}$ = 13.36, P < 0.001) and sex ($F_{(1,287)}$ = 12.61, P < 0.001; but no interaction between the two factors was identified ($F_{(23,287)}$ = 0.21, P = 1.000). The *Cntnap2* KO exhibited significant effects of time ($F_{(23,287)}$ = 5.32, P < 0.001) and sex ($F_{(1,287)}$ = 5.99, P = 0.015). There was no significant interaction between the time and sex ($F_{(23,287)}$ = 0.42, P = 0.992). There were no significant (P < 0.05) differences between the 1 hr bins as measured by Holm-Sidak test for multiple comparisons. **(B)** Grooming was assessed in a novel arena from mice of each genotype under short λ DLaN conditions at ZT 18. Time spent grooming for male (green) and female (purple) in WT (circles) and *Cntnap2* KO (triangles) mice are shown. Data were analyzed using a 2-way ANOVA with genotype and sex as factors (**S. Table 2.2**). Significant (P < 0.05) effects of genotype are indicated with a #. **(C)** Social interactions were assessed by measuring the time actively spent in social interactions with a novel stranger mouse under short λ DLaN conditions at ZT 18. Time spent grooming for male (green) and female (purple) in WT (circles) and *Cntnap2* KO (triangles) mice are shown. Data were analyzed using a 2-way ANOVA with genotype and sex as factors **(S. Table 2.2)**. Significant (P < 0.05) effects of genotype are indicated with a #.

Tables

Table 2.1. Reduced circadian outputs resulted from the long wavelength (λ) illumination. WT mice were used to test whether the long wavelength light has a diminished impact on 3 traditional assays for light input to the circadian system. For masking, mice were exposed to light (10 lx, 60 min) from ZT 14 to 15. For phase shifts, mice were held in constant darkness and exposed to light at CT 16 (10 lx, 15 min). For the c-Fos expression, mice held in DD were exposed to light at CT 16 and brains collected at CT 17. The number of immunopositive cells in both the left and right SCN from two consecutive coronal sections per animal were averaged. Equal numbers of male and female mice were used. Values are shown as means ± SEM. Data from the behavioral tests past the normality and equal variance tests and differences were evaluated by one way ANOVA followed by the Holm-Sidak Multiple comparison method. The c-Fos expression data did not past the equal variance test and the Kruskal-Wallis one way ANOVA on ranks was used to evaluate significances. In this and subsequent tables, $P = 0.05$ was considered significant, and significant differences are shown in bold.

Measures	**Untreated**	**Short λ enriched**	**Long λ enriched**	**One way ANOVA**
Masking (% reduction)	-3.0 ± 6.9 (n=14)	-51.0 ± 5.0 (n=11)	-13.6 ± 7.7 (n=11)	**$F_{(2, 35)}$=13.7, P < 0.001**
Phase shift (min)	-3.7 ± 4.0 (n=8)	-117.2 ± 5.9 (n=12)	-26.4 ± 3.9 (n=12)	**$F_{(2, 31)}$=149.3, P < 0.001**
c-Fos+ in SCN	5.6 ± 0.4 (n=4)	94.2 ± 6.5 (n=4)	18.8 ± 2.3 (n=4)	**$H_{(2)}$=2.651, P < 0.001**

Table 2.2. OPN4$^{dta/dta}$ mice were less affected by short λ enriched DLaN. Light input to the circadian system is mediated by the ipRGC population that can be selectively ablated in a line of mice with the gene coding for melanopsin (*OPN4*) expressing a component of the diphtheria toxin. Both male and female mice were used. We compared the impact of short wavelength enriched DLaN on activity rhythms and social interactions in WT and OPN4DTA/DTA littermates. Values are shown as means ± SEM. Because of the sample size, data were analyzed with a *t*-test. For parameters that did not pass normality tests, the Mann Whitney rank-sum test was run and the U statistic reported. *P* values < 0.05 were considered significant. The asterisks indicate significant differences between LD and DLaN treatments within genotype. Significant differences are shown in bold. a.u.= arbitrary units.

Measures	**WT LD**	**WT DLaN**	**Student's *t*-test**	**Opn4$^{dta/dta}$ LD**	**Opn4$^{dta/dta}$ DLaN**	**Student's *t*-test**
Masking (% reduction)	-8.9 ± 9.3	-42.1 ± 7.3*	**$t_{(12)}$ = 2.795, P = 0.016**	2.8 ± 10.4	10.0 ± 9.9	$t_{(12)}$ = -0.498, P = 0.628
Total activity (a.u./24 hrs)	3494.4 ± 538.6	1589.8 ± 267.4*	**$t_{(8)}$ = 5.408, P = 0.005**	2850.8 ± 889.9	2973.8 ± 801.9	$t_{(7)}$ = -0.368, P = 0.724
Power (% variation)	37.0 ± 3.7	17.8 ± 1.7*	**$t_{(8)}$ = 5.408, P = 0.005**	27.2 ± 1.9	28.9 ± 3.7	$t_{(7)}$ = -0.368, P = 0.724
Amplitude (Peak/trough)	316.7 ± 36.7	140.8 ± 23.5*	**$t_{(8)}$ = 4.031, P = 0.004**	271.1 ± 60.9	274.8 ± 67.0	$t_{(7)}$ = -0.040, P = 0.969
Activity in day (%)	19.0 ± 2.4	26.6 ± 4.5*	**$t_{(8)}$ = 5.408, P = 0.006**	27.2 ± 1.9	28.9 ± 2.8	$t_{(7)}$ = -0.368, P = 0.724
Fragmentation (bout #)	9.0 ± 0.6	9.8 ± 0.7	$t_{(8)}$ = 0.826, P = 0.425	7.6 ± 0.8	8.4 ± 0.8	$U_{(7)}$ = 4.0, P = 0.190
Onset variability (min)	13.9 ± 1.3	25.7 ± 6.5	$t_{(8)}$ =-1.767, P = 0.057	14.8 ± 3.1	16.7 ± 3.3	$t_{(7)}$ = -0.401, P = 0.350
Social interaction (sec)	54.9 ± 16.2	15.7 ± 3.1*	**$U_{(10)}$ =7.000, P = 0.007**	50.3 ± 12.6	40.8 ± 5.6	$t_{(10)}$ = 0.683, P = 510

Table 2.3. Long λ enriched illumination minimized DLaN disruption. Comparisons of age-matched WT and Cntnap2 KO mice under LD or DLaN regimen (n = 12/group). Values are shown as averages ± SEM. Data were analyzed with a 2-way ANOVA using genotype and treatment as factors. The Holm-Sidak test for multiple comparisons was used when appropriate. ∗ indicates significant differences between LD baseline and DLaN treatments. # indicates significant differences between WT and Cntnap2 KO controls. Significant differences are shown in bold. a.u.= arbitrary units.

	WT			***Cntnap2* KO**			**2-way ANOVA**	
Measures	**Baseline LD**	**Short λ DLaN**	**Long λ DLaN**	**Baseline LD**	**Short λ DLaN**	**Long λ DLaN**	**Genotype**	**Treatment**
Total activity (a.u./24 hrs)	3003.9 ± 320.6	2114.3 ± 237.0	3443.3 ± 524.1	1943.4 ± 135.3#	1639.4 ± 253.8	2145.6 ± 216.8	**$F_{(1,95)}$ = 14.16; *P* < 0.001**	**$F_{(2,95)}$ = 3.88; *P* = 0.024**
Power (% variance)	31.8 ± 1.1	22.6 ± 1.0*	30.6 ± 2.2	24.8 ± 1.2#	19.3 ± 1.4*	28.9 ± 2.0	**$F_{(1,95)}$ = 5.39, P = 0.022**	**$F_{(2,95)}$ = 10.97, P < 0.001**
Amplitude (Peak/trough)	250.1 ± 29.6	148.7 ± 1*	295.3 ± 45.9	183.9 ± 15.9#	132.1 ± 19.9*	212.1 ± 22.5	**$F_{(1,95)}$ = 5.49; *P* = 0.018**	**$F_{(2,95)}$ = 7.23; *P* = 0.001**
Activity in day (%)	18.7 ± 0.7	26.0 ± 1.9*	19.6 ± 1.7	26.0 ± 2.0	32.3 ± 2.0	19.3 ± 1.6	$F_{(1,95)}$ = 2.80; *P* = 0.098	**$F_{(2,95)}$ = 27.63; *P* < 0.001**
Onset variability (min)	18.2 ± 1.9	33.44 ± 5*	25.0 ± 3.0	23.5 ± 2.0	42.0 ± 6.1*	36.6 ± 2.9	**$F_{(1,95)}$ = 10.27; *P* = 0.002**	**$F_{(2,95)}$ = 16.10; *P* < 0.001**
Fragmentation (# bouts)	10.5 ± 0.9	10.7 ± 1.0	10.8 ± 2.0	11.6 ± 1.3	12.4 ± 1.5	11.6 ± 1.6	$F_{(1,95)}$ = 1.13; *P* =0.29	$F_{(2,95)}$ = 0.07; *P* = 0.93
Social interaction (sec)	48.8 ± 6.2	26.3 ± 6.8*	43.3 ± 9.6	23.4 ± 3.4#	8.6 ± 2.0*	16.9 ± 3.9	**$F_{(1,95)}$ = 15.04; *P* < 0.001**	**$F_{(2,95)}$ = 4.54; *P* = 0.013**
Grooming (sec)	13.4 ± 1.1	15.7 ± 2.0	10.1 ± 1.6	31.2 ± 1.8#	43.7 ± 2.8*	27.7 ± 2.5	**$F_{(1,151)}$ = 149.14; *P* < 0.001**	**$F_{(2,151)}$ = 11.51; *P* < 0.001**

Table 2.4. Long λ enriched illumination minimized DLaN evoked c-Fos expression in several brain regions. Comparisons of age-matched WT and Cntnap2 KO mice under LD or DLaN regimen (n = 6/group). Immunopositive cells were counted in the left and or right region of interest in two consecutive slice and the numbers averaged. Values are shown as averages ± SEM. Data were analyzed with a 2-way ANOVA using genotype and treatment as factors. The Holm-Sidak test for multiple comparisons was used when appropriate. ∗ indicates significant differences between LD controls and DLaN treatments. There were no significant interactions between genotype and treatment. SCN = suprachiasmatic nucleus; pHb = perihabenular nucleus; PVN = periventricular nucleus; LH = lateral hypothalamus; BLA = basolateral amygdala. Significant differences are shown in bold.

	WT			***Cntnap2* KO**			**2-way ANOVA**	
Brain region	**Baseline LD**	**Short λ DLaN**	**Long λ DLaN**	**Baseline LD**	**Short λ DLaN**	**Long λ DLaN**	**Genotype**	**Treatment**
SCN	4.6 ± 1.3	4.1 ± 0.8	4.6 ± 0.9	4.8 ± 1.5	3.3 ± 0.7	4.5 ± 0.7	$F_{(1,35)} = 0.09$; $P = 0.77$	$F_{(2,35)} = 0.62$; $P = 0.54$
pHb	30.1 ± 7.1	55.4 ± 6.7*****	34.7 ± 4.9	22.2 ± 1.6	63.1 ± 8.1*****	38.0 ± 6.4	$F_{(1,35)} = 0.047$; $P = 0.83$	**$F_{(2,35)} = 71.94$; $P < 0.001$**
PVN	28.4 ± 4.4	35.5 ± 4.8	29.6 ± 6.9	35.8 ± 7.6	35.5 ± 3.9	28.0 ± 7.0	$F_{(1,35)} = 0.19$; $P = 0.67$	$F_{(2,35)} = 0.76$; $P = 0.48$
LH	134.1 ± 42.0	133.6 ± 30.2	150. 9 ± 28.2	140.1 ± 40.0	140.9 ± 12.5	121.7 ± 19.9	$F_{(1,35)} = 0.055$; $P = 0.82$	$F_{(2,35)} < 0.001$; $P = 1$
BLA	170.2 ± 38.1	235.1 ± 46.3	160.2 ± 29.9	202.0 ± 42.0	346.3 ± 27.1*****	222.9 ± 25.8	**$F_{(1,35)} = 7.99$; $P = 0.008$**	**$F_{(2,35)} = 5.99$; $P = 0.006$**

Table 2.5. Short λ enriched illumination increases c-Fos expression in glutamatergic (vGlut2 positive) neurons in BLA. Comparisons of double labeling for c-Fos and vGLut2-ZsGreen positive cells in the BLA of WT and Cntnap2 KO mice under LD or short λ enriched DLaN regimen (n = 4/group). For this analysis, we counted the number of vGlut2-ZsGreen expressing neurons, then the number of these neuron that were also c-Fos positive. 5-6 fields per animal were measured and values averaged to come up with a number per animal. Values are shown as averages ± SEM. Data were analyzed with a 2-way ANOVA using genotype and treatment as factors. The Holm-Sidak test for multiple comparisons was used when appropriate. ∗ indicates significant differences between LD controls and short λ enriched DLaN. Significant differences are shown in bold.

Measures	**WT Baseline LD**	**WT Short λ DLaN**	***Cntnap2* KO Baseline LD**	***Cntnap2* KO Short λ DLaN**	**Genotype**	**Treatment**	**Interaction**
Total vGlut2+ cells (#)	208 ± 26	236 ± 13	246 ± 16	**174 ± 8*#**	$F_{(1, 15)}$ = 0.57, P = 0.46	$F_{(1, 15)}$ = 1.93, P = 0.19	**$F_{(1, 15)}$ = 10.51, P = 0.007**
c-Fos+ responsive-vGlut2+ cells (#)	44 ± 6	**95 ± 8***	50 ± 16	**93 ± 7***	$F_{(1, 15)}$ = 0.05, P = 0.82	**$F_{(1, 15)}$ = 28.77, P < 0.001**	$F_{(1, 15)}$ = 0.24, P = 0.64
c-Fos+ responsive-vGlut2+ cells/ Total vGlut2+ cells (%)	21.0 ± 1.0	**40 ± 5.0***	20 ± 5	**54 ± 6***	$F_{(1, 15)}$ = 2.19, P = 0.17	**$F_{(1, 15)}$ = 43.0, P < 0.001**	$F_{(1, 15)}$ = 3.15, P = 0.10

S. Table 2.1: Sex differences in WT and Cntnap2 KO mice under LD conditions. Comparisons of age-matched male and female WT and Cntnap2 KO mice under baseline LD conditions. Values are shown as averages ± SEM. Data were analyzed with a 2-way ANOVA using genotype and treatment as factors. The Holm-Sidak test for multiple comparisons was used when appropriate. ∗ indicates significant differences between sexes and # indicates significant differences between genotypes. There were no significant interactions between genotype and sex. Significant differences are shown in bold. a.u.= arbitrary units.

Measures	WT		*Cntnap2* KO		2-way ANOVA	
	Male Baseline LD	**Female Baseline LD**	**Male Baseline LD**	**Female Baseline LD**	**Genotype**	**Sex**
Total activity (a.u./24 hrs)	2756.8 ± 327.6 (n=12)	3276.6 ± 429.8 (n=11)	2073.8 ± 213.8 (n=12)	1812.9 ± 156.6# (n=12)	**$F_{(1,46)}$ = 13.28; *P* < 0.001**	$F_{(1,46)}$ = 0.19; *P* = 0.662
Power (% variance)	31.9 ± 1.5 (n=12)	32.5 ± 1.5 (n=11)	24.5 ± 1.4# (n=12)	24.3 ± 1.7# (n=12)	**$F_{(1,46)}$ = 19.92; P < 0.001**	$F_{(1,46)}$ = 0.03, P = 0.873
Amplitude (Peak/trough)	237.6 ± 29.2 (n=12)	251.4 ± 29.3 (n=11)	183.8 ± 14.9 (n=12)	167.2 ± 18.2# (n=12)	**$F_{(1,46)}$ = 8.54; *P* = 0.006**	$F_{(1,46)}$ = 0.01, P = 0.951
Social interaction (sec)	41.2 ± 6.4 (n=13)	56.0 ± 8.3 (n=11)	22.5 ± 5.2 (n=14)	22.5 ± 6.4 (n=10)	**$F_{(1,47)}$ = 15.62; *P* < 0.001**	$F_{(1,47)}$ = 1.26; *P* = 0.268
Grooming (sec)	14.4 ± 1.6 (n=17)	12.3 ± 1.6 (n=17)	35.8 ± 2.6# (n=19)	28.3 ± 2.0# (n=18)	**$F_{(1,69)}$ = 82.34; *P* < 0.001**	**$F_{(1,69)}$ = 5.37; *P* = 0.024**

S. Table 2.2: Sex differences in WT and *Cntnap2* KO mice under DLaN conditions. Comparisons of age-matched male and female WT and Cntnap2 KO mice under short λ DLaN conditions. Values are shown as averages ± SEM. Data were analyzed with a 2-way ANOVA using genotype and treatment as factors. The Holm-Sidak test for multiple comparisons was used when appropriate. ∗ indicates significant differences between sexes and # indicates significant differences between genotypes. There were no significant interactions between genotype and sex. Significant differences are shown in bold.

Measures	**WT**		***Cntnap2* KO**		**2-way ANOVA**	
	Male DLaN	**Female DLaN**	**Male DLaN**	**Female DLaN**	**Genotype**	**Sex**
Total activity (a.u./24 hrs)	1755.3 ± 257.6 (n=6)	2473.4 ± 359.5 (n=6)	2152.9 ± 388.3 (n=6)	1892.6 ± 216.5 (n=6)	$F_{(1,23)} = 0.08$; $P = 0.773$	$F_{(1,23)} = 0.53$; $P = 0.474$
Power (% variance)	21.0 ± 1.0 (n=6)	24.2 ± 1.6 (n=6)	25.2 ± 1.8 (n=6)	22.0 ± 0.9 (n=6)	$F_{(1,23)} = 0.52$, P = 0.479	$F_{(1,23)} = 0.01$, P =0.999
Amplitude (Peak/trough)	135.7 ± 19.5 (n=6)	161.7 ± 20.4 (n=6)	187.3 ± 25.7 (n=6)	156.8 ± 20.0 (n=6)	$F_{(1,23)} = 1.18$; $P = 0.291$	$F_{(1,23)} = 0.01$; $P = 0.919$
Social interaction (sec)	38.1 ± 11.3 (n=6)	17.8 ± 7.7 (n=6)	7.9 ± 3.0# (n=6)	11.0 ± 2.1# (n=6)	**$F_{(1,23)} = 6.20$; $P = 0.022$**	$F_{(1,23)} = 1.35$; $P = 0.259$
Grooming (sec)	18.0 ± 2.7 (n=8)	13.42 ± 2.8 (n=8)	44.4 ± 3.2# (n=11)	44.9 ± 4.5# (n=11)	**$F_{(1,37)} = 62.23$; $P < 0.001$**	$F_{(1,37)} = 0.31$; $P = 0.578$

References

Altimus CM, Güler AD, Alam NM, Arman AC, Prusky GT, Sampath AP, Hattar S. Rod photoreceptors drive circadian photoentrainment across a wide range of light intensities. Nat Neurosci. 2010;13(9):1107.

An K, Zhao H, Miao Y, Xu Q, Li Y-F, Ma Y-Q, Shi Y-M, Shen J-W, Meng J-J, Yao Y-G. A circadian rhythm-gated subcortical pathway for nighttime-light-induced depressive-like behaviors in mice. Nat Neurosci. 2020;23(7):869-80.

Angelakos CC, Tudor JC, Ferri SL, Jongens TA, Abel T. Home-cage hypoactivity in mouse genetic models of autism spectrum disorder. Neurobiol Learn Mem. 2019 165:107000. doi: 10.1016/j.nlm.2019.02.010.

Aubrecht TG, Weil ZM, Magalang UJ, Nelson RJ. Dim light at night interacts with intermittent hypoxia to alter cognitive and affective responses. American Journal of Physiology-Regulatory, Integrative and Comparative Physiology. 2013;305(1):R78-R86.

Baker EK, Richdale AL. Examining the behavioural sleep-wake rhythm in adults with autism spectrum disorder and no comorbid intellectual disability. J Autism Dev Disord. 2017;47(4):1207-22.

Bano-Otalora B, Martial F, Harding C, Bechtold DA, Allen AE, Brown TM, Belle MDC, Lucas RJ. Bright daytime light enhances circadian amplitude in a diurnal mammal. Proc Natl Acad Sci U S A. 2021 Jun 1;118(22):e2100094118. doi: 10.1073/pnas.2100094118. PMID: 34031246; PMCID: PMC8179182.

Bedrosian TA, Fonken LK, Walton JC, Nelson RJ. Chronic exposure to dim light at night suppresses immune responses in Siberian hamsters. Biol Lett. 2011;7(3):468-71. doi: 10.1098/rsbl.2010.1108.

Bedrosian TA, Nelson RJ. Timing of light exposure affects mood and brain circuits. Transl Psychiatry. 2017; 7(1):e1017. doi: 10.1038/tp.2016.262.

Bedrosian TA, Vaughn CA, Galan A, Daye G, Weil ZM, Nelson RJ. Nocturnal light exposure impairs affective responses in a wavelength-dependent manner. J Neurosci. 2013;33(32):13081-7.

Borniger JC, Maurya SK, Periasamy M, Nelson RJ. Acute dim light at night increases body mass, alters metabolism, and shifts core body temperature circadian rhythms. Chronobiol Int. 2014;31(8):917-25. doi: 10.3109/07420528.2014.926911.

Borniger JC, McHenry ZD, Abi Salloum BA, Nelson RJ. Exposure to dim light at night during early development increases adult anxiety-like responses. Physiol Behav. 2014;133(0):99-106. doi: http://dx.doi.org/10.1016/j.physbeh.2014.05.012.

Brown TM. Melanopic illuminance defines the magnitude of human circadian light responses under a wide range of conditions. J Pineal Res. 2020 69(1):e12655. doi: 10.1111/jpi.12655.

Bumgarner JR, Nelson RJ. Light at Night and Disrupted Circadian Rhythms Alter Physiology and Behavior. Integr Comp Biol. 2021 61(3):1160-1169. doi: 10.1093/icb/icab017.

Burgess HJ, Molina TA. Home Lighting Before Usual Bedtime Impacts Circadian Timing: A Field Study. Photochemistry and Photobiology. 2014;90(3):723-6.

Cain N, Gradisar M. Electronic media use and sleep in school-aged children and adolescents: A review. Sleep Med. 2010 11(8):735-42. doi: 10.1016/j.sleep.2010.02.006.

Cohen S, Conduit R, Lockley SW, Rajaratnam SMW, Cornish KM. The relationship between sleep and behavior in autism spectrum disorder (ASD): a review. J Neurodev Disord. 2014;6(1):44. doi: 10.1186/1866-1955-6-44. PubMed PMID: PMC4271434.

Collins B, Pierre-Ferrer S, Muheim C, Lukacsovich D, Cai Y, Spinnler A, Herrera CG, Winterer J, Belle MD, Piggins HD. Circadian VIPergic neurons of the suprachiasmatic nuclei sculpt the sleep-wake cycle. Neuron. 2020;108(3):486-99. e5.

Craig LA, McDonald RJ. Chronic disruption of circadian rhythms impairs hippocampal memory in the rat. Brain Res Bull. 2008;76(1–2):141-51. doi: http://dx.doi.org/10.1016/j.brainresbull.2008.02.013.

Devnani P, Hegde A. Autism and sleep disorders. J Pediatr Neurosci. 2015;10(4):304-7. doi: 10.4103/1817-1745.174438.

Dong H-Y, Wang B, Li H-H, Yue X-J, Jia F-Y. Correlation Between Screen Time and Autistic Symptoms as Well as Development Quotients in Children With Autism Spectrum Disorder. Frontiers in Psychiatry. 2021;12:140.

Elkhatib Smidt SD, Hitt T, Zemel BS, Mitchell JA. Sex differences in childhood sleep and health implications. Ann Hum Biol. 2021 48(6):474-484. doi: 10.1080/03014460.2021.1998624.

Engelhardt CR, Mazurek MO, Sohl K. Media use and sleep among boys with autism spectrum disorder, ADHD, or typical development. Pediatrics. 2013;132(6):1081-9. Epub 2013/11/20. doi: 10.1542/peds.2013-2066.

Engelmann M, Wotjak CT, Landgraf R. Direct osmotic stimulation of the hypothalamic paraventricular nucleus by microdialysis induces excessive grooming in the rat. Behav Brain Res. 1994;63(2):221-5.

Felix-Ortiz AC, Tye KM. Amygdala inputs to the ventral hippocampus bidirectionally modulate social behavior. J Neurosci. 2014;34(2):586-95.

Fernandez DC, Fogerson PM, Lazzerini Ospri L, Thomsen MB, Layne RM, Severin D, Zhan J, Singer JH, Kirkwood A, Zhao H, Berson DM, Hattar S. Light Affects Mood and Learning through Distinct Retina-Brain Pathways. Cell. 2018 175(1):71-84.e18. doi: 10.1016/j.cell.2018.08.004.

Figueiro MG, Pedler D. Red light: A novel, non-pharmacological intervention to promote alertness in shift workers. Journal of Safety Research. 2020;74:169-77.

Fombonne E. Epidemiology of pervasive developmental disorders. Pediatr Res. 2009 65(6):591-8. doi: 10.1203/PDR.0b013e31819e7203.

Fonken LK, Aubrecht TG, Meléndez-Fernández OH, Weil ZM, Nelson RJ. Dim Light at Night Disrupts Molecular Circadian Rhythms and Increases Body Weight. J Biol Rhythms. 2013;28(4):262-71. doi: 10.1177/0748730413493862. PubMed PMID: 23929553.

Fonken LK, Kitsmiller E, Smale L, Nelson RJ. Dim nighttime light impairs cognition and provokes depressive-like responses in a diurnal rodent. J Biol Rhythms. 2012;27(4):319-27.

Fonken LK, Lieberman RA, Weil ZM, Nelson RJ. Dim Light at Night Exaggerates Weight Gain and Inflammation Associated With a High-Fat Diet in Male Mice. Endocrinology. 2013;154(10):3817-25. doi: 10.1210/en.2013-1121.

Fonken LK, Haim A, Nelson RJ. Dim Light at Night Increases Immune Function in Nile Grass Rats, a Diurnal Rodent. Chronobiol Int. 2012;29(1):26-34. doi: 10.3109/07420528.2011.635831.

Fonken LK, Nelson RJ. Illuminating the deleterious effects of light at night. F1000 Med Rep. 2011;3:18. doi: 10.3410/M3-18. PubMed PMID: PMC3169904.

Fonken LK, Weil ZM, Nelson RJ. Mice exposed to dim light at night exaggerate inflammatory responses to lipopolysaccharide. Brain Behav Immun. 2013; 34:159-63. doi: https://doi.org/10.1016/j.bbi.2013.08.011.

Fournier C, Wirz-Justice A. Light, health and wellbeing: Implications from chronobiology for architectural design. World Health Design: Architecture, Culture, Technology. 2010;3(3):44-9.

Gibson EM, Wang C, Tjho S, Khattar N, Kriegsfeld LJ. Experimental 'Jet Lag' Inhibits Adult Neurogenesis and Produces Long-Term Cognitive Deficits in Female Hamsters. PLoS One. 2010;5(12):e15267. doi: 10.1371/journal.pone.0015267.

Güler AD, Ecker JL, Lall GS, Haq S, Altimus CM, Liao HW, Barnard AR, Cahill H, Badea TC, Zhao H, Hankins MW, Berson DM, Lucas RJ, Yau KW, Hattar S. Melanopsin cells are the

principal conduits for rod-cone input to non-image-forming vision. Nature. 2008 453(7191):102-5. doi: 10.1038/nature06829.

Hattar S, Liao HW, Takao M, Berson DM, Yau KW. Melanopsin-containing retinal ganglion cells: architecture, projections, and intrinsic photosensitivity. Science. 2002 295(5557):1065-70. doi: 10.1126/science.1069609.

Healy S, Garcia JM, Haegele JA. Environmental factors associated with physical activity and screen time among children with and without autism spectrum disorder. J Autism Dev Disord. 2020;50(5):1572-9.

Heo JY, Kim K, Fava M, Mischoulon D, Papakostas GI, Kim MJ, Kim DJ, Chang KJ, Oh Y, Yu BH, Jeon HJ. Effects of smartphone use with and without blue light at night in healthy adults: A randomized, double-blind, cross-over, placebo-controlled comparison. J Psychiatr Res. 2017 87:61-70. doi: 10.1016/j.jpsychires.2016.12.010.

Hong W, Kim D-W, Anderson DJ. Antagonistic control of social versus repetitive self-grooming behaviors by separable amygdala neuronal subsets. Cell. 2014;158(6):1348-61.

Hsu M, Dedhia M, Crusio WE, Delprato A. Sex differences in gene expression patterns associated with the *APOE4* allele. F1000Res. 2019 8:387. doi: 10.12688/f1000research.18671.2. PMID: 31448102; PMCID: PMC6685458.

International Commission on Illumination (CIE) to enable calculations and conversions of quantities related to ipRGC-influenced responses to light (IIL responses, or non-visual effects of light), following the international standard CIE S 026:2018. System for Metrology of Optical Radiation for ipRGC-Influenced Responses to Light. CIE, Vienna (DOI: 10.25039/S026.2018).

Ishihara A, Park I, Suzuki Y, Yajima K, Cui H, Yanagisawa M, Sano T, Kido J, Tokuyama K. Metabolic responses to polychromatic LED and OLED light at night. Sci Rep. 2021 11(1):12402. doi: 10.1038/s41598-021-91828-6.

Klepeis NE, Nelson WC, Ott WR, Robinson JP, Tsang AM, Switzer P, Behar JV, Hern SC, Engelmann WH. The National Human Activity Pattern Survey (NHAPS): a resource for assessing exposure to environmental pollutants. J Expo Anal Environ Epidemiol. 2001 May-Jun;11(3):231-52. doi: 10.1038/sj.jea.7500165. PMID: 11477521.

Lall GS, Revell VL, Momiji H, Al Enezi J, Altimus CM, Güler AD, Aguilar C, Cameron MA, Allender S, Hankins MW, Lucas RJ. Distinct contributions of rod, cone, and melanopsin photoreceptors to encoding irradiance. Neuron. 2010 66(3):417-28. doi: 10.1016/j.neuron.2010.04.037.

Lazzerini Ospri L, Prusky G, Hattar S. Mood, the Circadian System, and Melanopsin Retinal Ganglion Cells. Annu Rev Neurosci. 2017 Jul 25;40:539-556. doi: 10.1146/annurev-neuro-072116-031324.

LeGates TA, Fernandez DC, Hattar S. Light as a central modulator of circadian rhythms, sleep and affect. Nat Rev Neurosci. 2014;15(7):443-54. doi: 10.1038/nrn3743. PubMed PMID: 24917305; PMCID: PMC4254760.

Lee FY, Wang H-B, Hitchcock O, Loh DH-W, Whittaker DS, Kim Y-S, Aiken A, Kokikian C, Dell'Angelica EC, Colwell CS. Sleep/Wake Disruption in a Mouse Model of BLOC-1 Deficiency. Front Neurosci. 2018;12:759.

Lockley SW, Evans EE, Scheer FA, Brainard GC, Czeisler CA, Aeschbach D. Short-wavelength sensitivity for the direct effects of light on alertness, vigilance, and the waking electroencephalogram in humans. Sleep. 2006;29(2):161-8. PubMed PMID: 16494083.

Logan RW, Hasler BP, Forbes EE, Franzen PL, Torregrossa MM, Huang YH, Buysse DJ, Clark DB, McClung CA. Impact of Sleep and Circadian Rhythms on Addiction Vulnerability in Adolescents. Biol Psychiatry. 2018 83(12):987-996. doi: 10.1016/j.biopsych.2017.11.035

Lucas RJ, Lall GS, Allen AE, Brown TM. Chapter 1 - How rod, cone, and melanopsin photoreceptors come together to enlighten the mammalian circadian clock. In: Andries Kalsbeek MMTR, Russell GF, editors. Prog Brain Res: Elsevier; 2012. p. 1-18.

Lucas RJ, Peirson SN, Berson DM, Brown TM, Cooper HM, Czeisler CA, Figueiro MG, Gamlin PD, Lockley SW, O'Hagan JB. Measuring and using light in the melanopsin age. Trends Neurosci. 2014;37(1):1-9.

Lucassen EA, Coomans CP, van Putten M, de Kreij SR, van Genugten JH, Sutorius RP, de Rooij KE, van der Velde M, Verhoeve SL, Smit JW, Löwik CW, Smits HH, Guigas B, Aartsma-Rus AM, Meijer JH. Environmental 24-hr Cycles Are Essential for Health. Curr Biol. 2016 26(14):1843-53. doi: 10.1016/j.cub.2016.05.038

Lunn RM, Blask DE, Coogan AN, Figueiro MG, Gorman MR, Hall JE, Hansen J, Nelson RJ, Panda S, Smolensky MH, Stevens RG, Turek FW, Vermeulen R, Carreón T, Caruso CC, Lawson CC, Thayer KA, Twery MJ, Ewens AD, Garner SC, Schwingl PJ, Boyd WA. Health consequences of electric lighting practices in the modern world: A report on the National Toxicology Program's workshop on shift work at night, artificial light at night, and circadian disruption. Sci Total Environ. 2017 Dec 31;607-608:1073-1084. doi: 10.1016/j.scitotenv.2017.07.056.

Madisen L, Zwingman TA, Sunkin SM, Oh SW, Zariwala HA, Gu H, Ng LL, Palmiter RD, Hawrylycz MJ, Jones AR, Lein ES, Zeng H. A robust and high-throughput Cre reporting and characterization system for the whole mouse brain. Nat Neurosci. 2010 13(1):133-40. doi: 10.1038/nn.2467.

Mangieri LR, Lu Y, Xu Y, Cassidy RM, Xu Y, Arenkiel BR, Tong Q. A neural basis for antagonistic control of feeding and compulsive behaviors. Nature communications. 2018;9(1):52.

Mazurek MO, Engelhardt Cr Fau - Hilgard J, Hilgard J Fau - Sohl K, Sohl K. Bedtime Electronic Media Use and Sleep in Children with Autism Spectrum Disorder. J Dev Behav Pediatr.

2016;37(7):525–531, SEP (1536-7312 (Electronic)). doi: 10.1097/DBP.0000000000000314; PMCID: 27355885.

Mazurek MO, Sohl K. Sleep and Behavioral Problems in Children with Autism Spectrum Disorder. J Autism Dev Disord. 2016;46(6):1906-15. doi: 10.1007/s10803-016-2723-7.

Milosavljevic N, Cehajic-Kapetanovic J, Procyk CA, Lucas RJ. Chemogenetic activation of melanopsin retinal ganglion cells induces signatures of arousal and/or anxiety in mice. Curr Biol. 2016;26(17):2358-63.

Moaraf S, Vistoropsky Y, Pozner T, Heiblum R, Okuliarová M, Zeman M, Barnea A. Artificial light at night affects brain plasticity and melatonin in birds. Neurosci Lett. 2020;716:134639.

Mouland JW, Martial FP, Lucas RJ, Brown TM. Modulations in irradiance directed at melanopsin, but not cone photoreceptors, reliably alter electrophysiological activity in the suprachiasmatic nucleus and circadian behaviour in mice. J Pineal Res. 2021 70(4):e12735. doi: 10.1111/jpi.12735.

Nagare R, Rea MS, Plitnick B, Figueiro MG. Effect of White Light Devoid of "Cyan" Spectrum Radiation on Nighttime Melatonin Suppression Over a 1-h Exposure Duration. J Biol Rhythms. 2019 34(2):195-204. doi: 10.1177/0748730419830013.

Nagare R, Rea MS, Plitnick B, Figueiro MG. Nocturnal Melatonin Suppression by Adolescents and Adults for Different Levels, Spectra, and Durations of Light Exposure. J Biol Rhythms. 2019 Apr;34(2):178-194. doi: 10.1177/0748730419828056.

Nelson RJ, Chbeir S. Dark matters: effects of light at night on metabolism. Proc Nutr Soc. 2018 77(3):223-229. doi: 10.1017/S0029665118000198.

Norrholm SD, Das M, Légrádi G. Behavioral effects of local microinfusion of pituitary adenylate cyclase activating polypeptide (PACAP) into the paraventricular nucleus of the hypothalamus (PVN). Regul Pept. 2005;128(1):33-41.

Osibona O, Solomon BD, Fecht D. Lighting in the Home and Health: A Systematic Review. Int J Environ Res Public Health. 2021 18(2):609. doi: 10.3390/ijerph18020609.

Panda S, Antoch MP, Miller BH, Su AI, Schook AB, Straume M, Schultz PG, Kay SA, Takahashi JS, Hogenesch JB. Coordinated transcription of key pathways in the mouse by the circadian clock. Cell. 2002;109. doi: 10.1016/s0092-8674(02)00722-5.

Panda S, Nayak SK, Campo B, Walker JR, Hogenesch JB, Jegla T. Illumination of the Melanopsin Signaling Pathway. Science. 2005;307(5709):600-4. doi: 10.1126/science.1105121.

Plano SA, Casiraghi LP, García Moro P, Paladino N, Golombek DA, Chiesa JJ. Circadian and Metabolic Effects of Light: Implications in Weight Homeostasis and Health. Front Neurol. 2017 8:558. doi: 10.3389/fneur.2017.00558.

Rea MS, Nagare R, Figueiro MG. Predictions of melatonin suppression during the early biological night and their implications for residential light exposures prior to sleeping. Sci Rep. 2020 10(1):14114. doi: 10.1038/s41598-020-70619-5.

Rollag MD, Berson DM, Provencio I. Melanopsin, ganglion-cell photoreceptors, and mammalian photoentrainment. J Biol Rhythms. 2003;18(3):227-34. doi: 10.1177/0748730403018003005. PubMed PMID: 12828280.

Russart KLG, Nelson RJ. Light at night as an environmental endocrine disruptor. Physiol Behav. 2018 190:82-89. doi: 10.1016/j.physbeh.2017.08.029.

Schaafsma SM, Gagnidze K, Reyes A, Norstedt N, Månsson K, Francis K, Pfaff DW. Sex-specific gene-environment interactions underlying ASD-like behaviors. Proc Natl Acad Sci U S A. 2017 114(6):1383-1388. doi: 10.1073/pnas.1619312114.

Schmidt TM, Chen SK, Hattar S. Intrinsically photosensitive retinal ganglion cells: many subtypes, diverse functions. Trends Neurosci. 2011;34(11):572-80. doi: 10.1016/j.tins.2011.07.001. PubMed PMID: 21816493; PMCID: PMC3200463.

Schoonderwoerd RA, de Rover M, Janse JAM, Hirschler L, Willemse CR, Scholten L, Klop I, van Berloo S, van Osch MJP, Swaab DF, Meijer JH. The photobiology of the human circadian clock. Proc Natl Acad Sci U S A. 2022 119(13):e2118803119.

Shelton AR, Malow B. Neurodevelopmental Disorders Commonly Presenting with Sleep Disturbances. Neurotherapeutics. 2021 18(1):156-169. doi: 10.1007/s13311-020-00982-8.

Song P, Yan B, Lei F, Qiu Z, Zhang C, Wu Y, Chen S, Yang X, Shen D, Ma P. Continuous artificial light at night exacerbates diisononyl phthalate-induced learning and memory impairment in mice: Toxicological evidence. Food Chem Toxicol. 2021;151:112102

Stevenson TJ, Visser ME, Arnold W, Barrett P, Biello S, Dawson A, Denlinger DL, Dominoni D, Ebling FJ, Elton S, Evans N, Ferguson HM, Foster RG, Hau M, Haydon DT, Hazlerigg DG, Heideman P, Hopcraft JG, Jonsson NN, Kronfeld-Schor N, Kumar V, Lincoln GA, MacLeod R, Martin SA, Martinez-Bakker M, Nelson RJ, Reed T, Robinson JE, Rock D, Schwartz WJ, Steffan-Dewenter I, Tauber E, Thackeray SJ, Umstatter C, Yoshimura T, Helm B. Disrupted seasonal biology impacts health, food security and ecosystems. Proc Biol Sci. 2015 282(1817):20151453. doi: 10.1098/rspb.2015.1453.

Stiller A, Weber J, Strube F, Mößle T. Caregiver Reports of Screen Time Use of Children with Autism Spectrum Disorder: A Qualitative Study. Behav Sci (Basel) 2019 9(5):56. doi: 10.3390/bs9050056.

Stockman A, Sharpe LT. The spectral sensitivities of the middle-and long-wavelength-sensitive cones derived from measurements in observers of known genotype. Vision Res. 2000;40(13):1711-37.

Sun T, Song Z, Tian Y, Tian W, Zhu C, Ji G, Luo Y, Chen S, Wang L, Mao Y. Basolateral amygdala input to the medial prefrontal cortex controls obsessive-compulsive disorder-like checking behavior. Proceedings of the National Academy of Sciences. 2019;116(9):3799-804.

Touitou Y, Touitou D, Reinberg A. Disruption of adolescents' circadian clock: The vicious circle of media use, exposure to light at night, sleep loss and risk behaviors. J Physiol Paris. 2016 Nov;110(4 Pt B):467-479. doi: 10.1016/j.jphysparis.2017.05.001.

Townsend LB, Smith SL. Genotype- and sex-dependent effects of altered *Cntnap2* expression on the function of visual cortical areas. J Neurodev Disord. 2017 9:2. doi: 10.1186/s11689-016-9182-5.

Walker WH 2nd, Borniger JC, Gaudier-Diaz MM, Hecmarie Meléndez-Fernández O, Pascoe JL, Courtney DeVries A, Nelson RJ. Acute exposure to low-level light at night is sufficient to induce neurological changes and depressive-like behavior. Mol Psychiatry. 2020 25(5):1080-1093. doi: 10.1038/s41380-019-0430-4.

Walbeek TJ, Harrison EM, Gorman MR, Glickman GL. Naturalistic Intensities of Light at Night: A Review of the Potent Effects of Very Dim Light on Circadian Responses and Considerations for Translational Research. Front Neurol. 2021 12:625334. doi: 10.3389/fneur.2021.625334.

Wang H-B, Loh DH, Whittaker DS, Cutler T, Howland D, Colwell CS. Time-Restricted Feeding Improves Circadian Dysfunction as well as Motor Symptoms in the Q175 Mouse Model of Huntington's Disease. eNeuro. 2018;5(1):ENEURO.0431-17.2017. doi: 10.1523/ENEURO.0431-17.2017. PubMed PMID: PMC5752678.

Wang HB, Tahara Y, Luk SHC, Kim Y-S, Hitchcock ON, Kaswan ZAM, Kim YI, Block GD, Ghiani CA, Loh DH. Melatonin treatment of repetitive behavioral deficits in the Cntnap2 mouse model of autism spectrum disorder. Neurobiol Dis. 2020;145:105064.

Wang H-B, Whittaker DS, Truong D, Mulji AK, Ghiani CA, Loh DH, Colwell CS. Blue light therapy improves circadian dysfunction as well as motor symptoms in two mouse models of Huntington's disease. Neurobiology of Sleep and Circadian Rhythms. 2017;2:39-52. doi: https://doi.org/10.1016/j.nbscr.2016.12.002.

Werling DM, Geschwind DH. Sex differences in autism spectrum disorders. Curr Opin Neurol. 2013 26(2):146-53. doi: 10.1097/WCO.0b013e32835ee548.

Whitney MS, Shemery AM, Yaw AM, Donovan LJ, Glass JD, Deneris ES. Adult brain serotonin deficiency causes hyperactivity, circadian disruption, and elimination of siestas. J Neurosci. 2016;36(38):9828-42.

Wyse CA, Biello SM, Gill JM. The bright-nights and dim-days of the urban photoperiod: implications for circadian rhythmicity, metabolism and obesity. Ann Med. 2014 46(5):253-63. doi: 10.3109/07853890.2014.913422

Xiao H, Cai H, Li X. Non-visual effects of indoor light environment on humans: A review(). Physiol Behav. 2021 Jan 1;228:113195. doi: 10.1016/j.physbeh.2020.113195.

van Diepen HC, Schoonderwoerd RA, Ramkisoensing A, Janse JAM, Hattar S, Meijer JH. Distinct contribution of cone photoreceptor subtypes to the mammalian biological clock. Proc Natl Acad Sci U S A. 2021 118(22):e2024500118. doi: 10.1073/pnas.2024500118

Vethe D, Scott J, Engstrøm M, Salvesen Ø, Sand T, Olsen A, Morken G, Heglum HS, Kjørstad K, Faaland PM. The evening light environment in hospitals can be designed to produce less disruptive effects on the circadian system and improve sleep. Sleep. 2021;44(3):zsaa194.

Vong L, Ye C, Yang Z, Choi B, Chua S Jr, Lowell BB. Leptin action on GABAergic neurons prevents obesity and reduces inhibitory tone to POMC neurons. Neuron. 2011 71(1):142-54. doi: 10.1016/j.neuron.2011.05.028.

Chapter 4

Chapter 4

Role of inflammation in mediating the effects of dim light at night in the *Cntnap2* KO mouse model of autism.

Abstract

Our prior work suggests that exposure to dim light at night (DLaN) causes disruptions to the sleep/wake cycles as well as increased autism-like behaviors in the *Contactin Associated Protein-like 2* knockout (*Cntnap2* KO) mice. In this study, we sought to assess the contribution of inflammation to these DLaN driven behavioral changes. The wild-type (WT) and *Cntnap2* KO mice were held under control light/dark (LD) cycles or DLaN for 2 weeks and, after behavioral assays, the plasma and the prefrontal cortex (PFC) were sampled in the middle of the night. Under the DLaN, many of the plasma inflammatory markers were elevated in both genotypes and correlated with the behavioral deficits observed in these same mice. In addition, we found that the levels of IL-6 in the PFC were significantly increased in both genotypes. Furthermore, the mutant mice exposed to DLaN exhibited an increased number of microglia cells with a greater complexity in the PFC. We further tested the role of inflammation in mediating the effects of DLaN by treating the mice with the non-steroidal anti-inflammatory drug carprofen. This treatment effectively reduced the inflammatory signature and reduced the impacts of DLaN on social impairments and repetitive grooming. Together, our data suggest that exposure to DLaN increases inflammation while blocking the inflammatory reaction seems protective.

Introduction

The immune system is essential for the development and function of the central nervous system (CNS) besides its protecting role to pathogens (Tremblay et al., 2011; Morimoto et al., 2019). For example, microglia, the resident immune cells in the CNS, continuously surveil the brain environment and regulate the responses to injury and diseases while they also have “non-immune” roles in the healthy brains (Wake et al., 2013; Augusto-Oliveira et al., 2019). They are known to mediate synaptic remodeling (Hanamsagar et al., 2017; Nguyen et al., 2020), blood-brain barrier maintenance (Ronaldson et al., 2020), and secretion of neurotrophic factors (Konishi et al., 2019). Changes in microglial function and morphology have been demonstrated to cause impaired learning and memory (Parkhurst et al., 2013), reduced social interaction (Lowery et al., 2021), and increased anxiety behavior (Lituma et al., 2021). The released cytokines in the brain also play an essential role and have profound impacts on neuromodulating function and output behavior. For example, the interferon-gamma (IFN-γ) mediates neural connectivity and induces changes in social behavior through increased GABAergic signaling in the prefrontal cortex (PFC, Filianoet al., 2016). As another example, the interleukin-6 (IL-6) alters NMDA receptor mediated excitatory synaptic transmission and plasticity (Escobar et al., 2011) and inhibit the activity of GABAergic interneurons (Nelson et al., 2012; Basta-Kaim et al., 2015). These CNS neuromodulating functions are not restricted to development and continue into adulthood (e.g. Elmore et al., 2018; Liu et al., 2021).

Central and peripheral immune dysregulations are frequently observed in autism spectrum disorder (ASD), a complex neurodevelopmental disorder composed of a continuum of behavioral traits, including social-communication deficits and restricted interest/stereotypic behavior. Recent large-scale genome-wide association studies (GWAS) has demonstrated a statistical link between immune risk genes and ASD symptoms (Collins et al., 2013; Voineagu et al., 2013; Arenella et al., 2021). Supporting the genomic analysis, the investigations in ASD individuals have reported abnormal numbers of immune cells and altered levels of immune

molecules both centrally and peripherally (Nadeem et al., 2022; Robinson-Agramonte et al., 2022). In addition, significant associations between the imbalanced inflammatory/anti-inflammatory signaling and the challenging ASD behavior are reported (Nadeem et al., 2022). Finally, the contributions of immune dysregulations to the development of ASD are consistently replicated in preclinical models (Cupo et al., 2022; Massrali et al., 2022; Robinson-Agramonte et al., 2022). Together, these studies imply that dysregulated immune activities are prominent ASD characteristics and may contribute to the environmental insults on disease symptoms.

One of the environmental perturbations that may contribute to the expression of ASD symptoms through imbalanced immune pathways is the disruption of the circadian timing system. Circadian rhythms are an evolutionary timing system essential for optimal function and health in physiological systems including the immune system. In mammals, the circadian genes are found in immune cells including microglia, and regulate a broad range of immune activities such as the number of immune cells in the blood and lymphatic tissues (Born et al., 1997; Besedovsky et al., 2014; Kirsch et al., 2012), the activity of pattern-recognition receptors (Silver et al., 2012), the responses to endotoxin challenges (Straub et al., 2007), the recruitment of immune cells (Scheiermann et al., 2012), and phagocytosis (Keller et al., 2009). Supporting the multifunctional role of circadian rhythms in layers of immune regulations, studies have demonstrated that the disruption of the circadian system alters the inflammatory/anti-inflammatory balance (Downton et al., 2020; Gray et al., 2022) and can lead to more severe inflammatory outcomes (Poole et al., 2022; Qiu et al., 2022) and sometimes even higher mortality rates (Castanon-Cervantes et al., 2010).

Using the *Contactin Associated Protein-like 2* knockout (*Cntnap2* KO) mouse model of ASD, we have previously reported a link between the worsened ASD behavior and the circadian-disrupting environment (Wang et al., 2020; Wang et al., in prep). Our data demonstrated that 2 weeks of exposure to dim-light at night (DLaN, 5-10 lx) caused a mild disruption of diurnal rhythms in activity and sleep as well as reduced social behavior in both

Cntnap2 KO mutants and wild-type (WT) controls. The mutants further exhibited selective vulnerability to the impact of DLaN on repetitive grooming behavior. Given the tight connections between circadian rhythms and immune functions, the nightly illumination of circadian disruption is demonstrated to alter both the innate and adaptive immune functions, and leads to deleterious impacts on an organism's ability to respond to an immune challenge (Cissé et al., 2020; Okuliarova et al., 2021; Walker et al., 2021; Ziegler et al., 2021). Taking all together, we hypothesized that the DLaN treatment drives the behavioral changes by disrupting the immune balance in the testing animals.

To test this hypothesis, the WT mice and the *Cntnap2* KO mutants were held under control light/dark (LD) cycles or DLaN for 2 weeks and, after behavioral analysis, plasma and brains were collected in the middle of the night. To evaluate general immune profiles, the levels of an array of molecules involved in immune function were measured from the plasma. Since a dysfunctional prefrontal cortex (PFC) has implicated in ASD (Yizhar et al., 2012; Kim et al., 2014; Bicks et al., 2015), we evaluated the expression of the transcripts of a subset of inflammatory markers as well as the microglia number and morphology. Finally, we the tested the role of immune dysregulations underlying the DLaN impacts by pharmacologically blocking cyclooxygenase-2 (COX-2) signaling and measuring the behavioral consequences.

Materials and Methods

Animals and housing conditions

All animal procedures were performed in accordance with the UCLA animal care committee's regulations. The WT controls (C57BL/6J, https://www.jax.org/strain/000664) and the *Cntnap2* KO mutants (JAX #017482) were from our breeding colony maintained at the University of California, Los Angeles (UCLA). Weaned mice were genotyped (Transnetyx, Cordova, TN) and group-housed prior to experimentation. They were kept in temperature- and humidity-controlled cabinets with a 12 hr light (300 lx) and 12 hr dark (0 lx) LD cycles. When reaching the testing age (3-4 month of age), they were assigned to 1 of the 2 photic environments for 2 weeks: the LD control environment or the DLaN disrupting environment (5 lx instead of 0 lx in the dark phase) as previously described (Wang et al., 2020).

Multiplex cytokine measures

At the end of the treatment, blood samples from the 4 groups (WT: LD, DLaN; *Cntnap2* KO: LD, DLaN) were taken at ZT 18 in the dark room under dim red lights. The blood was collected (about 0.2-0.3 ml per animal) via cheek puncture into microvette EDTA tubes (Sarstedt, Nümbrecht, Germany). Tubes were gently inverted a few times and placed immediately on wet ice. Within one hour from the collection, samples were centrifuged at 10000 rpm for 15 minutes at 4°C. The supernatant plasma (0.1-0.2 ml) was then collected into pre-labeled Eppendorf tubes (Fisher Scientific, Hampton, NH). Tube lids were parafilmed and immediately stored at -80°C until further measurement using the Luminex multiplexed immunoassay at the UCLA Immune Assessment Core (IAC, https://www.uclahealth.org/pathology/services-immunoassays).

Cage activity of sleep/wake cycles

Daily locomotor activity was monitored using a top-mounted passive infra-red (IR) motion detector reporting to a VitalView data recording system (Mini Mitter, Bend, OR).

Detected movements were recorded in 3 min bins, and 10 days of data were averaged for analysis using the El Temps chronobiology program (A. Diez-Noguera, Barcelona, Spain; http://www.el-temps.com/principal.html). The activity rhythm analysis was conducted as previously described (Wang et al., 2018). Briefly, the rhythmic strength (%V) was determined from the amplitude of the $\chi 2$ periodogram at 24 hr with a threshold of 0.001 significance. The percentage of sleep-phase activity was determined by the relative distribution of activity during the day versus the night. Fragmentation and onset variability were determined using the Clocklab program (Actimetrics, Wilmette, IL; http://actimetrics.com/products/clocklab/) to analyze the recorded bouts.

Social and grooming behavioral tests

To avoid sleep disruptions, all behavioral tests were conducted in the middle of the dark phase (ZT 18). The animals were first habituated to the testing room and the testing arena for at least 30 mins. The social behavior was evaluated by introducing a never-met conspecific to the testing mouse. The two mice were allowed to interact for 10 mins, and their behavior was recorded. Duration of sniffing (nose to nose sniff and nose to anogenital sniff), social grooming (the testing mouse grooms the novel stranger mouse on any part of the body) and touching was scored and reported for the time of social behavior. If there were aggressive fights during the trial, the testing trial was stopped and removed from the dataset. The grooming test was performed to evaluate the level of their repetitive behavior. After the habituation, the testing mouse was recorded by a camcorder for 30 mins in the testing arena. The duration of grooming behavior during the trial was scored as previously described (Wang et al., 2020).

Microglia counting and morphological analysis

At the end of the treatment, mice were anesthetized with isoflurane in the middle of the night (ZT 18) and perfused with phosphate buffered saline (PBS, 0.1M, pH 7.4) containing 4% paraformaldehyde (PFA, Sigma). Brains were rapidly dissected out, post-fixed with 4% PFA

at 4°C overnight, and cryoprotected in a solution of 15% sucrose in PBS. The free-floating PFC sections (50 µm) were obtained using a Cryostat (Leica, Buffalo Grove, IL) and collected sequentially. Immunohistochemistry was performed as previously described (Wang et al., 2017; Lee et al., 2018). Briefly, the PFC sections were blocked for 1 hr at room temperature (1% BSA, 0.3% Triton X-100, 10% normal donkey serum in 1xPBS) and then incubated overnight at 4°C with a rabbit polyclonal antibody against the microglia cell surface protein - Ionized calcium-binding adaptor molecule 1 (Iba1, 1:1000, FUJIFILM Wako Pure Chemical Cooperation, Ohsawa et al., 2000) followed by a Cry3-conjugated donkey-anti-rabbit secondary antibody (Jackson ImmuoResearch Laboratories). Sections were mounted and coverslips applied with Vectashield mounting medium containing 4'-6-diamidino-2-phenylihodole (DAPI, Vector Laboratories, Burlingame, CA). Sections were visualized on a Zeiss AxioImager M2 microscope (Zeiss Thornwood NY) equipped with an AxioCam MRm and the ApoTome imaging system.

Microglia Counting

Tiled images were acquired from three sections to include the medial regions of the PFC using the Zeiss Zen software and a 20x objective. Five fields of fixed size were created to include most of the regions of interest and overlapped to the images. The number of Iba1-positive cells was determined in the 5 fields with the aid of the cell counter plugin of ImageJ by two scorers masked to the experimental groups. The numbers obtained from the 5 fields were summed to obtain one value/section and those from the 3 sections averaged to obtained one value/animal (n = 5).

Microglia Morphology

Ten images from 3 sections per animal were acquired using the Zeiss Zen software with a 40x objective. Only cells that could be well identified and without any overlap with other cells in the field were used for the analysis and 10-15 cells/animal were examined. Images were first skeletonized and then the quantitative description of the complexity of the processes

of microglia cells in the PFC was performed using the Sholl analysis plugin (Sholl, 1953) of ImageJ with a 10 µm-interval concentric circles. The number of crosses per shell was plotted against the shell distance from the soma. Measurements (area, circumference and diameter) of the soma were performed in the same images for all the cell using ImageJ. These analyses were performed by two observers masked to the experimental groups.

Quantitative real-time polymerase chain reaction (qPCR)

The WT controls and *Cntnap2* KO mutants were sacrificed at ZT 18 under dark under dim red lights. The prefrontal cortex (PFC) was sampled and the total RNA was extracted using TRIzol® reagent (Life Technologies) following the manufacturer's protocol, and further purified by treatment with Ambion® TURBO DNA-free™ (Life Technologies), followed by a second extraction with phenol/chloroform (Ghiani et al., 2011). Sample concentrations and purity were assessed using a ThermoScientific™ NanoDrop™ One Microvolume UV-Vis Spectrophotometer (Canoga Park, CA). Total RNA (600 ng) was reverse-transcribed using the iScriptTM cDNA Synthesis Kit (Bio-Rad Laboratories) then analyzed for the expressions of various transcript on a CFX ConnectTM Real-Time PCR Detection System (Bio-Rad Laboratories). Reactions were setup using the iQTM SYBR® Green Supermix (Bio-Rad Laboratories) and the QuantiTect® Primer Assay (Qiagen, Valencia, CA), and performed in triplicate following the manufacturer's directions. Negative controls (samples in which reverse transcriptase was omitted) were amplified individually using the same primer sets to ensure the absence of genomic DNA contamination. Amplification specificity was assessed by melting curve, while standard curves, made from serial dilutions of control RNA, were used for efficiency and quantification. Expression standardization was done using the housekeeping genes Gadph and Ubc. The average values from three technical replicates per sample were normalized to those obtained for Gapdh or Ubc in the same sample, and also to the geometric mean of those for the two housekeeping genes in the same sample with similar results. The relative expression level of the housekeeping gene Ubc, normalized to Gapdh, was indistinguishable from the theoretical value of 1.

Carprofen administration

The treatment carprofen or saline (control) was mixed in their drinking water (0.067 mg/ml) as previously described (Ingrao et al., 2013) and refreshed daily at ZT 12. The testing mice received either saline or carprofen solution beginning on day 1 when they were under the 2 weeks of DLaN. The consumption of saline or carprofen solution was monitored daily on a per-animal basis at the times when refreshing the solution. Daily consumption was calculated by subtracting the volume of solution before and after giving to the testing animals. It is estimated that the peak plasma concentration of carprofen would be achieved 12 h after the treatment with an expected half-life of 7.4 h (Ingrao et al., 2013). The social behavior and repetitive grooming were assayed at ZT 18 on day 13 and the testing mice were sacrificed for PFC collection at ZT 18 on day 15. The behavior was tested on day 0 and day 13 for another cohort of mice to evaluate individual changes before and after the treatment of saline or carprofen solution under DLaN.

Statistics

SigmaPlot (version 13, SySTAT Software, San Jose, CA) was used to run all the statistical analysis. To analyze the effects of *Cntnap2* mutation and DLaN on the plasma immune profiles, the consequent Iba1+ cell numbers, and the qPCR results of neuroinflammation markers in the PFC, we applied a 2-way analysis of variance (ANOVA) with genotype and treatment as factors on each immune molecule. The Sholl Intersection Profiles were analyzed by a 3-way ANOVA using radius, genotype, treatment as factors. To determine the effect of carprofen, the transcriptional level of IFN-γ and IL-6, the reciprocal social behavior, the grooming behavior, and parameters of locomotor activity rhythms were analyzed using a 2-way ANOVA with genotype and treatment as factors. The waveforms of activity rhythms were analyzed by using the repetitive 2-way ANOVA with time and treatment as factors. The Holm-Sidak test for multiple comparisons was used when appropriate. Correlations between plasma immune molecules and ASD-like behavior were examined by

applying Pearson correlation analysis. To examine the impacts of carprofen at individual changes, the Paired *t*-test was used to compare the social and grooming behavior before and after the treatment. Values were reported as the mean ± standard error of the mean (SEM). Differences were determined significant if $P < 0.05$.

Results

Cntnap2 mutants exhibited altered plasma immune profiles in the control environment and exaggerated responses to DLaN.

In this first set of measurements, we sought to measure the peripheral inflammatory state of the WT and *Cntnap2* mice (**Fig.3.1, Table 3.1)**. Even under control LD conditions, the *Cntnap2* KO exhibited an altered immune state compared to WT controls. The mutants had significantly higher levels of interferon-gamma (IFN-γ), leukemia inhibitory factor (LIF), interleukin-1 alpha (IL-1a), IL-1b, IL-3, IL-5, IL-12 (p40), IL-13, IL-17, chemokine (C-C motif) ligand 5 (CCL-5), chemokine (C-X-C motif) ligand 10 (CXCL-10). The mutants actually had lower levels of tumor necrosis factor-alpha (TNFα), IL-6, IL-10, CCL-11, CXCL-1, and CXCL-2. This data indicates that the *Cntnap2* mutation itself altered the peripheral immune profiles. After the DLaN treatment, there were a large number of molecules in which there were significant interactions between genotype and treatment (**Table 3.1**) as measured by a 2-way ANOVA.

Taking advantage of the fact that we have these measurements on mice which we also characterized the behavior, we used a correlational analysis **(Table 3.2)** to gain insights as to which molecular changes may be directly related to DLaN driven behavior changes in activity rhythms **(Fig. 3.2 A-D)**, social behavior **(Fig. 3.3 A)**, and repetitive grooming **(Fig. 3.3 B)**. The level of IL-3 was significantly associated with all the key parameters of the locomotor activity rhythms including the rhythmic power, the percentage of activity in the sleep phase, activity fragmentation, and cycle-to-cycle variabilities. In addition, the power of activity rhythms was also inversely correlated to the level of CXCL-1, and the activity fragmentation was also correlated with the level of IFN-γ. The levels of TNFα and IL-13 was proportional to the cycle-to-cycle variabilities. Significant correlations were also found between the level of plasma immune molecules and the ASD behavior. Social behavior exhibited modest inverse correlations with the levels of IL-3, IL-13, and CCL-11 **(Fig. 3.3 C-E)** while repetitive grooming

behavior was proportional to the levels of INFγ, IL-6, IL-13, and CCL-11 **(Fig. 3.3 G-I)**. Together this data is consistent with the hypothesis that DLaN serves as an environmental perturbation or "second hit" that drives inflammatory changes in *Cntnap2* mutant mice. In addition, these immune changes were associated with the behavioral consequences of a mild circadian disruption by night-time light exposure.

Cntnap2 mutants showed selectively increased microglia proliferation and hyper-ramification changes under DLaN.

Next, we sought to determine if the immune dysregulations induced by the DLaN disruption could also be observed centrally. Focusing on the PFC, using immunofluorescence staining, we found an increased number of Iba1+ cells selectively in the *Cntnap2* KO mutants under DLaN **(Fig. 3.4 A)**. In addition, the Sholl analysis identified differences in secondary or above processes in microglia morphology selectively in the *Cntnap2* KO mutants under the DLaN **(Fig. 3.4 B & C)**. The 3-way ANOVA identified significant effects of genotype ($F_{(1,259)}$ = 48.64, $P < 0.001$), treatment ($F_{(1,259)}$ = 16.88, $P < 0.001$), and the radius ($F_{(1,259)}$ = 30.71, $P < 0.001$) on the Sholl interaction profiles. However, the soma diameter, area and perimeter all remained unaltered **(Table 3.3)**, suggesting hyper-ramification of microglial transformation in mutants under DLaN. In addition, we used RT-PCR to demonstrate that levels of *IL-6* were elevated under DLaN while no changes were seen in *IFN-γ*, *CX3CR*, *P2Y*, *Tmem119*, and *IKB* in the PFC **(Fig. 3.4 D-E, Table 3.4)**.

Blocking COX-2 signaling effectively counteracts the negative impacts of DLaN on social impairments and grooming behavior.

The immune downstream effector, COX-2 signaling, is under circadian regulation (Ingle et al., 2015) and the regulatory network is connected with the immune molecules (e.g. IFN-γ and IL-6) that were induced peripherally by DLaN. To test the role of COX-2 signaling underlying the impacts of DLaN, nonsteroidal anti-inflammatory carprofen was administered to both genotypes of mice housed under DLaN for 2 weeks. The WT controls and the *Cntnap2*

KO mutants under DLaN had comparable body weights (WT: 20.3 ± 7.1 g vs *Cntnap2* KO: 19.7 ± 7.3 g) and consumed a similar amount of saline solution (WT: 147.9 ± 15.2 ml vs *Cntnap2* KO: 126.0 ± 8.7 ml) or carprofen solution (WT: 158.0 ± 16.0 ml vs *Cntnap2* KO: 141.4 ± 19.7 ml) during the two weeks of treatment. No effects of treatment ($F_{(2,35)}$ = 1.61, P = 0.22) or genotype ($F_{(1,35)}$ = 0.38, P = 0.54) were detected. At the central level, we found significant effects of treatment on levels of the levels of IFN-γ and IL-6 in the PFC, and the carprofen treatment effectively block DLaN-inducing increase in the levels of IFN-γ and IL-6 in the PFC **(Table 3.5)**. At the behavioral level, we found that the carprofen treatment reduced the impact of DLaN on social and repetitive grooming behavior **(Table 3.6)**. Compared to the conspecifics in the LD control environment, the *Cntnap2* mutants showed 52% reduction in their social interactions under the DLaN environment. In contrast, the mutants treated with the carprofen under DLaN showed comparable social behavior as the control group **(Fig. 3.5 A & B)**. The protecting effects were also observed in the WT control mice. The social behavior was reduced by 45% in the WT mice under DLaN, and the carprofen treatment rescued the behavior to the control levels. Similarly, without the carprofen treatment, there was an 104% increase in the grooming behavior in the *Cntnap2* KO mutants under DLaN compared to the conspecifics in the LD control environment **(Fig. 3.5 C & D)**. However, when the carprofen was given, the fold change in the grooming behavior was reduced to -20% compared to the control group, and there was no statistical difference between the two groups. DLaN does not impact repetitive grooming behavior in the WT mice, and there was no effect of carprofen on their grooming behavior. There was no significant rescuing effect of the carprofen treatment on the locomotor activity rhythms **(Table 3.7)**. The key parameters of the locomotor activity rhythms including the rhythmic power, amplitude, the percentage of activity in the sleep phase, activity fragmentation, and cycle-to-cycle variabilities were comparable between mice treated with saline solution or carprofen under DLaN. These results strongly support the hypothesis that the DLaN negatively affected the social and grooming behavior through a mechanism dependent upon COX-2 signaling at downstream level of circadian disruption.

Discussion

Across much of the world, the prevalent use light-emitting devices have dramatically altered night-time lighting environments and put many people into a situation in which they are not exposed to robust day/night rhythms in lighting. This is alarming because a proper day-night difference in the photic environment is essential for maintaining robust circadian organization to optimize the physiological function, including cognitive performance and immune function. Using a mouse model of ASD, we have previously demonstrated that DLaN brings detrimental effects on sleep/wake cycles, social preference, and repetitive grooming behavior (Wang et al., 2020). This present study explores the possibility that DLaN acts as a second hit to increase ASD behaviors through disrupting the immune balance.

We found that the *Cntnap2* KO showed altered immune state compared to WT controls. These findings are in agreement with the mounting evidence that ASD induces changes in the immune system (Rose et al., 2014; Xu et al., 2015). Prior studies in mouse models of ASD also found altered immune profiles in the peripheral and the central levels (Prata et al., 2017; Siniscalco et al., 2018). For example, changed levels of IL-1β, IL-6, and TNFα in the prefrontal cortex and hippocampus are found in the adult *Fmr1* KO mutants even without immune challenges (Pietropaolo et al., 2014; Hodges e al., 2017). As another example, the BTBR mouse model of ASD displays an inflammatory immune profile and anti-inflammatory treatments are effective in rescuing the behavior (Onore et al., 2013; Careaga et al., 2015; Nadeem et al., 2018; De Simone et al., 2020; Cristiano et al., 2022). Our study is the first reporting the abnormalities in a broad range of plasma immune profile in this *Cntnap2* KO preclinical model although it remains unclear how the *Cntnap2* mutation leads to a systematic change of the peripheral immune profiles. There are a number of possible mechanisms by which increased baseline inflammation can contribute to the phenotypes of the mutants. For example, the effect of the peripheral immune molecules on ASD behavior has been demonstrated in the BTBR mouse model of ASD. The social impairments in the BTBR mouse model of ASD are rescued when the peripheral immune profiles are corrected by bone marrow

transplantation from the WT mice. In contrast, the WT recipients to the BTBR bone marrow show increased grooming behavior (Schwartzer et al., 2017). The peripheral immune abnormalities may associate with the output behavior through the weakened blood-brain-barrier (BBB) that is reported in ASD populations (Theoharides et al., 2011; Fiorentino et al., 2016) and a rat model of *Cntnap2* KO (Memis et al., 2022). Although it has not been tested in the *Cntnap2* KO mice yet, the *Cntnap2* mutation-induced altered peripheral immune changes may penetrate the *Cntnap2*-leaking BBB and disrupt circuit wiring and synaptic functions during the critical period of the brain development, ultimately leading to aberrant output behavior. This premise is supported by studies showing that peripheral cytokines penetrating the BBB leads to evoked ASD behavior even in WT testing mice (Banks et al., 2005; Erickson et al., 2012).

The dramatic changes in the plasma immune profiles under DLaN suggests broad impacts on the immune regulatory network. Our data suggests that DLaN affects pro-inflammatory network (TNFα, IL-6), the T helper type-1 (Th1) cell pathway (IFN-γ, IL-2, IL-12), the T helper type-2 (Th2) cell pathway (IL5 and IL-13), and the Th17 cell pathway (IL-17). The imbalanced Th1/Th2 signaling and the dysregulated Th17 cell pathway are frequently observed in ASD patients and correlated with the severity of social impairments and stereotypic behavior (Ahmad et al., 2017; Bakheet et al., 2017; Dardani et al., 2022). Our correlation analysis is consistent with the conclusions of these studies and even suggests that IL-13 and CCL-11 may play a key in the DLaN-evoked changes. These two immune molecules were strongly evoked by DLaN in both genotypes with even higher vulnerability observed in the *Cntnap2* KO mutants. In addition, they were significantly correlated with both social impairments and stereotypic grooming behavior while other key immune molecules were associated with only either one. Prior work investigating the interactions between the plasma levels of IL-13 and CCL-11 and ASD characteristics are very limited; however, it has been shown that IL-13 upregulates CCL-11 productions (Matsukura et al., 2001; Zhou et al., 2012; Parajuli et al., 2015; Teixeira et al., 2018; Sirivichayakul et al., 2019) and the increased CCL-

11 may affect the autistic outputs by elevating reactive oxygen species and altering microglia (Parajuli et al., 2015). In addition, there might be synergistic effects of high levels of IL-13/CCL-11 and the imbalanced Th1/Th2 signaling and dysregulated Th17 cell pathway on ASD behavior.

At the central nervous level, we found evidence showing that the PFC was impacted in the mutants under DLaN. In the LD control environment, our work is consistent with a prior study showing that the adult *Cntnap2* KO mutants have no changes in the density and the soma area of the Iba1+ microglia, or the number of activated Iba1+ microglia, compared to the WT controls in the PFC (Cope et al.,2016). However, after DLaN exposure, the mutants appeared significant differences from the WT controls at the microglial level. Interestingly, changes in the PFC microglia suggest that the morphology became hyper-ramified rather than becoming phagocytic microglia. In addition, consistent with the microglia changes, the neuroinflammation markers such as *CX3CR*, *P2Y*, *Tmem119* were not evoked by DLaN. Our observation is similar to studies showing that the hyper-ramified morphology is inducible by chronic stress and independent from neuropathological markers such as IL1-β, CD68, or caspase (Hibwood et al., 2012, 2013; Hellwig et al., 2016; Rowson et al., 2016). Still, it remains to be determined if the observed hyper-ramified microglia are an arresting adaptive state or a transit transformation of the injury response to the DLaN. Nevertheless, the level of IL-6 was indeed evoked by DLaN in both the WT controls and the *Cntnap2* KO mutants. IL-6 exhibits neuromodulatory capabilities in neuronal glutamate and GABA receptors (El-Ansary et al., 2014; Kalkman et al., 2019), and associations between IL-6 levels and ASD behavior are frequently observed (Ashwood et al., 2011; Wei et al., 2012). In addition, Smith and colleagues demonstrated that blocking IL-6 signaling in pregnant mice prevented behavioral abnormalities in the offspring in the ASD model of maternal immune activation (MIA), pointing a specific role for IL-6 in the etiology of ASD (Smith et al., 2007). Together, the elevated IL-6 may disrupt the glutamatergic/GABAergic signaling in the PFC (Paine et al.,2016; Wang et al.,

2021) and ultimately lead to the social impairments and repetitive grooming behavior in mice under DLaN.

DLaN may disrupt the immune network via several mechanisms such as circadian-regulated toll-like receptors (Cermakian et al., 2014) and cytokine/chemokine secretions (Keller et al., 2009). One likely downstream effector is the COX-2. It is expressed in the peripheral system (e.g. kidney, gastrointestinal tract, and macrophages) as well as the CNS (Harris et al., 2006; Radi et al., 2006; Hoffmann et al., 2000), and under circadian regulation (De et al., 2010; Xu et al., 2012; Ingle et al., 2015). In addition, its level is inducible by environmental stimuli (Font-Nieves et al., 2012), and the COX-2 network is linked to key immune molecules identified in this study including IFN-γ (Ni et al., 2007), TNFα (Natarajan et al., 2018), IL-6 (Zhao et al., 2009), IL-12 (Muthian et al., 2006), and IL-17 (Lemos et al., 2009). The role of COX-2 in ASD symptoms is emerging recently and suggested by studies showing that COX-2 mediates long-term potentiation (Cowley et al., 2008) and neuromodulations (Abdolahi et al., 2019), and its inhibitor effective in other developmental disorders such as schizophrenia (Akhondzadeh et al., 2007; Muller et al., 2008; Zhang et al., 2021) and obsessive-compulsive disorder (Sayyah et al., 2011; Shalbafan et al., 2015). A recent study investigated 29 ASD patients without allergy/asthma found a significantly higher level of COX-2 compared to the control group (n = 28), suggesting overactivated COX-2 signaling may contribute to the ASD syndrome (Kordulewska et al., 2019). A latest preclinical study supported this observation and showed that overexpression of COX-2 in the mouse model induces reduced social preference in the 3-chamber test as well as increased repetitive digging behavior in the marble bury test (Kissoondoyal et al., 2022). Here our study is consistent with this work by demonstrating the successfully rescued social impairments and grooming behavior under the DLaN disruption using the carprofen treatment to suppress the COX-2 network.

Finally, the observed effects of DLaN on the altered immune profiles are likely independent of sleep loss. Sleep deprivation has profound effects on immune function, and

even the modest sleep restriction results in increased pro-inflammatory cytokine levels and declined social and cognitive flexibility (Vgontzas et al., 2004). However, we have previously demonstrated that DLaN does not reduce sleep time in either the *Cntnap2* KO mutants or the WT controls (Wang et al., 2020). The altered immune profiles caused by DLaN without involving sleep loss are consistent with other prior studies (Castanon-Cervantes et al., 2010; Brager et al., 2013).

In conclusion, we demonstrated pieces of evidence supporting the hypothesis that DLaN disruption functions as a second hit to drive autistic behavior in *Cntnap2* mutation mice. At the peripheral level, the levels of a number of immune markers exhibited significant interaction between genotype and DLaN treatment. At the CNS level, the microglia proliferation and morphology changes were observed in the *Cntnap2* KO mutants. At behavior level, while half of WT mice were impacted by DLaN and showed reduced social behavior, all of *Cntnap2* KO mutants were negatively affected. In addition, we demonstrated that the COX-2 signaling may mediate DLaN-driven changes in social impairments and the stereotypic behavior in the *Cntnap2* KO mouse model of ASD.

Figures

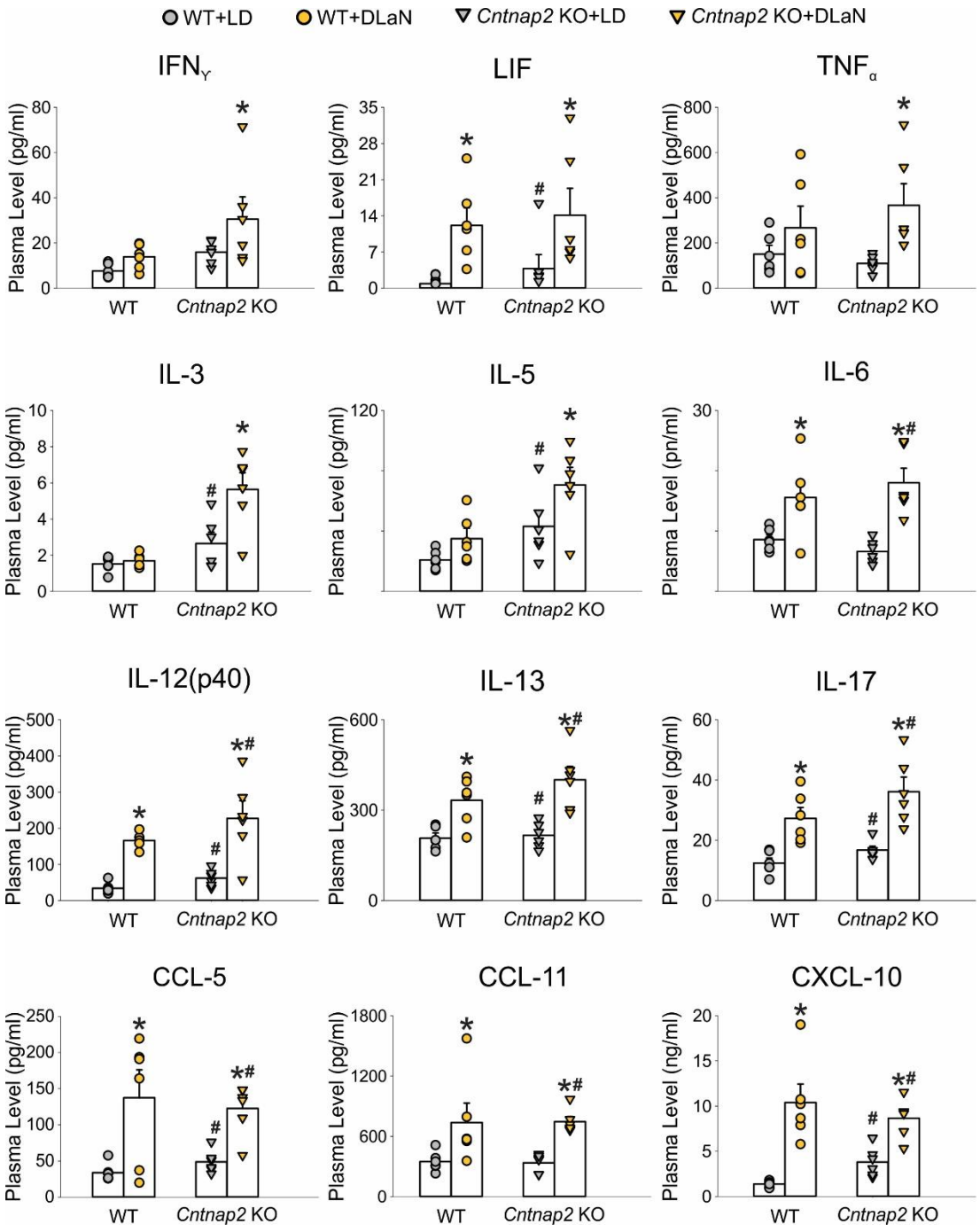

Fig. 3.1: The plasma immune profiles were already altered by the *Cntnap2* mutation and further changed by DLaN. Selected plasma immune molecules are shown and the full list of assayed immune molecules is reported in **Table 3.1**. The significant differences were analyzed by the 2-way ANOVA on the effects of photic environment and the genotype. **P* < 0.05 indicates the significant difference between the photic environments, and $^{\#}P$ < 0.05 indicates the significant difference between the genotypes. Detailed statics are described in **Table 3.1.**

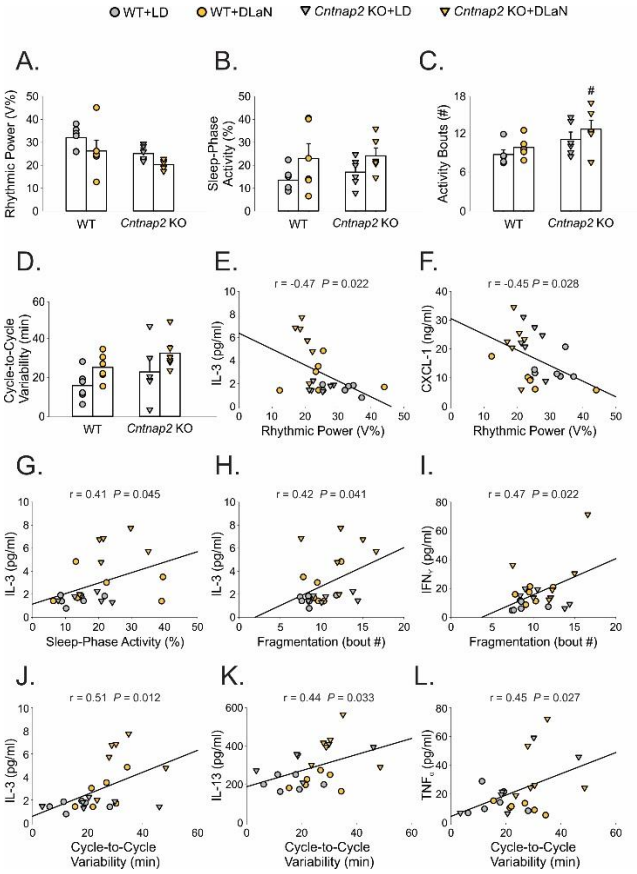

Fig. 3.2: The plasma immune molecules reflecting genotypic vulnerability were associated with the key parameters of locomotor activity rhythms. (A) The rhythmic power (V%) of the activity rhythms was analyzed by the 2-way ANOVA with the photic environment and the genotype as factors. WT+LD: 31.3 ± 2.2; WT+DLaN: 25.6 ± 4.6; *Cntnap2* KO+LD: 24.5 ± 1.4; *Cntnap2* KO+DLaN: 19.8 ± 0.9. Significant effects of genotype ($F_{(1,23)}$ = 6.72; P = 0.017) and environment ($F_{(1,23)}$ = 4.56; P = 0.045) were found. **(B)** The sleep-phase activity (%) was analyzed by the 2-way ANOVA with the photic environment and the genotype as factors. WT+LD: 13.2 ± 2.3; WT+DLaN: 22.5 ± 6.3; *Cntnap2* KO+LD: 16.6 ± 2.7; *Cntnap2* KO+DLaN: 23.6 ± 3.4. Significant effects of environment ($F_{(1,23)}$ = 4.95; P = 0.038) but not the genotype ($F_{(1,23)}$ = 0.39; P = 0.54) were found. **(C)** The fragmentation of activity rhythms (# bouts) was analyzed by the 2-way ANOVA with the photic environment and the genotype as factors. WT+LD: 8.7 ± 0.7; WT+DLaN: 9.8 ± 0.7; *Cntnap2* KO+LD: 11.0 ± 1.1; *Cntnap2* KO+DLaN: 12.6 ± 1.4. Significant effects of genotype ($F_{(1,23)}$ = 7.48; P = 0.013) but not the environment ($F_{(1,23)}$ = 2.00; P = 0.17) were found. **(D)** The cycle-to-cycle variability (min) was analyzed by the 2-way ANOVA with the photic environment and the genotype as factors. WT+LD: 15.8 ± 3.4; WT+DLaN: 25.1 ± 3.1; *Cntnap2* KO+LD: 22.8 ± 6.4; *Cntnap2* KO+DLaN: 32.4 ± 3.9. Significant effects of environment ($F_{(1,23)}$ = 5.56; P = 0.029) but not the genotype ($F_{(1,23)}$ = 3.17; P = 0.09) were found. **(E & F)** The correlations to the rhythmic power of the activity rhythms. Modest inverse correlations were found to levels of IL-3 and CXCL-1. **(G)** IL-3 level is proportional to the percentage of sleep-phase activity with a moderate correlation relationship. **(H & I)** Levels of IL-3 and TNF_{α} are proportional to the fragmentation level of activity rhythms with a mild to moderate correlation relationship. **(J-L)** Levels of IL-3, TNF_{α}, and IL-13 are proportional to the cycle-to-cycle variability of activity rhythms with a moderate correlation relationship. The correlation relationships were analyzed using the Pearson Correlation, and the coefficients are reported in **Table 3.2**.

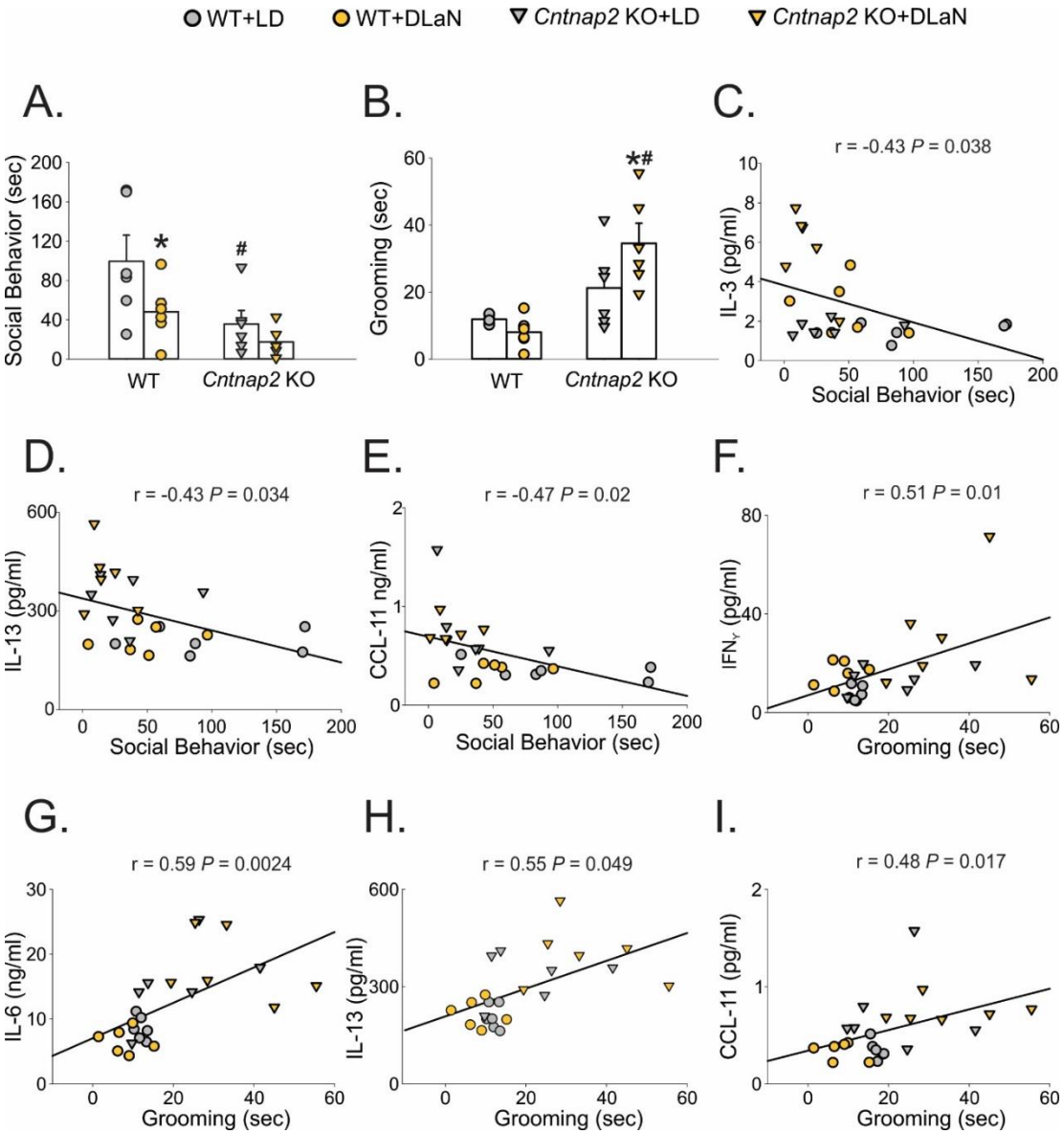

Fig. 3.3: The plasma immune molecules reflecting genotypic vulnerability were associated with the social impairment and repetitive grooming behavior and predicted the behavioral outcomes. (A) The social behavior (sec) was analyzed by the 2-way ANOVA with the photic environment and the genotype as factors. WT+LD: 99.5 ± 26.7; WT+DLaN: 48.0 ± 13.4; *Cntnap2* KO+LD: 35.6 ± 13.9; *Cntnap2* KO+DLaN: 17.5 ± 6.5. Significant effects of genotype ($F_{(1,23)}$ = 9.5; P = 0.006) and environment ($F_{(1,23)}$ = 5.17; P = 0.034) were found. **(B)** The grooming behavior (sec) was analyzed by the 2-way ANOVA with the photic environment and the genotype as factors. WT+LD: 11.9 ± 0.6; WT+DLaN: 8.1 ± 2.1; *Cntnap2* KO+LD: 21.2 ± 5.4; *Cntnap2* KO+DLaN: 34.6 ± 6.0. Significant effects of genotype ($F_{(1,23)}$ = 22.02; P < 0.001) but not the environment ($F_{(1,23)}$ = 1.55; P = 0.23) were found. **(C-E)** The correlations to the social behavior. Modest inverse correlations were found between social behavior and levels of IL-3, IL-13, and CCL-11. **(F-I)** The correlations to the repetitive grooming behavior. Levels of INFγ, IL-6, IL-13, and CCL-11 were proportional to the grooming time at mild to moderate level. The correlation relationships were analyzed using the Pearson Correlation, and the coefficients are reported in **Table 3.2**.

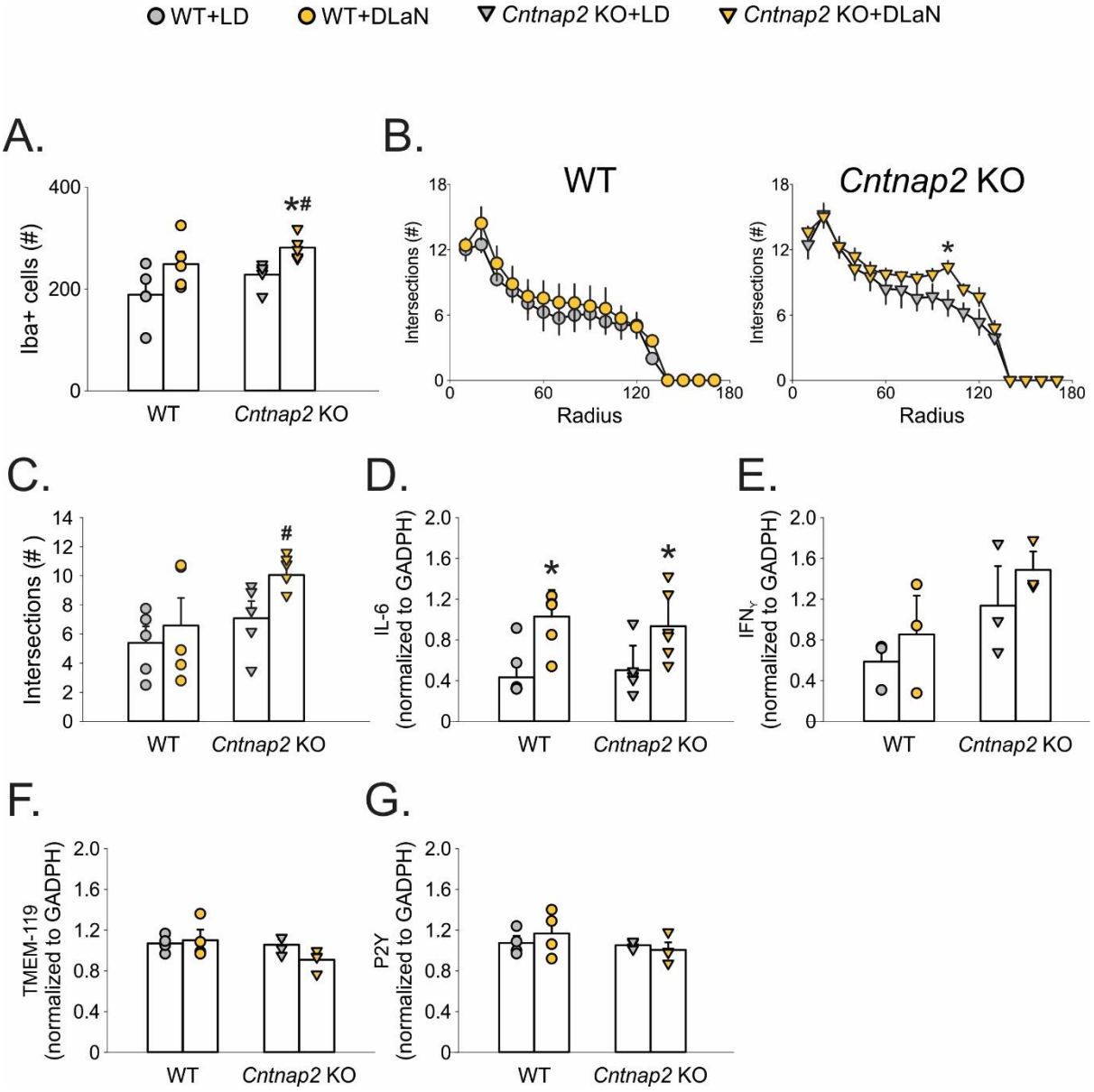

Fig. 3.4: DLaN evoked changes in immune profiles in the PFC with the strongest effects found on *Cntnap2* mutants. **(A)** The number of Iba1+ microglia cells in the PFC. The 2-way ANOVA analysis was applied with genotype and photic environment as factors. Detailed statics are described in **Table 3.3**. **(B)** The Sholl intersection profiles in the WT controls (left) and the *Cntnap2* KO mutants (right) in the LD control environment or under DLaN. The repetitive 2-way ANOVA were applied with radius and photic environment as factors. Within the WT controls, there was a significant effect from the radius (F = 40.04; $P < 0.001$) but not from the photic environment (F = 0.44; $P = 0.52$). Within the *Cntnap2* mutants, there was a significant interaction between the radius and the photic environment (F = 2.10; $P = 0.024$). **(C)** The Sholl intersection number at secondary or above process (100 um away from the soma center) of microglia in the PFC. The 2-way ANOVA analysis indicated a significant effect of genotype (F = 5.90; $P = 0.027$) but the effect of treatment did not reach significance (F = 3.94; $P = 0.065$). The post-hoc analysis identified significant difference between the WT controls and the *Cntnap2* mutants under DLaN (t = 2.36; $P = 0.031$). **(D-G)** The levels of *IL-6*, *INF$_Y$*, *Tmem-119*, and *P2Y* in the PFC were measured by qPCR. The 2-way ANOVA analysis was applied with genotype and photic environment as factors. Detailed statics are described in **Table 3.3**.

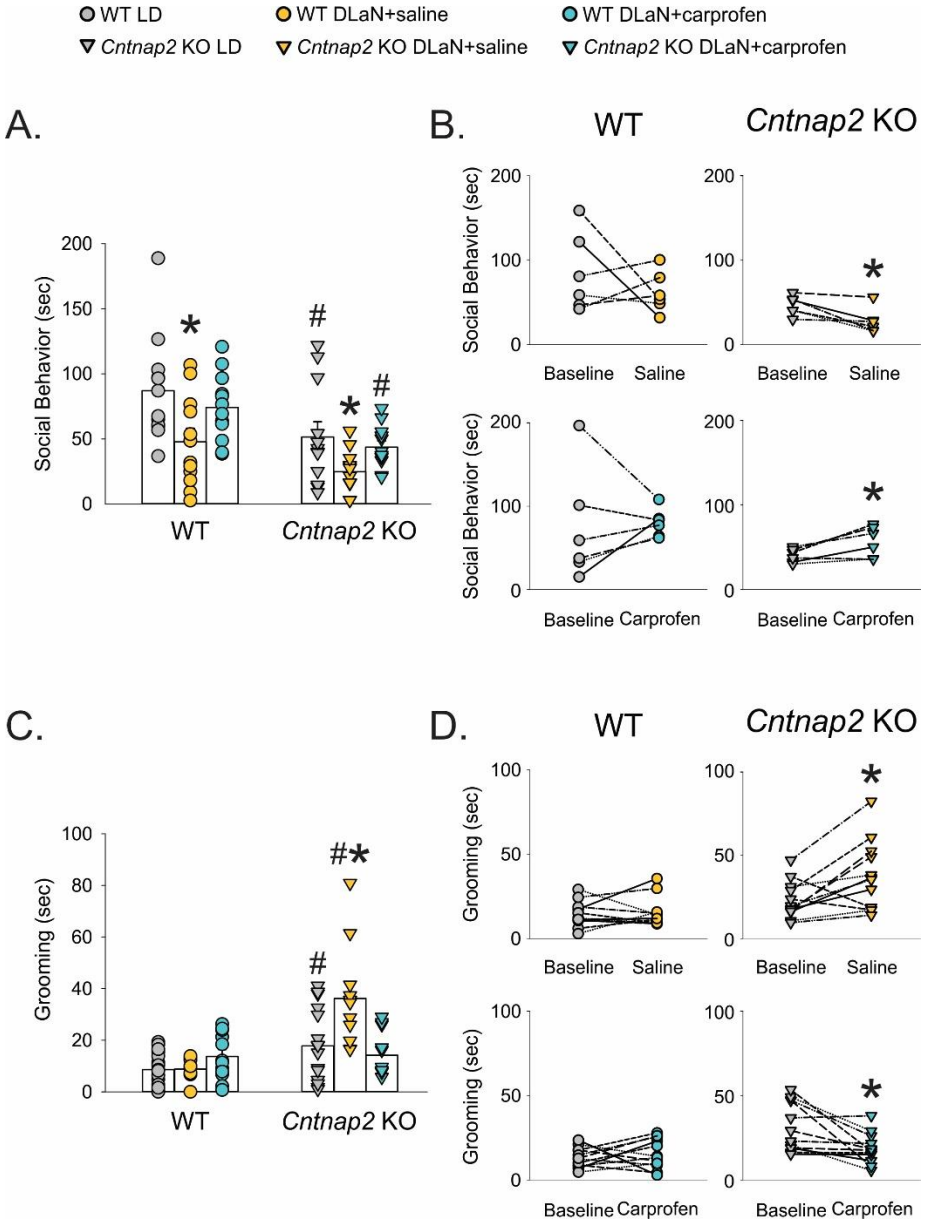

Fig. 3.5: COX-2 inhibitor blocked the DLaN-reducing effect on social behavior and the DLaN-evoking effect on repetitive grooming behavior. Both Social and grooming behavior were assayed at ZT 18. In the histograms, values from individual animals in the LD control environment, under the treatment of DLaN + saline solution, and under the treatment of DLaN + carprofen solution are reported. Data were analyzed using a 2-way ANOVA with genotype and treatment **(Table 6)**. Significant ($P < 0.05$) treatment differences are indicated with an * while the # indicates a genotypic difference. **(A)** The social behavior in the WT controls and *Cntnap2* KO mutants treated with carprofen solution was protected from the disruption of DLaN. **(B)** Time actively spent on social behavior from individual animals are shown. Paired *t*-test was used to analyze the changes before and after the treatment. An * over the treated values indicates significant difference ($P < 0.05$). **(C)** The repetitive grooming behavior in the *Cntnap2* KO mutants treated with carprofen solution was protected from the disruption of DLaN. The WT mice did not show evoked grooming behavior under DLaN, and there was no effect of carprofen on their grooming behavior. **(D)** The aberrant grooming behavior from individual animals are shown. Paired *t*-test was used to analyze the changes before and after the treatment. An * over the treated values indicates significant difference ($P < 0.05$).

Tables

Table 3.1. DLaN altered plasma immune profiles. Comparisons of age-matched WT and *Cntnap2* KO mice under the LD control environment or the DLaN disruptive environment (n = 6/group). Values are shown as averages ± SEM. Data were analyzed with a 2-way ANOVA using genotype and photic environment as factors. The Holm-Sidak test for multiple comparisons was used when appropriate. *indicates significant differences between the LD control and DLaN photic environments. # indicates significant differences between the WT controls and the *Cntnap2* KO mutants.

	WT LD	**WT DLaN**	***Cntnap2* KO LD**	***Cntnap2* KO DLaN**	**Genotype**	**Photic Environment**	**Interaction**
IFNγ	7.6 ± 1.4	13.9 ± 2.4	15.9 ± 2.3#	**30.5 ± 9.9***	**$F_{(1, 23)}$ = 6.67; *P* = 0.018**	$F_{(1, 23)}$ = 0.75; *P* = 0.4	**$F_{(1, 23)}$ = 4.68; *P* = 0.043**
LIF	0.9 ± 0.4	**12.2 ± 3.4***	3.8 ± 2.7#	**14.1 ± 5.2***	$F_{(1, 23)}$ = 0.62; *P* = 0.44	$F_{(1, 23)}$ = 0.024; *P* = 0.88	**$F_{(1, 23)}$ = 12.13; *P* = 0.002**
TNFα	150.2 ± 38.9	266.8 ± 95.8	109.3 ± 15.8#	**366.6 ± 95.3***	$F_{(1, 23)}$ = 0.21; *P* = 0.65	$F_{(1, 23)}$ = 1.19; *P* = 0.29	**$F_{(1, 23)}$ = 8.37; *P* = 0.009**
IL-1a	134.7 ± 20.5	**462.5 ± 149.7***	197.3 ± 30.7#	377.0 ± 52.9#	$F_{(1, 23)}$ = 0.024; *P* = 0.88	$F_{(1, 23)}$ = 0.99; *P* = 0.33	**$F_{(1, 23)}$ = 11.64; *P* = 0.003**
IL-1b	5.7 ± 1.7	13.4 ± 2.7	21.8 ± 6.1#	34.0 ± 11.7	**$F_{(1, 23)}$ = 8.82; *P* = 0.008**	$F_{(1, 23)}$ = 0.13; *P* = 0.72	$F_{(1, 23)}$ = 2.58; *P* = 0.12
IL-3	1.5 ± 0.2	1.7 ± 0.2	2.6 ± 0.6#	**5.6 ± 0.9***	**$F_{(1, 23)}$ = 23.95; *P* < 0.001**	**$F_{(1, 23)}$ = 7.41; *P* = 0.013**	**$F_{(1, 23)}$ = 9.28; *P* = 0.006**
IL-4	1.4 ± 0.2	1.0 ± 0.2	3.2 ± 1.2#	7.8 ± 4.0	**$F_{(1, 23)}$ = 5.06; *P* = 0.036**	$F_{(1, 23)}$ = 1.79; *P* = 0.2	$F_{(1, 23)}$ = 1.23; *P* = 0.28
IL-5	20.8 ± 2.8	34.9 ± 6.9	43.1 ± 9.8#	**70.7 ± 11.5***	**$F_{(1, 23)}$ =14.22; *P* = 0.001**	$F_{(1, 23)}$ = 0.77; *P* = 0.39	**$F_{(1, 23)}$ = 7.35; *P* = 0.013**
IL-6	8590.2 ± 807.5	**15590.4 ± 2769.94***	6629.6 ± 849.1#	**18009.1 ± 2424.1*#**	$F_{(1, 23)}$ = 0.017; *P* = 0.9	$F_{(1, 23)}$ = 1.54; *P* = 0.23	**$F_{(1, 23)}$ = 27.17; *P* < 0.001**
IL-10	3188.5 ± 553.5	**798.1 ± 113.1***	1389.4 ± 307.3#	832.3 ± 113.4	**$F_{(1, 23)}$ = 8.77; *P* = 0.008**	**$F_{(1, 23)}$ = 9.46; *P* = 0.006**	**$F_{(1, 23)}$ = 24.45; *P* < 0.001**
IL-12(p40)	34.3 ± 6.7	**166.1 ± 9.2***	62.2 ± 10.2#	**227.5 ± 49.0*#**	$F_{(1, 23)}$ = 3.64; *P* = 0.071	$F_{(1, 23)}$ = 0.51; *P* = 0.48	**$F_{(1, 23)}$ = 40.3; *P* < 0.001**
IL-13	207.2 ± 16.9	**333.0 ± 34.5***	216.4 ± 18.8#	**400.9 ± 44.7*#**	$F_{(1, 23)}$ = 1.87; *P* = 0.19	$F_{(1, 23)}$ = 1.08; *P* = 0.31	**$F_{(1, 23)}$ = 30.15; *P* < 0.001**
IL-15	73.3 ± 30.7	51.1 ± 8.7	74.8 ± 45.1	130.2 ± 51.1	$F_{(1, 23)}$ = 1.38; *P* = 0.26	$F_{(1, 23)}$ = 1.28; *P* = 0.27	$F_{(1, 23)}$ = 0.23; *P* = 0.63
IL-17	12.5 ± 1.7	**27.3 ± 3.6***	16.8 ± 1.3#	**36.1 ± 4.9*#**	**$F_{(1, 23)}$ = 4.99; *P* = 0.037**	$F_{(1, 23)}$ = 0.6; *P* = 0.45	**$F_{(1, 23)}$ = 33.77; *P* < 0.001**
CXCL-1	12893.4 ± 1764.8	**22517.5 ± 3425.9***	9628.6 ± 1902.6#	**22043.6 ± 4156.3*#**	$F_{(1, 23)}$ = 0.47; *P* = 0.5	$F_{(1, 23)}$ = 0.26; *P* = 0.62	**$F_{(1, 23)}$ = 16.31; *P* < 0.001**
CXCL-2	3768.8 ± 624.0	**14155.2 ± 3499.5***	2643.9 ± 657.0#	**9380.2 ± 1574.3*#**	$F_{(1, 23)}$ = 2.08; *P* = 0.17	$F_{(1, 23)}$ = 1.37; *P* = 0.26	**$F_{(1, 23)}$ = 23.6; *P* < 0.001**
CXCL-10	1366.9 ± 148.4	**10389.2 ± 2048.3***	3816.3 ± 727.0#	**8667.3 ± 957.9*#**	$F_{(1, 23)}$ = 0.11; *P* = 0.74	$F_{(1, 23)}$ = 3.69; *P* = 0.069	**$F_{(1, 23)}$ = 40.78; *P* < 0.001**
CCL-5	33.8 ± 5.5	**137.5 ± 38.6***	48.8 ± 7.0#	**122.7 ± 15.6*#**	F < 0.001; *P* = 1	F = 0.59; *P* = 0.45	**$F_{(1, 23)}$ = 20.87; *P* < 0.001**
CCL11	348.7 ± 42.5	**737.8 ± 193.7***	337.0 ± 41.2#	**746.6 ± 52.1*#**	$F_{(1, 23)}$ < 0.001; *P* = 0.99	$F_{(1, 23)}$ = 0.012; *P* = 0.92	**$F_{(1, 23)}$ = 17.5; *P* < 0.001**

Table 3.2. DLaN-altered plasma immune molecules were associated with the key parameters of activity rhythms and the severity of autistic behavior. The plasma immune molecules (from Table 3.1) and behavior tested from the same individual were analyzed for determining the correlations. All 4 groups (WT + LD, WT + DLaN, *Cntnap2* KO + LD, *Cntnap2* KO + DLaN) were pooled (n = 24) and the Pearson Correlation was applied. The correlation coefficients are reported and *p*-value below 0.05 was considered significant. The significant correlation coefficients are shown in bold and labeled with *.

	INF_{γ}	**TNF_{α}**	**IL-3**	**IL-6**	**IL-13**	**CCL11**	**CXCL-1**
Rhythmic Power (V%)	-0.35	-0.22	**-0.47***	-0.31	-0.4	-0.27	**-0.45***
Sleep-Phase Activity (%)	0.39	0.35	**0.41***	0.15	0.38	0.29	0.37
Fragmentation (# bouts)	**0.47***	0.15	**0.42***	0.13	0.27	0.22	0.32
Cycle-to-cycle variability (min)	0.25	**0.45***	**0.51***	0.22	**0.44***	0.3	0.24
Social Behavior(sec)	-0.32	-0.21	**-0.43***	-0.32	**-0.43***	**-0.47***	-0.21
Grooming (sec)	**0.51***	0.34	0.37	**0.59***	**0.55***	**0.48***	0.32

Table 3.3. DLaN evoked microglial changes in the prefrontal cortex. The microglia were marked with the Iba1 immunofluorescence staining, and the number and the morphology of Iba1+ cells were analyzed. The significant difference in sholl intersection number was found at the secondary and above process and reported here. Values are shown as averages ± SEM. Data were analyzed with a 2-way ANOVA using genotype and photic environment as factors. The Holm-Sidak test for multiple comparisons was used when appropriate. * indicates significant differences between LD control and DLaN photic environments. # indicates significant differences between WT controls and *Cntnap2* KO mice. N = 5/group.

	WT LD	**WT DLaN**	***Cntnap2* KO LD**	***Cntnap2* KO DLaN**	**Genotype**	**Photic Environment**	**Interaction**
Iba1+ Cells (#)	188.7 ± 27.3	249 ± 24.5	228.3 ± 12.6	**281.2 ± 11.8***	**$F_{(1, 15)} = 5.1$; $P = 0.038$**	**$F_{(1, 15)} = 7.45$; $P = 0.015$**	$F_{(1, 15)} = 0.015$; $P = 0.9$
Sholl Intersections (#)	5.4 ± 1.1	6.6 ± 1.9	7.1 ± 1.2	10.4 ± 0.6#	**$F_{(1, 19)} = 5.9$; $P = 0.027$**	$F_{(1, 15)} = 3.94$; $P = 0.065$	$F_{(1, 15)} = 0.83$; $P = 0.38$
Soma Diameter	9.7 ± 0.4	9.9 ± 0.6	9.5 ± 0.7	10.0 ± 0.3	$F_{(1, 15)} = 0.053$; $P = 0.82$	$F_{(1, 15)} = 1.8$; $P = 0.2$	$F_{(1, 15)} = 0.65$; $P = 0.43$
Soma Area	45.0 ± 2.5	44.8 ± 4.3	42.6 ± 5.5	44.7 ± 2.1	$F_{(1, 15)} = 0.47$; $P = 0.51$	$F_{(1, 15)} = 0.26$; $P = 0.62$	$F_{(1, 15)} = 0.39$; $P = 0.54$
Soma Perimeter	28.1 ± 1.0	28.2 ± 1.8	27.2 ± 0.4	28.3 ± 1.4	$F_{(1, 15)} = 0.27$; $P = 0.61$	$F_{(1, 15)} = 0.53$; $P = 0.48$	$F_{(1, 15)} = 0.43$; $P = 0.52$

Table 3.4. DLaN evoked neuroinflammatory transcripts in the prefrontal cortex. For each gene listed in the table, average values from three technical replicates per sample were normalized to Gapdh from the same sample. Values are shown as averages ± SEM. Data were analyzed with a 2-way ANOVA using genotype and photic environment as factors. The Holm-Sidak test for multiple comparisons was used when appropriate. *indicates significant differences between LD control and DLaN photic environments. # indicates significant differences between WT controls and *Cntnap2* KO mice. N = 5/group.

	WT LD	**WT DLaN**	***Cntnap2* KO LD**	***Cntnap2* KO DLaN**	**Genotype**	**Photic Environment**	**Interaction**
IL-6	0.4 ± 0.1	**1.0 ± 0.3***	0.5 ± 0.2	**0.9 ± 0.3***	$F_{(1,20)} = 0.015$; $P = 0.90$	**$F_{(1,20)} = 25.28$; $P < 0.001$**	$F_{(1,20)} = 0.65$; $P = 0.43$
IFN$_Y$	0.6 ± 0.2	0.9 ± 0.4	1.1 ± 0.4	1.5 ± 0.2	**$F_{(1,11)} = 5.90$; $P = 0.041$**	$F_{(1,11)} = 1.60$; $P = 0.24$	$F_{(1,11)} = 0.029$; $P = 0.87$
Cx3cr	1.0 ± 0.2	1.1 ± 0.2	1.0 ± 0.1	1.0 ± 0.2	$F_{(1,20)} = 1.03$; $P = 0.32$	$F_{(1,20)} = 0.54$; $P = 0.47$	$F_{(1,20)} = 0.55$ $P = 0.47$
IkB	0.9 ± 0.1	1.0 ± 0.2	1.0 ± 0.2	1.0 ± 0.2	$F_{(1,20)} = 0.21$; $P = 0.65$	$F_{(1,20)} = 0.29$; $P = 0.6$	$F_{(1,20)} = 0.98$; $P = 0.33$
P2y	1.0 ± 0.2	1.1 ± 0.2	1.0 ± 0.1	0.9 ± 0.2	$F_{(1,20)} = 1.81$; $P = 0.19$	$F_{(1,20)} = 0.19$; $P = 0.67$	$F_{(1,20)} = 3.02$; $P = 0.098$
Tmem119	1.0 ± 0.1	1.1 ± 0.2	1.0 ± 0.1	0.9 ± 0.1	$F_{(1,19)} = 2.12$; $P = 0.16$	$F_{(1,19)} = 0.098$; $P = 0.76$	**$F_{(1,19)} = 7.63$; $P = 0.012$**
Gapdh	1.0 ± 0.2	0.9 ± 0.2	1.0 ± 0.3	1.1 ± 0.3	$F_{(1,20)} = 1.16$; $P = 0.3$	$F_{(1,20)} = 0.06$; $P = 0.81$	$F_{(1,20)} = 0.58$; $P = 0.46$
Ubc	1.1 ± 0.2	1.2 ± 0.2	1.1 ± 0.2	1.0 ± 0.3	$F_{(1,20)} = 0.95$; $P = 0.34$	$F_{(1,20)} = 0.17$; $P = 0.69$	$F_{(1,20)} = 0.89$; $P = 0.36$

Table 3.5. The COX-2 inhibitor (carprofen) reduced DLaN-evoked IFN$_Y$ and IL-6 in the PFC. The WT and *Cntnap2* KO mice (n = 6/group) were treated with saline (control vehicle) or carprofen (0.067 mg/ml) under DLaN for 2 weeks. For each gene listed in the table, average values from three technical replicates per sample were normalized to Gapdh from the same sample. Values are shown as averages ± SEM. Data were analyzed with a 2-way ANOVA using genotype and photic environment as factors. The Holm-Sidak test for multiple comparisons was used when appropriate. *indicates significant differences between LD control and DLaN photic environments. # indicates significant differences between WT controls and *Cntnap2* KO mice.

	Genotype	**Treatment**	**Interaction**
IFN$_Y$	$F_{(1,29)} = 1.00$; $P = 0.33$	**$F_{(2,29)} = 6.21$; $P = 0.007$**	$F_{(2,29)} = 0.28$; $P = 0.76$
IL-6	$F_{(1,29)} = 0.55$; $P = 0.47$	**$F_{(2,29)} = 5.54$; $P = 0.011$**	$F_{(2,29)} = 0.18$; $P = 0.84$
Gapdh	$F_{(1,29)} = 0.17$; $P = 0.68$	$F_{(2,29)} = 1.09$; $P = 0.35$	$F_{(2,29)} = 0.063$; $P = 0.94$
Ubc	$F_{(1,29)} = 1.13$; $P = 0.3$	$F_{(2,29)} = 1.69$; $P = 0.21$	$F_{(2,29)} = 1.03$; $P = 0.37$

	WT LD control	**WT DLaN + Saline**	**WT DLaN + Carprofen**	***Cntnap2* KO LD control**	***Cntnap2* KO DLaN + Saline**	***Cntnap2* KO DLaN + Carprofen**
IFN$_Y$	0.6 ± 0.2	**1.0 ± 0.3***	0.4 ± 0.2	0.8 ± 0.1	**1.4 ± 0.4***	0.5 ± 0.2
IL-6	0.5 ± 0.2	0.9 ± 0.3	0.5 ± 0.3	0.6 ± 0.1	**1.2 ± 0.2***	0.5 ± 0.2
Gapdh	1.2 ± 0.0	1.3 ± 0.1	1.2 ± 0.0	1.2 ± 0.0	1.3 ± 0.1	1.2 ± 0.0
Ubc	1.2 ± 0.0	1.2 ± 0.0	1.2 ± 0.0	1.2 ± 0.0	1.3 ± 0.1	1.2 ± 0.0

Table 3.6. The COX-2 inhibitor (carprofen) counteracted DLaN-evoked social impairments and repetitive behavior. The WT and *Cntnap2* KO mice (n = 12/group) were treated with saline (control vehicle) or carprofen (0.067 mg/ml) under DLaN for 2 weeks. Then the autistic behavior was compared to the LD control group with a 2-way ANOVA to evaluate the effects of genotypes and treatments. Values are shown as averages ± SEM. The Holm-Sidak test for multiple comparisons was used when appropriate. *Indicates significant differences compared to the LD control environment. # indicates significant differences between WT controls and *Cntnap2* KO mice.

	Genotype	**Treatment**	**Interaction**
Social Behavior (sec)	F = 17.22; *P* < 0.001	**F = 7.4; *P* = 0.001**	F = 0.27; *P* = 0.77
Grooming (sec)	**F = 23.42; *P* < 0.001**	**F = 5.36; *P* = 0.007**	**F = 8.94; *P* < 0.001**
Distance Travelled	F = 3.14; *P* = 0.081	**F = 5.75; *P* = 0.005**	F = 1.76; *P* = 0.18

	WT	**WT**	**WT**	***Cntnap2* KO**	***Cntnap2* KO**	***Cntnap2* KO**
	LD control	**DLaN + Saline**	**DLaN + Carprofen**	**LD control**	**DLaN + Saline**	**DLaN + Carprofen**
Social Behavior (sec)	87.1 ± 12.2	**47.8 ± 10.4***	74.2 ± 7.8	51.46 ± 11.7#	**24.84 ± 4.78***	43.63 ± 4.92#
Grooming (sec)	8.6 ± 1.7	8.8 ± 1.1	13.7 ± 2.7	17.75 ± 3.67#	**36.16 ± 5.65*#**	14.17 ± 2.6
Distance Travelled	55.4 ± 3.0	57.1 ± 3.2	57.0 ± 2.9	65.58 ± 2.54#	49.43 ± 2.1	**52.05 ± 4.22***

Table 3.7. The COX-2 inhibitor (carprofen) did not prevent the sleep/wake cycles from the disruptions under DLaN. The WT and *Cntnap2* KO mice (n=8/group) were treated with saline (control vehicle) or carprofen (0.067 mg/ml) under DLaN for 2 weeks. The sleep/wake cycles was compared among the groups with a 2-way ANOVA to evaluate the effects of genotypes and treatments. Values are shown as averages ± SEM. The Holm-Sidak test for multiple comparisons was used when appropriate. *Indicates significant differences compared to the LD control environment. # indicates significant differences between WT controls and *Cntnap2* KO mice.

	Genotype	**Treatment**	**Interaction**
Period (hr)	$F_{(1,47)} = 0.00$; $P = 1.00$	$F_{(2,47)} = 0.11$; $P = 0.89$	$F_{(2,47)} = 1.48$; $P = 0.24$
Rhythmic Power (V%)	$F_{(1,47)} = 4.00$; $P = 0.052$	**$F_{(2,47)} = 7.34$; $P = 0.002$**	$F_{(2,47)} = 0.63$; $P = 0.54$
Total Activity (a.u.)	$F_{(1,47)} = 0.52$; $P = 0.47$	$F_{(2,47)} = 1.14$; $P = 0.33$	$F_{(2,47)} = 2.58$; $P = 0.088$
Amplitude (peak-trough, a.u.)	$F_{(1,47)} = 1.90$; $P = 0.18$	$F_{(2,47)} = 1.37$; $P = 0.27$	$F_{(2,47)} = 0.78$; $P = 0.47$
Sleep-Phase Activity (%)	$F_{(1,47)} = 0.93$; $P = 0.34$	**$F_{(2,47)} = 5.11$; $P = 0.01$**	$F_{(2,47)} = 2.65$; $P = 0.082$
Fragmentation (# bouts)	$F_{(1,47)} = 0.46$; $P = 0.50$	$F_{(2,47)} = 1.26$; $P = 0.29$	$F_{(2,47)} = 0.13$; $P = 0.88$
Cycle-to-cycle variability (min)	$F_{(1,47)} = 0.081$; $P = 0.78$	**$F_{(2,47)} = 3.8$; $P = 0.03$**	$F_{(2,47)} = 1.81$; $P = 0.18$

	WT	**WT**	**WT**	***Cntnap2* KO**	***Cntnap2* KO**	***Cntnap2* KO**
	LD control	**DLaN + Saline**	**DLaN + Carprofen**	**LD control**	**DLaN + Saline**	**DLaN + Carprofen**
Period (hr)	24.2 ± 0.1	24.0 ± 0.1	23.9 ± 0.1	24.0 ± 0.1	24.0 ± 0.1	24.1 ± 0.2
Rhythmic Power (V%)	35.2 ± 2.6	**23.3 ± 2.6***	29.3 ± 2.0	28.3 ± 2.9	21.7 ± 0.5	25.9 ± 3.2
Total Activity (a.u.)	2812.2 ± 267.8	2193.0 ± 283.5	1674.9 ± 92.9	1983.2 ± 245.0	1918.9 ± 258.2	2233.4 ± 573.5
Amplitude (peak-trough, a.u.)	192.7 ± 38.8	121.8 ± 24	142.6 ± 17.4	186.1 ± 21.1	161.9 ± 19.8	209.1 ± 48.9
Sleep-Phase Activity (%)	18.6 ± 1.5	23.4 ± 2.8	17.2 ± 1.5	16.9 ± 1.7	**23.3 ± 1.6***	**23.1 ± 1.0*#**
Fragmentation (# bouts)	21.3 ± 3.4	21.6 ± 1.8	18.9 ± 1.6	21.7 ± 1.9	24.1 ± 2.5	19.8 ± 1.7
Cycle-to-cycle variability (min)	30.9 ± 9.1	**62.4 ± 10.8***	54.5 ± 7.5	23.1 ± 1.0	42.6 ± 5.7	59.4 ± 8.0

Reference

Abdolahi, Mina, et al.,. "The neuromodulatory effects of ω-3 fatty acids and nano-curcumin on the COX-2/iNOS network in migraines: A clinical trial study from gene expression to clinical symptoms." Endocrine, Metabolic & Immune Disorders-Drug Targets (Formerly Current Drug Targets-Immune, Endocrine & Metabolic Disorders) 19.6 (2019): 874-884.

Akhondzadeh, Shahin, et al.,. "Celecoxib as adjunctive therapy in schizophrenia: a double-blind, randomized and placebo-controlled trial." Schizophrenia research 90.1-3 (2007): 179-185.

Ahmad, Sheikh F., et al.,. "Imbalance between the anti-and pro-inflammatory milieu in blood leukocytes of autistic children." Molecular Immunology 82 (2017): 57-65.

Arenella, Martina, et al. "Potential role for immune-related genes in autism spectrum disorders: Evidence from genome-wide association meta-analysis of autistic traits." Autism (2021): 13623613211019547.

Augusto-Oliveira, Marcus, et al. "What do microglia really do in healthy adult brain?." Cells 8.10 (2019): 1293.

Bakheet, Saleh A., et al.,. "Resveratrol ameliorates dysregulation of Th1, Th2, Th17, and T regulatory cell-related transcription factor signaling in a BTBR T+ tf/J mouse model of autism." Molecular neurobiology 54.7 (2017): 5201-5212.

Banks, William A. "Blood-brain barrier transport of cytokines: a mechanism for neuropathology." Current pharmaceutical design 11.8 (2005): 973-984.

Basta-Kaim, A., Fijał, K., Slusarczyk, J., Trojan, E., Głombik, K., Budziszewska, B., … Lason, W. (2015). Prenatal administration of lipopolysaccharide induces sex-dependent changes in glutamic acid decarboxylase and parvalbumin in the adult rat brain. Neuroscience, 287, 78–92.

Besedovsky L, Born J, and Lange T (2014) Endogenous glucocorticoid receptor signaling drives rhythmic changes in human T-cell subset numbers and the expression of the chemokine receptor CXCR4. FASEB J 28:67-75.

Bicks, Lucy K., et al. "Prefrontal cortex and social cognition in mouse and man." Frontiers in psychology 6 (2015): 1805.

Born J, Lange T, Hansen K, Molle M, and Fehm HL (1997) Effects of sleep and circadian rhythm on human circulating immune cells. J Immunol 158:4454-4464.

Castanon-Cervantes, O., Wu, M., Ehlen, J. C., Paul, K., Gamble, K. L., Johnson, R. L., Besing, R. C., Menaker, M., Gewirtz, A. T., Davidson, A. J. (2010) Dysregulation of inflammatory responses by chronic circadian disruption. J. Immunol. 185, 5796 – 5805.

Cermakian, Nicolas, Susan Westfall, and Silke Kiessling. "Circadian clocks and inflammation: reciprocal regulation and shared mediators." Archivum immunologiae et therapiae experimentalis 62.4 (2014): 303-318.

Collins, Ann L., and Patrick F. Sullivan. "Genome-wide association studies in psychiatry: what have we learned?." The British Journal of Psychiatry 202.1 (2013): 1-4.

Cope, Elise C., et al.,. "Immature neurons and radial glia, but not astrocytes or microglia, are altered in adult Cntnap2 and Shank3 mice, models of autism." ENeuro 3.5 (2016).

Cowley, T. R., B. Fahey, and S. M. O'mara. "COX-2, but not COX-1, activity is necessary for the induction of perforant path long-term potentiation and spatial learning in vivo." European Journal of Neuroscience 27.11 (2008): 2999-3008.

Dardani, Christina, et al.,. "Immunological pathways underlying autism: Findings from Mendelian randomization and genetic colocalisation analyses." medRxiv (2022).

De Zavalía, Nuria, et al.,. "Circadian variations of prostaglandin E2 and F2 α release in the golden hamster retina." Journal of neurochemistry 112.4 (2010): 972-979.

Downton, Polly, James O. Early, and Julie E. Gibbs. "Circadian rhythms in adaptive immunity." Immunology 161.4 (2020): 268-277.

El-Ansary, Afaf, and Laila Al-Ayadhi. "GABAergic/glutamatergic imbalance relative to excessive neuroinflammation in autism spectrum disorders." Journal of neuroinflammation 11.1 (2014): 1-9.

Ekdahl, C. T., Zaal Kokaia, and Olle Lindvall. "Brain inflammation and adult neurogenesis: the dual role of microglia." Neuroscience 158.3 (2009): 1021-1029.

Filiano, Anthony J., et al.,. "Unexpected role of interferon-γ in regulating neuronal connectivity and social behaviour." Nature 535.7612 (2016): 425-429.

Erickson, Michelle A., Kenji Dohi, and William A. Banks. "Neuroinflammation: a common pathway in CNS diseases as mediated at the blood-brain barrier." Neuroimmunomodulation 19.2 (2012): 121-130.

Escobar, M., Crouzin, N., Cavalier, M.,Quentin, J., Roussel, J., Lanté, F.,et al.,. (2011). Early, time-dependent disturbances of hippocampal synaptic transmission and plasticity after in utero immune challenge. Biol. Psychiatry 70, 992–999.

Fiorentino, Maria, et al.,. "Blood–brain barrier and intestinal epithelial barrier alterations in autism spectrum disorders." Molecular autism 7.1 (2016): 1-17.

Fonken, Laura K., Zachary M. Weil, and Randy J. Nelson. "Mice exposed to dim light at night exaggerate inflammatory responses to lipopolysaccharide." Brain, Behavior, and Immunity 34 (2013): 159-163.

Font-Nieves, Miriam, et al.,. "Induction of COX-2 enzyme and down-regulation of COX-1 expression by lipopolysaccharide (LPS) control prostaglandin E2 production in astrocytes." Journal of Biological Chemistry 287.9 (2012): 6454-6468.

Hanamsagar, Richa, and Staci D. Bilbo. "Environment matters: microglia function and dysfunction in a changing world." Current opinion in neurobiology 47 (2017): 146-155.

Harris, Raymond C. "COX-2 and the kidney." Journal of cardiovascular pharmacology 47 (2006): S37-S42.

Hellwig, Sabine, et al.,. "Altered microglia morphology and higher resilience to stress-induced depression-like behavior in CX3CR1-deficient mice." Brain, Behavior, and Immunity 55 (2016): 126-137.

Hinwood, Madeleine, et al.,. "Evidence that microglia mediate the neurobiological effects of chronic psychological stress on the medial prefrontal cortex." Cerebral cortex 22.6 (2012): 1442-1454.

Hinwood, Madeleine, et al.,. "Chronic stress induced remodeling of the prefrontal cortex: structural re-organization of microglia and the inhibitory effect of minocycline." Cerebral cortex 23.8 (2013): 1784-1797.

Hoffmann, C. "COX-2 in Brain and Spinal Cord-Implications for Therapeutic Use." Current medicinal chemistry 7.11 (2000): 1113-1120.

Hu, Chun-Chun, et al.,. "Alterations in plasma cytokine levels in chinese children with autism spectrum disorder." Autism Research 11.7 (2018): 989-999.

Ingle, Kevin A., et al.,. "Cardiomyocyte-specific Bmal1 deletion in mice triggers diastolic dysfunction, extracellular matrix response, and impaired resolution of inflammation." American Journal of Physiology-Heart and Circulatory Physiology 309.11 (2015): H1827-H1836.

Ingrao, Joelle C., et al.,. "Aqueous stability and oral pharmacokinetics of meloxicam and carprofen in male C57BL/6 mice." Journal of the American Association for Laboratory Animal Science 52.5 (2013): 553-559.

Kalkman, Hans O. "Novel treatment targets based on insights in the etiology of depression: role of IL-6 trans-signaling and stress-induced elevation of glutamate and ATP." Pharmaceuticals 12.3 (2019): 113.

Keller, Maren, et al.,. "A circadian clock in macrophages controls inflammatory immune responses." Proceedings of the National Academy of Sciences 106.50 (2009): 21407-21412.

Kim, Ji-Woon, et al. "Subchronic treatment of donepezil rescues impaired social, hyperactive, and stereotypic behavior in valproic acid-induced animal model of autism." PloS one 9.8 (2014): e104927.

Konishi, Hiroyuki, Hiroshi Kiyama, and Masaki Ueno. "Dual functions of microglia in the formation and refinement of neural circuits during development." International Journal of Developmental Neuroscience 77 (2019): 18-25.

Hughes, Alexandria N., and Bruce Appel. "Microglia phagocytose myelin sheaths to modify developmental myelination." Nature neuroscience 23.9 (2020): 1055-1066.

Kissoondoyal, Ashby. "Abnormal COX2/PGE2 Signalling in the Developing Cerebellum-A Link to Autism Spectrum Disorders." (2022).

Kirsch S, Thijssen S, Alarcon Salvador S, Heine GH, van Bentum K, Fliser D, Sester M, and Sester U (2012) T-cell numbers and antigen-specific T-cell function follow different circadian rhythms. J Clin Immunol 32:1381-1389.Korn T, Bettelli E, Oukka M, and Kuchroo VK (2009) IL-17

Kordulewska, Natalia Karolina, et al.,. "A novel concept of immunological and allergy interactions in autism spectrum disorders: Molecular, anti-inflammatory effect of osthole." International Immunopharmacology 72 (2019): 1-11.

Labrecque, Nathalie, and Nicolas Cermakian. "Circadian clocks in the immune system." Journal of biological rhythms 30.4 (2015): 277-290.

Lemos, Henrique P., et al.,. "Prostaglandin mediates IL-23/IL-17-induced neutrophil migration in inflammation by inhibiting IL-12 and IFNγ production." Proceedings of the National Academy of Sciences 106.14 (2009): 5954-5959.

Lituma, Pablo J., et al.,. "Altered synaptic connectivity and brain function in mice lacking microglial adapter protein Iba1." Proceedings of the National Academy of Sciences 118.46 (2021).

Lowery, Rebecca L., et al.,. "Loss of P2Y12 has behavioral effects in the adult mouse." International Journal of Molecular Sciences 22.4 (2021): 1868.

Maes M., Sirivichayakul S., Kanchanatawan B., Vojdani A. Breakdown of the paracellular tight and adherens junctions in the gut and blood brain barrier and damage to the vascular barrier in patients with deficit schizophrenia. Neurotox. Res. 2019;36:306–322. doi: 10.1007/s12640-019-00054-6.

Masi A, Quintana DS, Glozier N, Lloyd AR, Hickie IB, Guastella AJ. Cytokine aberrations in autism spectrum disorder: a systematic review and meta-analysis. Mol Psychiatry (2015) 20:440–6. doi: 10.1038/mp.2014.59

Matsukura, Satoshi, et al.,. "Interleukin-13 upregulates eotaxin expression in airway epithelial cells by a STAT6-dependent mechanism." American journal of respiratory cell and molecular biology 24.6 (2001): 755-761.

Morimoto, Keiko, and Kazunori Nakajima. "Role of the immune system in the development of the central nervous system." Frontiers in Neuroscience (2019): 916.

Mosser, Coralie-Anne, et al.,. "Microglia in CNS development: Shaping the brain for the future." Progress in neurobiology 149 (2017): 1-20.

Muller, Norbert, and Markus J. Schwarz. "COX-2 inhibition in schizophrenia and major depression." Current pharmaceutical design 14.14 (2008): 1452-1465.

Muthian, Gladson, et al.,. "COX-2 inhibitors modulate IL-12 signaling through JAK-STAT pathway leading to Th1 response in experimental allergic encephalomyelitis." Journal of clinical immunology 26.1 (2006): 73-85.

Natarajan, Kasthuri, et al.,. "NF-κB-iNOS-COX2-TNF α inflammatory signaling pathway plays an important role in methotrexate induced small intestinal injury in rats." Food and chemical toxicology 118 (2018): 766-783.

Nelson, T., Engberink, A.O., Hernandez, R., Puro, A., Huitron-Resendiz, S., Hao, C., … Gruol, D. (2012). Altered synaptic transmission in the hippocampus of transgenic mice with enhanced central nervous systems expression of interleukin-6. Brain, Behavior, and Immunity, 26, 959–971.

Nguyen, Phi T., et al.,. "Microglial remodeling of the extracellular matrix promotes synapse plasticity." Cell 182.2 (2020): 388-403.

Ni, Jia, et al.,. "COX-2 inhibitors ameliorate experimental autoimmune encephalomyelitis through modulating IFN-γ and IL-10 production by inhibiting T-bet expression." Journal of neuroimmunology 186.1-2 (2007): 94-103.

Ohsawa, Keiko, et al.,. "Involvement of Iba1 in membrane ruffling and phagocytosis of macrophages/microglia." Journal of cell science 113.17 (2000): 3073-3084.

Parajuli B, Horiuchi H, Mizuno T, Takeuchi H, Suzumura A. CCL11 enhances excitotoxic neuronal death by producing reactive oxygen species in microglia. Glia (2015) 63:2274–84. doi: 10.1002/glia.22892

Radi, Zaher A., and Nasir K. Khan. "Effects of cyclooxygenase inhibition on the gastrointestinal tract." Experimental and Toxicologic Pathology 58.2-3 (2006): 163-173.

Ronaldson, Patrick T., and Thomas P. Davis. "Regulation of blood–brain barrier integrity by microglia in health and disease: a therapeutic opportunity." Journal of Cerebral Blood Flow & Metabolism 40.1_suppl (2020): S6-S24.

Rowson, Sydney A., et al.,. "Neuroinflammation and behavior in HIV-1 transgenic rats exposed to chronic adolescent stress." Frontiers in psychiatry 7 (2016): 102.

Rose, Destanie, and Paul Ashwood. "Potential cytokine biomarkers in autism spectrum disorders." Biomarkers in medicine 8.9 (2014): 1171-1181.

Rotondo, D., Abul, H. T., Milton, A. S., and Davidson, J.. 1988. Pyrogenic immunomodulators increase the level of prostaglandin E2 in the blood simultaneously with the onset of fever. Eur. J. Pharmacol. 154:145–152.

Sayyah, Mehdi, et al.,. "A preliminary randomized double–blind clinical trial on the efficacy of celecoxib as an adjunct in the treatment of obsessive–compulsive disorder." Psychiatry research 189.3 (2011): 403-406.

Scheiermann, C. et al.,. Adrenergic nerves govern circadian leukocyte recruitment to tissues. Immunity 37, 290–301 (2012).

Schwartzer, Jared J., et al.,. "C57BL/6J bone marrow transplant increases sociability in BTBR T+ Itpr3tf/J mice." Brain, behavior, and immunity 59 (2017): 55-61.

Shalbafan, M., et al.,. "Celecoxib as an adjuvant to fluvoxamine in moderate to severe obsessive-compulsive disorder: a double-blind, placebo-controlled, randomized trial." Pharmacopsychiatry 48.04/05 (2015): 136-140.

Silver, Adam C., et al.,. "The circadian clock controls toll-like receptor 9-mediated innate and adaptive immunity." Immunity 36.2 (2012): 251-261.

Sirivichayakul S., Kanchanatawan B., Thika S., Carvalho A.F., Maes M. A new schizophrenia model: Immune activation is associated with induction of different neurotoxic products which together determine memory impairments and schizophrenia symptom dimensions. CNS Neurol. Disord. Drug Targets. 2019;18:124–140. doi: 10.2174/1871527317666181119115532.

Straub, R. H., Cutolo, M. (2007) Circadian rhythms in rheumatoid arthritis: implications for pathophysiology and therapeutic management. Arthritis Rheum. 56, 399 – 408.

Teixeira A.L., Gama C.S., Rocha N.P., Teixeira M.M. Revisiting the Role of Eotaxin-1/CCL11 in Psychiatric Disorders. Front. Psychiatr. 2018;9:241. doi: 10.3389/fpsyt.2018.00241.

Theoharides, Theoharis C., and Bodi Zhang. "Neuro-inflammation, blood-brain barrier, seizures and autism." Journal of neuroinflammation 8.1 (2011): 1-5.

Tremblay, Marie-Ève, et al. "The role of microglia in the healthy brain." Journal of Neuroscience 31.45 (2011): 16064-16069.

Voineagu, Irina, and Valsamma Eapen. "Converging pathways in autism spectrum disorders: interplay between synaptic dysfunction and immune responses." Frontiers in human neuroscience 7 (2013): 738.

Wake, Hiroaki, et al. "Microglia: actively surveying and shaping neuronal circuit structure and function." Trends in neurosciences 36.4 (2013): 209-217.

Xu, Yi-Qiao, et al.,. "Diurnal variation of hepatic antioxidant gene expression in mice." (2012): e44237.

Xu, Ningan, Xiaohong Li, and Yan Zhong. "Inflammatory cytokines: potential biomarkers of immunologic dysfunction in autism spectrum disorders." Mediators of inflammation 2015 (2015).

Yizhar, Ofer. "Optogenetic insights into social behavior function." Biological psychiatry 71.12 (2012): 1075-1080.

Zhan, Yang, et al.,. "Deficient neuron-microglia signaling results in impaired functional brain connectivity and social behavior." Nature neuroscience 17.3 (2014): 400-406.

Zhang, Shengxiang. "Microglial activation after ischaemic stroke." Stroke and vascular neurology 4.2 (2019).

Zhang, Yan, et al.,. "Associations between expression of indoleamine 2, 3-dioxygenase enzyme and inflammatory cytokines in patients with first-episode drug-naive Schizophrenia." Translational psychiatry 11.1 (2021): 1-8.

Zhao, Yutong, et al.,. "Regulation of COX-2 expression and IL-6 release by particulate matter in airway epithelial cells." American journal of respiratory cell and molecular biology 40.1 (2009): 19-30.

Zhou, Xiuxia, et al.,. "MAPK regulation of IL-4/IL-13 receptors contributes to the synergistic increase in CCL11/eotaxin-1 in response to TGF-β1 and IL-13 in human airway fibroblasts." The Journal of Immunology 188.12 (2012): 6046-6054.

Ziebell, Jenna M., P. David Adelson, and Jonathan Lifshitz. "Microglia: dismantling and rebuilding circuits after acute neurological injury." Metabolic brain disease 30.2 (2015): 393-400.

Chapter 5

Chapter 5

Scheduled feeding improves behavioral outcomes and reduces inflammation in a mouse model of Fragile X syndrome.

Abstract

Fragile X syndrome (FXS) is a neurodevelopmental disorder caused by the abnormal expansion of CGG repeats in the fragile X mental retardation 1 (*Fmr1*) gene. Sleep disruptions are experienced by many FXS patients and we sought to explore these symptoms along with the possible benefits of a scheduled feeding intervention using the *Fmr1* KO model of FXS. We found clear evidence for sleep and circadian disturbances in the *Fmr1* KO mouse model including delay in the onset of sleep, fragmented rhythms with increases in cycle to cycle variability. The mutants exhibited clear deficits in their circadian behavioral response to light with reduced masking, light-induced phase shifts, and resetting to 6 hr shifts in the LD cycle. Interestingly, disruptions in social and repetitive behavior were correlated with sleep duration and fragmentation. In the attempt to improve the rhythms, we applied a timed-restricted feeding regimen (TRF, 6-h feeding/18-h fast cycle) as a circadian-based strategy that boasts circadian rhythms independently of light. We found that this intervention significantly improved activity and sleep in the mutants. Strikingly, TRF also reduced repetitive behavior and increase social interactions in the Fmr1 KO mice. Finally, the feeding schedule reduced the elevated levels of Interferon-gamma (IFN-γ) and Interleukin-12 (IL12) in the *Fmr1* KO mutants, suggesting that TRF may be an effective way to reduce inflammation. Together, our study points out that the *Fmr1* KO exhibit specific deficits in the light-input pathway to the circadian system and raises the possibility that these deficits may contribute to the sleep disruption that is so commonly experienced by FXS patients. The sleep disruptions were found to be correlated with the expression of ASD behavioral deficits in individual animals. Using the information that we gained about the deficits, we designed a circadian-based intervention that improved behavioral outcomes and reduced the inflammatory signature of the *Fmr1* KO mice.

Introduction

The fragile X mental retardation protein (FMRP), an RNA-binding protein essential for the synaptic plasticity (Zalfa et al., 2006; Soden et al., 2010; Kute et al., 2019), is encoded by the fragile X mental retardation 1 (*FMR1)* gene on the X chromosome. The mutation with an expansion of CGG repeats causes transcriptional silencing of the *FMR1* gene and the loss of FMRP. This cascade is the cause of Fragile X syndrome (FXS), one of the most common forms of developmental delay and autistic-like behavior. Common symptoms include impairments in social interaction, social anxiety, delayed speech development, gaze avoidance, sensory hypersensitivity, and stereotypic movements and behaviors. FXS is likely the most common monogenic cause of Autism Spectrum Disorder (ASD) and it is estimated that 40-60% of male and 20% of female patients with FXS meet the criteria for ASD. So while ASD is highly heterogenetic without established etiology, *Fmr*1 knock-out (KO) mutants are one of the ASD mouse models that has been validated for elucidating disease mechanisms and is widely used for preclinical development of drug candidates (Thomas et al., 2012; Kazdoba et al., 2014).

While social deficits and repetitive behaviors are hallmark symptoms of FXS, sleep disturbances are extremely common (Kronk et al., 2009; Budimirovic et al., 2022). Poor sleep is harmful to not only brain health but also to many physiological levels (Casavi et al ., 2022; Nelson et al., 2022; Small et al., 2022). Unfortunately, there have been only a limited number of studies studying the interaction between sleep disturbances and FXS traits. One possible mechanism that may underlie disruptions in the timing of sleep are disturbances to the circadian timing system. The circadian clock is well known to regulate the timing of sleep/wake cycles as well as drive the consolidation of sleep at night (Colwell et al., 2003; Pandi-Perumal et al., 2022). Animal models presenting both ASD-like behavior and circadian deficits are undoubtedly valuable to study for the development of new treatments targeting these symptoms.

In this study, we sought to comprehensively examine the sleep/circadian disturbances in the *Fmr1* knock-out (KO) mice, and answer the question of whether or not the sleep/circadian disturbances are associated with their ASD behaviors. It is worth noting that much of the literature concerning behavioral deficits in the *Fmr1* KO line were conducted in the middle of the day when the mice were normally asleep, and this daytime protocol may cause sleep disruption. To address this issue, we first sought to make use of non-invasive monitoring systems to assess the sleep behavior and the activity rhythms in their home cages, and then we characterized the ASD behavior in their active phase to minimize disruptions to their sleep/wake rhythms. The same mice that were recorded for their sleep/wake cycles and tested for their ASD behavior were used to determine the underlying correlations between the two domains. Finally, guided by our understanding of the deficits in the *Fmr1* KO line, we utilized a circadian-based intervention (timed-restricted feeding, 6-h feeding/18-h fast) and determined its impact on sleep/wake rhythms and well as social deficits, and repetitive behavior.

Methods

Animals

The experimental protocols were approved by the UCLA Animal Research Committee and adhered to the UCLA Division of Laboratory Animal Medicine (DLAM) and National Institute of Health (NIH) guidelines. The *Fmr1* KO mice ($Fmr1^{tm4Cgr}$) on the C57BL/6J background (JAX ID: 003025) and the WT controls (JAX ID: 000664) were acquired from the JAX lab. All mice were genotyped (Transnetyx, Cordova, TN) again at 2 months of age and group-housed prior to any experimentation. The studies were carried out when mice were the ages of 3-5 months and all tested mice were males. All experimental animals were males in this study. They were housed in light-tight ventilated cabinets in temperature- and humidity-controlled conditions, with free access to food and water (*ad lib*) except the experimental groups with the timed-restricted feeding (TRF).

Animals tested for ASD-like behavior were habituated to the testing room at least 30 mins before the experiments started. The behavioral assays were performed under dim red light (< 2 lx at the level of the testing arena) during the active phase of the testing animals (ZT 16-18).

Immobility-Based Sleep Behavior

The sleep behavior under 12h:12h LD cycles was recorded using Anymaze automatic mouse tracking software (Stoelting Co., Wood Dale, IL) that tracked the (40 sec or greater as previously described (Wang et al., 2016; Whittaker et al., 2018). This threshold was previously determined by Fisher and his colleagues to have 99% correlation with EEG-defined sleep (Fisher et al., 2016). From 5 days of recordings, 2 days with the best recording quality were picked for the analysis. A sleep bout was defined as a time period in which activity stayed above the bout threshold (3 counts of sleep per minute for longer than one minute at a time). Acquiring data were exported in 1-min bins and the total sleep during the light phase and the dark phase was obtained.

Locomotor cage activity rhythms

To characterize the sleep/wake cycles, the WT controls and the *Fmr1* KO mutants were housed under a scheduled 12h:12h LD cycles. The mice were habituated to this cycle for 2 weeks to ensure entrainment to the appointed LD schedule before activity data was used for analysis. The animals were then released into constant darkness (12h:12h dark-dark, DD) for the assessment of the endogenous rhythms. They were kept in DD for at least 2 weeks with free access to food and water. The locomotor activity under LD cycles and DD was monitored using running wheel sensors that tracked wheel-running activity. In the set of TRF experiments, the locomotor activity rhythms were monitored using a top-mounted passive infra-red (IR) motion detector. Both the wheel-running recordings and the IR recordings were reported to a VitalView data recording system (Mini Mitter, Bend, OR) as previously described. 10 days of recordings were used for analysis and waveform presentations. The analysis was conducted by using the El Temps (A. Diez-Nogura, Barcelona, Spain) and ClockLab programs as previously described (Loh et al., 2014; Lee et al 2018). The periodogram generated by the El Temps provided measures on the period, or the length of one activity cycle, and the power of the rhythmicity. The power, or percent variance (%V), assessed the strength of the mouse's periodicity corrected for activity amount and normalized to variance percent derived from peak significance (P = 0.05). The fragmentation and the imprecision of daily onset of sleep/wake cycles were determined by the ClockLab. Fragmentation was determined by the number of activity bouts per day (maximum gap: 1 min; threshold 3 counts/min), and the imprecision was determined by calculating the variability of the time of activity onset between the best-fit line of the 10 analyzed days.

Light-regulating circadian behavior

A cohort of *Fmr1* KO mice and age-matched WT controls were housed under a 12:12 LD cycle (300 lx full-spectrum light) first and then went through the following behavioral assays to determine the deficient light-regulating circadian behavior in the *Fmr1* KO mice. The testing

mice were individually housed in cages with running wheels as described above, and the entrainment was confirmed and manually checked by senior testers.

Photic suppression on nocturnal activity (negative light masking)

After entrainment to the LD cycle, the testing mice were exposed to 1 h of light (300 lx) at ZT 14 (2 h after lights off). The number of wheel revolutions during this pulse of white light was compared to the number of wheel revolutions during the equivalent hour collected from the previous day. The fold changes were reported: [(rev during the 1-h light exposure) – (rev during the dark baseline)]/(rev during the dark baseline) %.

Phase shift of wheel-running activity onsets to a single light pulse

After entrainment to the housing LD cycle, the testing mice were released into DD for 10 days. The circadian time (CT) of their free-running sleep/wake cycles were monitored with the VitalView. The time of activity onset under DD was defined as CT 12. On day 11, a 60-min light exposure (50 lx) was given at CT 16. After the light pulse, the mice stayed in DD for the following 10 days. And the best-fit lines of the activity onsets of sleep/wake cycles before and after the light exposure were measured.

Phase shift of wheel-running activity onsets to a 6h-phase advanced photic environment

After stable entrainment, the LD cycles were advanced by 6-h from the original LD cycles. The sleep/wake cycles were continuously monitored by the wheel-running system and the VitalView. The entrainment was quantified by the difference between the running activity onset and the new ZT 12 in each recording day. A testing mouse was determined to be full entrained when the animal circadian phase was equal to the environment and there was no phase shifting for the consecutive 5 days.

Skeleton Photoperiod

After stable entrainment to the LD 12:12 cycle, mice were placed in a skeleton photoperiod consisting of 1:11: 1:11 LD. The 1-hr light treatments at 300 lux were given at

the beginning (ZT 0) and the end (ZT 11) of the original light phase. The mice were kept in this photic condition for at least 2 weeks with free access to food and water.

Stereotypic Behavior

The marble burying test was used to evaluate the repetitive digging behavior (Yrigollen et al., 2019). The testing mice were habituated to the testing room for at least 30 mins before the test. An array of 4 marbles by 6 marbles was placed in the testing arena with a layer of 4-cm deep shavings. The testing mouse was introduced to the arena from the corner and allowed to freely behave during the trial. Their behavior was recorded for 30 mins and the testing mouse was carefully returned to their home cages. After the test, the number of buried marbles was counted. Mable buried more than ⅔ area were counted, and all marbles were cleaned with 70% ethanol before the next use. Time spent on digging was manually scored and the distance travelled was derived from the automatic mouse-tracking system (Anymaze software, Stoelting Co., Wood Dale, IL).

The grooming test was conducted as our previous work (Wang et al 2020). The behavior of self-grooming was defined as the cleaning, licking, or washing of the limbs, tail, and body surface areas, typically from a head to tail direction, but excludes bouts of scratching. Time spent on self-grooming was manually scored and the distance travelled was derived from the automatic mouse-tracking system (Anymaze software).

Social Behavior

The three-chamber test of social behaviour was adapted with minor modifications from our previous study (Wang et al 2020). The testing mice were allowed to freely explore an arena with three chambers where the central chamber remained empty. When being habituated to the three-chamber arena, the *Fmr1* KO mice and their WT controls explored the arena evenly. No preference toward the left or the right chamber was observed (left/right ratio: WT: 0.95 ± 0.14; $P = 0.43$ by paired *t*-test. *Fmr1* KO: 0.82 ± 0.1; $P = 0.085$ by paired *t*-test). The three-chamber test consisted of two parts: the first stage assessed the preference of social approach

toward the stranger mouse, and the second stage assessed the ability of social discrimination of the testing mouse. In the first stage (social approach), an up-turned metal-grid pencil cup was placed in the side chambers: one remained empty as the novel object (the object chamber), and a never-met stranger mouse that mached the sex, age, and genotype of the testing mouse was placed in the second up-turned cup (the social chamber). Therefore, the testing mouse was tested for the preference between the object chamber and the social chamber in this first testing stage. In the second stage (social discrimination), the first stranger mouse and the cup remained the same while a second never-met stranger mouse that mached the sex, age, and genotype of the testing mouse was placed in the second up-turned cup. In other words, the social chamber in the first stage became a familiar chamber in the second stage, and the object chamber in the first stage became a novel chamber in the second stage. Thus, the testing mouse was tested for the preference between the familiar chamber and the novel chamber in this second testing stage. Time spent in each chamber and the distance travelled were derived from the automatic mouse-tracking system (Anymaze software).

The 5-trial social test was conducted as previously described (Mineur et al., 2006). The testing mouse was first habituated to a testing arena for 30 mins and then introduced to a never-met stranger mouse for 4 trials. The testing mouse was allowed to explore and interact with the stranger mouse for 2 mins in each trial. A second stranger mouse was introduced to the testing mouse during the 5th trial for 2 mins. The resting interval between trials was 5 mins. Active social behavior such as physical contacts (e.g. crawling over, social grooming), nose-to-nose sniffing, nose-to-anus from the testing mouse to the stranger mice were scored manually. Testing mice that showed aggressive behavior were withdrawn from the experiment, and the stranger mice showed aggressive behavior were removed from the testing trial and the pool of stranger mice.

Time-restricted feeding (TRF) paradigm

The TRF were conducted as previously described (Wang et al 2018; Whittaker et al 2018). For animals treated with TRF, they were first entrained to a 12:12 LD (300 lx vs 0 lx respectively) for a minimum of 2 weeks prior to any experiment. Next, they were exposed to a feeding paradigm of food (standard chow) available for 6 h during the middle of the active phase during ZT 15-21. To monitor the sleep/wake cycles, experimental mice were singly housed in cages with an infrared motion sensor. Food availability was achieved by manually adding and removing food from the mouse cages, and a careful examination was carried out to ensure no small food fragments were dropped and remained in the cages. The food consumption was manually measured by weighing food at the beginning and the end of the feeding cycles (control: 24 h vs TRF: 6 h). The experimental groups and their controls (*ad lib*) were held in these conditions for a total of 2 weeks.

Blood sampling and measurements of plasma immune molecules

In the beginning of the light phase, the blood was collected (~0.5 mL per animal) via cheek puncture into microvette tubes coded with EDTA (Sarstedt, Numbrecht, Germany). Tubes were gently inverted a few times and placed immediately on wet ice. Within 1 h following collection, samples were centrifuged at 2500 rpm for 15 min at 4° C. The plasma was then collected into prelabeled Eppendorf tubes (Fisher Scientific, Hampton, NH), and the lids were sealed with parafilm and immediately stored at 80° C until assessed using the Luminex Multiplexed Assay at UCLA (https://www.uclahealth.org/pathology/services-immunoassays).

Statistics

To determine the impact of loss of FMRP on the waveforms of sleep/wake cycles, we used a repeated measures two-way analysis of variance (ANOVA) with time and genotype factors. To analyze the difference between light phase and dark phase in sleep bouts, we used a 2-way ANOVA with genotype and treatment as factors. Post hoc Holm-Sidak pairwise comparisons were applied after the ANOVA. To determine if the *Fmr1* KO mutants show

genotypic difference compared to WT mice in behavior, the student *t*-test was applied. Correlations between circadian/sleep parameters and ASD-like behavior were examined by applying Pearson correlation analysis. Statistical analysis was performed using SigmaPlot. The dataset was examined for normality (Shapiro–Wilk test) and equal variance (Brown–Forsythe test). Values were reported as the mean ± standard error of the mean (SEM). Differences were determined significant if $P < 0.05$.

Results

The Fmr1 KO mutants exhibited shorter and fragmented sleep in the light phase.

To determine if the *Fmr1* KO had deficits in immobility-defined sleep behavior, the animals were examined using a combination of video recording and mouse tracking system under standard 12:12 LD cycles **(Fig. 4.1 A)**. The 2-way ANOVA was used to analyze the temporal pattern of sleep (1-h bins) of the WT controls and the *Fmr1* KO mutants and revealed a significant effect of time ($F_{(23, 287)}$ = 31.94; P < 0.001) and genotype ($F_{(23, 287)}$ = 11.95; P < 0.001). The further measures of sleep behavior from both the light phase and dark phase were then scrutinized using the 2-way ANOVA with the effect of genotype and time **(Table 4.1)**. Even though both genotypes showed day-night differences in all our sleep measures, the *Fmr1* KO mutants exhibited sleep disturbances specifically in the light phase. Compared to the WT controls, the *Fmr1* KO mutants had 11% less sleep time **(Fig. 4.1 B)** with 21% more number of sleep bouts **(Fig. 4.1 C)** in the light phase. In addition, the average length and the maximum length of sleep bouts were significantly reduced by 25-28% in the mutants compared to the controls **(Fig. 4.1 D and 4.1 E)**. The reduced sleep time, shorter bout length, and a greater number of sleep bouts are all evidence for a fragmented sleep pattern in the *Fmr1* KO mutants.

T*he Fmr1 KO mutants exhibited reduced rhythmic strength and reduced nocturnality.*

Next, we sought to determine if *Fmr1* KO mutants show circadian deficits in locomotor activity rhythms. The age-matched WT controls and *Fmr1* KO mutants were housed in running-wheel cages under standard 12:12 LD cycles for 2 weeks and then released into DD **(Fig. 4.2 A; Table 4.2)**. Under the LD environment, the hourly average waveforms suggested that the *Fmr1* mutants exhibited a clear circadian rhythm in their locomotor activity cycles with a rhythmic amplitude comparable to their WT controls **(Fig. 4.2 B)**. Analysis using the 2-way ANOVA confirmed the effects of time ($F_{(23, 287)}$ = 8.84; P = 0.003) and genotype ($F_{(23, 287)}$ = 39.75; P < 0.001) on the locomotor activity rhythms. We found that the most dramatic

difference occurred in the first 3 h of the light phase (ZT 0-3). A closer look with the post hoc *t*-test applying on measures of activity rhythms further confirmed that the *Fmr1* mutants had reduced rhythmic strength **(Fig. 4.2 C)** and more light-phase activities during ZT 0-3 than their WT controls **(Fig. 4.2 E)**. When the animals were released into DD, both *Fmr1* mutants and the WT controls exhibited very similar free-running period (tau) **(Fig. 4.2 A; Table 4.3)**, suggesting that both genotypes robust circadian oscillations. However, the *Fmr1* KO mutants exhibited weaker rhythmic strength **(Fig. 4.2 H)** and increased cycle-to-cycle variabilities **(Fig. 4.2 J)** compared to the WT controls, suggesting that the mutants have deficits synchronizing to the environment. Together, our data suggest that the *Fmr1* KO mice exhibit deficits in the circadian regulation of locomotor activity and specifically raise the possibility of problems in the synchronization to the LD cycle.

The Fmr1 KO mutants showed difficulties in responding to photic timing cues at behavioral levels.

We sought to test the possibility that the *Fmr1* KO mutants show deficits in their response to light using three classic assays of the circadian light response including light evoked suppression of activity (negative masking), light induced phase shifts of the circadian system in constant darkness, and the response of the circadian system to 6-h phase shifts in the LD cycle. First, light-masking assay tested if light exposure could effectively suppress the locomotor activity of nocturnal mice. At baseline (the equivalent hour in the day prior to testing), there was no difference between the *Fmr1* KO mutants and the WT controls in the locomotor activity level (2639.8 ± 345.6 a.u. vs 2229.7 ± 171.6 a.u., $P = 0.28$); however, during the 1-hr light pulse, levels of activity were suppressed by 77.8 ± 5.8% in the WT controls while only 32.5 ± 10.0% in the *Fmr1* mutants compared to their baseline activity (**Fig. 4.3 A**). The genotypic differences were prominent when we tracked the individual changes (**Fig. 4.3 B**). Next, we measured the direct light-induced phase shifts of the circadian system of the mice by exposing them to light (50 lx, CT 16) when they were in DD. The WT controls showed a phase delay of 2.3 ± 0.4 h while the *Fmr1* KO mutants only showed a delay of 1.1 ± 0.1 h in

the activity onset the next day (**Fig. 4.3 C and 4.3 D**). Finally, we examined the number of cycles the mice took to re-entrain to a 6 h shift of the LD cycle. While WT mice re-synchronized in 4.9 ± 0.7 days, the Fmr1 KO took 10.3 ± 0.5 days to adjust to the 6 h advance (**Fig. 4.3 E and 4.3 F**).

In another behavioral test of the ability of the circadian system to entrain to the photic environment is to place the mice in a skeleton photoperiod (SPP) in which the full 12 h of light is replaced by two 1-hr light exposures. In these experiments, all of the mice were first entrained to the standard LD cycle and then released into the SPP for 2 weeks **(Fig. 4.4, Table 4.3)**. Our recordings demonstrated that the WT controls were able to entrain to this challenging environment and exhibited robust circadian rhythms with a tau of 24.0 ± 0.0 h (**Fig. 4.4 A**). The *Fmr1* KO mutants, however, failed to stability entrain to the SPP and exhibited a tau of 23.7 ± 0.2 h (**Fig. 4.4 A**). Compared to the WT controls, the *Fmr1* KO mutants under SPP showed reduced rhythmic strength, increased light-phase activity, and larger cycle-to-cycle onset variability **(Fig. 4.4 C-G)**. Overall cage activity did not vary between the genotypes. So, in all four behavioral tests, we found evidence that the *Fmr1* KO mice exhibited deficits in their circadian light response.

Light-phase sleep measures correlated with the severity of dark-phase measured autistic behavior.

The social and stereotypic symptoms are the hallmarks symptoms in ASD, and there are clinical studies suggested a link between the reduced nighttime sleep quality and the exacerbated challenging behavior in the day (Abel et al., 2018; Cohen et al., 2018; Yavuz-Kodat et al., 2020; Sadikova et al., 2022). However, such association has not been tested in any ASD mouse models. To address this issue, we sought to first test a battery of ASD behaviors at night (ZT 16 to ZT 18), a phase when animals are naturally awake and active, and then study the correlation between the sleep measures and ASD behavior.

The active-phase social behavior was first tested with the three-chamber test. In the first stage of testing social approach, the *Fmr1* KO mutants showed robust social interests toward the stranger mouse when they were given the choice between an asocial object and a social subject. The 2-way ANOVA indicated that there was a significant effect of the chamber ($F_{(1, 31)}$ = 5.7; P = 0.024) but not the genotype ($F_{(1, 31)}$ = 0.1; P = 0.75). The post-hoc *t*-test confirmed that *Fmr1* KO mice spend a similar amount of time in the social chamber as their WT controls (WT: 212.4 ± 23.4 sec, *Fmr1* KO: 223.9 ± 17.5 sec; P = 0.68). However, the genotypic difference was found in the social memory. In the following second testing stage, when the asocial object was replaced with a second novel mouse and the same stranger mouse from the first stage had become a familiar mouse, the WT controls spent 222.8 ± 13.5 sec in the novel-mouse chamber and 143.4 ± 11.2 sec in the familiar-mouse chamber (61.2 ± 16.0% fold change toward the novel mouse). The *Fmr1* KO mutants spent 209.5 ± 14.2 sec in the novel-mouse chamber and 172.6 ± 1.7 sec in the familiar-mouse chamber (21.7 ± 9.1% fold change toward the novel mouse) **(Fig. 4.5 A, Table 4.4)**. The reduced time in exploring and staying the novel-mouse chamber suggested that the *Fmr1* KO mutants were not able to distinguish the second novel mouse from the first familiar mouse.

The possibility of impaired social memory was further tested by the 5-trial social test. In this test, the first stranger mouse becomes a familiar mouse after 4 times of introduction to the testing mouse. When the second novel mouse is introduced in the 5th trial, the testing mouse typically shows a boosted interest in exploring the second novel mouse. Our results showed that, when the first stranger mouse was introduced to the testing mouse, the *Fmr1* KO mutants showed a similar level of social interest as their WT controls (**Table 4.4**). As expected, when the second novel stranger mouse replaced the first familiar mouse and was introduced to the testing animals, WT controls showing elevated social behavior in the 5th trial. In contrast, the *Fmr1* KO mutants were not affected by the induction of the second novel mouse, and did not show a boosted interest in exploring the second novel mouse (**Fig. 4.5B, Table 4.4**).

Next, when the active-phase repetitive behavior was examined by the marble bury test, we found that the *Fmr1* KO mutants buried 129.8% more number of marbles and spent 433.9% more time in digging behavior than the WT controls (**Fig. 4.5 C**; **Table 4.5**). When this 30-min trial was divided into three 10-min intervals, the repetitive digging behavior was significant in the *Fmr1* mutants compared with the WT controls through all the three 10-min interval (**Fig. 4.5 D**). The 2-way ANOVA demonstrated that there was a significant effect of the genotype ($F_{(1, 107)} = 11.04$; $P = 0.001$) but not the interval ($F_{(2, 107)} = 0.42$; $P = 0.66$). In the grooming test that tested a different form of their repetitive behavior, the *Fmr1* KO mutants exhibited aberrant grooming behavior by showing 113.2% more time in grooming than their WT controls (**Fig. 4.5 E**, **Table 4.5**).

Finally, the same mice that were recorded for their sleep/wake cycles and tested for their ASD behavior were used to determine the underlying correlations between the two domains. Significant correlations were found in the social memory tested by the 5-trial social interaction test, the percentage of buried marbles, and the grooming time **(Table 4.6)**. The social memory showed a moderate-strong correlation with the sleep time and the sleep bout length in the light phase **(Fig. 4.5 G & H)**. The grooming time had a strong correlation with the sleep time, the number of sleep bouts, and the sleep bout length in the light phase **(Fig. 4.5 I & L)**. In addition, we also found moderate correlation between the grooming time and the circadian rhythmic power as well as activity onset variability **(Table 4.6)**.

In short, our work demonstrated that even when tested at their circadian active phase, the *Fmr1* KO mutants exhibited robust deficits in social memory and repetitive behavior. Moreover, the shorter and the more fragmented the daytime sleep, the more severe of social memory impairment and the repetitive behavior.

The time-restricted feeding paradigm ameliorated sleep disturbances and improved the deficits in social memory and repetitive grooming behavior in the Fmr1 KO.

The correlations between the fragmented sleep and the severity of ASD output behavior raised a possibility that the interventions improving the sleep and circadian rhythms may ameliorate the observed ASD behavioral deficits in the *Fmr1* KO mutants. Scheduled feeding can be a powerful regulator of circadian rhythms (Long and Satchidananda, 2022; Manoogian et al., 2022) and has been shown to be effective in disease models (Whittaker et al., 2018; Gao et al., 2022; Gupta et al., 2022). We therefore sought to determine if a TRF paradigm (6-h feeding/18-h fast, 2 weeks of treatment) could benefit the *Fmr1* KO mice. In this study, we had 2 genotypes held under *ad lib* as well as TRF conditions. Initially, we confirmed the food consumption was very similar by the second week (**S. Fig. 4.2**). Both the genotypes were able to learn the protocol and were eating as much as their *ad lib* controls after 5 days. At the end of the two treatment, the TRF groups weighted less than the *ad lib* groups (**S. Fig. 4.2**). Nevertheless, we found no evidence suggesting that the lighter body weights in the TRF groups negatively implicated any physiological outcomes. As a gross output measure, the locomotor activities or the sleep/wake cycles were not different between the feeding groups. Both WT and *Fmr1* KO mutants treated with TRF show a similar level of cage activities as well as the rhythmic amplitude to their *ad lib* controls **(Fig. 4.7 A & B, Table 4.7)**.

The TRF treatment benefited a number of aspects of the daily rhythms in activity and sleep. The effects of genotypes and the feeding treatments were analyzed using a 2-way ANOVA with genotype and treatment as factors **(Table 4.7)**. When the sleep behavior was assayed, there was a robust improvement in their sleep **(Fig. 4.6, Table 4.7)**. The 2-way ANOVA analysis confirmed the enhancing effects of TRF treatment on sleep time and sleep consolidation. During the light phase, the TRF-treated *Fmr1* KO mutants spend more time sleeping with longer sleep bout length and a smaller number of sleep bouts than the *ad lib* feeding mutants. It suggested that the sleep fragmentations in the *Fmr1* KO mutants were

ameliorated by the TRF treatment. The beneficial effects of TRF treatment on sleep behavior were also observed in the WT controls **(Table 4.7)**. In addition, we found that TRF improved the power of the rhythmic power as well as reducing the inappropriate light-phase activity, and the number of activity bouts **(Fig. 4.6, Table 4.7)**. Moreover, the TRF-treated *Fmr1* KO mutants showed a significant reduction in the cycle-to-cycle variation and the number of activity bouts, suggesting more precise and consolidated circadian rhythms in the treated mutants. Therefore, TRF benefitted the rhythms in sleep and activity.

We also observed the benefits of TRF treatment on the ASD output behavior. The social memory and the grooming behavior were selected due to their significant correlations to the circadian and sleep measures **(Table 4.6)**, and the effects of genotypes and the feeding treatments were determined by the 2-way ANOVA analysis **(Table 4.8)**. The social memory was evaluated by the 5-trial social interaction test, and there was a significant improvement in the mutants treated with TRF **(Fig. 4.7)**. Their social interests in interacting with the second novel mouse were significantly increased to the WT-like level, suggesting that the treated mutants were able to distinguish the novel mouse from the familiar mouse. In addition, we also observed a trend that both the WT controls and *Fmr1* KO mutants showed increased social behaviours during the first 4 testing sessions compared to their *ad lib* controls (WT: 20.0% increase, *Fmr1* KO: 42.0% increase), even though the effect of TRF treatment was not identified by the 2-way ANOVA analysis. Regarding the repetitive grooming behavior, the TRF-treated *Fmr1* KO mice showed a significant reduction in time spent on self-grooming **(Fig. 4.7)**. This reduction was not due to any changes in their locomotor ability as there was no feeding effects on the distance travelled during the test among the TRF groups and *ad lib* groups **(Fig. 4.7)**. In summary, TRF not only improved the sleep/wake cycles but also improved the deficits in social memory as well as the self-grooming behavior in the *Fmr1* KO mutants.

Time-restricted feeding treatment reduced the elevated IL-12 and INF$_Y$ pathway in the Fmr1 KO mice.

Abnormal immune responses have been suggested to play a role in FXS and ASD pathophysiology (Reynolds et al., 2021; Dias et al., 2022; Robinson-Agramonte et al., 2022). To investigate whether or not our TRF treatment corrected the altered cytokine profiles in the *Fmr1* KO mutants, the plasma samples were collected at the end of the TRF treatment. Our assessment revealed a number of cytokines altered in the *Fmr1* KO mice, and the changes were countered by the treatment of TRF **(Table 4.9)**. The comparison within the *ad lib* group revealed that the *Fmr1* KO mutants had elevated levels of Interleukin-12 (p40) [IL-12 (p40)], Interferon-gamma (IFN$_Y$), and Chemokine Ligand-9 (CXCL-9) compared to WT. The genotypic differences in these pro-inflammatory makers were no longer significant in the TRF-treated groups **(Fig. 4.8)**. The 2-way ANOVA identified the significant effects of TRF treatment on IL-2, IL-12 (p40), IFN$_Y$, and CXCL-9.

We next asked whether there was a correlation between the levels of these proinflammatory markers and the expression of the behavioral phenotypes. We focused our attention on IL-12 (p40) and IFN$_Y$ axis because their levels were elevated in the KO and were successfully reduced by the TRF treatment. Our analysis confirmed our hypothesis and revealed significant correlations **(Fig. 4.8; Table 4.10)**. Markers of poor sleep such as higher activity in the light phase, shorter sleep time/sleep bout length, and higher numbers of sleep bouts were significantly associated with higher levels of IL-12 and IFN$_Y$. The levels of IL-12 and IFN$_Y$ were significantly associated with the social memory impairments and the severity of repetitive grooming behavior. Together, our data demonstrate that TRF treatment effectively reduced the levels of pro-inflammatory cytokines in the *Fmr1* KO mutants, and might act on the IL-12 (p40) - IFN$_Y$ axis to improve sleep/wake cycles as well as the ASD behaviors.

Discussion

It is becoming increasingly clear that robust daily sleep/wake rhythms are essential to good health. A wide range of growing studies have demonstrated that disrupted circadian rhythms and poor sleep lead to a cluster of symptoms, including metabolic deficits, cardiovascular problems, abnormal immune activities, and cognitive deficits (Abdul et al., 2021; Cheng et al., 2021; Johnson et al., 2021; Bisdounis et al., 2022). Many of these same symptoms are seen in FXS and ASD patients (Parente et al., 2022; Protic et al., 2022), indicating a potentially bidirectional link between the circadian clocks and the core symptoms. In this present study, we demonstrated that the loss of *Fmr1* had negative impacts on temporal pattern of sleep and locomotor activity with strong deficits in the respond to the environment lighting. The disrupted rhythms as were significantly associated with the social memory impairments and the repetitive behavior. In addition, we demonstrated that the circadian-based treatment strategy, TRF, was effective in countering the behaviors deficits as well as the basal inflammatory signature in the *Fmr1* KO mutants.

Using similar assays, prior work found that *Fmr1/Fxr2* double KO and *Fmr1 KO/Fxr2* heterozygous animals exhibit a loss of rhythmic activity in a LD cycle (Zhang et al., 2008). Using a home-cage monitoring system to assess total sleep time in *Fmr1* KO mice, Saré and colleagues also found evidence for genotypic effects on sleep during in adults only in the light phase (Saré et al., 2017). Other studies measuring home cage activity found that *Fmr1* KO mice show significantly less daily movement during their active phase (the dark cycle) and that the mutants have more bouts of activity during the light cycle compared with WT (Bonasera et al., 2017). Hypoactivity during the night was also a prominent feature of male *Fmr1* KO uncovered by home cage activity by another group (Angelakos et al., 2019). Broadly, these are consistent in finding hypoactivity during the dark and shortened, fragmented sleep during the day. We did not see the shortening of free-running circadian period (tau) when activity is measured in DD (also see Angelakos et al., 2019). The free-running period, as measured by locomotor behavior in DD, is an extremely sensitive marker of output of the core molecular

clock that drives circadian oscillations (Takahashi et al., 2008). Measurements of clock gene expression in the central clock (SCN) did not find alterations in the rhythmic patterns of transcriptions of any of the core clock genes (*Per1*, *Per2*, *Bmal1*, or *Cry1*) in the *Fmr1* KO (Zhang et al., 2008). Based on the lack of changes in tau or clock gene expression in the SCN, we do not see evidence for deficits in the core circadian clock in these mutants which leaves us to consider deficits in the photic regulation and outputs of the circadian time system in order to explain the behavioral phenotype. Collectively, this work indicates that the *Fmr1* KO mice exhibit disruptions in the temporal patterning of activity and sleep which fits with a general pattern of deficits seen in mouse models of monogenic neurological disorders (Angelakos et al., 2019; Brown et al., 2019; Shi and Johnson, 2019; Takumi et al., 2019; Wang et al., 2020).

One interesting and novel findings of our experiments is the clear behavioral evidence for impairments in the light regulation of the circadian system in the *Fmr1* KO mutants (**Fig. 4.3**). A higher portion of light-phase activities in their home cages have been reported (Bonasera et al., 2017); however, it is to our knowledge that this is the first study examining this perspective thoroughly. We applied three classic circadian assays followed by the challenge of SPP environment. The *Fmr1* KO mutants showed deficiency in all our assays: Compared to the WT controls, the mutants showed 58% reduction in their negative light-masking behavior, 53% reduction in their phase-shifting magnitude, they took twice as long to re-entrain to a 6-h shift in the LD cycle (5 vs. 10 days). The deficits in the *Fmr1* KO were highlighted when place on a skeleton photoperiod (1:11:1:11) in which the mutants failed to stably entrain while WT mice have no problem adjusting to this lighting condition (**Fig. 4.4**). Prior work suggests that the central circadian clock in the SCN may not be impacted by the *Fmr1* mutation. The temporal expression of core clock genes (e.g. *Per1*, *Bmal1*) as well as the multiunit electrical activity in the SCN were found intact in the mutants (Zhang et al 2006). Still, our data along with the work by Zhang et al., 2006 were not able to rule out the possibility that there might be deficiency caused by the lack of FMRP in the output part or the downstream pathways of the SCN. Considering that FMRP is essential for synaptic functions and the loss

of FMRP can lead to abnormal neurotransmitter signaling, it is possible that the neuronal outputs from the SCN could be compromised by the loss of FMRP. Future studies aiming the SCN outputs such as rhythms of core body temperature, cortisol, and melatonin will help to scrutinize this hypothesis. It will be important to determine whether these deficits in light input that were so prominent in the mouse model are also present in the FXS patients. The possible finding that the circadian light response may be compromised has a number of practical implications that could alter disease management of FXS.

One of the key features of the present study is that assessments of the mutants compared to WT controls during their active phase (ZT 16-18) and that we were able to measure sleep as well as social and repetitive behaviors in the same animals which enabled us to test for correlations (**Fig. 4.5**). We feel that these features are meaningful as most published work studied the mutants at their rest phase (Spencer et al., 2011; Sørensen et al 2015; Petroni et al., 2022), potentially bringing in a confound factor of sleep disruption/deprivation to their results. In other words, the daytime-testing protocol could function as a stressor to the mutants which could exacerbate the observed phenotypes. For example, the contactin associated protein-like 2 (*Cntnpa2* KO) mouse model of ASD show stronger repetitive grooming behavior in the light phase than the dark phase (Wang et al., 2020). Therefore, we feel that it is important to test the behavior of nocturnal animals in the night during their active phase. Prior work in ASD patients reported that the daytime symptoms are worse when the prior night's sleep is poor (Schreck et al., 2004; Sikora et al., 2012; Taylor et al., 2012; Budimirovic et al., 2022). In addition, interventions using either behavioral (Malow et al., 2014) or pharmacological (Wright et al., 2011) approach to improve sleep are effective to reduce symptoms severity in ASD patients. To our knowledge, the present study is the first to explore possible correlations between the sleep measures and the ASD behavior in a rodent model. When the sleep is shorter and more fragmented, both social memory and the repetitive behavior were negatively affected. This data provides strong support for the concept of

bidirectional links between sleep and ASD symptoms. Importantly, we have a number of behavioral and pharmacological interventions that can improve sleep.

We went on to test the hypothesis that improving the sleep and circadian rhythms may ameliorate the observed ASD behavioral deficits in the *Fmr1* KO mutants using a scheduled feeding protocol. The feeding treatment was chosen over light therapy because of the deficient responses to photic timing cues in the *Fmr1* KO mutants. Even with a short treatment of 2 weeks, the TRF treatment drove significant improvements in the *Fmr1* KO mutants. TRF increased rhythmic power, reduced variability, and improved nocturnality in the activity rhythms as well as lengthened and consolidated sleep bouts during the light phase **(Fig. 4.6)**. Moreover, significant improvements in the social memory and a reduction in repetitive grooming behavior were observed (**Fig. 4.7**). Importantly, our cytokine results highlight the possible role of inflammation as the mechanistic link between sleep/wake rhythms and ASD behavior. Peripheral cytokines are known to affect different behaviors, and when chronically augmented, can have profound and long-term effects on behavior in patients and animal models, even resulting in neuropsychiatric disorders. Altered immune profiles and exacerbated responses to immune challenges are reported in both FXS patients (Ashwood et al., 2010; Careaga et al., 2014; Van Dijck et al., 2020) and the *Fmr1* KO mice (Pacey et al., 2015; Hodges et al., 2020; Bertrand et al., 2021), suggesting that the lack of FMRP may lead to broad effects on imbalanced immune activities. And associations between the impaired ASD behavior and levels of dysregulated cytokines have been documented in patients and preclinical models (Siniscalco et al., 2018; Matta et al., 2019). For example, Increased levels of IL-6, IL-12 are associated with increased stereotypy, impaired cognitive abilities, abnormal anxiety, and decreased social interactions in ASD (Konsman et al., 2008; Ashwood et al., 2011; Wei et al., 2012; Fallah et al., 2020). Moreover, counteracting changes in immune profiles is suggested to improve the ASD behavior in the Fmr1 KO mice (Goo et al., 2020). Here our study suggests that the IL-12 (p40) and IFN-γ may play a key role in how TRF improves the *Fmr1* KO mutants. The levels of IFN-γ and IL-12 (p40) showed genotypic

difference in the *ad lib* control group, respond to the TRF treatment, and their levels were also significantly correlated with the level of sleep measures and the severity of behavioral impairments **(Fig. 4.8; Table 4.10)**. Neuroinflammation, which is associations with reduced GABA level as well as glutamate excitotoxicity (El-Ansary et al., 2014; Park et al., 2022), have been observed in the prefrontal cortex, hippocampus, and the amygdala region that are essential for mediating sleep, learning and memory, social behavior and repetitive behavior in the *Fmr1* KO mutants as well as other ASD animal models (Arsenault et al., 2016; Hodges et al., 2017; Yuskaitis et al., 2019; Cristiano et al., 2022). Whether or not the TRF treatment counters the neuroinflammation in these candidate regions will need to be addressed in the future study.

Figures

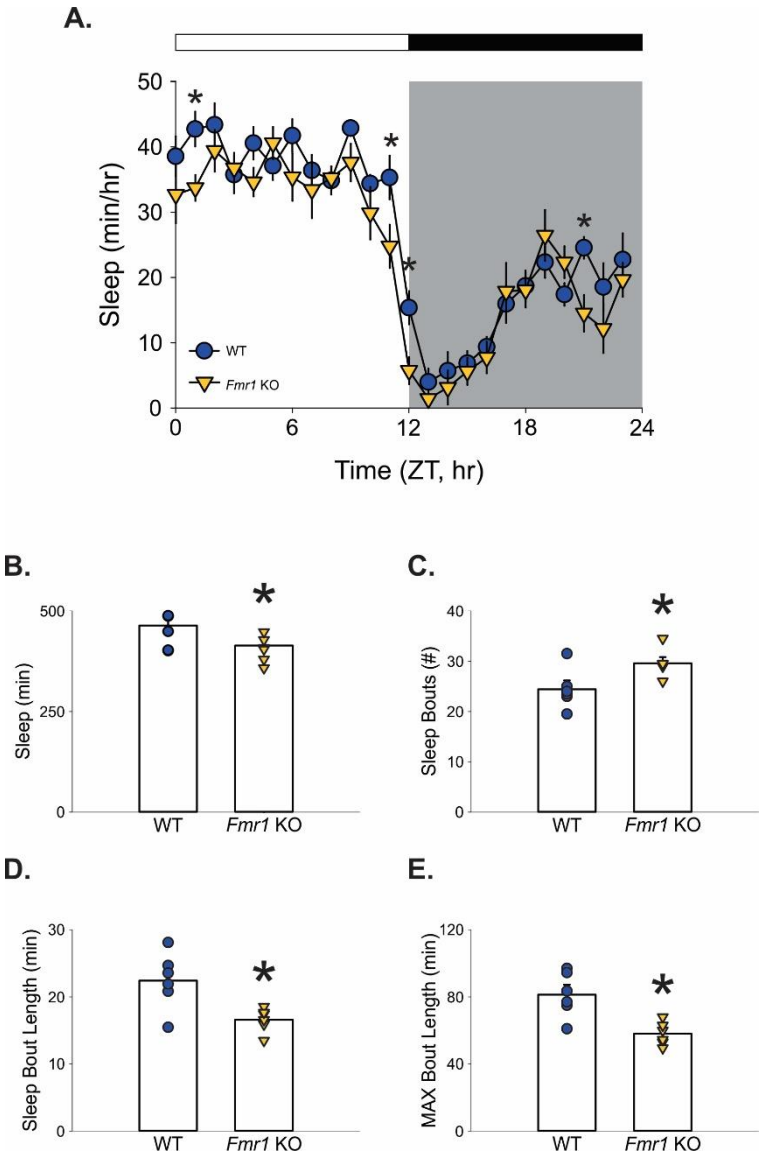

Fig. 4.1: The *Fmr1* KO mutants exhibited shorter and fragmented sleep in the light phase. (A) Waveforms of daily rhythms in sleep behavior under standard 12:12 h light-dark (LD) cycles in both WT (blue circle) and *Fmr1* KO (yellow triangle) mice (n = 6/genotype). By definition, ZT 0 is when lights turn off and ZT 12 is when lights turn on. The sleep waveform (1 h bins) of each genotype were analyzed using a 2-way ANOVA with genotype and time as factors, followed by Holm-Sidak's multiple comparisons test, *$P < 0.05$. The effects of time ($F = 31.94$; $P < 0.001$) and genotype ($F = 11.95$; $P < 0.001$) were significant. The WT controls and the *Fmr1* KO mutants exhibited clear rhythms in sleep, with reductions in the mutants mostly found in the light phase. The white/black bar on the top indicates the 12:12 h LD cycle, and the gray shading in the waveforms indicates the time of the dark phase. **(B-E)** Measures of immobility-defined sleep in the light phase. Values show means ± SEM. Significant differences ($P < 0.05$) are indicated with an asterisk (*). Detailed numbers are reported in **Table 4.1**.

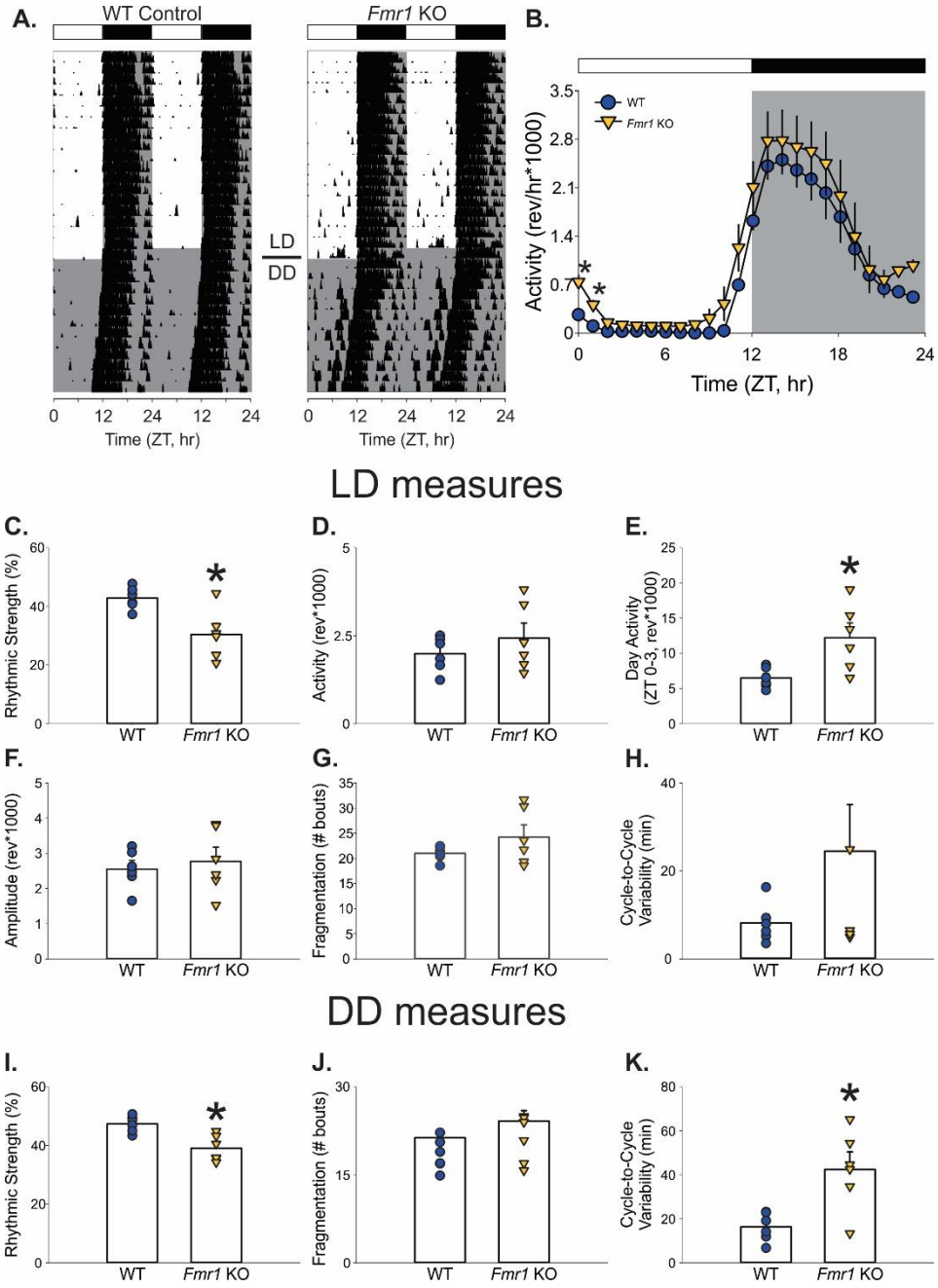

Fig. 4.2: The *Fmr1* KO mutants exhibited unstable locomotor activity rhythms and reduced nocturnality. (A) The representative wheel-running actograms of daily rhythms in cage activity under standard LD cycles followed by the constant darkness (DD) in both WT (left) and *Fmr1* KO (right) mice. The activity levels in the actograms were normalized to the same scale (85% of the maximum of the most active individual). Each row represents two consecutive days, and the second day is repeated at the beginning of the next row. **(B)** Waveforms of daily rhythms in cage activity in both WT (blue circle) and *Fmr1* KO (yellow triangle) mice under the LD cycles (n = 6/genotype). The activity waveform (1 hr bins) was analyzed using a 2-way ANOVA with treatment and time as factors followed by Holm-Sidak's multiple comparisons test, **P* < 0.05. There were significant effects of time (F = 8.84; *P* = 0.003) and genotype (F = 39.75; *P* < 0.001) on the temporal of the locomotor activity rhythms. Note that most genotypic differences were found at the beginning of the light phase. **(C-K)** Measures of locomotor activity rhythms under LD **(C-H)** and DD **(I-K)**. Histograms show means ± SEM, and the genotypic differences were analyzed by the student *t*-test (**P* < 0.05). The white/black bars on the top of the actograms and waveforms indicate the 12:12 h LD cycle, and the gray shading in the waveforms indicates the time of dark exposure. Detailed numbers are reported in **Table 4.2**.

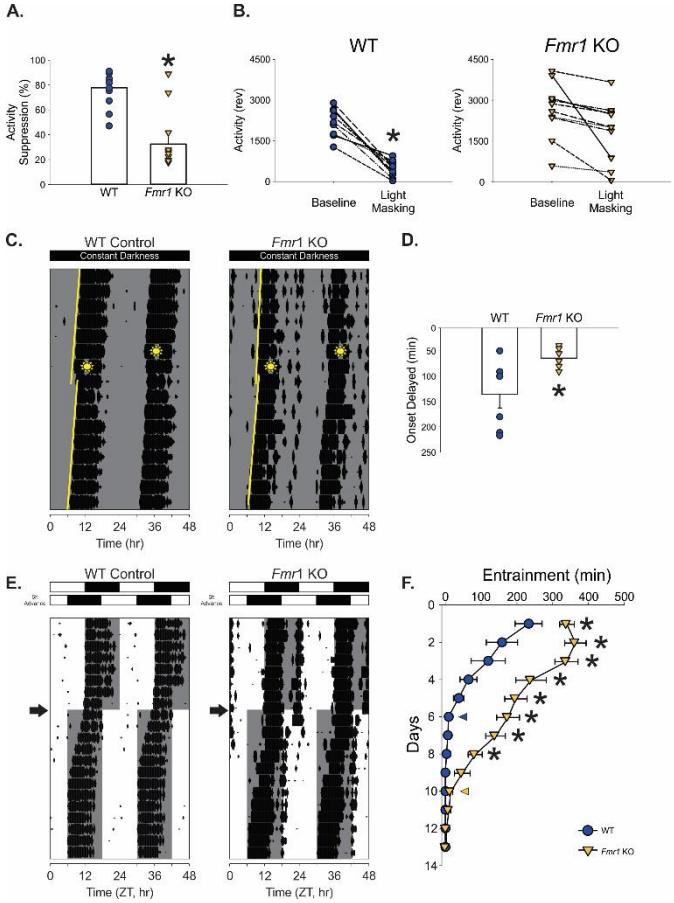

Fig. 4.3: The *Fmr1* KO mutants showed deficits in light-regulated circadian behaviors. (A, B) The photic-suppressing (masking) activity in mice exposed to lights (full spectrum) at 300 lx for an hour at ZT 14 (n=10/group). The activity level during the light exposures was compared to the activity level during the equivalent hour (ZT 14 to 15) on the day before the treatment (baseline activity). **(A)** The genotypic difference in the fold change is determined by the student's *t*-test, and the mutants showed significantly lower suppression compared to the WT controls (WT: 77.8 ± 5.8%; *Fmr1* KO: 32.5 ± 10.0%; t = 4.13, *P* < 0.001). **(B)** The individual changes in the activity levels during the baseline window and the light masking are determined using the paired *t*-test in the WT controls (left, 2229.7 ± 171.6 a.u. vs 473.0 ± 99.4 a.u., t = 9.34, *P* < 0.001) and the *Fmr1* KO mutants (right, 2639.8 ± 345.6 a.u vs 1852.5 ± 371.1 a.u., t = 1.64, *P* = 0.12) **(C, D)** Light-induced phase delay of free-running activity rhythms in mice exposed to lights at 50 lx for 60 mins at circadian time (CT) 16. By definition, CT 12 is the beginning of activity cycle under DD conditions. Examples of light-induced phase shifts of wheel-running activity rhythms **(C)** of the WT controls (left) and the *Fmr1* KO mutants (right) and quantified phase delay **(D)** are shown (n = 7/group). In the representative actograms, the yellow lines indicate the best-fit line of the activity onset across the 10 days before and after the light pulse, and the amount of the phase delay is determined from the difference between the two lines on the next day after the light pulse. The sunny-shape symbols indicate when mice were exposed to light (CT16). Compared to the WT controls (-135.6 ± 26.9 mins), the *Fmr1* KO mutants showed reduced phase shift of their activity rhythms (-64.3 ± 7.7). The phase shifts were compared using student's *t*-test (t = 33.5, P = 0.001). **(E, F)** Entrainment induced by a 6 h-phase advanced LD cycle. Examples of light-induced phase shifts of wheel-running activity rhythms **(E)** of the WT controls (left) and the *Fmr1* KO mutants (right) are shown. The white/black bars on the top of actograms indicate the LD cycle before (upper) and after (lower) the 6 h phase advance. The gray shading in the waveforms indicates the time of dark phase. The arrows next to the actograms indicate the day when 6 h-phase advance was applied. The entrainment shifting in the WT controls (blue circle) and the *Fmr1* KO mutants (yellow triangle) is quantified by the difference between the activity onset and the new ZT12 on each day **(F)**. The dash lines indicate the day when the activity rhythms are considered well entrained. Significant effects on genotype (F = 28.03, *P* < 0.001), time (F = 60.95, *P* < 0.001), and the interaction between the two factors (F = 9.29, *P* < 0.001) were found using a 2-way repetitive measure ANOVA.

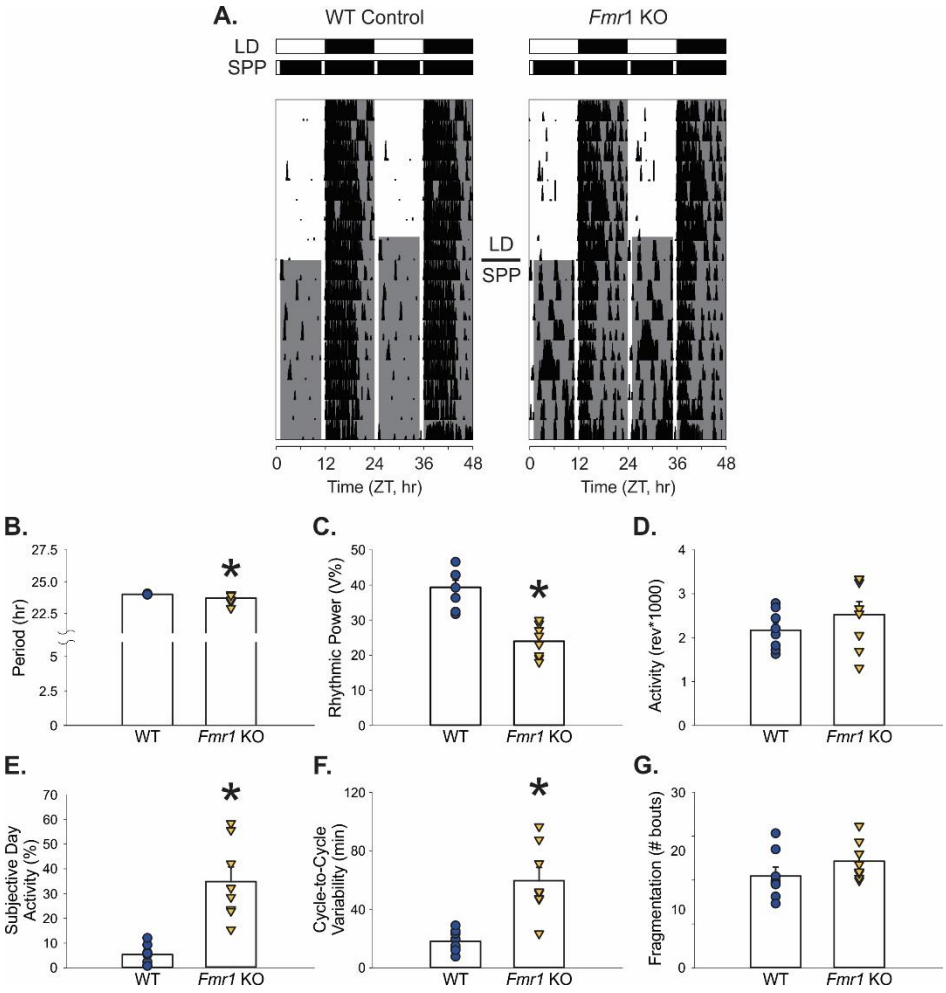

Fig. 4.4: The *Fmr1* KO mutants exhibited difficulty in adapting to the skeleton photic period (SPP). (A) The representative actograms of daily rhythms in cage activity under standard LD cycles followed by the SPP challenge (1:11:1:11 LD cycles) in both WT (left) and *Fmr1* KO (right) mice. The white/black bars on the top of actograms indicate the baseline LD cycle (upper) and the SPP LD cycles (lower). The gray shading in the waveforms indicates the time of the dark phase. The black arrows indicate the day when the SPP was applied. **(B-G)** Measures of locomotor activity rhythms under the SPP environment, and the histograms show means ± SEM. The genotypic differences were analyzed by the student's *t*-test (**P* < 0.05). Detailed numbers are reported in **Table 4.3** (n = 8/group).

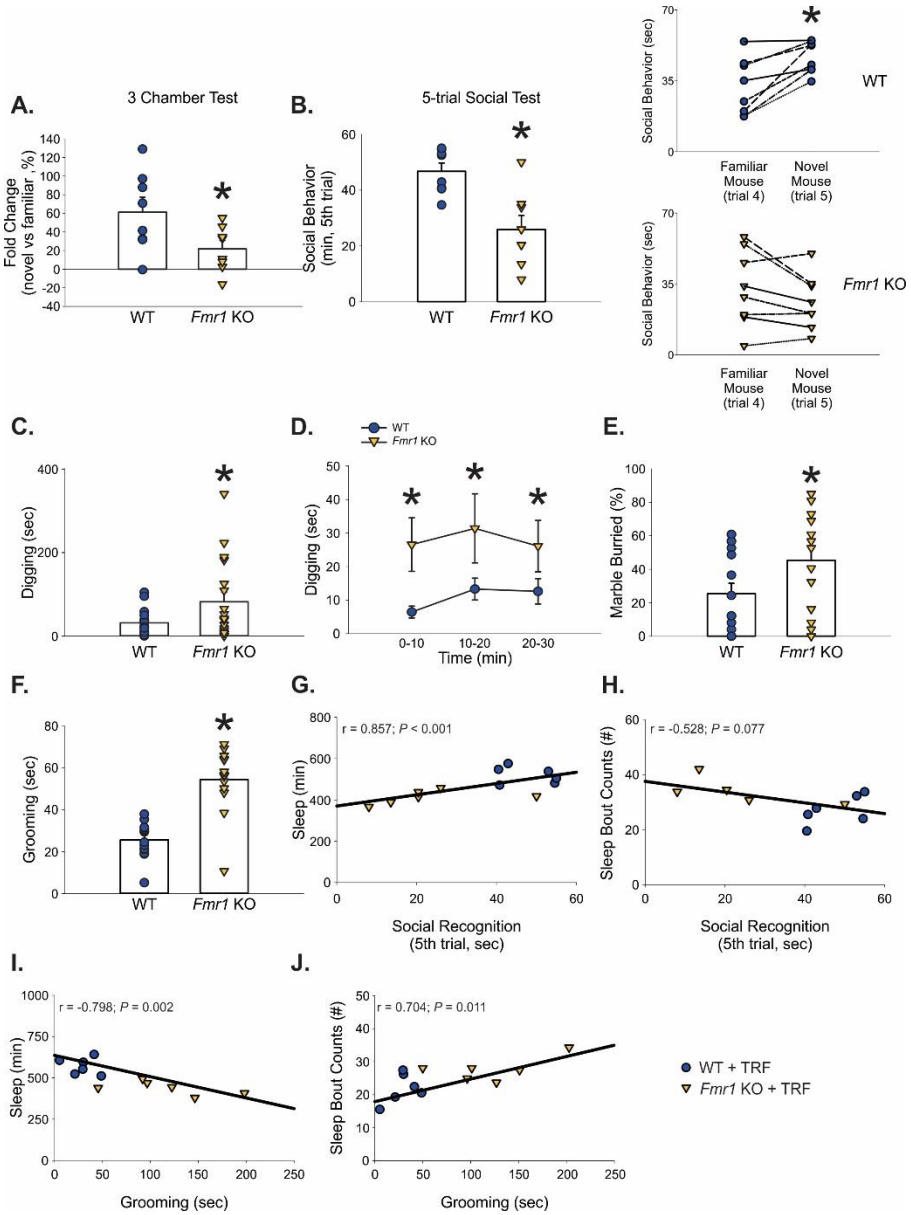

Fig. 4.5: Light-phase sleep measures correlated with the severity of dark-phase measured autistic behavior. (A) The fold change of social recognition was tested in the second stage of the three-chamber test. Time spent in the novel mouse chamber was compared with the time staying in the familiar mouse chamber. The genotypic differences were analyzed by the student's *t*-test (**P* < 0.05; n=8/group). **(B)** The left panel shows the time spent in social behavior when the second novel stranger mouse was introduced to the testing mouse in the 5-trial social interaction test. The right panel shows the individual changes in their social interaction with the familiar mouse and the novel mouse in the 5-trial social interaction test (WT controls on the top, and *Fmr1* KO mutants at the bottom). The difference was determined using the paired *t*-test (**P* < 0.05). Detailed numbers are reported in **Table 4.4** (n = 8/ group). **(C-F)** The digging, burying, and grooming behaviors were tested in the dark phase (n=14/group). The histograms were analyzed using the student's *t*-test (**P* < 0.05). Digging behavior in the three 10-min sections was analyzed using the 2-way ANOVA with the genotypes and sections as the variables. Detailed numbers are reported in **Table 4.5**. **(G-J)** The correlations among sleep time, sleep fragmentation (# bouts), social recognition, and grooming behavior. Data were analyzed using the Pearson Correlation, and the coefficients are reported in **Table 4.6** (n = 6/genotype).

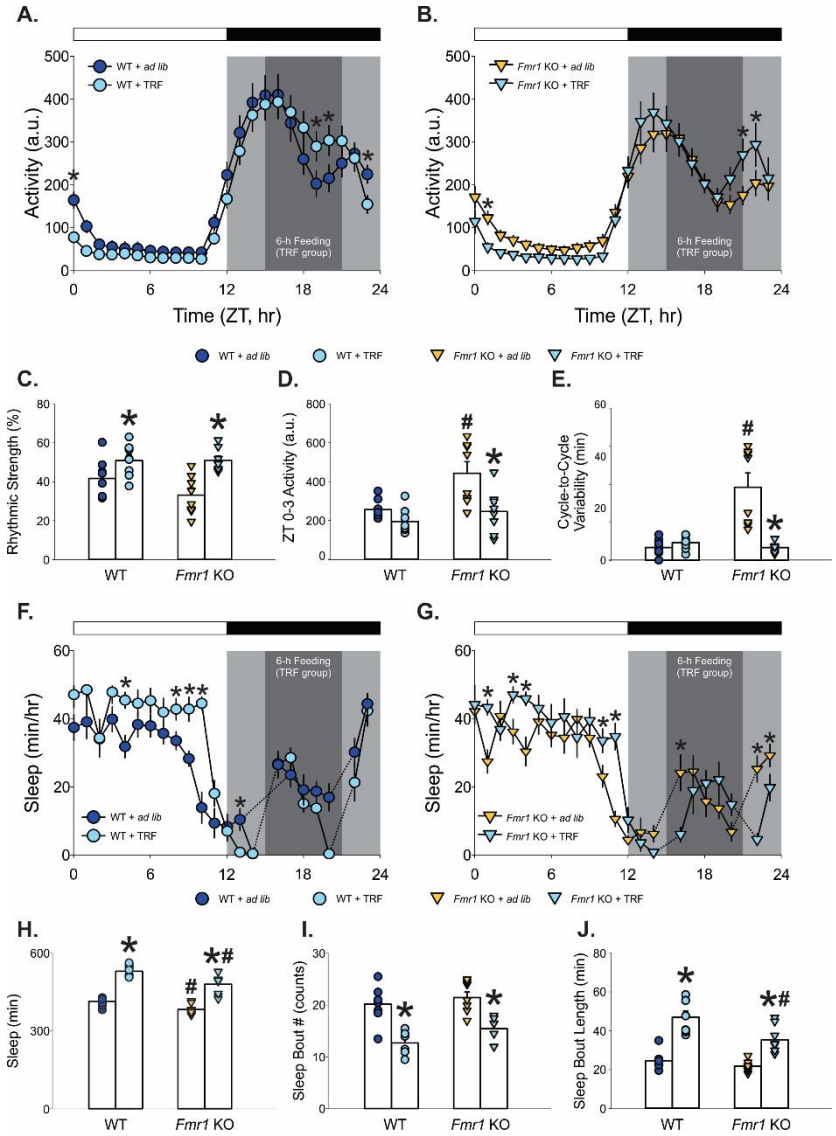

Fig. 4.6: The TRF intervention effective in the sleep/wake rhythms in the *Fmr1* KO mutants. (A, B) Waveforms of daily rhythms in cage activity in the WT (circle) and *Fmr1* KO (triangle) mice under the *ad lib* (empty) or the TRF (filled) feeding paradigms (n = 8/group). The activity waveform (1 hr bins) was analyzed using a 2-way ANOVA with time and the feeding treatments as factors followed by Holm-Sidak's multiple comparisons test. There were significant interactions between time and feeding treatment on the temporal of the locomotor activity rhythms found in the WT controls ($F = 1.68$, $P = 0.027$) and the *Fmr1* KO mutants ($F = 1.63$, $P = 0.036$). TRF reduces inappropriate activity at the beginning of the light phase and enhances the activity in the middle-late dark phase in both genotypes. **(C-E)** Measures of locomotor activity rhythms. **(F, G)** Waveforms of daily rhythms in the immobility-defined sleep. The sleep waveform (1 hr bins) was analyzed using a 2-way ANOVA with time and the feeding treatments as factors followed by Holm-Sidak's multiple comparisons test. There were significant interactions between time and feeding treatment on the temporal of the sleep behavior rhythms. **(H-J)** Measures of immobility-defined sleep in the light phase. The histograms were analyzed by the 2-way ANOVA on the effects of feeding treatment and genotype. $^{*}P < 0.05$ indicates the significant difference between the feeding treatments, and $^{\#}P < 0.05$ indicates the significant difference between the genotypes. Details are described in **Table 4.7**.

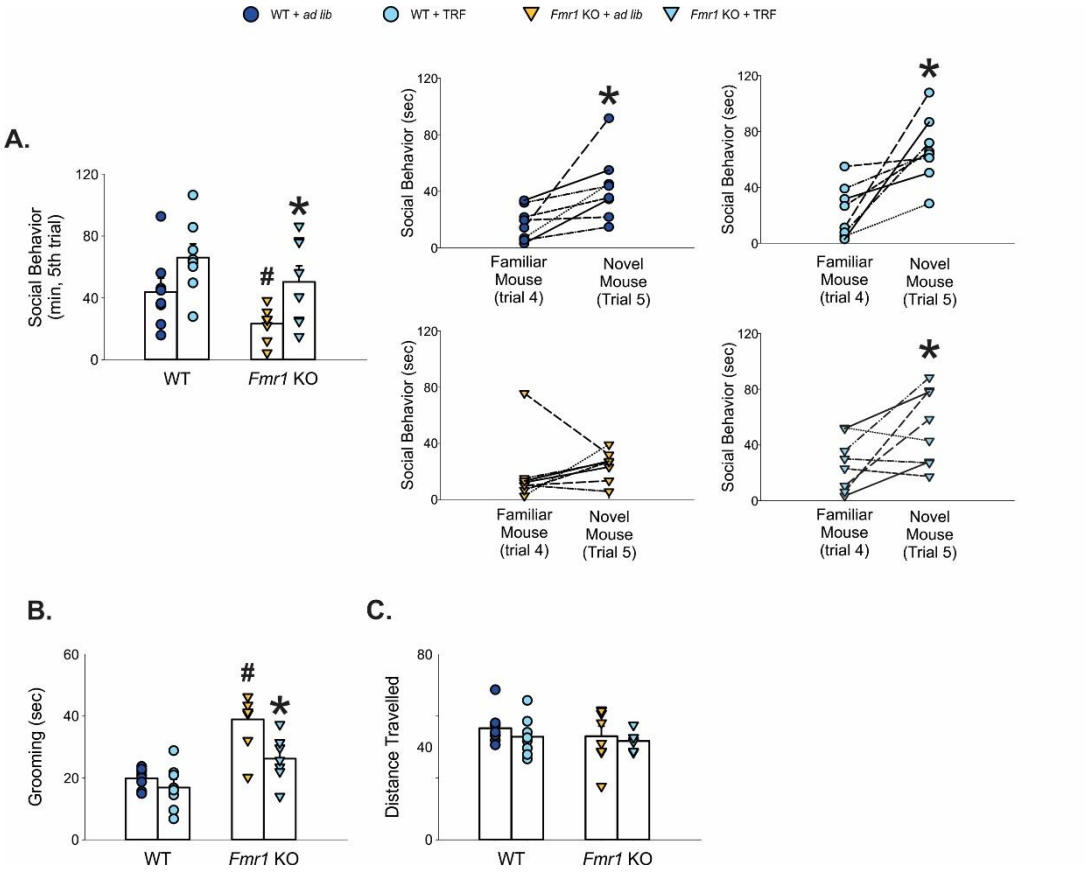

Fig. 4.7: TRF improved the social memory and the stereotypic grooming behavior in the *Fmr1* KO mutants. (A) The left panel shows the time spent in social behavior when the second novel stranger mouse was introduced to the testing mouse in the 5-trial social interaction test. The significant differences were analyzed by the 2-way ANOVA on the effects of feeding treatment and genotype. **P* < 0.05 indicates the significant difference between the feeding treatments, and $^{\#}P$ < 0.05 indicates the significant difference between the genotypes. The right panel shows the individual changes in their social interaction with the familiar mouse and the novel mouse in the 5-trial social interaction test (top: *ad lib*, bottom: TRF, left: WT controls, right: *Fmr1* KOs). The difference was determined using the paired *t*-test (**P* < 0.05, n=8/group). **(B)** The aberrant grooming behavior was corrected by the TRF treatment. The significant differences were analyzed by the 2-way ANOVA on the effects of feeding treatment and genotype (n=8/group). **P* < 0.05 indicates the significant difference between the feeding treatments, and $^{\#}P$ < 0.05 indicates the significant difference between the genotypes. **(C)** Distance travelled in the grooming test. TRF did not alter the overall locomotion in the treated mice. Details are described in **Table 4.8**.

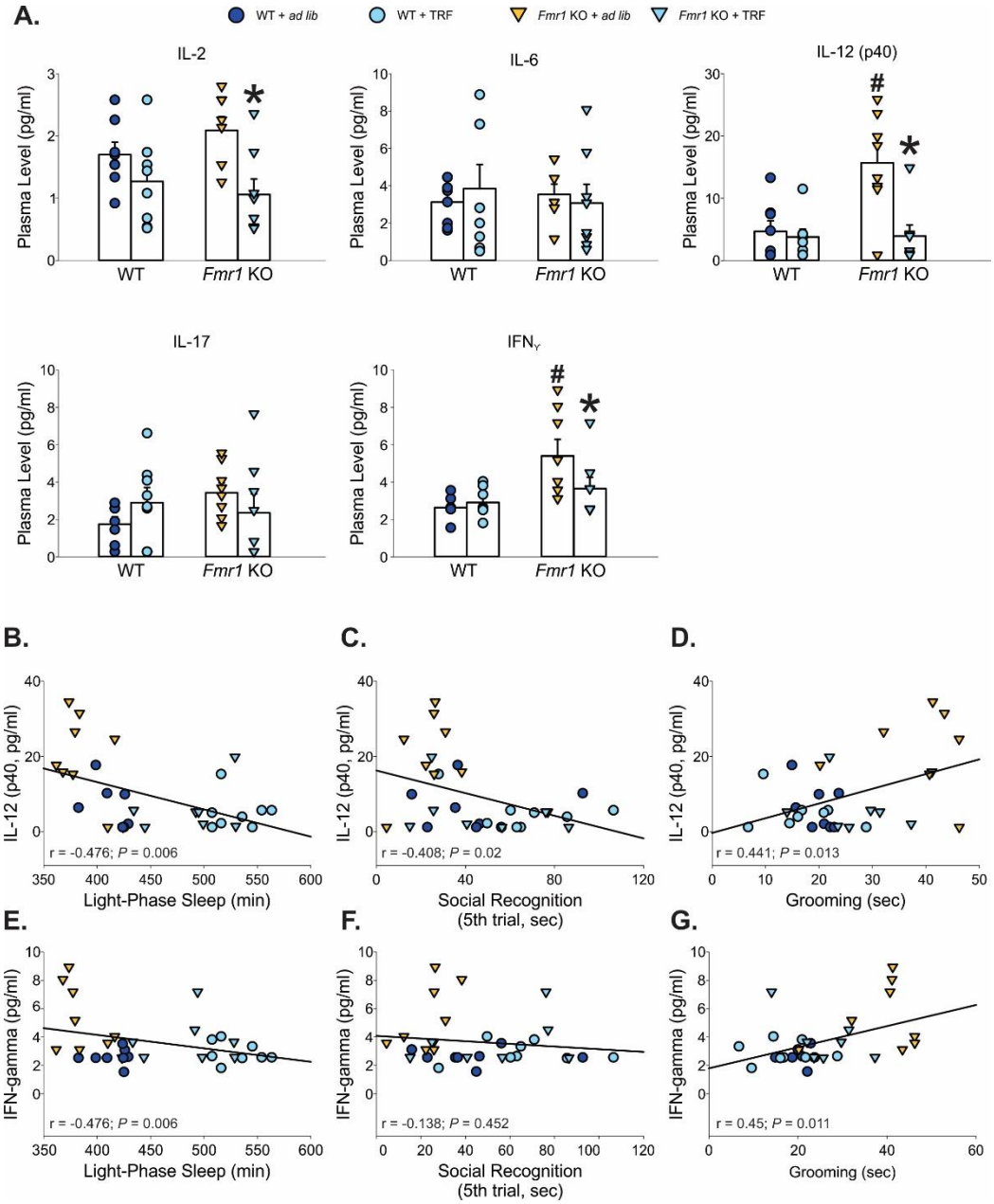

Fig. 4.8: The plasma levels of IL-12 and INF$_Y$ are associated with measures of sleep/wake rhythms as well as the autistic behaviors, and corrected by the TRF treatment in the *Fmr1* KO mutants. (A) Selected plasma pro-inflammatory markers are shown. The full list of assayed makers is reported in **Table 4.9** (n = 8/group). The significant differences were analyzed by the 2-way ANOVA on the effects of feeding treatment and genotype. *P < 0.05 indicates the significant difference between the feeding treatments, and $^{\#}P$ < 0.05 indicates the significant difference between the genotypes. **(B-G)** The correlations between IL-12/IFN-γ and sleep time, social recognition, and grooming behavior. Data were analyzed using the Pearson Correlation, and the coefficients are reported in **Table 4.10**.

Tables

Table 4.1 The sleep in the light phase were fragmented in the *Fmr1* KO mutants. Comparisons of sleep behavior in age-matched WT and *Fmr1* KO mice (n = 6/group). Values are shown as averages ± SEM. Data were analyzed with a 2-way ANOVA using genotype and treatment as factors. The Holm-Sidak test for multiple comparisons was used when appropriate. $^{*}P < 0.05$ indicates significant differences between *Fmr1* KO mutants and the controls. $^{\#}P < 0.05$ indicates significant differences between the light and dark phases.

	WT controls			***Fmr1* KO**			**2-way ANOVA**		
Measures	**24-hr cycle**	**Light Phase**	**Dark Phase**	**24-hr cycle**	**Light Phase**	**Dark Phase**	**Genotype**	**Time**	**Interaction**
Sleep Duration (min)	645.1 ± 30.2	463.6 ± 19.4$^{\#}$	181.5 ± 13.5	568.6 ± 29.8	**414.0 ± 14.8$^{*\#}$**	154.6 ± 17. 7	**$F_{(1,23)}$ = 6.37; *P* = 0.02**	**$F_{(1,23)}$ = 319.45; *P* < 0.001**	$F_{(1,23)}$ = 0.56; *P* = 0.46
Bout counts (#)	49.9 ± 2.7	24.4 ± 1.8	25.5 ± 2.1	50.3 ± 2.0	**29.6 ± 1.2$^{*\#}$**	20.7 ± 1.9	$F_{(1,23)}$ = 0.017; *P* = 0.9	**$F_{(1,23)}$ = 5.70; *P* = 0.027**	**$F_{(1,23)}$ = 9.33; *P* = 0.006**
Avg. Bout Length (min)	15.7 ± 1.1	22.4 ± 1.9$^{\#}$	9.0 ± 0.7	13.1 ± 0.6	**16.6 ± 0.8$^{*\#}$**	9.5 ± 0.6	**$F_{(1,23)}$ = 6.77; *P* = 0.017**	**$F_{(1,23)}$ = 100.86; *P* < 0.001**	**$F_{(1,23)}$ = 9.64; *P* = 0.006**
MAX Bout Length (min)	55.9 ± 3.8	81.3 ± 6.0$^{\#}$	30.5 ± 3.0	48.3 ± 2.7	**58 ± 3.09$^{*\#}$**	38. 7 ± 3.8	$F_{(1,23)}$ = 4.02; *P* = 0.059	**$F_{(1,23)}$ = 85.96; *P* < 0.001**	**$F_{(1,23)}$ = 17.33; *P* < 0.001**

Table 4.2. *Fmr1* KO mutants exhibited an altered temporal pattern of locomotor activity rhythms with abnormally more activity in the beginning of the light phase. The locomotor activity rhythms of *Fmr1* KO mutants and their WT controls at adult age in the standard 12 h:12 h LD cycles and constant darkness (DD) were monitored using the wheel running system (n = 6/group). Values are shown as averages ± SEM. All parameters passed the normality tests, and the results of student's *t*-tests are reported. Significant differences (*$P < 0.05$) are shown in bold.

	WT controls	***Fmr1* KO**	**Difference**	***P* value**
12:12 LD cycles				
Period (h)	24.0 ± 0.0	23.9 ± 0.1	-0.1	0.85
Power (% variance)	42.8 ± 1.7	**30.4 ± 3.8***	-12.4	**0.008**
Cage Activity (rev)	19874.8 ± 2197.1	24302.0 ± 4294.0	4427.2	0.34
Amplitude (rev)	2553.5 ± 246.3	2771.3 ± 406.4	217.8	0.63
Activity in the Light Phase (ZT 0-3, rev)	418.1 ± 50.7	**1099.2 ± 164.7***	681.2	**0.002**
Cycle-to-cycle variability (min)	8.1 ± 2.0	24.5 ± 10.6	16.4	0.39
Fragmentation (# bouts)	21.0 ± 0.6	24.2 ± 2.5	3.2	0.39
DD				
Tau (h)	23.6 ± 0.1	23.4 ± 0.2	0.1	0.38
Power (% variance)	47.4 ± 1.2	**39.1 ± 2.0***	-8.3	**0.003**
Cage Activity (rev)	27224.7 ± 1495.4	27914.0 ± 3216.7	1721.3	0.836
Onset variability (min)	16.3 ± 2.9	**42.5 ± 7.9***	26.2	**0.007**
Fragmentation (# bouts)	21.3 ± 1.2	24.1 ± 1.8	-2.8	0.187

Table 4.3. *Fmr1* KO mutants showed difficulty in entraining to the 2-light pulse skeleton photoperiod. The locomotor activity rhythms of *Fmr1* KO mutants and their WT controls under the skeleton photoperiod were monitored using the wheel running system (n = 8/group). Values are shown as averages ± SEM. All parameters passed the normality tests, and the results of student's *t*-tests are reported. Significant differences (**P* < 0.05) are shown in bold.

	WT controls	***Fmr1* KO**	**Difference**	***P* value**
Period (h)	24.0 ± 0.0	**23.7 ± 0.2***	-0.3	**0.021**
Power (% variance)	39.4 ± 2.0	**24.0 ± 1.8***	-15.4	**< 0.001**
Cage Activity (rev)	21710.6 ± 1662.1	25257.3 ± 2953.8	3546.7	0.28
Activity in the subject day (rev)	5.29 ± 1.5	**34.7 ± 6.0***	29.4	**< 0.001**
Onset variability (min)	18.1 ± 2.8	**59.5 ± 9.1***	41.5	**< 0.001**
Fragmentation (# bouts)	20.9 ± 0.2	24.3 ± 1.7	3.4	0.19

Table 4.4. Fmr1 KO mutants exhibited deficits in social discrimination. Comparisons of social discrimination behavior in age-matched WT and *Fmr1* KO mice (n = 8/group) were assessed using the 3-chamber test and the 5-trial social interaction test. In the second stage of the 3-chamber test, the testing mouse was given the choice between a chamber with a familiar mouse and another chamber with a novel mouse. Time spent in the chambers was tracked by the AnyMaze software and the social discrimination was assessed by the fold change between the two chambers [(novel chamber - familiar chamber)/ familiar chamber *100%]. In the 5-trial social test, the social behavior with the familiar mouse (trial 1-4) and the novel stranger mouse (trial 5) was recorded and scored. All parameters passed the normality tests, and the results of student's *t*-tests are reported. Significant differences (**P* < 0.05) are shown in bold.

	WT controls	***Fmr1* KO**	**Difference**	***P* value**
Social Recognition in the 3-chamber test (the 2nd test stage)				
Familiar-mouse chamber (sec)	143.4 ± 11.2	**172.6 ± 1.7***	29.2	**0.028**
Novel-mouse chamber (sec)	222.8 ± 13.5	209.5 ± 14.2	-13.3	0.48
Fold change between chambers (%)	61.3 ± 16.0	**21.8 ± 9.2***	-39.5	**0.038**
5-trial social recognition test				
Familiar mouse (trial 1-4, sec)	154.4 ± 16.4	150.4 ± 22.4	-4.0	0.88
Novel mouse (trial 5, sec)	46.8 ± 3.0	**25.9 ± 5.1***	-20.8	**0.002**

Table 4.5. *Fmr1* KO mutants exhibited robust repetitive behavior. The repetitive digging, burying and grooming behavior in the *Fmr1* KO mutants and their WT controls (n = 14/genotype) were assessed in the marble bury test and the grooming test. Values are shown as averages ± SEM. All parameters passed the normality tests, and the results of student's *t*-tests are reported. Significant differences (**P* < 0.05) are shown in bold.

	WT controls	***Fmr1* KO**	**Difference**	***P* value**
Marble Bury Test				
Digging in total of 30 mins (sec)	19.8 ± 4.2	**105.8 ± 28.0***	86.0	**0.02**
Buried Marbles (%)	19.6 ± 6.1	**45.8 ± 8.6***	25.9	**0.017**
Distance Travelled (m)	49.1 ± 3.5	**63.9 ± 2.7***	14.9	**0.0017**
Grooming Test				
Grooming (sec)	25.5 ± 2.3	**54.4 ± 4.3***	28.9	**< 0.001**
Distance Travelled (m)	67.7 ± 2.6	**78.0 ± 2.4***	10.3	**0.0061**

Table 4.6. Sleep disturbances were associated with the impairment of social recognition and the severity of repetitive behavior. A cohort of age-matched WT and *Fmr1* KO mice were housed under standard LD cycles and tested for the associations. Data from both genotypes were pooled (for a greater statistical power, n = 6/genotype) and the Pearson Correlation was applied. Based on our finding that the most prominent sleep phenotypes were observed in their light-phase sleep, measures from the light-phase sleep were used here. The correlation coefficients are reported and $P < 0.05$ was considered significant. The significant correlation coefficients are shown in bold and labeled with *.

	3-chamber social test (2^{nd} stage, chamber fold change)	Social recognition (trial 5, sec)	Digging (sec)	Marble Buried (%)	Grooming (sec)
Rhythmic Strength (V%)	0.18	0.43	0.13	-0.051	**-0.62***
Activity in the Light Phase (ZT 0-3)	-0.4	-0.013	**0.64***	0.58	0.35
Onset variability (min)	-0.37	-0.4	0.23	**0.61***	**0.63***
Sleep (min)	0.47	**0.86***	-0.3	-0.52	**-0.8***
Sleep Bout Counts (#)	-0.39	-0.53	0.27	**0.78***	**0.7***
Avg. Sleep Bout Length (min)	0.44	**0.59***	-0.29	**-0.71***	**-0.75***
MAX Sleep Bout Length (min)	0.49	**0.76***	-0.4	**-0.65***	**-0.78***

Table 4.7. TRF improved the sleep/wake cycles in the *Fmr1* KO mutants. The locomotor activity rhythms and the immobility-defined sleep of *Fmr1* KO mutants and their WT controls under ad lib or TRF conditions (n = 8/genotype/treatment). Based on our finding that the most prominent sleep phenotypes were observed in their light-phase sleep,and considering that the sleep recordings were paused for food adding/removal in the dark phase, we decided to focus on effects of TRF on the light-phase sleep. In other words, the sleep time, sleep bout counts, and bout length were derived from their sleep in the light phase. Values are shown as averages ± SEM. Data were analyzed with 2-way ANOVA using genotype and treatment as factors. The Holm-Sidak test for multiple comparisons was used when appropriate. $^{*}P < 0.05$ indicates significant differences between *ad lib* and TRF treatments. $^{\#}P < 0.05$ indicates significant differences between WT controls and *Fmr1* KO mice.

	WT		***Fmr1* KO**		**2-way ANOVA**		
Measures	***Ad Lib***	**TRF**	***Ad Lib***	**TRF**	**Genotype**	**Treatment**	**Interaction**
Period (hr)	24.0 ± 0.0	24.0 ± 0.0	24.1 ± 0.1	24.0 ± 0.0	$F_{(1, 31)} = 0.12$; $P = 0.73$	$F_{(1, 31)} = 0.32$; $P = 0.58$	$F_{(1, 31)} = 0.6$; $P = 0.44$
Power (% variance)	41.8 ± 3.8	**50.9 ± 3.1***	33.2 ± 3.8	**51.1 ± 2.2***	$F_{(1, 31)} = 1.9$; $P = 0.18$	**$F_{(1, 31)} = 19.41$; $P < 0.001$**	$F_{(1, 31)} = 2.04$; $P = 0.17$
Cage Activity (a.u.)	4306.7 ± 517.4	4063.7 ± 395.6	3747.9 ± 402.1	3750.1 ± 471.4	$F_{(1, 31)} = 1.08$; $P = 0.31$	$F_{(1, 31)} = 0.082$; $P = 0.78$	$F_{(1, 31)} = 0.085$; $P = 0.77$
Amplitude (a.u.)	391.6 ± 38.4	370.6 ± 37.5	300.4 ± 35.2	353.7 ± 38.8	$F_{(1, 31)} = 2.37$; $P = 0.14$	$F_{(1, 31)} = 0.21$; $P = 0.65$	$F_{(1, 31)} = 1.12$; $P = 0.3$
Light-Phase Activity (ZT 0-3, a.u.)	255.3 ± 18.9	194.3 ± 24.3	443.1 ± 59.6$^{\#}$	**245.9 ± 42.0***	**$F_{(1, 31)} = 10.44$; $P = 0.03$**	**$F_{(1, 31)} = 12.14$; $P = 0.002$**	$F_{(1, 31)} = 3.38$; $P = 0.07$
Onset variability (min)	6.8 ± 1.6	9.4 ± 1.3	38.5 ± 7.5$^{\#}$	**6.8 ± 0.9***	$F_{(1, 31)} = 15.58$; $P < 0.001$	$F_{(1, 31)} = 15.70$; $P < 0.001$	**$F_{(1, 31)} = 21.68$; $P < 0.001$**
Fragmentation (# bouts)	29.3 ± 1.7	**23.4 ± 1.0***	29.5 ± 1.8	**23.4 ± 1.1***	$F_{(1, 31)} = 0.11$; $P = 0.74$	**$F_{(1, 31)} = 21.91$; $P < 0.001$**	$F_{(1, 31)} = 0.23$; $P = 0.64$
Sleep (min)	414.9 ± 6.3	**524.5 ± 11.9***	383.7 ± 7.4$^{\#}$	**481.0 ± 15.7*$^{\#}$**	**$F_{(1, 31)} = 18.35$; $P < 0.001$**	**$F_{(1, 31)} = 127.19$; $P < 0.001$**	$F_{(1, 31)} = 0.96$; $P = 0.34$
Bout counts (#)	20.2 ± 1.3	**12.7 ± 0.8***	21.4 ± 1.1	**15.4 ± 0.9***	$F_{(1, 31)} = 4.21$; $P = 0.05$	**$F_{(1, 31)} = 47.94$; $P < 0.001$**	$F_{(1, 31)} = 0.59$; $P = 0.45$
Avg. Bout Length (min)	24.6 ± 1.7	**47.0 ± 3.2***	21.7 ± 1.04	**35.3 ± 2.7*$^{\#}$**	**$F_{(1, 31)} = 11.04$; $P = 0.002$**	**$F_{(1, 31)} = 68.3$; $P < 0.001$**	$F_{(1, 31)} = 4.03$; $P = 0.055$
MAX Bout Length (min)	96.4 ± 4.3	**136.6 ± 3.3***	88.3 ± 3.1	**108.4 ± 4.7*$^{\#}$**	**$F_{(1, 31)} = 25.03$; $P < 0.001$**	**$F_{(1, 31)} = 68.76$; $P < 0.001$**	**$F_{(1, 31)} = 7.64$; $P = 0.01$**

Table 4.8. TRF improved the social recognition memory and stereotypic grooming behavior in the *Fmr1* KO mutants. The active social behavior assessed in the 5-trial social test and the grooming behavior assessed in the grooming test of *Fmr1* KO mutants and their WT controls under ad lib or TRF conditions (n=8/genotype/treatment). Values are shown as averages ± SEM. Data were analyzed with 2xANOVA using genotype and treatment as factors. The Holm-Sidak test for multiple comparisons was used when appropriate. $^{*}P < 0.05$ indicates significant differences between *ad lib* and TRF treatments. $^{\#}P < 0.05$ indicates significant differences between WT controls and *Fmr1* KO mice.

Measures	**WT**		***Fmr1* KO**		**2-way ANOVA**		
	Ad Lib	**TRF**	***Ad Lib***	**TRF**	**Genotype**	**Treatment**	**Interaction**
Familiar mouse (trial 1-4, sec)	80.5 ± 12.3	96.5 ± 14.4	67.5 ± 4.7	95.8 ± 14.7	$F_{(1, 31)} = 0.36$; $P = 0.55$	$F_{(1, 31)} = 3.77$; $P = 0.062$	$F_{(1, 31)} = 0.29$; $P = 0.59$
Novel mouse (trial 5, sec)	43.8 ± 8.9	66.1 ± 8.8	23.3 ± 4.0$^{\#}$	**50.3 ± 10.4***	**$F_{(1, 31)} = 5.37$; $P = 0.028$**	**$F_{(1, 31)} = 9.88$; $P = 0.004$**	$F_{(1, 31)} = 0.092$; $P = 0.76$
Grooming (sec)	19.9 ± 1.2	16.9 ± 2.7	38.9 ± 3.3$^{\#}$	**26.2 ± 3.1$^{*\#}$**	**$F_{(1, 31)} = 35.05$; $P < 0.001$**	**$F_{(1, 31)} = 10.66$; $P = 0.003$**	$F_{(1, 31)} = 4.1$; $P = 0.053$
Distance Travelled (m)	72.2 ± 4.2	66.6 ± 4.7	67.0 ± 6.6	63.2 ± 2.2	$F_{(1, 31)} = 0.98$; $P = 0.33$	$F_{(1, 31)} = 1.14$; $P = 0.3$	$F_{(1, 31)} = 0.039$; $P = 0.85$

Table 4.9. TRF alters the plasma cytokine in the *Fmr1* KO mutants and their WT controls. The level of plasma cytokines in the *Fmr1* KO mutants and their WT controls under ad lib or TRF conditions (n = 8/genotype/treatment). Values are shown as averages ± SEM. Data were analyzed with 2xANOVA using genotype and treatment as factors. The Holm-Sidak test for multiple comparisons was used when appropriate. $^{*}P < 0.05$ indicates significant differences between *ad lib* and TRF treatments. $^{\#}P < 0.05$ indicates significant differences between WT controls and *Fmr1* KO mice.

	WT		***Fmr1* KO**		**2-way ANOVA**		
Measures	***Ad Lib***	**TRF**	***Ad Lib***	**TRF**	**Genotype**	**Treatment**	**Interaction**
TNFα	4.1 ± 1.0	2.6 ± 0.8	3.9 ± 0.6	2.5 ± 1.0	$F_{(1, 31)} = 0.03$; $P = 0.86$	$F_{(1, 31)} = 3.42$; $P = 0.075$	$F_{(1, 31)} = 0.009$; $P = 0.93$
IL-2	1.7 ± 0.2	1.3 ± 0.3	2.1 ± 0.2	**1.1 ± 0.3***	$F_{(1, 31)} = 0.16$; $P = 0.69$	**$F_{(1, 31)} = 11.14$; $P = 0.002$**	$F_{(1, 31)} = 1.83$; $P = 0.19$
IL-3	0.9 ± 0.1	0.7 ± 0.1	1.0 ± 0.1	0.8 ± 0.2	$F_{(1, 31)} = 0.32$; $P = 0.58$	$F_{(1, 31)} = 1.51$; $P = 0.23$	$F_{(1, 31)} < 0.001$; $P = 0.98$
IL-5	14.1 ± 2.1	**5.9 ± 1.1***	12.4 ± 1.3	8.9 ± 1.9	$F_{(1, 31)} = 0.17$; $P = 0.68$	**$F_{(1, 31)} = 14.35$; $P < 0.001$**	$F_{(1, 31)} = 2.34$; $P = 0.14$
IL-6	3.1 ± 0.5	3.9 ± 1.3	3.5 ± 0.6	3.1 ± 1.0	$F_{(1, 31)} = 0.046$; $P = 0.83$	$F_{(1, 31)} = 0.023$; $P = 0.88$	$F_{(1, 31)} = 0.5$; $P = 0.49$
IL-10	4.8 ± 1.4	3.9 ± 1.5	3.4 ± 0.9	3.9 ± 1.9	$F_{(1, 31)} = 0.24$; $P = 0.63$	$F_{(1, 31)} = 0.027$; $P = 0.87$	$F_{(1, 31)} = 0.25$; $P = 0.63$
IL-12 (p40)	6.2 ± 2.3	5.0 ± 1.7	20.9 ± 4.0$^{\#}$	**5.2 ± 2.4***	**$F_{(1, 31)} = 8.44$; $P = 0.007$**	**$F_{(1, 31)} = 10.85$; $P = 0.003$**	**$F_{(1, 31)} = 7.97$; $P = 0.009$**
IL-15	40.2 ± 8.0	62.4 ± 25.5	49.7 ± 16.4	48.9 ± 14.4	$F_{(1, 31)} = 0.016$; $P = 0.9$	$F_{(1, 31)} = 0.44$; $P = 0.51$	$F_{(1, 31)} = 0.51$; $P = 0.48$
IL-17	1.8 ± 0.4	2.9 ± 0.8	3.4 ± 0.5	2.4 ± 1.0	$F_{(1, 31)} = 0.66$; $P = 0.42$	$F_{(1, 31)} = 0.0026$; $P = 0.96$	$F_{(1, 31)} = 2.61$; $P = 0.12$
CCL-2	17.9 ± 4.6	12.3 ± 4.8	9.3 ± 1.6	11.2 ± 5.4	$F_{(1, 31)} = 1.42$; $P = 0.24$	$F_{(1, 31)} = 0.22$; $P = 0.64$	$F_{(1, 31)} = 0.87$; $P = 0.36$
CCL-5	7.1 ± 0.6	6.0 ± 1.2	7.23 ± 1.2	5.4 ± 0.9	$F_{(1, 31)} = 0.05$; $P = 0.82$	$F_{(1, 31)} = 2.56$; $P = 0.12$	$F_{(1, 31)} = 0.11$; $P = 0.74$
IFN-γ	2.6 ± 0.2	2.9 ± 0.3	5.4 ± 0.9$^{\#}$	**3.7 ± 0.6***	**$F_{(1, 31)} = 10.97$; $P = 0.03$**	$F_{(1, 31)} = 1.96$; $P = 0.17$	$F_{(1, 31)} = 3.66$; $P = 0.066$
CXCL-1	105.6 ± 17.5	91.0 ± 33.3	83.9 ± 14	90.3 ± 20.2	$F_{(1, 31)} = 0.28$; $P = 0.6$	$F_{(1, 31)} = 0.038$; $P = 0.85$	$F_{(1, 31)} = 0.25$; $P = 0.62$
CXCL-5	368.4 ± 103.9	357.1 ± 155.5	346.6 ± 25.4	181.2 ± 48.4	$F_{(1, 31)} = 0.67$; $P = 0.42$	$F_{(1, 31)} = 0.017$; $P = 0.9$	$F_{(1, 31)} = 0.003$; $P = 0.96$
CXCL-9	207.4 ± 54.3	225.9 ± 53.9	346.6 ± 25.4$^{\#}$	**181.2 ± 48.4***	$F_{(1, 31)} = 1.15$; $P = 0.29$	$F_{(1, 31)} = 2.79$; $P = 0.11$	**$F_{(1, 31)} = 4.37$; $P = 0.046$**

Table 4.10. Plasma levels of IL-12 (p40) and IFN were associated with the level of sleep disturbances and the severity of autistic behavior. Data from Table 7, 8 and 9 were analyzed for determining the correlations. All 4 groups (WT + ad lib, WT + TRF, *Fmr1* KO + ad lib, *Fmr1* KO + TRF) were pooled and the Pearson Correlation was applied. The correlation coefficients are reported and *p*-value below 0.05 was considered significant. The significant correlation coefficients are shown in bold and labeled with *.

Measures	IL-12 (p40, pg/ml)	IFN-γ (pg/ml)	CXCL-9 (pg/ml)
Rhythmic Strength (V%)	-0.34	-0.15	0.072
Activity in the Light Phase (ZT 0-3, a.u.)	**0.73***	**0.59***	0.58
Onset variability (min)	**0.19***	0.69	0.01
Sleep (min)	**-0.48***	**-0.48***	0.34
Sleep Bout Counts (#)	0.26	0.16	-0.16
Avg. Sleep Bout Length (min)	**-0.36***	-0.24	0.25
MAX Sleep Bout Length (min)	**-0.38***	**-0.42***	0.34
Social recognition (trial 5, sec)	**-0.41***	-0.14	0.34
Repetitive Behavior (grooming, sec)	**0.44***	**0.45***	0.26

Reference

Abel, Emily A., et al. "Sleep and challenging behaviors in the context of intensive behavioral intervention for children with autism." Journal of autism and developmental disorders 48.11 (2018): 3871-3884.

Abdul, Fazal, et al. "Disruption of circadian rhythm and risk of autism spectrum disorder: role of immune-inflammatory, oxidative stress, metabolic and neurotransmitter pathways." Reviews in the Neurosciences (2021).

Angelakos CC, Tudor JC, Ferri SL, Jongens TA, Abel T (2019). Home-cage hypoactivity in mouse genetic models of autism spectrum disorder. Neurobiol Learn Mem 165, 107000. doi:10.1016/j.nlm.2019.02.010.

Ashwood, Paul, et al. "Plasma cytokine profiles in Fragile X subjects: is there a role for cytokines in the pathogenesis?." Brain, behavior, and immunity 24.6 (2010): 898-902.

Arsenault, Jason, et al. "FMRP expression levels in mouse central nervous system neurons determine behavioral phenotype." Human gene therapy 27.12 (2016): 982-996.

Bertrand, Marylène, et al. "NMR metabolomic analysis: an aid to understanding neuroinflammatory processes in nociceptive defects of Fmr1 KO mice, model of Fragile X syndrome." 14èmes journées scientifiques RFMF. 2021.

Bisdounis, Lampros, et al. "Psychological and behavioural interventions in bipolar disorder that target sleep and circadian rhythms: a systematic review of randomised controlled trials." Neuroscience & Biobehavioral Reviews 132 (2022): 378-390.

Bonasera SJ, Chaudoin TR, Goulding EH, Mittek M, Dunaevsky A. Decreased home cage movement and oromotor impairments in adult Fmr1-KO mice. Genes Brain Behav. 2017 16(5):564-573. doi: 10.1111/gbb.12374.

Brown, L. A., Fisk, A. S., Pothecary, C. A., & Peirson, S. N. (2019). Telling the Time with a Broken Clock: Quantifying Circadian Disruption in Animal Models. Biology (Basel) 8(1), 18. doi:10.3390/biology8010018

Budimirovic, Dejan B., et al. "Sleep problems in fragile X syndrome: Cross-sectional analysis of a large clinic-based cohort." American Journal of Medical Genetics Part A 188.4 (2022): 1029-1039.

Careaga, Milo, et al. "Group I metabotropic glutamate receptor mediated dynamic immune dysfunction in children with fragile X syndrome." Journal of neuroinflammation 11.1 (2014): 1-10.

Casavi, Vizayieno, et al. "Relationship of quality of sleep with cognitive performance and emotional maturity among adolescents." Clinical Epidemiology and Global Health (2022): 100958.

Cheng, Wai-Yin, et al. "Circadian disruption-induced metabolic syndrome in mice is ameliorated by oat β-glucan mediated by gut microbiota." Carbohydrate Polymers 267 (2021): 118216.

Colwell CS, Michel S. Sleep and circadian rhythms: do sleep centers talk back to the clock? Nat Neurosci. 2003 Oct;6(10):1005-6. doi: 10.1038/nn1003-1005. PMID: 14513032; PMCID: PMC2573023.

Cohen, Simonne, et al. "Sleep patterns predictive of daytime challenging behavior in individuals with low-functioning autism." Autism Research 11.2 (2018): 391-403.

Cristiano, Claudia, et al. "Behavioral, Anti-Inflammatory, and Neuroprotective Effects of a Novel FPR2 Agonist in Two Mouse Models of Autism." Pharmaceuticals 15.2 (2022): 161.

Dias, Caroline M., et al. "Glial dysregulation in human brain in Fragile X-related disorders." bioRxiv (2022).

El-Ansary, Afaf, and Laila Al-Ayadhi. "GABAergic/glutamatergic imbalance relative to excessive neuroinflammation in autism spectrum disorders." Journal of neuroinflammation 11.1 (2014): 1-9.

Fallah, Hamid, et al. "IFNG/IFNG-AS1 expression level balance: implications for autism spectrum disorder." Metabolic Brain Disease 35.2 (2020): 327-333.

Gao, Ying, et al. "Beneficial effects of time-restricted feeding on gentamicin cytotoxicity in mouse cochlea and vestibular organs." Laryngoscope investigative otolaryngology 7.2 (2022): 530-539.

Goo, Nayeon, et al. "The effect of fecal microbiota transplantation on autistic-like behaviors in Fmr1 KO mice." Life Sciences 262 (2020): 118497.

Gupta, Charlotte C., et al. "A Time to Rest, A Time to Dine: Sleep, Time-Restricted Eating, and Cardiometabolic Health." Nutrients 14.3 (2022): 420.

Hodges, Samantha L., et al. "Adult Fmr1 knockout mice present with deficiencies in hippocampal IL-6 and TNFα expression." Neuroreport 28.18 (2017): 1246.

Hodges, Samantha L., et al. "Lipopolysaccharide-induced inflammation leads to acute elevations in pro-inflammatory cytokine expression in a mouse model of Fragile X syndrome." Physiology & Behavior 215 (2020): 112776.

Johnson, Dayna A., et al. "Understanding the determinants of circadian health disparities and cardiovascular disease." Chronobiology international (2021): 1-8.

Kazdoba, Tatiana M., et al. "Modeling fragile X syndrome in the Fmr1 knockout mouse." Intractable & rare diseases research 3.4 (2014): 118-133.

Kronk, Rebecca, Ronald Dahl, and Robert Noll. "Caregiver reports of sleep problems on a convenience sample of children with fragile X syndrome." American journal on intellectual and developmental disabilities 114.6 (2009): 383-392.

Kronk, Rebecca, et al. "Prevalence, nature, and correlates of sleep problems among children with fragile X syndrome based on a large scale parent survey." Sleep 33.5 (2010): 679-687.

Kute, Preeti Madhav, et al. "NMDAR mediated translation at the synapse is regulated by MOV10 and FMRP." Molecular brain 12.1 (2019): 1-14.

Lee FY, Wang HB, Hitchcock ON, Loh DH, Whittaker DS, Kim YS, Aiken A, Kokikian C, Dell'Angelica EC, Colwell CS, Ghiani CA. Sleep/Wake Disruption in a Mouse Model of BLOC-1 Deficiency. Front Neurosci. 2018 Nov 15;12:759. doi: 10.3389/fnins.2018.00759. PMID: 30498428; PMCID: PMC6249416.

Loh DH, Kuljis DA, Azuma L, Wu Y, Truong D, Wang HB, Colwell CS. Disrupted reproduction, estrous cycle, and circadian rhythms in female mice deficient in vasoactive intestinal peptide. J Biol Rhythms. 2014 Oct;29(5):355-69. doi: 10.1177/0748730414549767. Epub 2014 Sep 24. PMID: 25252712; PMCID: PMC4353614.

Long, Hong, and Satchidananda Panda. "Time-restricted feeding and circadian autophagy for long life." Nature Reviews Endocrinology 18.1 (2022): 5-6.

Malow, Beth A., et al. "Parent-based sleep education for children with autism spectrum disorders." Journal of autism and developmental disorders 44.1 (2014): 216-228.

Manoogian, Emily NC, et al. "Time-restricted eating for the prevention and management of metabolic diseases." Endocrine reviews 43.2 (2022): 405-436.

Matta, Samantha M., Elisa L. Hill-Yardin, and Peter J. Crack. "The influence of neuroinflammation in Autism Spectrum Disorder." Brain, behavior, and immunity 79 (2019): 75-90.

Mineur, Yann S., Linh X. Huynh, and Wim E. Crusio. "Social behavior deficits in the Fmr1 mutant mouse." Behavioural brain research 168.1 (2006): 172-175.

Nelson, Kathy L., Jean E. Davis, and Cynthia F. Corbett. "Sleep quality: An evolutionary concept analysis." Nursing Forum. Vol. 57. No. 1. 2022.

Pacey, Laura KK, et al. "Persistent astrocyte activation in the fragile X mouse cerebellum." Brain and behavior 5.10 (2015): e00400.

Pandi-Perumal, Seithikurippu R., et al. "Timing is everything: circadian rhythms and their role in the control of sleep." Frontiers in neuroendocrinology (2022): 100978.

Park, Gaeun, et al. "Decreased in vivo glutamate/GABA ratio correlates with the social behavior deficit in a mouse model of autism spectrum disorder." Molecular brain 15.1 (2022): 1-12.

Parente, Martina, et al. "Brain Cholesterol Biosynthetic Pathway Is Altered in a Preclinical Model of Fragile X Syndrome." International journal of molecular sciences 23.6 (2022): 3408.

Petroni, Valeria, et al. "Autistic-like behavioral effects of prenatal stress in juvenile Fmr1 mice: the relevance of sex differences and gene–environment interactions." Scientific Reports 12.1 (2022): 1-12.

Protic, Dragana D., et al. "Fragile X Syndrome: From Molecular Aspect to Clinical Treatment." International journal of molecular sciences 23.4 (2022): 1935.

Reynolds, Kathryn E., Victoria Krasovska, and Angela L. Scott. "Converging purinergic and immune signaling pathways drive IL-6 secretion by Fragile X cortical astrocytes via STAT3." Journal of Neuroimmunology 361 (2021): 577745.

Robinson-Agramonte, Maria de los Angeles, et al. "Immune Dysregulation in Autism Spectrum Disorder: What Do We Know about It?." International Journal of Molecular Sciences 23.6 (2022): 3033.

Sadikova, Eleonora, Kristen Dovgan, and Micah O. Mazurek. "Longitudinal Examination of Sleep Problems and Symptom Severity in Children with Autism Spectrum Disorder." Journal of Autism and Developmental Disorders (2022): 1-9.

Saré RM, Harkless L, Levine M, Torossian A, Sheeler CA, Smith CB. Deficient Sleep in Mouse Models of Fragile X Syndrome. Front Mol Neurosci. 2017 10:280. doi: 10.3389/fnmol.2017.00280

Schreck, Kimberly A., James A. Mulick, and Angela F. Smith. "Sleep problems as possible predictors of intensified symptoms of autism." Research in developmental disabilities 25.1 (2004): 57-66.

Siniscalco, Dario, et al. "Inflammation and neuro-immune dysregulations in autism spectrum disorders." Pharmaceuticals 11.2 (2018): 56.

Sørensen, Emilie M., et al. "Hyperactivity and lack of social discrimination in the adolescent Fmr1 knockout mouse." Behavioural pharmacology 26.8-9 (2015): 733-740.

Spencer, Corinne M., et al. "Modifying behavioral phenotypes in Fmr1KO mice: Genetic background differences reveal autistic-like responses." Autism research 4.1 (2011): 40-56.

Shi SQ, Johnson CH (2019). Circadian biology and sleep in monogenic neurological disorders and its potential application in drug discovery. Curr Opin Behav Sci 25, 23-30. doi:10.1016/j.cobeha.2018.06.006.

Sikora, Darryn M., et al. "The relationship between sleep problems and daytime behavior in children of different ages with autism spectrum disorders." Pediatrics 130.Supplement_2 (2012): S83-S90.

Small, Gary W., et al. "Brain health consequences of digital technology use." Dialogues in clinical neuroscience (2022).

Soden, Marta E., and Lu Chen. "Fragile X protein FMRP is required for homeostatic plasticity and regulation of synaptic strength by retinoic acid." Journal of Neuroscience 30.50 (2010): 16910-16921.

Takumi T, Tamada K, Hatanaka F, Nakai N, Bolton PF (2019). Behavioral neuroscience of autism. Neurosci Biobehav Rev. pii, S0149-7634(18)30372-5. doi:10.1016/j.neubiorev.2019.04.012.

Taylor, Matthew A., Kimberly A. Schreck, and James A. Mulick. "Sleep disruption as a correlate to cognitive and adaptive behavior problems in autism spectrum disorders." Research in developmental disabilities 33.5 (2012): 1408-1417.

Thomas AM, Bui N, Perkins JR, Yuva-Paylor LA, Paylor R. Group I metabotropic glutamate receptor antagonists alter select behaviors in a mouse model for fragile X syndrome. Psychopharmacology (Berl) 2012; 219:47 – 58.

Wang HB, Whittaker DS, Truong D, Mulji AK, Ghiani CA, Loh DH, Colwell CS. Blue light therapy improves circadian dysfunction as well as motor symptoms in two mouse models of Huntington's disease. Neurobiol Sleep Circadian Rhythms. 2017 Jan 20;2:39-52. doi: 10.1016/j.nbscr.2016.12.002. PMID: 31236494; PMCID: PMC6575206.

Van Dijck, Anke, et al. "Reduced serum levels of pro-inflammatory chemokines in fragile X syndrome." BMC neurology 20.1 (2020): 1-12.

Wang, Huei-Bin, et al. "Time-restricted feeding improves circadian dysfunction as well as motor symptoms in the Q175 mouse model of Huntington’s disease." Eneuro 5.1 (2018).

Whittaker DS, Loh DH, Wang HB, Tahara Y, Kuljis D, Cutler T, Ghiani CA, Shibata S, Block GD, Colwell CS. Circadian-based Treatment Strategy Effective in the BACHD Mouse Model of Huntington's Disease. J Biol Rhythms. 2018 Oct;33(5):535-554. doi: 10.1177/0748730418790401. Epub 2018 Aug 7. PMID: 30084274.

Wright, Barry, et al. "Melatonin versus placebo in children with autism spectrum conditions and severe sleep problems not amenable to behaviour management strategies: a randomised controlled crossover trial." Journal of autism and developmental disorders 41.2 (2011): 175-184.

Yavuz-Kodat, Enise, et al. "Disturbances of continuous sleep and circadian rhythms account for behavioral difficulties in children with autism spectrum disorder." Journal of Clinical Medicine 9.6 (2020): 1978.

Yrigollen, Carolyn M., and Beverly L. Davidson. "CRISPR to the Rescue: Advances in Gene Editing for the FMR1 Gene." Brain sciences 9.1 (2019): 17.

Yuskaitis, Christopher J., Eleonore Beurel, and Richard S. Jope. "Evidence of reactive astrocytes but not peripheral immune system activation in a mouse model of Fragile X syndrome." Biochimica et Biophysica Acta (BBA)-Molecular Basis of Disease 1802.11 (2010): 1006-1012.

Zalfa, Francesca, Tilmann Achsel, and Claudia Bagni. "mRNPs, polysomes or granules: FMRP in neuronal protein synthesis." Current opinion in neurobiology 16.3 (2006): 265-269.

Zhang J, Fang Z, Jud C, Vansteensel MJ, Kaasik K, Lee CC, Albrecht U, Tamanini F, Meijer JH, Oostra BA, Nelson DL. Fragile X-related proteins regulate mammalian circadian behavioral rhythms. Am J Hum Genet. 2008 Jul;83(1):43-52. doi: 10.1016/j.ajhg.2008.06.003.

Chapter 6

Chapter 6

Conclusion

Circadian rhythms are driven by an endogenous timing system that helps organisms adapt to their environment. In order to function adaptively, this timing system has evolved specialized sensory systems that enable the endogenous clock to synchronize to regular changes in the physical environment. From an evolutionary perspective, daily changes in lighting provide a predictable measure of time and organisms have adapted to use dawn and dusk as potent time givers (zeitgeber). However, the high prevalence of artificial lights and changes in lifestyle have been challenging this natural design. Although there are undoubtable benefits of illumination at night, a growing number of studies warns of the cost. Many of the findings of the research described in this dissertation demonstrate the health consequences in model organisms and specifically suggest that some populations may be particularly vulnerable to the costs of light at night.

Overall, our work supports the 2-hit hypothesis that the ASD risk gene (i.e. *Cntnap2* here) predispose the subjects (the first hit) and make them more susceptible to environmental disruption (i.e. DLaN, the second hit), leading to worse outcomes compared to the conspecifics without carrying ASD risk mutations. Using the *Cntnap2* KO mouse model of ASD, we demonstrated that the *Cntnap2* mutants showed vulnerabilities at many levels. At the molecular and cell levels, the mutants under DLaN showed stronger changes in their plasma immune profiles and microglia proliferation as well as morphology. At tissue levels, the *Per2*-driven bioluminescence rhythms were shifted and dampened in the SCN and hippocampus more in the mutants than in the WT controls. At behavioral levels, the *Cntnap2* mutants showed a higher vulnerability than the WT controls in at least the repetitive grooming behavior to the 2 weeks of DLaN disruption. The social impairment was more affected in mutants than the WT controls and the repetitive grooming behavior was even selectively evoked in the mutants but not in the WT controls. Together, our work provides clear evidence that there is

synergistic interplay between the *Cntnap2* mutation and circadian disruption. It should be noted that all mice tested in this dissertation research were at adult age (3-5 month of age). Although we did not test the 2-hit hypothesis in mice at adolescent or even younger ages, it is most likely that the genetic vulnerability to DLaN would be even more dominant given that a wealthy number of studies have demonstrated prominent impacts of environmental factors on ASD characteristics during early life stages (Wang et al., 2017; Imbriani et al., 2021). Another notable finding in our work is that we did not find sex as a third factor mediating the interaction between *Cntnap2* mutation and DLaN disruption. Sex differences in ASD diagnosis and severity of ASD characteristics suggest a female protective effect in ASD (Werling, 2016; Dickerson et al., 2017; Petroni et al., 2022). In addition, a recent study suggested sex as a third-hit and reported male-specific deficits in social behavior and gene expression in the *Cntnap2* KO offspring treated with the paradigm of maternal immune activation (Schaafsma et al., 2017). However, even though we found that female *Cntnap2* KO mutants had less pronounced social impairments and repetitive grooming behavior in the LD control environment, they were equally impacted by the DLaN to the male mutants. One possible hypothesis is that the unobserved female protecting effects may result from reduced estrogen levels or dysregulated estrogen receptors in the *Cntnap2* mouse lines. This hypothesis is supported by studies showing neuroprotective effects of estrogen (Hwang et al., 2020) and significant correlations between ASD and decreased estrogen receptor-β (Chakrabarti et al., 2009) and altered aromatase level (Sarachana et al., 2011). Future studies are needed to carefully test this hypothesis. Nevertheless, our work strongly suggests that avoiding the environmental second hit by maintaining a clean photic environment should be considered as part of the ASD disease management.

In addition, this dissertation research unravels a mechanistic pathway underlying the impact of DLaN. This line of research started with exploration of the sensory part of the pathway. A critical role for melanopsin (encoded by *OPN4*) is supported by multiple lines of literature and has been implicated in mediating photic effects on circadian rhythms and as well

as variety of other behaviors (Milleret al., 2006; LeGates et al., 2012; Milosavljevic et al., 2016; Maruani et al., 2022). We demonstrated the loss of melanopsin expressing ipRGCs in the *OPN4*$^{DTA/DTA}$ mutants prevented the effects of DLaN on diurnal activity rhythms as well as social and repetitive behavior. Next, the role of melanopsin inputs was further supported by clear differences in the impact of DLaN driven behavior outcomes in the WT controls and the *Cntnap2* mutants between the short and long wavelength-enriched DLaN with the same energy (0.02 W/m^2) and luminescence (10 lx). The primary difference between the two illuminations was the melanopic lx (short vs long wavelength-enriched lighting: 1:15). All the behavioral outputs were much less impacted by the long wavelength-enriched DLaN than the short wavelength-enriched DLaN. The melanopsin expression ipRGCs send a mon-synaptic connection to the SCN (Lucas et al., 2014; Sondereker et al., 2020), and desynchronized peripheral clocks due to disrupted SCN rhythms are associated with varieties of diseases (Roenneberg et al., 2016). We hypothesize that the effects of DLaN are mediated by the disruption in the SCN rhythms (see **Fig. 5.1**) although this has not been resolved in these experiments. Finally, we demonstrated dysregulated inflammation and evoked cyclooxygenase-2 (COX-2) signaling were the downstream pathway connecting circadian disruption and affected ASD behavior. At the plasma level, our investigation suggested imbalanced Th1/Th2 signaling and the dysregulated Th17 cell pathway in testing mice under DLaN. Moreover, the dysregulated cytokines were significantly correlated to the social impairments and repetitive grooming behavior. In the prefrontal cortex, we found that DLaN evoked IL-6 level, a cytokine as well as a neuromodulator that may disrupt the glutamatergic/GABAergic balance (Paine et al., 2016; Wang et al., 2021). And when the COX-2 signaling was pharmacologically blocked by nonsteroidal anti-inflammatory carprofen treatment, the disrupting effects of DLaN on social impairments and repetitive grooming behavior were neutralized, along with reduction of IFN-γ and IL-6 in the prefrontal cortex. Importantly, DLaN-induced circadian disruptions on locomotor activity rhythms were not affected by the treatment of COX-2 inhibitor, suggesting that the beneficial effects of COX-2

inhibitor results from the action at the downstream of SCN outputs. Together, our work suggests a mechanistic pathway underlying DLaN impacts on ASD behavior **(Fig. 5.2)**:

Lights at night -> melanopsin (the photoreceptor) -> SCN (the master clock) disruption -> dysregulated inflammation and evoked COX-2 signaling -> exacerbated ASD behavior and disrupted sleep/wake cycles

The role of SCN and its causal relationship to DLaN-driven ASD behaviors was evaluated in a preliminary set of experiments. It is known that the SCN is one of the recipients of melanoptic inputs (Lucas et al., 2014; Sondereker et al., 2020), and we have shown that the molecular clocks in the SCN are shifted and dampened by the DLaN in the WT controls and the *Cntnap2* mutants using the Per2::Luc monitoring approach (Wang et al., 2020). Still, whether or not there is a causal relationship between the SCN disruption and the worsened ASD behavior under DLaN is still an open question. One way to test this hypothesis is to place mice under a special lighting condition in which their SCN rhythms are not disrupted even though the testing mice are exposed to nightly illumination. Under these conditions, if the test mice do not show impacted ASD behavior, it would support the hypothesis that the DLaN disrupts the ASD behavior through the SCN disruption. On the other hand, if the test mice still exhibit impacted ASD behavior without the SCN disruption, it would reject our hypothesis and suggest that there are direct effects of lights on ASD behavior independently from SCN regulations. This special condition can be achieved by placing the mice on T7 LD cycles. The T7 LD cycles are a photic environment that switches light and dark with a period of 3.5 hours [Period (T) = 7 hours] rather than the regular 12 hours (T = 24 hours). Circadian rhythms are not synchronized to this T7 cycle, and the activity rhythms free-run. And because of the free-running activity rhythms, the test mice are exposed to lights at all circadian phases including their subjective night. Moreover, prior research has demonstrated that, even though there are light exposures at subjective night, the SCN rhythms are not affected and remain comparable to the rhythms in the T24 standard LD cycles (LeGates et al., 2012; Moriya et al., 2015; Engeland et al., 2018). Therefore, we used the T7 LD cycle to test the causal link between the

SCN disruption and worsened ASD behavior. WT controls and *Cntnap2* mutants were distributed into three photic conditions for 2 weeks: the LD (T24) control group, the DLaN exposed LD (T24) positive control group, and the T7 test group. The social and grooming behavior were tested in the middle of their subjective night (ZT or CT 18). We found no difference in the social and grooming behavior between the T7 groups and the LD control groups while the two autistic behavior were negatively impacted by nighttime lights in our positive control group **(Fig. 5.1)**. This set of experiment suggests that SCN disruption is required for the worsened ASD behavior under DLaN.

In addition to the test of 2-hit hypothesis and the proposed of the mechanistic pathway underlying DLaN impacts on ASD behavior, our work in this dissertation research also suggests at least three circadian-based interventions helping ASD population. First of all, we showed that the timed supplement of melatonin was effective **(Chapter 2)**. It should be noted that the mouse strain used throughout the dissertation studies does not generate endogenous melatonin. This is due to the deficits in the synthesis pathway of melatonin in the C57 mouse strain (Ebihara et al., 1986); however, the M1 and M2 melatonin receptors are still expressed and functional. We demonstrated that nightly melatonin improved the sleep/wake cycles, and the grooming behavior was even returned to WT levels. However, such improvements were diminished if melatonin supplement was given in the day. Second, we demonstrated that shifting the spectral composition of light at night to longer wavelength was a good alternative **(Chapter 3)**. Compared with conspecifics under the short-wavelength enriched DLaN, the *Cntnap2* KO mutants under long-wavelength enriched DLaN showed 44% stronger circadian power, 61% greater rhythmic amplitude, 39% less daytime activity, and 13% smaller cycle-to-cycle variability in their sleep/wake cycle measurements, and 13% more social behavior as well as 28% reduced repetitive grooming behavior. Third, we showed that aligning the feeding window to the active phase was capable of rescuing the *Fmr1* KO mouse model in a LD environment **(Chapter 5)**. When the time-restricted feeding (TRF) treatment was given, the mutants showed 54% increased circadian power, 44% better nocturnality, 25% longer sleep

duration, and 28% reduced sleep fragmentation than the conspecifics with *ad lib* treatment. Social memory and repetitive grooming behavior were also improved by 116% and 33% in the mutants respectively. Together, these rescue studies all support the emerging idea that better understanding the role of circadian rhythms in ASD may bring new insights to disease mechanisms and assist the development of novel treatments.

There are several lines of studies can be conducted in the future based on this current dissertation study. For example, it remains to be determined if the DLaN-induced inflammation is prevented under T7 LD cycle. The SCN regulates immune profiles through the projections to the paraventricular hypothalamus and hypothalamus-pituatry-adrenal axis to release norepinephrine, adrenaline, and glucocorticoids (Kalsbeek et al., 2012). Under T7 LD cycle, the SCN rhythms remains un-impacted (LeGates et al., 2012; Moriya et al., 2015; Engeland et al., 2018) and thus we expect that the downstream immune regulations would be undisturbed. In addition, it has been demonstrated that the testing animals have undistinguishable amount of sleep in the standard environment and in the T7 LD cycle, so we do not expect that the immune regulations would be affected due to sleep loss which may be a confounding factor leading to increased pro-inflammatory cytokine levels and declined social and cognitive flexibility (Killgore et al., 2017; Gordon; Grant et al., 2018). We hypothesize that the unaltered ASD behavior is due to undisrupted immune regulations in the plasma and in the central nervous tissues. In addition, as a second line of future work, we would like to determine if the dysregulated glutamatergic subpopulation in the basolateral amygdala (BLA) drives DLaN-induced ASD behavioral impairments. Alterations in the BLA is implicated for ASD (Sturm et al., 2013; Felix-Ortiz and Tye, 2014; Sun et al., 2019) and perturbations in the excitatory/inhibitory balance in this brain region is likely leading to disruptive behavior outcome (Zhong et al., 2022). By comparing levels of c-Fos induction in several brain regions including those in the hypothalamus and limbic system under long or short wavelength DLaN, we have demonstrated a high level of c-Fos expression in the glutamatergic cell population (labeled by vesicular glutamate transporter, vGlut2) in the BLA region responding to DLaN disruption

(Chapter 3). To achieve our goal, we have established WT controls and Cntnap2 KO mutants carrying vGlut2-ires-Cre genetic construct for DREADD (designer receptors exclusively activated by designer drugs) technology that allows spatial and temporal control of the activity of specific neurons. The role of glutamatergic (vGlut2+) subpopulation in BLA could be tested by two sets of experiments: 1) to determine if activation of vGlut2+ neurons in BLA using DREADD under standard LD environment is sufficient to replicate the disruptive behavior evoked by DLaN exposure; and 2) to determine if suppression of vGlut2+ neurons in BLA using DREADD under DLaN is sufficient to prevent the negative behavioral consequences. We expect that these experiments will answer the question if vGlut2+ neurons in BLA are sufficient and required to DLaN-driven ASD behavioral impairments. Finally, as a third line of future study, it is of our interest to investigate if inflammation induced by DLaN is also present in other brain areas implicated for ASD characteristics. Hippocampus, for example, is associated with ASD behavior by evidence from the neuropathological and imaging studies in ASD patients (Raymond et al., 1989; Bauman et al., 2005; Lawrence et al., 2010). Dysregulated neuroinflammation in hippocampus is suggested to modulate sociability and repetitive behavior in preclinical models (Makinoda et al., 2008; Depino et al., 2011; Provenzano et al., 2016). Moreover, anti-inflammation treatment rescues social communication and stereotyped behavior in the BTBR T+ Itpr3tf/J (BTBR) mice with reductions in neuro-inflammatory markers such as interleukin-1β, Iba-1, tumor necrosis factor-a, and interleukin -6 in the hippocampus (Zhang et al., 2019). And neuroinflammation in BLA is likely to disrupt the excitatory/inhibitory balance in this brain region and thus leading to disruptive behavior (Zhong et al., 2022). For example, a study leveraging a combination of maternal immune activation regimen and optogenetics demonstrates that neuroinflammation in the BLA increases BLA firing outputs along with ASD behavioral impairments (Li et al., 2018). At this moment, whether or not the *Cntnap2* mutants under DLaN exhibit increased inflammation in hippocampus and BLA is unknown; however, we did find abnormalities such as disrupted circadian profiles or increased glutamatergic signaling in the hippocampus and

BLA **(Chapter 2 & 3)**. Put all together, we hypothesize that the dysregulated inflammation in these regions might be a convergent mechanism underlying disrupted circadian profiles and increased glutamatergic signaling underlying DLaN-evoked disruptive behavior.

In conclusion, my doctoral research demonstrates the 2-hit hypothesis by showing that there are synergistic effects of DLaN and *Cntnap2* mutation. The *Cntnap2* mutants are more vulnerable to the environmental disruption from molecular to behavior levels. In addition, my doctoral research unravels a primitive mechanistic pathway from photic inputs to behavioral outputs underlying DLaN impacts, and demonstrates that circadian-based intervention can be beneficial to ASD populations. It is my hope that my doctoral research provides a proof of concept that disrupted profiles of circadian rhythms are likely to exacerbate ASD symptoms and correcting their circadian rhythms could be an effective treatment.

Figures

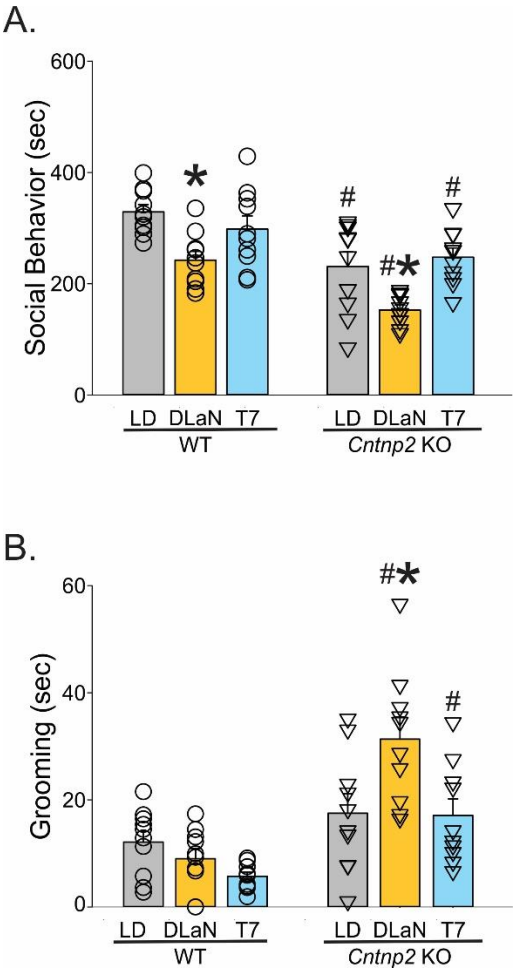

Fig. 5.1: Social and grooming behavior were not affected by lights at subjective nights in the T7 environment. (A) The social behavior in WT controls (circles) and *Cntnap2* KO (triangles) was evaluated by analyzing the time actively spent in social interactions by the testing mouse with the novel stranger mouse. N = 10/genotype/environment with equal males and females. The stranger and testing mice were matched for age, sex, and genotype. Experiments were conducted at CT 18. A 2-way ANOVA was applied and revealed significant effects of genotype ($F_{(1, 30)} = 30.13$, $P < 0.001$) and environment ($F_{(1, 30)} = 13.28$, $P < 0.001$) on the social behavior. Significant ($P < 0.05$) treatment differences are indicated with an * while the # indicates a genotypic difference. **(B)** The grooming behavior was assessed in a novel arena from mice of each genotype under each lighting condition. N = 10/genotype/environment with equal males and females. Experiments were conducted at CT 18. A 2-way ANOVA was applied and revealed significant effects of genotype ($F_{(1, 30)} = 34.80$, $P < 0.001$), environment ($F_{(1, 30)} = 5.36$, $P = 0.008$), and interactions ($F_{(1, 30)} = 5.06$, $P = 0.01$) between the two factors on the grooming behavior. Significant ($P < 0.05$) treatment differences are indicated with an * while the # indicates a genotypic difference.

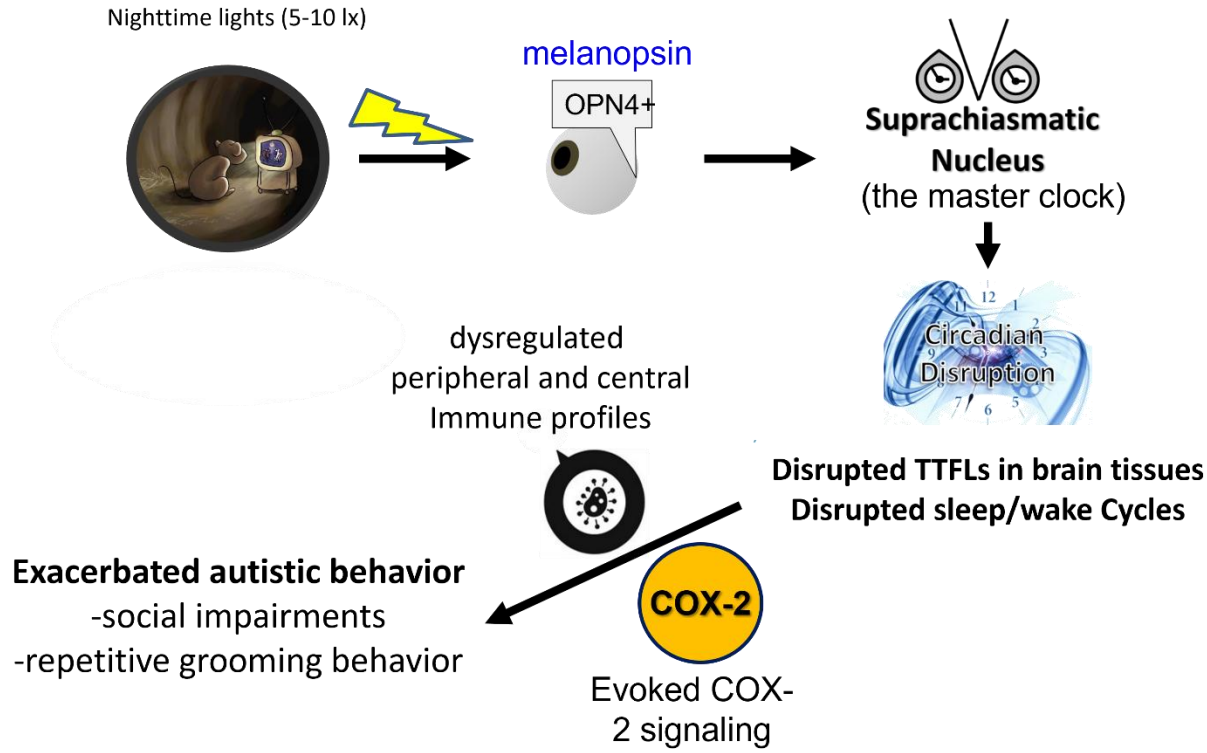

Fig. 5.2: Proposed mechanistic pathway underlying DLaN impacts on social impairments and repetitive grooming behavior. Our work suggests that the nighttime lights are received by the photoreceptor-melanopsin (*OPN4*) and transmitted to the master clock-suprachiasmatic nucleus (SCN). This inappropriate photic inputs at night disrupts the SCN rhythms and results in circadian disruptions in central nervous tissues and sleep/wake cycles. At the downstream of pathway, the circadian disruption induces dysregulated inflammation in the plasma and prefrontal cortex (PFC) and ultimately negatively impacts social and grooming behavior by evoking cyclooxygenase-2 (COX-2) signaling.

Reference

Chakrabarti, Bhismadev, et al. "Genes related to sex steroids, neural growth, and social–emotional behavior are associated with autistic traits, empathy, and Asperger syndrome." Autism Research 2.3 (2009): 157-177.

Badia, Pietro, et al. "Bright light effects on body temperature, alertness, EEG and behavior." Physiology & behavior 50.3 (1991): 583-588.

Bauman, Margaret L., and Thomas L. Kemper. "Neuroanatomic observations of the brain in autism: a review and future directions." International journal of developmental neuroscience 23.2-3 (2005): 183-187.

Depino, Amaicha Mara, Luciana Lucchina, and Fernando Pitossi. "Early and adult hippocampal TGF-β1 overexpression have opposite effects on behavior." Brain, behavior, and immunity 25.8 (2011): 1582-1591.

Dickerson, Aisha S., et al. "Potential sex differences relative to autism spectrum disorder and metals." Current environmental health reports 4.4 (2017): 405-414.

Engeland, William C., et al. "The adrenal clock prevents aberrant light-induced alterations in circadian glucocorticoid rhythms." Endocrinology 159.12 (2018): 3950-3964.

Felix-Ortiz AC, Tye KM. Amygdala inputs to the ventral hippocampus bidirectionally modulate social behavior. J Neurosci. 2014;34(2):586-95.

Gordon, Amie M., Wendy Berry Mendes, and Aric A. Prather. "The social side of sleep: Elucidating the links between sleep and social processes." Current directions in psychological science 26.5 (2017): 470-475.

Grant, Leilah K., et al. "Impaired cognitive flexibility during sleep deprivation among carriers of the Brain Derived Neurotrophic Factor (BDNF) Val66Met allele." Behavioural brain research 338 (2018): 51-55.

Hwang, Wu Jeong, et al. "The role of estrogen receptors and their signaling across psychiatric disorders." International Journal of Molecular Sciences 22.1 (2020): 373.

Imbriani, Giovanni, et al. "Early-life exposure to environmental air pollution and autism spectrum disorder: a review of available evidence." International Journal of Environmental Research and Public Health 18.3 (2021): 1204.

Killgore, William DS, et al. "Sleep deprivation impairs recognition of specific emotions." Neurobiology of Sleep and Circadian Rhythms 3 (2017): 10-16.

Lawrence, Y. A., et al., "Parvalbumin-, calbindin-, and calretinin-immunoreactive hippocampal interneuron density in autism." Acta Neurologica Scandinavica 121.2 (2010): 99-108.

Li, Yan, et al. "Maternal and early postnatal immune activation produce dissociable effects on neurotransmission in mPFC–amygdala circuits." Journal of Neuroscience 38.13 (2018): 3358-3372.

LeGates, Tara A., et al. "Aberrant light directly impairs mood and learning through melanopsin-expressing neurons." Nature 491.7425 (2012): 594-598.

Lucas, Robert J., et al. "Measuring and using light in the melanopsin age." Trends in neurosciences 37.1 (2014): 1-9.

Maruani, Julia, and Pierre A. Geoffroy. "Multi-Level Processes and Retina–Brain Pathways of Photic Regulation of Mood." Journal of Clinical Medicine 11.2 (2022): 448.

Makinodan, Manabu, et al. "Maternal immune activation in mice delays myelination and axonal development in the hippocampus of the offspring." Journal of neuroscience research 86.10 (2008): 2190-2200.

Miller, Mark W. "Apparent effects of light pollution on singing behavior of American robins." The Condor 108.1 (2006): 130-139.

Milosavljevic, Nina, et al. "Chemogenetic activation of melanopsin retinal ganglion cells induces signatures of arousal and/or anxiety in mice." Current Biology 26.17 (2016): 2358-2363.

Moriya, Shunpei, et al. "Housing under abnormal light–dark cycles attenuates day/night expression rhythms of the clock genes Per1, Per2, and Bmal1 in the amygdala and hippocampus of mice." Neuroscience research 99 (2015): 16-21.

Petroni, Valeria, et al. "Autistic-like behavioral effects of prenatal stress in juvenile Fmr1 mice: the relevance of sex differences and gene–environment interactions." Scientific Reports 12.1 (2022): 1-12.

Piontkewitz, Yael, et al. "Effects of risperidone treatment in adolescence on hippocampal neurogenesis, parvalbumin expression, and vascularization following prenatal immune activation in rats." Brain, behavior, and immunity 26.2 (2012): 353-363.

Provenzano, Giovanni, et al. "Comparative gene expression analysis of two mouse models of autism: transcriptome profiling of the BTBR and En2−/− hippocampus." Frontiers in Neuroscience 10 (2016): 396.

Roenneberg, Till, and Martha Merrow. "The circadian clock and human health." Current biology 26.10 (2016): R432-R443.

Sarachana, Tewarit, et al. "Sex hormones in autism: androgens and estrogens differentially and reciprocally regulate RORA, a novel candidate gene for autism." PloS one 6.2 (2011): e17116.

Sondereker, Katelyn B., Maureen E. Stabio, and Jordan M. Renna. "Crosstalk: The diversity of melanopsin ganglion cell types has begun to challenge the canonical divide between image-forming and non-image-forming vision." Journal of Comparative Neurology 528.12 (2020): 2044-2067.

Sturm, Volker, et al. "DBS in the basolateral amygdala improves symptoms of autism and related self-injurious behavior: a case report and hypothesis on the pathogenesis of the disorder." Frontiers in Human Neuroscience 6 (2013): 341.

Sun T, Song Z, Tian Y, Tian W, Zhu C, Ji G, Luo Y, Chen S, Wang L, Mao Y. Basolateral amygdala input to the medial prefrontal cortex controls obsessive-compulsive disorder-like checking behavior. Proceedings of the National Academy of Sciences. 2019;116(9):3799-804.

Wang, Chengzhong, et al. "Prenatal, perinatal, and postnatal factors associated with autism: A meta-analysis." Medicine 96.18 (2017).

Wang, Huei Bin, et al. "Melatonin treatment of repetitive behavioral deficits in the Cntnap2 mouse model of autism spectrum disorder." Neurobiology of disease 145 (2020): 105064.

Werling, Donna M. "The role of sex-differential biology in risk for autism spectrum disorder." Biology of sex differences 7.1 (2016): 1-18.

Zhang, Quanzhi, et al. "Folic acid improves abnormal behavior via mitigation of oxidative stress, inflammation, and ferroptosis in the BTBR $^{T+ tf/J}$ mouse model of autism." The Journal of nutritional biochemistry 71 (2019): 98-109.

Zhong, Haiquan, et al. "Neonatal inflammation via persistent TGF-β1 downregulation decreases GABAAR expression in basolateral amygdala leading to the imbalance of the local excitation-inhibition circuits and anxiety-like phenotype in adult mice." Neurobiology of Disease (2022): 105745.